SMART POLYMERIC CARRIERS:
TARGETED DELIVERY OF THERAPEUTIC AGENTS

by
Merve Karaçivi
B.S., Chemistry, Yıldız Technical University, 2009
M.S., Chemistry, İstanbul Technical University, 2011

Submitted to the Institute for Graduate Studies in
Science and Engineering in partial fulfillment of
the requirements for the degree of
Doctor of Philosophy

Graduate Program in Chemistry
Boğaziçi University
2019

SMART POLYMERIC CARRIERS:
TARGETED DELIVERY OF THERAPEUTIC AGENTS

APPROVED BY:

Prof. Rana Sanyal	……
(Thesis Supervisor)	
Prof. Amitav Sanyal	……
(Thesis Co-Advisor)	
Prof. İlknur Doğan	……
Prof. Sevgi Güngör	……
Assist. Prof. Oktay Demircan	……
Assist. Prof. Özgül Gök	……

DATE OF APPROVAL: 14.05.2019

ACKNOWLEDGEMENTS

First I would like to thank my thesis supervisors Prof. Rana Sanyal and Prof. Amitav Sanyal for letting me to study in their lab, making me love chemistry much more, helping me through my research whenever I need help and motivating me patiently. Moreover I want to send my special thanks to Prof. Rana Sanyal she was always like a big sister to me.

I would like to express my thanks to my thesis advisors and members of my thesis committee Prof. İlknur Doğan, Prof. Sevgi Güngör, Assist. Prof. Oktay Demircan and Assist. Prof. Özgül Gök for their careful and constructive review of the final manuscript of the thesis.

I am so much thankful to all my labmates for their very kind interest and generous help during my research in the laboratory. I am very grateful each of them because of being like a brother or a sister to me.

My deepest thanks go to my family, especially my nephew Arda and my niece Zeynep for their endless love, patience and support.

Finally I would also want to thank the graduate scholarship program by The Scientific and Technological Research Council of Turkey (TÜBİTAK) (2211-D) for supporting me during my PhD education. I would like to thank BU/BAP for contributing the funding and resources contributed to this thesis.

ABSTRACT

SMART POLYMERIC CARRIERS: TARGETED DELIVERY OF THERAPEUTIC AGENTS

In cancer research, studies about polymer drug conjugates and targeted delivery of chemotherapy agents are gaining great attention due to their ability to enhance biodistribution profiles and improve efficacy of chemotherapy agents. In the scope of this thesis four different polymer drug conjugates were synthesized using acrylate based carriers. In each case, drug molecules were covalently attached to the polymeric carrier through biodegradable linkers. These polymeric carriers aim to accumulate the active drug in the tumor via passive and active targeting. Each carrier, due its size, has the capacity to take advantage of enhanced permeation and retention (EPR) effect. Along with the size, active targeting via small molecule targeting units are also utilized. As such, in the first project, anti-angiogenic drug Combretastatin A4 (CA4) was conjugated to polymer backbone through a hydrolyzable ester linker. A second drug, alendronate (ALN) was also conjugated to the system as a bone targeting agent aiming to accumulate the conjugate in bone tissue. For the next three studies, anti-neoplastic agent Docetaxel (DTX) and 5-Fluorouracil (5-FU) derivatives were used as the active drug moiety. These constructs were ornamented further to accumulate in breast and ovarian tumors. In each case, different linkers were utilized in order to affect the release profile of the abovementioned drug molecules. In vitro studies were undertaken to demonstrate the effect of the active agents on a variety of the cell lines.

ÖZET

AKILLI İLAÇ TAŞIYICILAR: TERAPÖTİK AJANLARIN HEDEFLİ TESLİMİ

Kanser araştırmalarında polimer ilaç konjugatları ve kemoterapi ajanlarının hedefe yönelik uygulamaları bu tür formülasyonların barındırdıkları ilaçların biyodağılım profillerini ve etkinliklerini artırabilme potansiyellerinden dolayı her geçen gün önem kazanmaktadırlar. Bu tez kapsamında akrilat bazlı dört farklı polimer ilaç konjugatı sentezlenmiştir. Herbir projede ilaç molekülleri polimerik taşıyıcılara biyobozunur bağlanyıcılarla bağlanmıştır. Bu polimerik taşıyıcıların amacı ilaçların tümör dokusuna pasif ve aktif hedefleme yoluyla toplanmasını sağlamaktır. Her taşıyıcı boyutundan dolayı arttırılmış geçirgenlik ve alıkonma etkisinden (EPR) faydalanma kapasitesine sahiptir. Moleküler boyut dışında küçük moleküllü hedefleme birimleri de aktif hedefleme için kullanılmıştır. Buna örnek olarak ilk projede antianjiyojenik bir ilaç olan CA4, polimer omurgasına hidrolize olabilen bir ester bağlayıcısı üzerinden bağlanmıştır. İkinci ilaç Alendronat ise kemik dokusunda birikimin sağlanabilmesi için hedefleyici grup olarak polimere bağlanmıştır. Diğer üç çalışmada ise anti-neoplastik ilaçlar Dosetaxel ve 5-FU, aktif ilaç molekülleri olarak kullanılmışlardır. Bu polimerlerin ileriki aşamalarda meme ve yumurtalık dokularında birikmesi hedeflenmiştir. Tüm çalışmalarda yukarıda bahsedilen ilaçların salım profillerinin düzenlenmesi için farklı bağlayıcılar kullanılmıştır. Ayrıca polimerlerin aktivitelerinin belirlenmesi için farklı kanser hücre hatlarında sitotoksisite çalışmaları yapılmıştır.

TABLE OF CONTENTS

ACKNOWLEDGEMENTS 3
ABSTRACT 4
ÖZET 5
TABLE OF CONTENTS 6
LIST OF FIGURES 11
LIST OF TABLES 16
LIST OF ACRONYMS/ABBREVIATIONS 17
1. Introduction 1
1.1. Cancer 1
1.2. EPR EFFECT 4
1.3. Polymer-Drug Conjugates 5
1.4. Combination Drug Delivery Systems 9
1.5. Diagnosis in Cancer and Drug Delivery Systems 12
1.6. Active Targeting and Effects of Targeting Groups in Polymer Molecules 15
1.7. Reactive Monomers and Post Polymerization Modification Strategies 23
1.8. Activated Ester Monomers 25
1.9. N-Hydroxysuccinimide (NHS) Based Reactive Groups for Targeting Group Conjugations 26
1.10. Polymerization Techniques 29
1.10.1. Free Radical Polymerization 30
1.10.2. Reversible-Addition Fragmentation and Chain Transfer Reaction (RAFT) 30
1.11. Stimuli Responsive Controlled Drug Release 31
1.11.1. Ph Responsive Polymer Drug Conjugates 32
1.11.2. Enzyme Responsive Polymer Drug Conjugates 35
1.11.3. Redox Responsive Polymer Drug Conjugates and Glutathion Sensitive Structures 38

2. TARGETING TO THE BONE: ALENDRONATE DIRECTED CA4 BEARING ANTI-ANGIGENIC POLYMER DRUG CONJUGATES 41
2.1. Introduction 41
2.2. Experimental Section 44
2.2.1. Materials 44
2.2.2. Instrumentation 45
2.2.3. Synthesis and Characterization of CA4MA (3) 46
2.2.4. Synthesis and Characterization of P(OEGMA-CA4-NHS) (4) 46
2.2.5. Synthesis and Characterization of P(OEGMA-CA4-ALN) (6) 46
2.2.6. Synthesis and Characterization of P(OEGMA-CA4) (7) 47
2.2.7. Synthesis and Characterization of P(OEGMA-NHS) (8) 47
2.2.8. Synthesis and Characterization of P(OEGMA-ALN-NHS) (9) 47
2.2.9. Synthesis and Characterization of P(OEGMA-ALN) (10) 48
2.2.10. Synthesis and Characterization of P(OEGMA-CA4-NHS-FMA) (12). 48
2.2.11. Synthesis, Characterization of P(OEGMA-CA4-ALN-NHS-FMA) (13) 449
2.2.12. Synthesis, Characterization of P(OEGMA-CA4-FMA) (14) 49
2.2.13. Synthesis, Characterization of P(OEGMA-CA4-ALN-FMA) (15) . 49
2.2.14. *In vitro* Drug Release 50
2.2.15. Serum Stability of CA4 50
2.2.16. Hydroxyapatite Binding Assay 50
2.2.17. *In vitro* Cell Viability Assay on HUVEC's, Saos-2 and U-2 OS Human Osteosarcoma Cell Lines 51
2.2.18. Endothelial Cell Tube Formation Assay on HUVECs 51
2.2.19. Internalization of FMA Containing Polymers 52
2.3. Results and Discussion 52
2.3.1. Synthesis and Characterization of CA4 Conjugated Copolymers 52
2.3.2. Hydroxyapatite Binding Assay 55
2.3.3. Drug Release Profiles of Copolymers 56
2.3.4. in vitro Cytotoxicity of Copolymers on HUVECs, Saos-2, and U2-OS Cells. 57
2.3.5. Cell Internalization Studies 59

2.3.6. Endothelial Tube Formation Assay on HUVECs..... 60
2.4. Conclusions..... 62
3. INTEGRIN TARGETED ANTI-ANGIOGENIC AND ANTI-NEOPLASTIC AGENT CARRYING COPOLYMERS FOR OVARIAN CANCER TREATMENT.....63
3.1. Introduction..... 63
3.2. Experimental Section..... 65
3.2.1. Materials..... 65
3.2.2. Instrumentation..... 65
3.2.3. Synthesis, Characterization of P(OEGMA-CA4-NHS) (18) 66
3.2.4. Synthesis, Characterization of P(OEGMA-CA4-RGD) (19)..... 66
3.2.5. Synthesis, Characterization of P(OEGMA-CA4) (20)..... 67
3.2.6. Synthesis, Characterization of P(OEGMA-CA4-NHS-DTX) (21).. 67
3.2.7. Synthesis, Characterization of P(OEGMA-CA4-RGD-DTX) (22) . 68
3.2.8. Synthesis, Characterization of P(OEGMA-CA4- DTX) (23)..... 68
3.2.9. Synthesis, Characterization of P(OEGMA-CA4-NHS-FMA) (24) . 69
3.2.10. Synthesis, Characterization of P(OEGMA-CA4-RGD-FMA) (25) . 69
3.2.11. Synthesis, Characterization of P(OEGMA-CA4-FMA) (26)..... 70
3.2.12. Synthesis, Characterization of P(OEGMA-CA4-NHS-FMA-DTX) (27) 70
3.2.13. Synthesis, Characterization of P(OEGMA-CA4-RGD-FMA-DTX) (28) 71
3.2.14. Synthesis, Characterization of P(OEGMA-CA4 –FMA-DTX) (29) 71
3.2.15. In vitro drug release..... 71
3.2.16. In *Vitro* Cell Viability Assay on SK-OV-3 and Caov-3 Human Ovarian Cancer Cell lines..... 72
3.2.17. Animal Study..... 72
3.3. Results and Discussion..... 73
3.3.1. Synthesis and Characterization of CA4 and DTX Bearing Copolymers 73
3.3.2. Drug Release Profiles of Copolymers..... 80
3.3.3. In vitro cytotoxicities of copolymers on SK-OV-3 and Caov-3 human ovarian cancer cells 81

3.4. Conclusion 83
4. cRGDfK TARGETED REDOX RESPONSIVE 5-FU PRODRUG CONJUGATES FOR BREAST CANCER THERAPY 84
4.1. Introduction 84
4.2. Experimental Section 86
4.2.1. Materials 86
4.2.2. Instrumentation 87
4.2.3. Synthesis, Characterization of SCEDEMA (31) 87
4.2.4. Synthesis, Characterization of Compound 32 88
4.2.5. Synthesis, Characterization of MA-5'DFCR (33) 88
4.2.6. Synthesis, Characterization of P(OEGMA-NHS-5'DFCR) (34) 89
4.2.7. Synthesis, Characterization of P(OEGMA-5'DFCR-RGD) (35) 89
4.2.8. Synthesis, Characterization of P(OEGMA-5'DFCR) (36) 90
4.2.9. Synthesis, Characterization of P(OEGMA-5'DFCR-NHS-FMA) (37) 90
4.2.10. Synthesis, Characterization of P(OEGMA-5'DFCR-FMA-RGD) (38) 91
4.2.11. Synthesis, Characterization of P(OEGMA-5'DFCR-FMA) (39) 91
4.2.12. *In vitro* Drug Release 92
4.2.13. Cell Lines 92
4.2.14. *In vitro* Cell Viability Assay on MDA-MB-453 and MDA-M-231 Cells 92
4.3. Results and Discussion 93
4.3.1. Synthesis, Characterization of 5'-DFCR Conjugated Copolymers 93
4.3.2. Drug Release Profiles of Copolymers 97
4.3.3. Determination of *in vitro* Cytotoxicity of Copolymers on MDA-MB-453 and MDA-MB-231 Cells 98
4.4. Conclusion 99
5. NOVEL CATHEPSIN B LABILE DIPEPTIDE LINKER VAL-CIT AND ANTI-NEOPLASTIC DRUG DOCETAXEL CONJUGATED MONOMER FOR CANCER TREATMENT 101
5.1. Introduction 101
5.2. Experimental Section 103

5.2.1. Materials 103
5.2.2. Instrumentation 104
5.2.3. Synthesis of t-Butyl-4-aminobenzoate (41) 104
5.2.4. Synthesis of Fmoc-Val-Cit (42) 105
5.2.5. Synthesis of Fmoc-Val-cit-tertiary amino benzoate (43) 105
5.2.6. Synthesis of Val-cit-tertiary amino benzoate (44) 106
5.2.7. Synthesis of MA-Val-cit-tertiary amino benzoate (45) 106
5.2.8. Synthesis of MA-Val-cit-amino benzoic acid (46) 107
5.2.9. Synthesis of MA-Val-cit-amino benzoyl-DTX (47) 107
5.2.10. Synthesis of P(OEGMA-MA-VC-benzoyl-DTX-NHS) (48) 108
5.2.11. Synthesis of P(OEGMA-MA-VC-benzoyl-DTX-RGD) (49) 108
5.2.12. Cell Lines 109
5.2.13. *In vitro* Cell Viability Assay on A549 Cells 109
5.3. Results and Discussion 110
5.3.1. Synthesis of Val-Cit dipeptide and chemotherapy drug docetaxel bearing monomer 110
5.3.2. Determination of *in vitro* Cytotoxicity of Targeted Copolymer on A549 Cell Line 113
5.4. Conclusion 114
6. CONCLUSIONS 115
REFERENCES 117
APPENDIX A: ADDITIONAL DATA 150

LIST OF FIGURES

Figure 1.1. Schematic illustritaion of abnormal cell growth. 1

Figure 1.2. General scheme of angiogenesis process. 2

Figure 1.3. Vicious cycle of bone metastases of breast cancer cells. 3

Figure 1.4. Schematic Illustration of EPR effect. 4

Figure 1.5. General illustration of dendrimeric structure. 9

Figure 1.6. Polymer based combination therapies. 11

Figure 1.7. Combination of therapeutic and diagnostic agents. 13

Figure 1.8. Schematic Illustration of Active Targeting. 16

Figure 1.9. General Scheme of Bisphosphonate Molecules. 17

Figure 1.10. General strategy for PPM reactions 23

Figure 1.11. Different types of reactive monomers applied for post polymerization modification reactions. 24

Figure 1.12. Schematic illustration and synthetic route for rhBMP-2 attached AH-modified CPC. 28

Figure 1.13. General mechanism of free radical polymerization reaction technique. 30

Figure 1.14. Major types of RAFT agents. 31

Figure 1.15. Stimuli responsive controlled drug release. 32

Figure 1.16. pH-sensitive linker bearing polymer drug conjugate. 33

Figure 1.17. Schematic illustration of dendritic structure bearing enzymatically cleavable phe-lys linker. 37

Figure 2.1. Scheme for synthesis and evaluation of bone-targeted antiangiogenic copolymers. 44

Figure 2.2. Synthetic Route for Drug, Targeting Moiety Appended Copolymers 52

Figure 2.3. Synthetic Route for FMA Containing Fluorescent Copolymers. 55

Figure 2.4. Binding kinetics of Copolymers 56

Figure 2.5. Release of CA4 from Copolymers 57

Figure 2.6. Viabilities of HUVECs, Saos-2 and U2-OS cells 59

Figure 2.7. Microscopy images of Saos-2 cells labeled copolymers. 60

Figure 2.8. Anti-angiogenic assay using HUVECs on Matrigel 61

Figure 3.1. Monomers that are used in polymerization reaction. 74

Figure 3.2. Enzymatic and plasma release of DTX and CA4 from P(OEGMA-CA4-DTX-RGD) and P(OEGMA-CA4-DTX). 80

Figure 3.3. Viabilities of SK-OV-3 cells and Caov-3 cells 82

Figure 4.1. Process of turning drug capecitabine into 5-FU *via* enzymes. 85

Figure 4.2. The effect of disulfide bonds on releasing 5'-DFCR. 86

Figure 4.3. Synthetic route of 5'-DFCR bearing monomer 94

Figure 4.4. Synthesis of 5'-DFCR and cRGDfK bearing copolymers. 94

Figure 4.5. Synthesis of 5'-DFCR, FMA and cRGDfK bearing copolymers 96

Figure 4.6. Release profiles of copolymers 97

Figure 4.7. Viabilities of MDA-MB-453 and MDA-MB-231 cells 98

Figure 5.1. Design of methacrylated val-cit linker and PABA spacer bearing 103

Figure 5.2. General synthesis of Val-Cit dipeptide bearing and Docetaxel containing monomer. 111

Figure 5.3. Expanded ^{1}H NMR spectrums of copolymers 48 and copolymer 49 112

Figure 5.4. Synthesis of P(OEGMA-MA-Val-Cit-benzoyl-DTX-RGD) copolymer 113

Figure 5.5. Viabilities of A549 cells treated with free DTX and P(OEGMA-CA4-DTX-RGD) 113

Figure A.1. ^{1}H-NMR of CA4MA (3) 151

Figure A.2. ^{13}C-NMR of CA4MA (3) 152

Figure A.3. FT-IR^{-1} of CA4MA (3) 153

Figure A.4. ^{1}H-NMR of P(OEGMA-CA4-NHS) (4) 154

Figure A.5. ^{1}H-NMR of P(OEGMA-CA4-ALN) (6) 155

Figure A.6. ^{1}H-NMR of P(OEGMA-CA4) (**7**) 156

Figure A.7. ^{1}H-NMR of P(OEGMA-NHS) (8) 157

Figure A.8. ^{1}H-NMR of P(OEGMA-NHS-ALN) (9) 158

Figure A.9. ^{1}H-NMR of P(OEGMA-ALN) (10) 159

Figure A.10. ^{1}H-NMR of P(OEGMA-CA4-NHS-FMA) (12) 160

Figure A.11. ^{1}H-NMR of P(OEGMA-CA4-NHS-ALN-FMA (13) 161

Figure A.12. ^{1}H-NMR Spectrum of P(OEGMA-CA4-NHS) (18) 162

Figure A.13. ^{1}H-NMR Spectrum of P(OEGMA-CA4-RGD) (19) 163

Figure A.14. ^{1}H-NMR Spectrum of P(OEGMA-CA4) (20) 164

Figure A.15. ^{1}H-NMR Spectrum of P(OEGMA-CA4-NHS-DTX) (21) 165

Figure A.16. ^{1}H-NMR Spectrum of P(OEGMA-CA4-RGD-DTX) (22) 166

Figure A.17. ^{1}H-NMR Spectrum of P(OEGMA-CA4-DTX) (23) 167

Figure A.18. ^{1}H-NMR Spectrum of P(OEGMA-CA4-NHS-FMA) (24) 168

Figure A.19. ^{1}H-NMR Spectrum of P(OEGMA-CA4-RGD-FMA) (25) 169

Figure A.20. ^{1}H-NMR Spectrum of P(OEGMA-CA4-FMA) (26) 170

Figure A.21. ^{1}H-NMR Spectrum of P(OEGMA-CA4-NHS-DTX-FMA) (27) 171

Figure A.22. ^{1}H-NMR Spectrum of P(OEGMA-CA4-RGD-DTX-FMA) (28) 172

Figure A.23. ^{1}H-NMR Spectrum of P(OEGMA-CA4-DTX-FMA) (29) 173

Figure A.24. ^{1}H-NMR Spectrum of HSEMA (30) 174

Figure A.25. ^{1}H-NMR Spectrum of SCEDEMA (31) 175

Figure A.26. ^{13}C-NMR Spectrum of SCEDEMA (31) 176

Figure A.27. FT-IR^{-1} Spectrum of SCEDMA (31) 177

Figure A.28. ^{1}H-NMR Spectrum of MA-DO-5'DFCR monomer (32) 178

Figure A.29. ^{13}C-NMR Spectrum of MA-DO-5'DFCR monomer (32) 179

Figure A.30. FT-IR^{-1} Spectrum of MA-DO-5'DFCR monomer (32) 180

Figure A.31. ^{1}H-NMR Spectrum of MA-5'DFCR in $CDCl_3$ (33) 181

Figure A.32. ^{1}H-NMR Spectrum of MA-5'DFCR in DMSO-*d6* (33) 182

Figure A.33. ^{13}C-NMR Spectrum of MA-5'DFCR (33) 183

Figure A.34. FT-IR^{-1} Spectrum of MA-5'DFCR (33) 184

Figure A.35. ^{1}H-NMR Spectrum of P(OEGMA-NHS-5'DFCR) (35) 185

Figure A.36. ^{1}H-NMR Spectrum of P(OEGMA-RGD-5'DFCR) (36) 186

Figure A.37. ^{1}H-NMR Spectrum of P(OEGMA-5'DFCR) (37) 187

Figure A.38. ^{1}H-NMR Spectrum of P(OEGMA-NHS-5'DFCR-FMA) (38) 188

Figure A.39. ^{1}H-NMR Spectrum of P(OEGMA-RGD-5'DFCR-FMA) (39) 189

Figure A.40. ^{1}H-NMR Spectrum of P(OEGMA-5'DFCR-FMA) (40) 190

Figure A.41. ^{1}H-NMR Spectrum of tert-butyl 4-aminobenzoate (41) 191

Figure A.42. ^{1}H-NMR Spectrum of Fmoc-VC (42) 192

Figure A.43. ^{1}H-NMR Spectrum of Fmoc-VC-tert-butyl-4-aminobenzoate(43) 193

Figure A.44. ^{13}C-NMR Spectrum of Fmoc-VC-tert-butyl 4-aminobenzoate (43) 194

Figure A.45. FT-IR^{-1} Spectrum of Fmoc-VC-tert-butyl 4-aminobenzoate (43)…..... 195

Figure A.46. ^{1}H-NMR Spectrum of VC-tert-butyl 4-aminobenzoate (44) 196

Figure A.47. ^{13}C-NMR Spectrum of VC-tert-butyl 4-aminobenzoate (44) 197

Figure A.48. FT-IR^{-1} Spectrum of VC-tert-butyl 4-aminobenzoate (44) 198

Figure A.49. ^{1}H-NMR Spectrum of MA-VC-tert-butyl 4-aminobenzoate (45)…..... 199

Figure A.50. ^{13}C-NMR Spectrum of MA-VC-tert-butyl 4-aminobenzoate (45) 200

Figure A.51. FT-IR^{-1} spectrum of MA-VC-tert-butyl 4-aminobenzoate (45) 201

Figure A.52. ^{1}H-NMR Spectrum of MA-VC-4-aminobenzoic acid (46) 202

Figure A.53. ^{13}C-NMR Spectrum of MA-VC-4-aminobenzoic acid (46) 203

Figure A.54. FT-IR^{-1} Spectrum of MA-VC-4-aminobenzoic acid (46)..... 204

Figure A.55. ^{1}H-NMR Spectrum of MA-VC-4-aminobenzoyl-DTX (47) 205

Figure A.56. ^{13}C-NMR Spectrum of MA-VC-4-aminobenzoyl-DTX (47) 206

Figure A.57. FT-IR^{-1} Spectrum of MA-VC-4-aminobenzoyl-DTX (47) 207

Figure A.58. ^{1}H NMR Spectrum of P(OEGMA-MA-VC-4-aminobenzoyl-DTX-NHS) (48) 208

Figure A.59. ^{1}H NMR Spectrum of P(OEGMA-MA-Val-Cit-4-aminobenzoyl-DTX-RGD) (49) 209

LIST OF TABLES

Table 2.1. Polymerization Conditions and Characterization of Copolymers. 53

Table 2.2. Properties of copolymers. 53

Table 2.3. Calculated EC_{50} values after continuous incubation HUVECs, U2-OS and Saos-2 cells for 48 h. 58

Table 3.1. Polymerization Conditions and Characterization of Copolymers. 79

Table 3.2. Properties of Copolymers. 79

Table 3.3. EC_{50} values of free drugs and copolymers after incubation of SK-OV-3 and Caov-3 cells for 48 hours. 82

Table 4.1. Polymerization conditions and obtained polymers' characterizations. 95

Table 4.2. Properties of Copolymers. 95

Table 4.3. EC_{50} values of MDA-MB-453 and MDA-MB-213 cells treated with free 5-FU, targeted and non-targeted copolymers. 99

LIST OF ACRONYMS/ABBREVIATIONS

5’-DFCR	5’-Deoxy-5-Fluorocytidine
5’-DFUR	5-fluoro-5’-deoxyurudine
ACN	Acetonitrile
AIBN	2,2′-Azobis(2-methylpropionitrile)
ATCC	American Type Culture Collection
ATR-FT-IR	Attenuated Total Reflection Fourier Transform Infrared
AUC	Area Under the Curve
BP	Bisphosphonate
CA4	Combretastatin A4
CAF	Cancer-Associated Fibroblasts
CPT	Campthotesin
CCK-8	Cell Counting Kit-8
$CDCl_3$	Deuterated Chloroform
CH_2Cl_2	Dichloromethane
CPC	Calcium Phosphate Cement
CRP	Controlled Living Radical Polymerization
cRGDfK	Cyclic Arginine-Gylcine-Aspartic acid-Phenyl alanine-Lysine
DCC	*N,N′*-Dicyclohexylcarbodiimide
DDS	Drug Delivery System
DMAc	Dimethylacetamide
DMAP	4-Dimethylaminopyridine
DTX	Docetaxel
EDCI	1-Ethyl-3-(3-Dimethylaminopropyl) Carbodiimide

EPR	Enhanced Retention and Permeability
FDA	Food and Drug Administration
FMA	Fluorescein-O-methacrylate
FT-IR	Fourier Transform Infrared
GFLG	Glycine-Phenylalanine-Leucine-Glycine
GPC	Gel Permeation Chromatography
GSH	Glutathione
HA	Hydroxylapatite
HER2	Human Epidermal Growth Factor Receptor Type 2
HSEMA	2-((2-hydroxyethyl)disulfanyl)ethyl methacrylate
HIF	Hypoxia-Inducible Factors
HPMA	N-(2-Hydroxylpropyl) Methacrylamide
HUVEC	Human Umbilical Vein Endothelial Cell
J	Coupling Constant
kDa	Kilo Dalton
LC-MS	Liquid Chromatography–Mass Spectrometry
MALDI-TOF	Matrix-assisted laser desorption/ionization-Time of Flight
MDR	Multidrug-Resistant
MeOH	Methanol
MHz	Mega Hertz
mRNA	Messenger RNA
MTD	Maximum Tolerated Dose
MWCO	Molecular Weight Cut-Off
NCI	National Cancer Institue
NHS	N-Hydroxy Succinimide

NIR	Near Infra-Red
NMR	Nuclear Magnetic Resonance
NMP	Nitroxide Mediated Polymerization
NO	Nitric Oxide
NSCLC	Non-Small Cell Lung Cancer
OS	Overall Survival
PABA	Paraaminobenzyl acid
PABC	Paraaminobenzyl alcohol
PAMAM	Poly(amidoamine)
PBLG	Poly(γ-benzyl-l-Glutamate)
PBS	Phosphate Buffer Saline
PCL	Poly(ε-caprolactone)
PDI	polydispersity index
PEG	Poly(ethylene glycol)
PFP	Pentafluorophenyl
PFS	Progression-Free Survival
PK	Pharmacokinetic
PLAA	Poly(l-aspartamide)
PLGA	Poly(lactic-co-glycolic acid)
PMDETA	*N,N,N′,N″,N‴*-Pentamethyldiethylenetriamine
PPM	Post Polymerization Modification
PPO	Poly(Propylene Oxide)
PSMA	Prostate-Specific Membrane Antigen
PVA	Polyvinyl alcohol
PVP	Poly(vinylpyrrolidone)

RAFT	Reversible Addition- fragmentation Chain Transfer
RC	Regenerated Cellulose
RGD	Arginylglycylaspartic Acid
RNA	Ribonucleic Acid
ROS	Reactive Oxygen Species
rt	Room Temperature
SCEDEMA	2-((2-(N-succunimidylcarboxyoxy)ethyl)disulfanyl)ethyl methacrylate
SCEMA	2-(N-succinimidylcarboxyoxy)ethyl methacrylate
SD	Standard Deviation
SSPS	Solid Phase Peptide Synthesis
TEA	Triethyl amine
TFA	Trifluoroacetic acid
THF	Tetrahydrofuran
TNF-α	Tumor Necrosis Factor-α
TT	Thiazolidine-2-thione
UV	Ultraviolet
VC	Valine-Citrulline
VEGF	Vascular Endothelial Growth Factor
Vis	Visible

1. INTRODUCTION

1.1. Cancer

Cancer is complicated disease containing various crucial changes in cell morphology which finally leads to tumor formulation. The biological end point of the cancer is uncontrolled growing of cells and proliferation [1] (Figure 1.1). Cancer cells derived from normal cells in which the DNA has become mutated. In normal cells, when DNA is damaged, the cell can repair itself but in cancer cells, these injured cells don't die. Instead, it causes abnormal cell growth that all have the same DNA deficiency [2]. DNA damage can occur due to hereditary or it may happen at any time in peoples' life. All over the World, there are millions of people who suffer from cancer. Recent research showed that, 8.8 million people died from cancer in 2015 which is one in six deaths in worldwide [3].

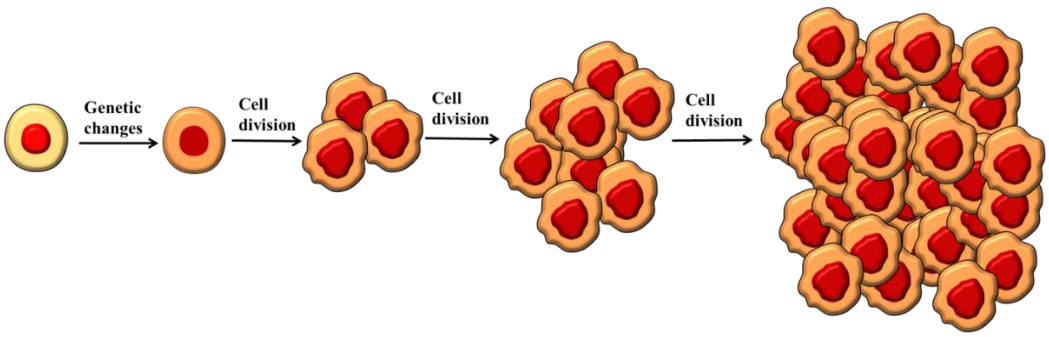

Figure 1.1. Schematic illustritaion of abnormal cell growth.

Cancer initiation and advancement depends on environmental and cellular factors which can act together or in consecutive time. According to latest researches, the environmental factors play main role in developing cancer when compared to genes [4]. Risk of to get cancer may also increase due to infectious agents, cancer-causing agents and age. It has been known that, there are more than 100 types of cancer. Lung, breast, colon,

pancreatic and prostate cancer are the noteworthy types that killed the most people in the World according to National Cancer Institute (NCI) [5].

Most of the cancers start in the one place in the body which is called as primary cancer and the place where cancer starts is called as primary site. Sometimes, cancer cells may spread to other parts of the body far away from the origin place of the tumor *via* blood or lymph [6]. This process is called as metastases. That new constitution of the cancer in the new place is called as metastatic cancer. The most encountered regions for metastatic cancer to grow are liver, lungs, brain, skin and bones [7].

Similar to healthy tissues or organs, tumors need to create new blood supply to obtain their requirements for growing, survival and managing metabolic affairs. On the other hand, blood vessel supply is crucial by extracting residuals from cellular metabolism. This process is accomplished through angiogenesis essentially [8]. (Figure 1.2). Angiogenesis is new blood cell constitution from pre-existing vasculature and it is very critical indication of cancer in common with metabolism. The basic initiator of angiogenesis is hypoxia which has important role in tumor adaptation. Hypoxia adjusts the expression of many genes which are under the control of hypoxia-inducible factors (HIF). Due to hypoxia is major regulator of aggressive tumor growth, HIF regulated genes contribute to cancer expansion and progression. In other words, angiogenesis is mainly formed by hypoxia resultant angiogenic growth factors [9].

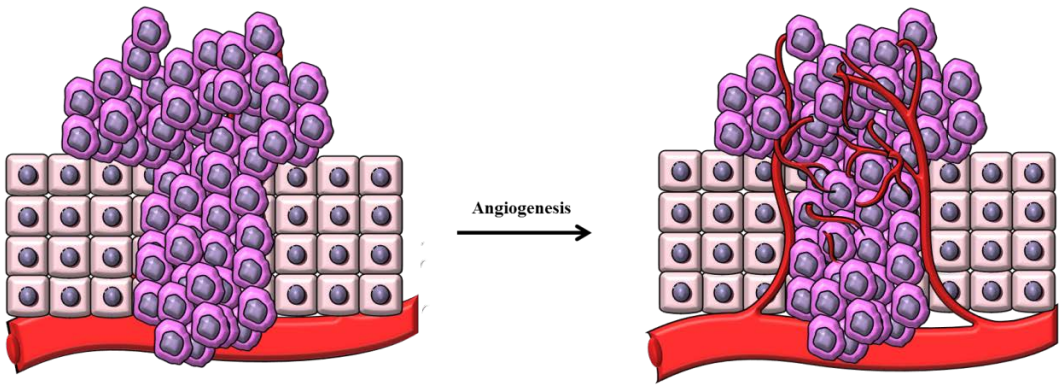

Figure 1.2. General scheme of angiogenesis process.

Among metastatic cancers, the most encountered type is metastatic bone cancer (Figure 1.3). Bone metastases are routine problems of cancer and common in 65-80% of patients with prostate and breast cancer. Although primary bone cancer is seen rarely, for patients with other tumors, metastatic cells spread to bone preferentially. This is because assorted hallmarks of the bone marrow such as well vascularized structure, may give reason for attraction of tumor cells [10, 11].

Current chemotherapy methods have problems associated with poor water solubility, rapid clearance from metabolism and uncontrolled drug release [12]. In this regard, to overcome all these complications, smart nanocarriers have been designing by researchers. According to this approach, drug is attached to polymeric scaffold *via* biological sensitive linker and hydrophilic polymeric backbone is used as a vehicle. These polymeric structures may include linear polymer-drug conjugates, polymeric micelles, dendrimers, liposomes, quantum dots and nanoparticles [13]. (Figure 1.3).

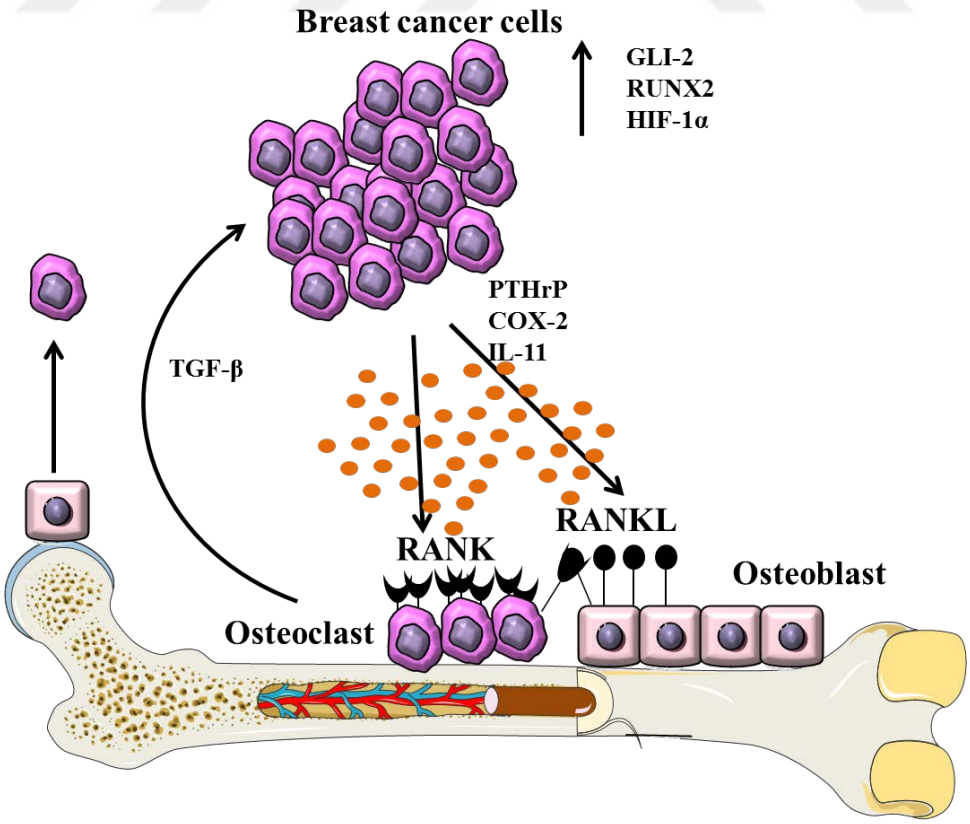

Figure 1.3. Vicious cycle of bone metastases of breast cancer cells.

1.2. EPR Effect

Generally ignored property of conjugated polymeric systems is their poor selectivity and random distribution within body. In addition to that, arriving of low percentage of drug to tumor location is a big challenge due to reaching the tumor tissue may not be sufficient as a result of rapid clearance from body. To point out all these drawbacks, passive targeting in other words the enhanced permeability and retention (EPR) effect is explored as milestone in cancer treatment researches [14]. EPR effect is well-known phenomenon of tumors in terms of their physiologic and anatomic features when compared to healthy tissue and it is considered when tumor tissues exhibit specific extravasation and retention of macromolecules.

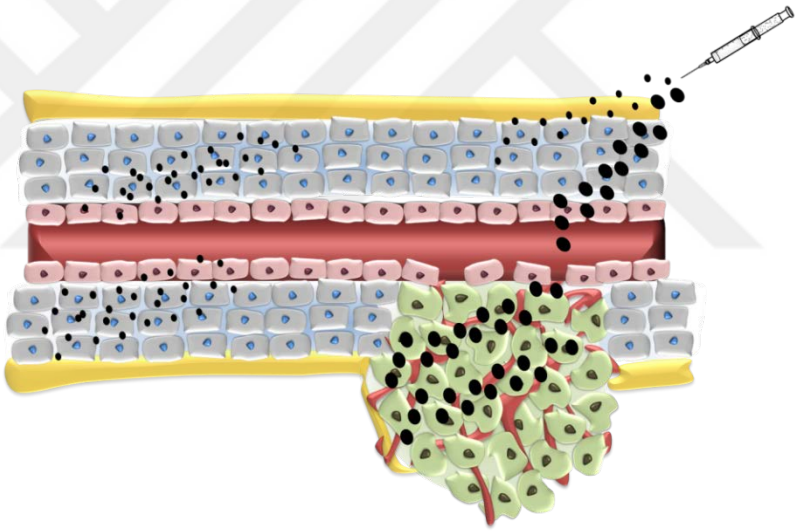

Figure 1.4. Schematic Illustration of EPR effect.

In 1986, Matsumuda and Maeda were the first researches that have mentioned about EPR effect [15]. They showed deficiency of blood vessels on tumor tissue. As a result of this fact, production of vascular permeability factors reaches the highest point. Enhanced vascular permeability is encountered almost in most of the tumors. That complication causes transporting of nutrients and oxygen to tumor in sufficient manner results in rapid tumor growth. Large macromolecules can accumulate in tumor tissues due to their big sizes and they can’t leak out from tumor vessel rapidly because of abnormal excretory system in

tumor. However, such big macromolecules can't penetrate normal tissue because of well-ordered and tight constitution in healthy tissues.

Different from macromolecules, low molecular weight chemotherapy agents cannot be hold in tumor because of their rapid clearance from system (Figure 1.4). This exclusive occurrence in tumor is utilized as notable principle in targeted drug delivery systems. EPR based tumor targeting systems are generally expected to be drug attached macromolecules to have long circulating time for accumulation in targeted region and release its drug in required time. The best way of keeping drug in the blood flow long enough is attaching them to water soluble polymeric structures.

1.3. Polymer-Drug Conjugates

The first opinion of polymer drug conjugate in which therapeutic agent was covalently linked to polymeric structure emerged in 1960's. Jatkewitz and co-workers designed a poly(vinyl pyrrolidone) polymer and attached mescaline *via* dipeptide spacer in 1955 [16]. Just before 1970's, Ringsdorf developed more complex polymer drug conjugates models [17]. As reported by Ringsdorf, optimal polymer drug conjugates should have biocompatible backbone and therapeutic agents should attach the polymer scaffold *via* biologically sensitive linkers. Then in the recent past, polymer drug conjugates gained much attention by researchers. Due to poor water solubility of chemotherapy agents, hydrophilic polymer backbones have been used to change characteristics of drugs. By using this strategy, hydrophobic drugs were acquired water solubility, specific accumulation in tumor, extended half-life in plasma and triggered release profile. For obtaining ideal polymer-drug conjugates, some key factors should be considered such as molecular weight, characteristic of polymer backbone, conjugation type of drug and sort of linker. As next steps, administration and dose amounts of polymer drug conjugations should be planned.

Polyethylene glycol (PEG) is one of the most widely investigated synthetic polymer, which is highly water soluble, biocompatible and commercially available. The most common and known structure of PEG is ending with hydroxyl groups. At the beginning, PEG was used as altering proteins and peptides. Then, PEG was attached to small molecules

covalently such as drugs and targeting groups to overcome non-specific biodistribution of small molecules and poor water solubility. Chemical structure, steric hindrances and molecular weights of the conjugated molecules play leading role for successful conjugation to PEG molecule. On the other hand, since PEG has just two functional terminal groups, drug payload in PEG backbone was highly limited. To accomplish this problem, multiarmed, forked and branched PEG structures as well as modified PEG molecules were developed [18]–[20]. In the last decades, promising results have been obtained with several PEGylated structures. Oncaspar®, that is used for leukemia has been evaluated and just approved clinically and in 2006, FDA approved Oncaspar® for the first-line analysis on leukemia patients. Opaxio is obtained *via* conjugation of PLGA and paclitaxel and it is also in the clinical trials for both lung and ovarian cancer.

Acrylated polymer drug conjugates are prepared by copolymerization of two or more different monomers *via* radical polymerization. For this purpose, specific monomers are used for controlling the facilities of the end product. Alkenyl polymer conjugates can be attached with different groups such as targeting moieties, drugs, dyes. Among these structures, copolymers may have high drug content in the polymer scaffold because of reactive pendant groups. In recent years, attachment of drugs to copolymers *via* covalent bond such as poly[N-(2-hydroxypropyl) methacrylamide] (PHPMA), poly(vinyl alcohol) (PVA) and poly(2-hydroxyethyl methacrylate) (PHEMA) has been studied by many researchers. All over these copolymers, HPMA backbone-based copolymers gained much more attention. In 1979, Kopecek and co-workers published a study about HPMA copolymer-drug conjugation [21]. In another study, enzymatically cleavable tetra peptide spacer Gly-Phe-Leu-Gly (GFLG) was utilized for conjugation of chemotherapy drug Doxorubicin to HPMA polymer backbone [22]. However, researchers considered the importance of molecular weight, size and shape of the copolymers to be sure about long circulation in the blood stream, renal elimination and nonbiodegradability in the body [23]. Researchers also explored that, the highly branched star polymer with doxorubicin GFLG conjugate showed more efficient tumor accumulation and slower renal filtration when compared to linear structure and free drug [24]. As a subsequent study, it was claimed that increasing of molecular weight of the polymer within limits, can be effective on inhibiting tumor growth. On the other hand, more increased Mw didn’t give effective responses [25]. In 2001, also the first studies about combinations of drugs came in to the cancer research area.

Kopecek and his colleagues synthesized copolymer bearing Doxorubicin and Mesochlorin e6 which is photoactivable agent and they proved the enhanced activity of the combination against each drug alone [26]. Another study on drug combination therapy was carried out by Greco and Vincent, in 2005. They showed improved effect of HPMA polymer attached with Doxorubicin and Aminoglutethimide (AMG) which is aromatase inhibitor used for endocrine diseases [27]. As different chemotherapy agent Paclitaxel (PTX) was combined with carboplatin for breast cancer [28] and vinorelbine for non-small cell lung cancer (NSCLC) [29]. In addition to these studies, Phase II trials were completed with 5-Fluorouracil (5-FU), cisplatin and fulminic acid combinations with Paclitaxel for gastric cancer patients [30]. The other important combination study was carried out by Ulbrich and his collaborators. They designed HPMA copolymer carrying both Dexamethasone as antiflammatory agent (DEX) and Doxorubicin resulted with indicating improved activity of combination [31]. The same group published other study about combination therapy in which HPMA polymer conjugated with Doxorubicin and Gemcitabine (GEM). The presence of these two drugs on one macromolecule improved angiogenesis inhibition capacity of molecule when compared to each drugs a lone. Furthermore, polymer that carries both drugs induced apoptosis more than one drug containing polymer [32]. Among drug carriers, polysaccharides have important and crucial role for development of cancer treatments. Owing to their high biocompatibility and biodegradability, they are preferred by researchers mostly against synthetic polymers for medical applications. Hyaluronic acid (HA) which can be used as targeting group, is one of the most known anionic biopolymers. It has high binding affinity through the CD44 cell surface adhesion receptor that has overexpression on many cancer cells. As a result, HA and drug combinations are expected to enhance cellular uptake and long-acting delivery of drug [33]. There are many studies on combination therapy of HA and chemotherapy drugs such as paclitaxel [34] and doxorubicin [35]. One more polysaccharide for drug delivery is Chitosan. Chemotherapy agents that are combined with chitosan can be counted as atorvastatin [36], salicylic acid [37] and stavudine [38]. Although heparin is known as anticoagulant, sometimes it is applied for drug conjugations. As drug carrier, heparin may have some drawbacks because of its anticoagulant activity which is not tolerable in cancer treatment. But by increasing drug content in the polymer may reduce the anticoagulant activity of heparin to ignorable degree. As a result, in cancer treatments, heparin is not most-preferred drug carrier because of its hemorrhagic complication risk [39]. Like heparin, dextran showed insufficient responses in cancer treatments.

Primally, dextran was considered to be appropriate choice for drug delivery applications because of its plasma expanding ability, but then it is proved that it showed high toxicity in Phase I clinical trials [40, 41]. For Phase II clinical trials, β-cyclodextrin was applied for non-small lung cancer patients. In this study, Camptothesin (CRLX101) was used as chemotherapy agent [42]. After that, conjugation of β-cyclodextrin to linear polymers in wire form has gained much attention. Thus, high amounts of drugs can be conjugated to potential functional hydroxyl groups on the backbone [43]. In the meantime, cellulose [44], pullulan [45] and pectin [46] are used as drug carrier polysaccharides.

Group of poly(aminoacid) based drug carriers may include poly(l-lysine) (PLL), poly(aspartic acid) (PAA) and poly(-glutamic acid) (PGA) because of their biodegradability and biocompatibility in the body. It was mainly encountered that, PEGylation method was used for modifying PLL as a drug carrier [47]. By utilizing from this method, tumor accumulation was improved. On the other hand, PAA based copolymers were used for bone targeted drug delivery area due to their high binding affinity to bone mineral hydroxyapatite [48]. In addition to all these poly(aminoacid) drug carriers, the most applied macromolecular structure is PGA. Drug conjugation is achieved *via* γ-carboxyl groups on PGA molecule. PGA can be taken in to cancer cell and release its drug although it biodegrades before delivery to tumor. It is crucial factor for PGA to have important role in drug delivery platform [49]. In Phase III clinical trials, PGA-paclitaxel (Opaxio^{TM}) and PGA-camptothecin were tested. According to results, PGA-paclitaxel was more effective on women when compared to men. That gender dependent results were attributed to estrogen level which triggers paclitaxel release [50]. For more effective drug delivery system, cyclic arginine-glycine-aspartic acid (cRGDfK) were added to PGA-paclitaxel conjugation to target $\alpha_v\beta_3$ receptor which has overexpression on various cancer types. As a consequence, enhanced tumor accumulation and less toxicity than free drug was obtained [51]. Dendrimers are three dimensional macromolecules that can be constructed with central core, narrow polydispersity index, good control over structure (Figure 1.5). Dendrimers have multiple functional groups at the periphery that provides drug conjugation in high content [52]. Among dendrimer molecules, poly(amidoamine) (PAMAM) dendrimers have gained much more attention in drug delivery researches. Due to chemotherapy drugs have poor solubility in water, some researchers studied on conjugation of drugs to PAMAM dendrimers.

Thomas *et al*. conjugated to antibodies on PAMAM dendrimer with imaging agent to explore affinity of structures to antigen-expressing cells [53]. In 2012, Yan li and co-workers used 4th generation of PEGylated PAMAM dendrimer to conjugate Doxorubicin on it. Nevermore, transferrin and tamoxifen molecules were linked to dendrimer for dual targeting to brain glioma [54]. One of the most important studies was folate conjugated dendrimers. In the study, folic acid was conjugated to PAMAM dendrimer since folate has overexpression in some cancer types such as breast and ovarian cancers. In addition to folic acid as a targeting group, methotrexate (MTX) was also conjugated to dendrimer to observe tumor accumulation differences between targeted and nontargeted structures [55]. On the other hand, dendrimer molecules gave opportunity for intranasal or intravaginal drug administration unlike classical intravenous ways [56].

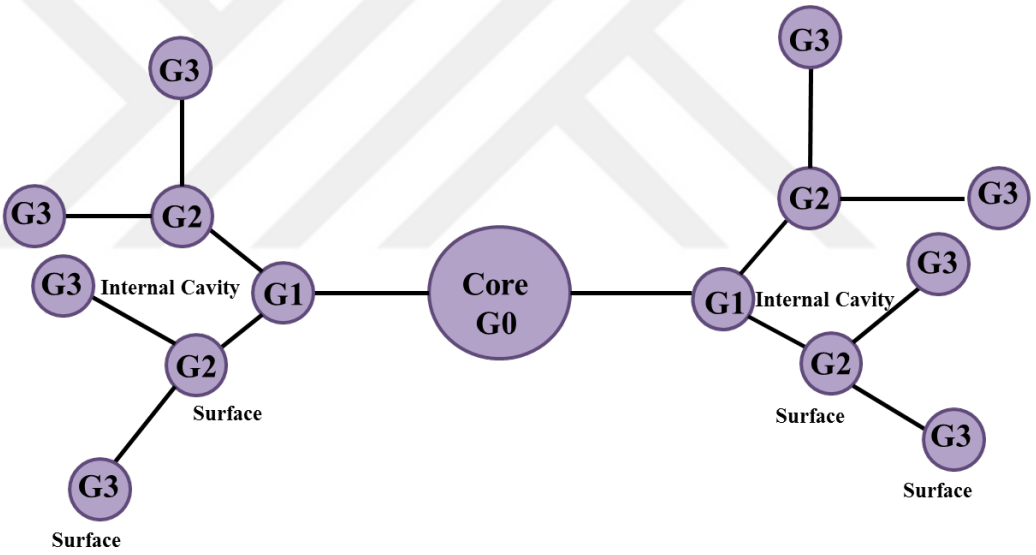

Figure 1.5. General illustration of dendrimeric structure.

1.4. Combination Drug Delivery Systems

There is enormous effort in improvement of drug delivery systems for increasing their therapeutic profiles and decreasing their side effects and toxicities. However, some diseases, especially cancer, has complex morphology and development process which makes it so difficult to diagnose, treat and end up. That’s why, combination therapy that refers

administration of two or more drugs simultaneously or at the same time for treatment of cancer has gained great attention in recent years. Different from mono-drug administration, multi-drug therapy can provide both enhanced therapeutic effect and accomplishment for complex mechanisms of drug resistance [57]. AIDS, malaria and cancer are the most known diseases that can be treated by using combination therapy. In 1999, three or four anti-HIV drugs were combined for treatment of HIV, namely the highly active antiretroviral therapy (HAART) at first time [58]. As for malaria disease, anti-malaria drugs are so resistant to malarian parasites which are mutated as a result of selection and dissemination. Thus, combination therapy for malaria is being used as first treatment method that is coming to mind [59]. Combined drug administration ideas also have promising studies on multiple sclerosis (MS) patients who have relapsing-remitting process. Mount Sinai School of Medicine (CombiRx) has been investigating utility of interferon-beta-1α (Avonex, Rebif®) and glatiramer acetate (Copaxone®) combinations. Another application of drug combination study has been proceeding on diabetics in which glucagon-like peptide-1 (GLP-1) and gastrin were combined. In that study, diabetic NOD mice were treated with drug combination and regulated glycemic levels were achieved [60]. Combination therapy is a widely encountered strategy on cancer treatment at most. As it is known well, cancer therapies have several side effects. However, combined drug administration may enhance therapeutic efficacy of drugs although they have different cytotoxicity profiles of each. In other words, whereas almost each of cancer drugs are highly toxic alone, combining drug treatment can provide better results and decreased cytotoxicity profiles [61]. There are several types of combination therapy such as based on small molecules, monoclonal antibodies and polymer-drug conjugates. In this thesis, we are focusing on polymer drug conjugate-based combination therapy. As mentioned before, polymer drug conjugate platform is an increasing trend for the current decades. Especially, mono-drug carrying polymers draw attention to their clinical trials, thereby their studies and applications have been extended to design of multi-drug carrying nanostructures [62]. The concept of polymer drug conjugation systems for combination therapy may include several types such as polymer drug conjugate and free drug, two different polymer drug conjugates, one polymeric carrier containing two different drugs and polymer drug conjugate with polymer enzyme conjugate in which enzyme conjugate is responsible for releasing drug. Schematic illustrations of mentioned types were shown in Figure 1.6.

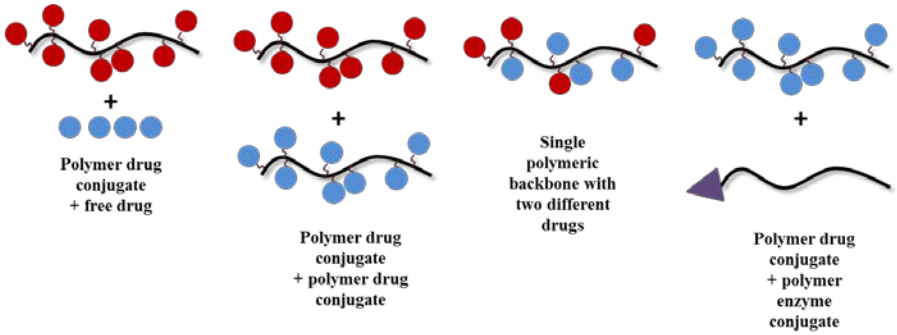

Figure 1.6. Polymer based combination therapies.

Over the past decades, polymer-drug conjugation systems have emerged as encouraging idea to drug delivery area since they contain targeting groups, imaging agents etc. Despite all studies, there are just few embodies of two or more drug combinations with single polymeric backbone. The first example of this combination type was done by using HPMA as a polymeric carrier. Aminoglutethimide (AGM) which is used for endocrine therapy and chemotherapy agent doxorubicin were attached to HPMA backbone [27]. Both drugs were attached to polymer *via* peptidyl linker that can be cleaved in lysosome of cells. According to obtained *in vitro* results on breast cancer cells, single polymer carrying both two drugs was more efficient than two polymer drug conjugate combination that were attached with drugs separately [63]. Another promising study of combination therapy is achieved by using PEG to attach drug Epirubicin (EPI) and Nitroxide (NO) that enables cells to communicate with each other throughout the body. Due to increasing loading capacity of the PEG, researchers designed a dendrimeric structure of PEG for obtaining two chemically available conjugation sites at terminus. However, EPI and NO didn't exhibit synergistic effect and caused cardiotoxicity indeed [64]. In case of using single chain for conjugation of both drugs, showed better anti-cancer activity because of providing same body distribution to polymer conjugate and less cardiotoxicity was achieved [65]. Satchi Fainaro and her crew performed a pioneering study on polymer drug conjugate with antiangiogenic drug TNP-470 (Caplostatin) which is being developed as clinically by SynDevRx, Inc [66]. After obtaining compelling results on different tumor models such as melanoma, colon and prostate cancers, they developed their design by attaching another agent Alendronate to their polymer. Alendronate is not only pharmacologically active agent for osteoporosis and some bone diseases, but also used for targeting moiety [67]. According to *in vivo* results on human osteosarcoma tumor model, complete tumor regression was observed, thus combination of

TNP-470 and alendronate is approved as anti-angiogenic and anti-tumor effective chemotherapy agent. As a latter study, HPMA based combination study was performed again by the same group, this time conjugated chemotherapy drug was paclitaxel instead of TNP-470 [68]. Enhanced anti-angiogenic effect on bone tissue which was metastasized from prostate and breast cancer tissue was achieved. In the later years, different versions of HPMA based copolymers emerged in combination therapies platform. Gemcitabine (GEM) and doxorubicin containing HPMA copolymer was confirmed as good carrier for delivery of two drugs to the desired tumor region [32]. When compared to controls and free drugs, both two drugs bearing copolymer was more effective to rat tumor model. Additionally, that conjugate displayed anti-angiogenic properties on tumor and cell apoptosis was induced more effectively. In case of anti-inflammatory agent dexamethasone (DEX) and doxorubicin conjugated copolymer, researchers compared activities of free drugs of each and copolymer. Consequently, it was determined that using polymer drug conjugate is more beneficial in terms of therapeutic index [69].

1.5. Diagnosis in Cancer and Drug Delivery Systems

Diagnosis, especially in cancer research area, means process of discovering the presence of tumor. That process also includes identifying tumor type, size, location and stage [70]. In cancer treatments, early diagnosis is very important and crucial for patient survival because if precancerous changes in the body is detected, cancer can be treated before it becomes malignant. For cancer detection, determination of markers in body fluid is one of the most applied methods [71]. Among them all, nanostructures can be used for tumor cell detection *in vitro* and *in vivo* right along with their drug delivery applications. If therapeutic and diagnostic agents are conjugated in single molecule, it is called as theranostic agents (Figure 1.7). Dendrimers, polymers, proteins and inorganic compounds are generally applied structures for designing theranostic agents [72, 73]. The most important feature of theranostic nanostructures is their localization and accumulation capability in diseased tissues than healthy tissues due to EPR effect. Especially, polymer based theranostic agents can be obtained by loading hydrophobic dyes in the inner core of self-assembled amphiphilic polymers.

Additionally, functionalization of polymer surfaces with dye and targeting agents can be regarded as other option for theranostic agent preparation [74]. The most common imaging technique is magnetic resonance imaging (MRI). In this technique, magnetic field is used and in cancer tissue hydrogen atoms are excited by finding applicable resonant frequency. Hydrogen atoms of each tissue have their own relaxation times, because of this phenomenon, contrast is created between different tissues.

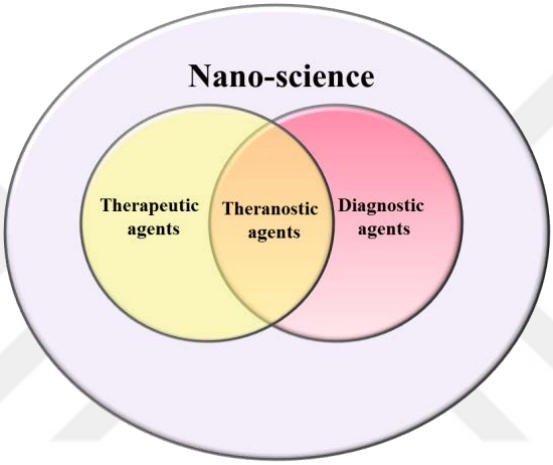

Figure 1.7. Combination of therapeutic and diagnostic agents.

For MRI applications, super paramagnetic iron-oxide (SPIO) and gadolinium (Gd) metals are mostly used examples. In one example, maleimide−PEG−poly(lactic acid) amphiphilic block copolymer was self-assembled and nanoparticle was obtained. Maleimide functional groups were attached on the surface for targeting group attachment. This prepared nanoparticle was loaded with both drug DOX and SPIO for tracking the conjugate in the body and determining tumor accumulation and penetration [75]. Similar to this study, poly(lactic-*co*-glycolic acid) (PLGA) was utilized for obtaining nanoparticle. This time, docetaxel and SPIO was encapsulated in to self-assembled structure that was obtained strong contrast with [76]. PLGA-PEG block copolymer was used in other research by Yang in which DOX and $MnFe_2O_4$ was loaded. Breast cancer targeted nanoparticle was detected by MRI in tumor tissue very sensitively [77].

Another imaging agent used for MRI is gadolinium that is applied by loading it in to special ligands. These ligands embody may include diethylenetriaminepentaacetic acid (DTPA) and tetraazacyclododecanetetraacetic acid (DOTA). In one study, Gd loaded DOTA was attached to side chains of PGA polymer and MRI signal was investigated on breast cancer tumor tissue [78]. By using hydrophobic PLGA core, liposome shell was designed also. For targeting desired region, liposome shell was prepared by using folate coated Gd-DTPA. On the other hand PEGylation method was used to obtain hydrophilicity and effective DOX loading was achieved [79]. For utilization from polymers as theranostic agents by using MRI and targeted drug delivery, HPMA backbone based copolymers [80] and multi-arm star block copolymers [81] are also applied.

By administration of some radioisotopes such as ^{76}Br, ^{99}mTc, ^{64}Cu, ^{90}Y intravenously or orally, radionuclide imaging can be benefited from. Unlike MRI, radionuclide imaging is more likely about discovering the stage of disease by using cellular metabolism. In one of the most important examples, HPMA polymeric carrier was conjugated to ^{90}Y and ^{99}mTc both, as well as RGD4C. As a result, enhanced cell internalization on endothelial cells was observed. In case of tumor studies that are carried on SCID mouse xenograft model of human prostate carcinoma, tumor growth retaining results were satisfying [82]. Lammers and his co-workers studied on ^{131}I loaded HPMA polymeric carrier which is also conjugated with DOX or/and gemcitabine (GEM). This study is considered as one of the most challenging works due to hosting both combined drug therapy and radionuclide imaging [83].

As for the fluorescence imaging method that we also used in our study is applied in various fields like biology, biochemistry and engineering. Most of the natural molecules like aminoacids and lipids may fluoresce when they are exposed to UV-vis light [84]. The most advantageous aspect of this method is its low cost. In the UV-near infrared (NIR) wavelength range, fluorescence imaging is as sensitive as radioisotopes used in positron emission tomography (PET) and single-photon emission computed tomography (SPECT). In 2010, folate targeted and indocyanine-green coated nanoparticles were prepared for examining cell uptake and therapeutic index of molecule on different cancer cells [85]. By using again, the same dye, Nile red was also encapsulated in to dendritic-core multi-shell nanoparticle. This nanoparticle was loaded with three different drugs which are DOX, methotrexate and sodium ibandronate. After 6 hours of administration of nanoparticle, sensitive contrast was observed

within tumor tissues in F9 teratocarcinoma bearing mice [86]. In other study, DOX-conjugated monomethoxy PEG block-poly(L-lactide-co-mercaptoethanol) copolymer, rhodamine B-conjugated mPEG-b-p(LA-co-ME), and folic acid conjugated PEG-b-PLA copolymers were self-assembled to get multifunctional micelles. Those micelles were loaded with fluorescence imaging and targeting moiety as well. As expected, targeted micelles were accumulated in hepatocarcinoma tumor tissue better than free drug and non-targeted version of micelle [87]. With all these studies mentioned above, some compelling works on quantum dots (QDs) based theranostic agents were also performed [88]. On the other hand, there are some researches on natural polymer-based and fluorescent agent containing theranostic systems. One of them is achieved by using chitosan as colloidal polymeric carrier. According to results, 2 hours later from injection of fluorescent chitosan carrier to breast cancer and lung cancer cells, more than 80% of breast cancer cells and 100% of lung cancer cells exhibited fluorescent features [89].

1.6. Active Targeting and Effects of Targeting Groups in Polymer Molecules

Active targeting is utilizing affinity of conjugated targeting moieties or special ligands to targeted tissue or cells for enhanced delivery system (Figure 1.8). Targeting groups can be regarded as crucial for mechanism of cellular uptake. While EPR effect enhances the transport of polymeric structures to tumor site through long circulation time, the attached targeting molecule improves endocytosis of macromolecules. Detection of targeting group by its target substrate is fundamental consideration for cellular uptake. Ideal targeting groups may include proteins, antibodies, nucleic acids. However, sugars, lipids and proteins which are overexpressed on diseased tissue can be shown as examples of targeted molecules [90, 91].

Binding ability of targeting systems depend on two mainly attitudes: transfer capacity and targeting selectivity. Transfer ability of macromolecule to targeted tissue has connection with structure of polymer. On the other hand, targeting selectivity is directly related to biodistribution of targeting group conjugated polymer. In addition to that, it is very important to determine if targeting groups have any interaction with off-target molecules or cells in the body.

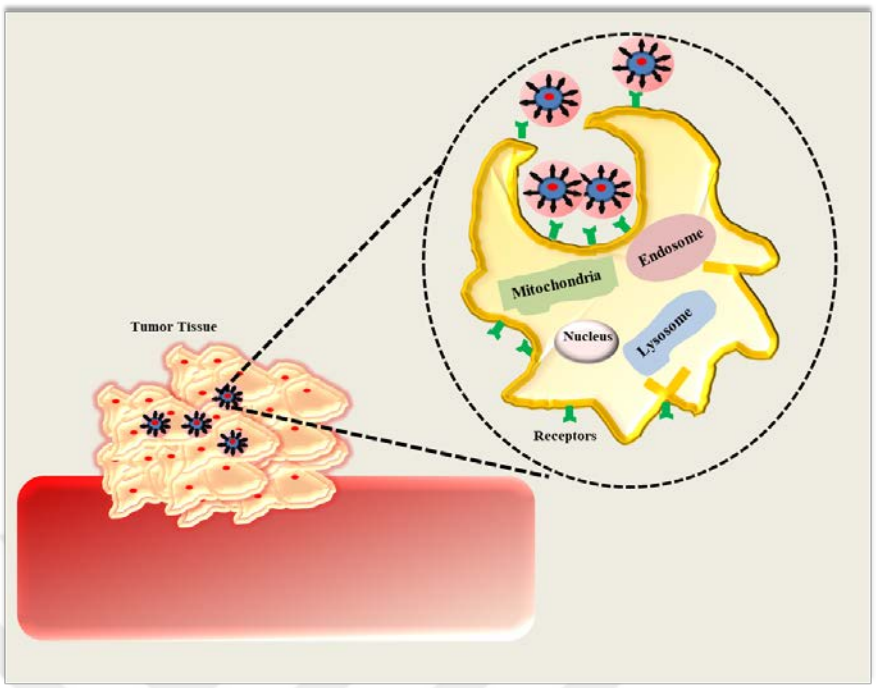

Figure 1.8. Schematic Illustration of Active Targeting.

For effective active targeting system, targeting group attached polymer requires to be in the close area with targeted molecule. Due to blood flow in the immune system organs is low, affinity of polymers for the targeted molecules can't compete with systemic clearance of body [92]. Consequently, polymers with targeting groups need comprehensive blood circulation time. Because of targeting ligands are in the extravascular region of tumors, polymeric structures need to apply EPR effect to interact with their targeting ligands. That phenomenon is replying the question for why blood circulation time of polymers should be adjusted to get ideal interaction between targeted and targeting groups.

Bisphosphonate (BP) molecules are the counterpart of naturally occurring structures pyrophosphates and they are the most effective antiresorptive drug for treatment of osteoporosis, bone metastases and Paget's disease. Nevermore, BP structures have high binding affinity to Hydroxylapatite (HA) mineral which is naturally exists in the bone tissue. BP structures may include Alendronate, Zoledronate, Ibandronate and Eridronate. BP molecules have other assistant groups (R^1 and R^2) on their geminal carbons as well (Figure 1.9).

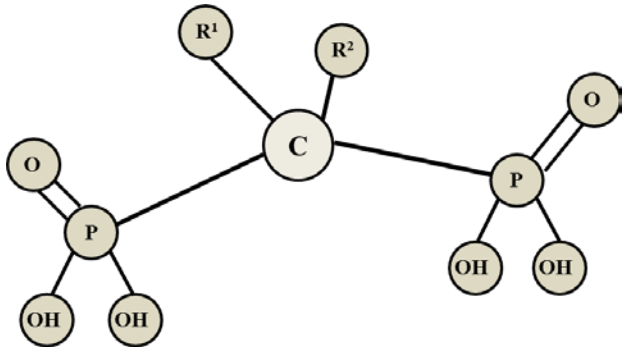

Figure 1.9. General Scheme of Bisphosphonate Molecules.

These substituents enhance bone seeking ability of BP and increases the affinity of BP to bone. In addition, octapeptides, aspartic acid and tetracycline molecules are the well-known bone targeting moieties. By modification of R^1 and R^2 groups on the BP, affinity of BP to bone can be arranged. For all these reasons, BP molecules have emerged in cancer research area for advanced bone metastases and skeleton complications. Due to BP molecules are water soluble and they have acidic character, they distribute in the body insufficiently. Hence, they excrete from body through urinary system mainly. BPs have a half-life of several months because P-C-P bond in structure is highly stable which provides long remaining period for molecule. BP molecules are one of the most applied structures among bone targeting moieties so that there are lots of studies have been done to find out binding ability of these structures to the HA.

In 2006, Ulbrich and co-workers studied on whether the number of targeting moieties on polymer effects the adsorption rate of polymer or not. As a result, authors discovered that there must be multiple targeting ligand on polymer to be sure at least one targeting moiety is exposed to HA. The research on BP molecules as targeting groups have started for few decades. In the same research, authors designed a novel drug delivery system that contains biocompatible *N*-(2-hydroxypropyl)methacrylamide (HPMA) copolymer as polymer backbone and hydroxy bisphosphonate as a targeting moiety. Additionally, these polymer conjugates are also attached with radiotherapeutics ^{125}I, ^{111}In and Doxorubicin as anti-cancer drug. For that purpose, monomers bearing reactive TT groups were selected for supplying the attachment of drug and L-tyrosine amide. These reactive TT group containing polymers were functionalized with corresponding amine groups of Doxorubicin, L-Tyrosine and

bisphosphonate groups *via* aminolysis reaction. On the other hand, to investigate the rate of Doxorubicin release from the polymer, two different copolymers with different spacers were prepared. GFLG which is a peptide with four aminoacids enabled polymer to release doxorubicin enzymatically with the help of Cathepsin B [93]. In the next study, Kopecek and co-workers utilized the same polymer backbone as a polymeric carrier to synthesize another HPMA copolymer and bisphosphonate containing drug delivery system [94]. The process of synthesizing these polymers with different molecular weight, contains the attachment of Alendronate, L-tyrosine and FITC to HPMA polymer precursor which was obtained by using RAFT polymerization technique. Like in previous work, side chains of polymer were terminated in reactive TT groups for attachment of Alendronate which has NH_2 group. As a result of reaction, polymers that have bone targeting moiety, dye and monomer which was going to be radiolabeled with ^{125}I was synthesized. In this study, researchers wanted to explore the correlation between molecular weight of polymers and alendronate content. Among low molecular weight polymers, the highest binding capacity was obtained with high content alendronate containing conjugate. On the other hand, if the high molecular weight conjugates were considered closely, binding capacities of polymers don't depend on alendronate content. For bone accumulation, all alendronate containing conjugates were deposited in bone more than non-targeted control polymers. The elimination of conjugates from the body was evaluated after intravenous administration. According to results, in low molecular weight polymers, short elimination time was observed, whereas high molecular weight polymers cleared from the body in longer time.

Another HPMA based Alendronate containing copolymer-drug conjugation system has been reported by Satchi-Fainaro and co-workers in 2009 [95]. In this study, copolymer which was conjugated with Alendronate as a targeting moiety and Paclitaxel as an anti-angiogenic drug, was produced. Paclitaxel is one of the most known and effective drugs in widespread clinical use. Despite it has prominently been used for curing cancer in industry, it has various side effects like in other chemotherapy drugs. Therefore, paclitaxel exhibits dose-limiting toxicities. Because of all these reasons, researchers have been developed a new and elegant strategy to target bone metastasis by attaching Paclitaxel to macromolecule. By doing this, it was aimed to benefit from EPR effect and also targeting potential of Alendronate that was also attached to macromolecule.

Paclitaxel was attached to macromolecule after two steps in which via FK-PABC linker. After that, it was conjugated to HPMA-ONp copolymer. This dipeptide PABC linker gives a stability to molecule by the carbonate linkage. For demonstration of PTX release from conjugate via cleavage with lysosomal enzyme cathepsin B, HPMA copolymer-GGGG-PTX conjugate that contains non-cleavable GGGG linker and HPMA copolymer-GGFK-PTX conjugate that contains cleavable GGFK linker were also prepared. On the other hand, Alendronate moieties were attached to polymer *via* functional –ONp groups. As a result, of 10% mole ONp groups, 2.5% mole were bound to Alendronate and 4% mole were bound to PTX. By treating HPMA-GGFK-PTX conjugate with Cathepsin B enzyme, release of PTX amount was higher. In 2011, Ronit Satchi-Fainaro and co-workers published another follow up study that they published in 2009 [96]. In addition to their previous research, proliferation assays of the human MDA-MB-231 and murine 4T1 mammary adenocarcinoma cancer cells, CEC and CEP cell levels, white blood and red blood cell assays were achieved as *in vitro* studies. Furthermore, anti-tumor efficacy and toxicity profiles of conjugates in mice bearing 4T1-mCherry murine mammary adenocarcinoma were done as *in vivo* studies.

Another example of utilization of the bisphosphonate targeted drug delivery systems, was reported by the same group in 2009 [68]. HPMA based copolymers were synthesized by using Reversible addition- fragmentation chain transfer (RAFT) polymerization technique. Different from the study mentioned above, TNP-470 was used as anti-angiogenic drug, instead of Paclitaxel. TNP-470 and Alendronate were attached to copolymer through Gly-Gly-Pro-Nle, Cathepsin K cleavable linker. FITC labeled monomer was also used for obtaining enhanced visibility. The major purpose of the study is to get noticed novelty and importance of combined therapy of HPMA copolymer-ALN-TNP-470 conjugate. Because over the past few decades, combination therapy has gained much attention among researchers. It was also claimed that, using multiple drug may enhance anti-tumor efficacy by acting in different mechanisms. In that study, the first step was conjugation of Alendronate and TNP-470 to copolymer. After conjugation, as i*n vitro* studies, inhibitory effects of both Alendronate and TNP-470 on HUVECs, Saos-2, and MG-63-RAS cells, internalization tests on HUVECs and Saos-2 cells were investigated. Addition to *in vitro* experiments, *in vivo* studies on SCID mice bearing MG-63-RAS human osteosarcoma were also carried out.

In a subsequent study, the same group reported a follow up paper which is about HPMA based copolymer-drug conjugation system and also contains MA-Tyr monomer that can be radiolabeled [97]. In addition to experiments that was told in previous work, red blood cell and white blood cell assays, CEC and CEP measurements were achieved. The proliferation inhibitory effect of conjugate on K7M2 murine osteosarcoma cell was studied. Like in previous study, Alendronate containing monomer was synthesized by using Solid Phase Peptide Synthesis method and conjugated to monomer via TT reactive group. TNP-470 was attached to polymer with the help of amine group on the polymer. (Gly-Gly-Pro-Nle-NH_2). For polymerization reaction via RAFT technique, MA-FITC and MA-Tyr monomers were also prepared. In vitro cell growth inhibition of free TNP-470, Alendronate and ALN-TNP-470 were evaluated on K7M2 murine osteosarcoma cells. The *in vitro* results demonstrated that both free and conjugated ALN-TNP-470 inhibited cell proliferation at IC_{50} of 10 μM. One of the most recent studies about bisphosphonate targeted drug delivery is published by Ronit Satchi-Fainaro and co-workers again in 2015 [98]. Different from other studies mentioned above, herein targeting agent Alendronate and anti-mimotic drug Paclitaxel were covalently attached to Pullulan, which is natural polysaccharide derivative polymer. While Paclitaxel was bound to Pullulan, through Cathepsin K-sensitive tetra peptide spacer GlyGlyProNle, Alendronate was bound through PEG spacer. Bioconjugates are challenging structures for utilizing drug delivery researches. The obtained bioconjugate Pull-(GGPNle-φ-PTX)-(PEG-ALN) has been designed to enhance the delivery of Paclitaxel to tumor tissue actively. The main idea of the study is to synthesize a colloidal polymer which has polysaccharide-based backbone and to attach bisphosphonate and drug for treatment of breast cancer with bone metastasis. After synthesis of the structure, biological experiments were performed routinely. HA binding test was performed in two manner. At different pH values, Alendronate hasn't showed specific binding ability to HA, whereas binding property of Pull-(GGPNle-φ-PTX)-(PEG-ALN) conjugate was pH dependent. After 5 minutes, 72% of free Alendronate was bound to HA. At the end of the 3 hours, the percent value was 80%.

On the other hand, Pull-(GGPNle-φ-PTX) -(PEG-ALN) conjugate has showed 60% binding ability at pH 5.5. but at pH 7.4 binding percent was 40% respectively. Selective distribution of cancer drugs to desirable tissues or cells in the body is very crucial and important requirement in cancer treatment. Defining the physiological differences between

normal cells and tumor cells clearly, is the main need of sending chemotherapy drugs to desired sides with minimal harm to normal cells. Technologies about targeted delivery of cancer agents are being developed day by day due to minimize side effects and increase effects of drugs. In last decades, some types of targeting groups have been investigating by researchers such as anti-body or peptide mediated structures [99]. Among all targeting groups, the most encountered studies are about peptide conjugated macromolecules. Especially, integrins which are transmembrane receptors in the human body and have overexpression on cancer tissues make them promising targets for peptide conjugated structures in cancer treatments [100, 101]. After studies of Ruoslahti and Pierschbacher on peptides as targeting tools, RGD molecule has gained great attention with its capability of being recognized by $\alpha_v\beta_3$ integrin receptors on the cell surfaces [102]–[104]. Thus, that molecule with tripeptide sequence arginine, glycine and aspartic acid have been appeared in the cancer treatment and research area. One of the first studies about conjugation of RGD peptide to polymers was accomplished by Kawasaki, in 90's. PEG was used as macromolecule for enhancing blood circulation and eliminating adverse effects of drug in the body. According to their results, after co-injection of RGD conjugated PEG6k molecule to tumor tissue, [105] inhibition of lung metastasis on B16-BL6 melanoma mice was observed [106]. Other researcher Saiki advanced that former study by doing serial experiments and obtaining different RGD attached PEG molecules to see if anti-metastatic effect can be prolonged [107]. All these accomplished studies proved anti-invasive ability of RGD molecule for inhibiting metastasis of cancer. Komazawa designed a new compound which is poly(carboxyethylmethacrylamide) (CEMA) based and RXDS conjugated molecule where X is Glycine, Lysine or Isoleucine. This product was able to prevent metastasis on various mice models [108, 109]. While poly(CEMA)-RXDS conjugate decreases lung and liver metastasis on some tumor models, just poly(CEMA) and RXDS molecules didn't show noteworthy effects on same tumors. From here, with the same compound but by using chitin as a polymer backbone, RGD conjugates of polymers showed high anti-metastatic efficacy on same tumor models in independent administration times [110, 111]. In one study which was performed by Polyak and his crew [112], RGD and doxorubicin were conjugated to terminal end groups of bifunctional PEG chain *via* pH sensitive hydrazone linker. As reported by the researchers, targeted copolymer that was monitored through fluorescence imaging, accumulated in DA3 murine breast cancer tumor model. The same group sustained this study by synthesizing poly(α-L-glutamic acid) (PGA)

based paclitaxel attached macromolecule which has RGD as a targeting moiety [113]. Prepared conjugate that has RGD molecule and RAD molecule (as a control) on it showed encouraging results in the matter of their antiangiogenic performance and tumor accumulation ability. On the other hand, systematic toxicity was improved when compared to free drug paclitaxel. As for HPMA based backbone macromolecules, designing integrin targeted pHPMA based copolymers was pioneered by Wan *et al*.[66]. Studies that were done by using ECV304 endothelial cells for cell internalization and localization of conjugates showed enhanced uptake. As a latter study, Ray and his group synthesized pHPMA based copolymer that was conjugated with Docetaxel and RGD molecules [114]. The amount of targeting group was determined as ~5 %w/w and size of the molecule was 3 nm in diameter as well. However, the authors wanted to show difference of tumor accumulation behaviors between targeted and non-targeted versions of this copolymer. For this reason, another copolymer that has no targeting ligand on it but with high molecular weight (~7 nm in diameter) was prepared also. As a result, single dose of either compounds in DU145 prostate cancer xenograft model was acceptable for tumor accumulation and tumor size regression. In same year, same people proved that RGD bearing HPMA polymer showed 2-fold better tolerated dose in the same animal model when compared to non-targeted counterpart [115]. As regards biodistribution studies that were carried out by using ^{125}I radiolabeled copolymers, same profile with previous study was encountered. Tumor accumulation was 3-fold higher for the targeting group containing molecules [116].

Targeted drug delivery systems in which RGD was used as targeting moiety, are not only about linear polymers but also dendrimeric structures. One of the first studies of integrin targeted dendrimeric structure was reported by Shukla and his group in 2005 [117]. In their study, generation 5 PAMAM dendrimer bearing RGD was prepared to find out if the molecule can target and directly bind to $\alpha_v\beta_3$ integrin receptors [118]. Furthermore, PEG-PAMAM-cysaconityl-DOX and cRGDyC bearing PAMAM structure were constructed for evaluation of *in vivo* studies in orthotopic murine C6 glioma tumor model [119] and murine B16 melanoma tumor model [120]. To conclude, RGD modified copolymers exhibited better tumor accumulation and increased survival rates *in vivo*. The similar trend was followed by loading PAMAM-RGD conjugate on to poly(lactic-co-glycolic acid)-poly(lactic acid) (PLGA-PLA) implants in which intratumor drug accumulation and tumor regression were higher when compared to free drug Doxorubicin and non-targeted counterparts [121]. More

interestingly, same group proved that mesenchymal stem cells (MSCs) which have tumor targeting behavior, were providing similar tumor penetration, accumulation and survival rate with RGD conjugated compounds [122]. In very recent years, Xu *et al*. designed redox-responsive polymeric structure [123] that was combined with PEG block and GGRGD, with the size of lower than 70 nm in diameter. The studies that were done with HepG2 tumor bearing mice showed enhanced tumor accumulation and survival rates as against non-targeted structures.

1.7. Reactive Monomers and Post Polymerization Modification Strategies

Post polymerization modification (PPM), in other words post polymerization functionalization is well known phenomenon since polymer science studies have been started (Figure 1.10). In seventeenth century, various researches about PPM on natural polymers were done by chemists [124]. But then, due to PPM studies on natural polymers weren't recognized and applied well enough, some of the pioneers of the polymer chemistry started to apply PPM reactions on synthetic polymers. In 1948, Serniuk and co-workers conjugated butadiene polymers to thiols by using thiol-ene reaction [125]. Solid state peptide synthesis was brought in to polymer science research area by Meriffield [126]. On the other hand some preliminary studies on PPM reactions of epoxides [127] and halogenated polymers [128] were reported in later years.

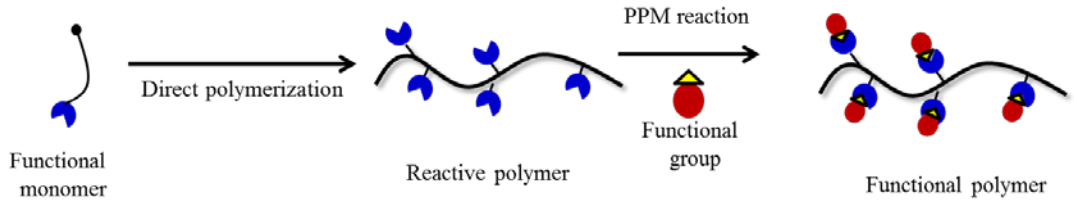

Figure 1.10. General strategy for PPM reactions.

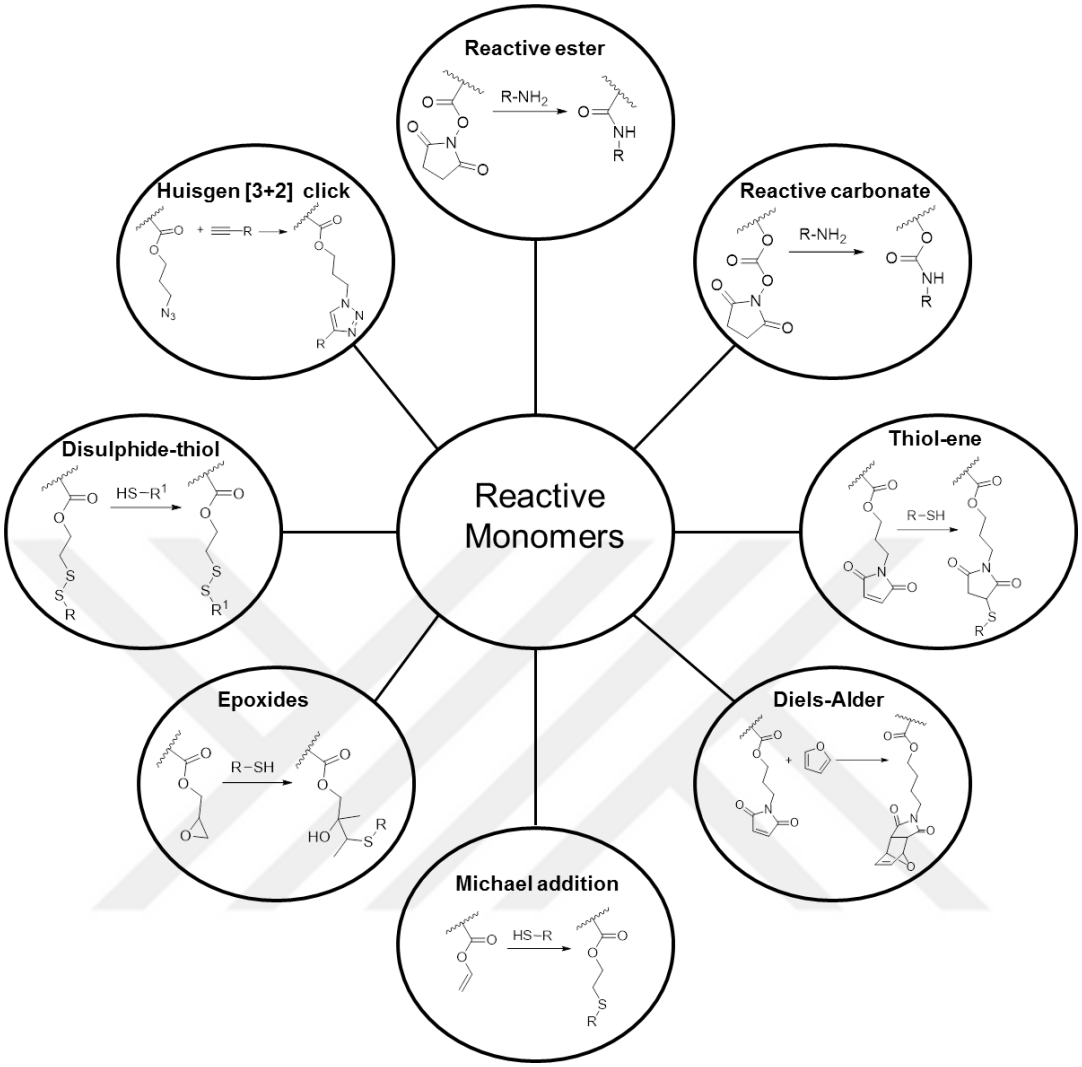

Figure 1.11. Different types of reactive monomers applied for post polymerization modification reactions.

However, discovery of living/controlled radical polymerization methods brought along new coupling reaction types such as thiol-ene reactions and cycloaddition reactions. To benefit from PPM reactions in polymer chemistry, some reactive monomers (Figure 1.11) that have functional groups on it were utilized. These functional groups allow selective transformation of reactive groups into other desired functional groups. Among all reactive monomers, activated esters which are mostly utilized in this thesis are well known and beneficial molecules.

Activated esters provide stable amide bonds with amines, which is the main requirement for targeting group conjugations in biological applications. Nevermore, activated carbonate groups can form hydrolyzable carbamate groups with amines which is advantageous for drug conjugations.

1.8. Activated Ester Monomers

The first appearance of activated ester monomers in research area was in 1970s by Ferruti and Ringsdorf [74, 75]. Conjugation reaction of active ester and amine molecules are one of the most encountered PPM reaction type. The reason for that is active ester moieties are very reactive even with weak nucleophiles and resulting amide bond is very stable. N-hydroxysuccinimide (NHS) based active ester monomers and their polymers are the most known molecules. Although they are used so regular, active ester molecules' solubility is restricted in some solvents such as dimethyl sulfoxide (DMSO) and dimethyl formamide (DMF). Moreover, as a result of using NHS based monomers for PPM reactions, some side reactions such as ring opening formation can show up [131]. By using excess amine molecules like triethylamine (TEA), these side reactions can be eliminated [132]. As an alternative, pentafluorophenyl (PFP) ester molecules and polymers are appealing choices for PPM reactions due to their higher reactivity when compared to NHS based esters. In addition, they are more stable and soluble in desired solvents [133]. Thiazolidine-2-thione (TT) molecules are another alternative reactive group that are used for obtaining reactive ester containing polymers. Ulbrich published a study about hydrolytic stability of TT groups and their ability of fast aminolysis in aqueous media [134]. But it was observed that, TT containing polymers didn't show obvious difference against amines and thiols under equal reaction conditions. Hawker and his crew proved that 4-vinyl-benzoate (VB) based active ester containing polymers are more reactive than methacrylated derivatives. They used VB molecules to get dendrimers in high yields [135]. Theato's study also exhibited that, VB polymers can react with less nucleophilic aromatic amines rapidly, unlike TT and methacrylate containing polymers [136]. In 2010, our group synthesized orthogonally functionalizable polymers by using 2-(N-succinimidylcarboxyoxy)ethyl methacrylate (SCEMA) monomer that contains NHS group *via* carbonate linker. In addition to SCEMA monomer, NHSMA was also used for utilizing activated ester moiety. Consequently,

allylamine was conjugated to resulted copolymer *via* carbonate group and it completely converted to carbamate group at ambient conditions while ester group was preserved [137].

1.9. N-Hydroxysuccinimide (NHS) Based Reactive Groups for Targeting Group Conjugations

Among many other activated ester monomers, NHS bearing monomers are arising as a very impressive type of functional monomer due to their resistance to hydrolysis and ability of reacting with primary and secondary amines efficiently. The study of Ringdorf and Ferruti about free radical polymerization of methacrylated and acrylated NHS with AIBN can be accepted one of the earliest publication among all [138, 139]. However, even though NHS based monomers are very reactive, they have poor solubility in most of organic solvents which limits usage of them as homopolymers. Hence NHS based monomers are generally copolymerized with other monomers to improve solubility of their final copolymer products thus facilitating aminolysis with different amines of extended polarity [140].

What is attractive about NHS based monomers is their ability to aminolysis and of making stable amide bond with amines as mentioned above. For utilizing these properties of NHS groups, they are commonly used for attaching different targeting groups *via* hydrolytically stable amide bond for targeted drug delivery applications. One of the earliest studies about NHS groups in which they are used for targeting group conjugation is published by Chao Deng and co-workers in 2006 [141]. RGD conjugated and biodegradable triblock copolymers were prepared. Before conjugation, researchers activated side-chain carboxylic acid group with NHS for accurate conjugation with amine of RGD molecule. In the upcoming years, NHS activation gained great attention for targeting group conjugation. In 2011, other RGD attachment *via* NHS activation was published by Biswas [142]. Biocompatible and water-soluble block copolymers were prepared. As a copolymerization technique, Ring opening metathesis polymerization (ROMP) was utilized. In addition to attaching cRGDfK molecule as a targeting group, amine containing dye was used for imaging application. In the same year, another study was published in which vascular targeting ligand bis-cyclic E-[c(RGDfK)$_2$] molecule was conjugated to copolymer *via* NHS activation again [51]. In addition to RGD molecule chemotherapy drug Paclitaxel (PTX) was

conjugated to polymer. This copolymer showed promising result *in vitro* and *in vivo* studies and time dependent tumor accumulation at tumor site was preferable when compared to non-targeted derivatives. In the recent past, our group prepared polymeric micelle by employing dendron-polymer construct types [143]. Like in previous examples, cRGDfK peptide was conjugated to periphery of AB type diblock polymer-dendron *via* NHS group. After conjugation of targeting group to prepared set of micelles, Docetaxel (DTX) encapsulation was executed. Overall, it was observed that RGD bearing micelles showed more promising results. Another molecule that can be utilized as targeting group and also bears amine moiety is folic acid which has high binding affinity to folate receptor that overexpress on some types of tumors. Just like RGD molecule, amine bearing folic acid conjugation to the constructs was employed by using NHS activated ester moieties in general. In 2011, Ronit Satchi-Fainaro highlighted the importance of natural macromolecule pullulan, chosen as the delivery agent [144]. Folic acid conjugation to the pendant PEG chain was achieved by using NHS ester activation yielded 63% of NHS group consumption approximately.

Bisphosphonate groups are popular type of targeting groups due to their high binding affinity for natural occurring bone mineral hydroxyapatite (HA). Angiogenesis is one of the most encountered problem for cancer patients during their treatment process. Bisphosphonates are utilized for targeted drug delivery especially for metastatic bone cancer. Since they have amine group at the periphery, they are generally conjugated to activated ester moieties to get stable amide bond. Ronit-Satchi Fainaro and coworkers are the precursor researchers about bisphosphonate drug delivery studies, especially utilizing from alendronate as bisphosphonate targeting group is their well-known studies. In 2011, they used NHS group as activation moiety for attaching alendronate [145]. They designed dendrimer that bears PTX and alendronate for targeting bone neoplasm. This heterobifunctional dendrimer was conjugated with PTX and then alendronate was attached *via* NHS activation. Concerning the alendronate conjugation to the polymers *via* NHS groups, many substantial studies have been published in recent years. As an example, one another attractive study was reported by our group which is about bone targeted drug delivery [146]. Combretastatin A4 (CA4) that is antiangiogenic drug was gained methacrylate group *via* –OH group and copolymerized with P(OEGMA) and NHSMA. After copolymerization reaction, resulted copolymer was attached with alendronate *via* NHS

moiety. After all, P(OEGMA) based polymeric macromolecule targeting bone cancer and also bears antiangiogenic drug on it was synthesized.

In the same year, recombinant human bone morphogenetic protein-2 (rhBMP-2) that naturally occurs in the body was tethered on to surface of calcium phosphate cement (CPC) matrix, by utilizing affinity of CPC to alendronate molecule [147]. rhBMP-2 is used for inducing bone formation and biomaterial carriers such as degradable polymers [148], [149] hydrogels [150, 151] and inorganic nanoparticles [152, 153] have been searched for employing from rhBMP-2 with maximum efficacy. According to some considerable studies, rhBMP-2 should be loaded in to biomaterial for the best output [154]–156]. However, selected biomaterials must have appropriate matrix that provide long-term localization for rhBMP-2 and also, they should protect rhBMP-2 until binding to targeted cells. Jioayang Zou and his colleagues designed a biomaterial by immobilization of rhBMP-2 on to the CPC (Figure 1.12). For this purpose, alendronate was conjugated with Heparin *via* NHS activity as a first step, and then Alendronate-Heparin (AH) conjugate was adsorbed on to CPC. rhBMP-2 was further incorporated on to surface through electrostatic interactions. As a matter of fact, according to *in vivo* studies, rhBMP-2 induced osteogenic bioactivity on the AH-CPC surface and enhanced bone regeneration.

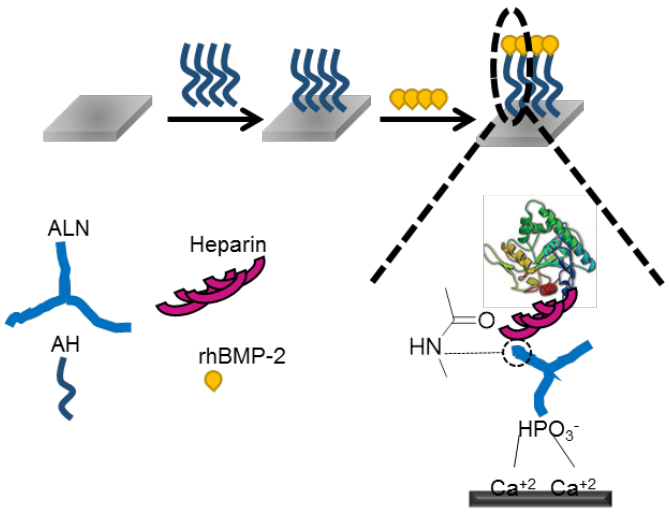

Figure 1.12. Schematic illustration and synthetic route for rhBMP-2 attached AH-modified CPC.

Moreover, another group from China published a study in which they anchored NHS group to the both sides of PEG-diacid before alendronate conjugation [157]. As a result, with the help of alendronate moiety, this novel molecule was bound with calcium phosphate core to obtain nanoparticle and Methotrexate (MTX) was loaded in to nanoparticle to observe cellular inhibition of cancer cells.

Another targeting groups which are used frequently are antibodies. Antibodies are immunoglobulins (Ig) and they have adjusted characteristics thus they can identify some specific antigens in the body [158]. For conjugation of so much important materials to nanomolecules, utilization from NHS activated esters is encountered in the literature often. In one of the important studies which was published in 2010, researchers conjugated monoclonal antibody Trastuzumab *via* NHS groups [159]. For Trastuzumab conjugation, acid bearing four armed DOTA chelate was used. After activating acid groups with NHS, trastuzumab was anchored to DOTA that was also labeled with Lutetium-177 providing enhanced tumor visibility. After a few years, same trends for trastuzumab conjugation to the Cu-64 labelled DOTA [160] and PEG molecule [161] were applied. As additional interesting studies, NHS activation was also applied for obtaining constructs for gene delivery [162] and ligand formation [163].

1.10. Polymerization Techniques

Polymerization can be called as a chemical reaction between small monomers to construct long polymer chains or macromolecules. Because of one polymer chain may be formed by hundreds or thousands of monomers, molecular weights of polymers are very large. Among all the polymerization techniques, free radical polymerization is the most widely applied method but due to drawbacks of this technique such as poor control on molecular weight and side reactions, some controlled living radical polymerization (CRP) techniques have been advanced in last decades. These techniques may include Atom transfer radical polymerization (ATRP) [164], Nitroxide mediated polymerization (NMP) [165], Reversible addition-fragmentation chain transfer polymerization (RAFT) [166, 167]. Polymerization techniques that are applied in this thesis are briefly introduced below.

1.10.1. Free Radical Polymerization

Free radical polymerization is one of the chain growth polymerization techniques in which polymer chain grows by the addition of monomers sequentially. In the growing process, double bond of the monomer's acrylate part is broken and radical ion is formed for propagation of polymer chain [168]. Free radical polymerization has much advantages and it has widespread application areas on the other hand it has also considerable amount of limitations in use such as fast irreversible termination step and noncontrollable molecular weight distribution [169]. Due to moisture removal is not crucial in the reaction process, polymerization reaction can be accomplished in desired solution or bulk phase. Free radical polymerization technique has four specific steps in order; initiation, propagation, transfer and termination (Figure 1.13). As a result of free radical polymerization reaction, high molecular weight polymer molecules and unreacted monomer units remain in the polymerized mixture which is accepted as specificity of this technique.

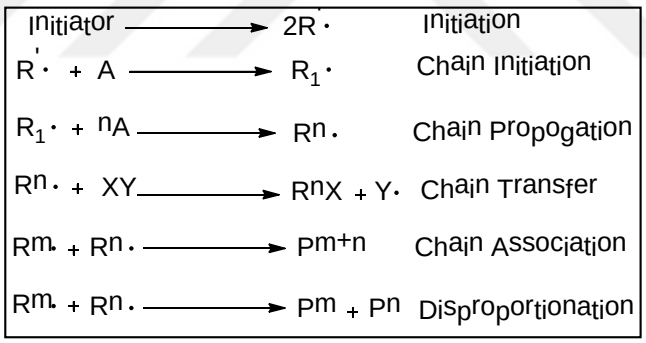

Figure 1.13. General mechanism of free radical polymerization reaction technique.

1.10.2. Reversible-Addition Fragmentation and Chain Transfer Reaction (RAFT)

Among all controlled radicalic polymerization techniques, RAFT polymerization is the most recent and well-known type polymerization. The first studies about RAFT and dithiocarbonyl structures based RAFT were reported in 1998 [170]. The main characteristic of RAFT polymerization is that the product which has a similar activity to precursor transfer agent itself, also serves like a chain transfer agent. The polymeric products and starting polymeric molecule generally have similar properties except their molecular weight, due to

reaction is stopped *via* degenerative chain transfer [171]. Typical RAFT agent has R and Z groups that determine reactivity and solubility of RAFT agent in the reaction, thus choosing suitable RAFT agent depends on the selected monomer's structure. The most applied RAFT agents are dithiocarbamates, trithiocarbonates and thiobenzoates (Figure 1.14)

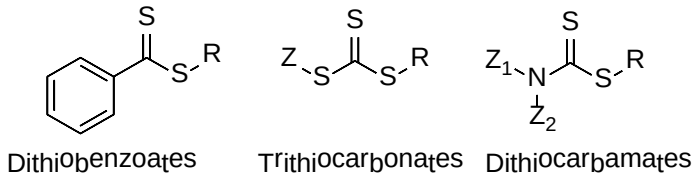

Figure 1.14. Major types of RAFT agents.

One of the key points of RAFT polymerization is deciding on which RAFT agent is the most appropriate for the polymerization. Typically, choosing right agent depends on construction of monomer and how does that agent affect the chain transfer activity of monomer in polymerization process [172].

1.11. Stimuli Responsive Controlled Drug Release

Due to novel drug therapies are interested by researchers for a long time, delivery and biodistribution profiles of drugs gained great attention. As it is known, when drug is administered in body, concentration of drug in plasma and clearance from body is followed and reported carefully. For increasing effectivity of drug thus bringing it to cancer treatment platform, determining important concentrations of drug such as lethal dose and ineffective dose is so crucial. To do this, release profiles, characteristics of drug in the body and tumor responses should be investigated. One of the biggest problem of releasing drug is premature drug release that causes side effects, nonspecific biodistribution in body and low efficacy [173]. Similarly, sometimes drugs can't be released in the tumor tissue leading to low drug concentration hence low toxicity is encountered. For improving therapeutic efficacies of chemotherapy agents, release profiles of drugs have been studied for a long time. Polymeric molecules that release drugs have been developed in terms of in which conditions they can release their drug.

In general, there are two main stimulus that triggers drug release (Figure 1.15). They are endogenous stimulus like pH of the environment, redox or enzymes. Another one is exogenous stimulus which are light, temperature, magnetic field and ultrasound [174, 175]. In cancer therapy, bio responsive nanoparticles are known as good facilitators for cell uptake and releasing drug in tumor environment. That's why, that kind of molecules have different benefits such as no need of exogenous stimulies thereby sufficient accumulation in the tumor *via* passive or active targeting can be achieved. In the tumor environment or inside the cancer cells, pH values of the lysosome (4.5-5.5) and endosome (pH 5.5-6.8) are low. There are extra-cellular and degradative enzymes that can facilitate drug release by cleaving enzyme responsive linkers. On the other hand, in the cell nucleus and cytosol, glutathion levels are so high when compared to healthy cells. All these unique features in the cancer cells can be counted as natural release stimulies to provide enhanced drug and protein release [176]. In this thesis, we designed different copolymers in which chemotherapy drugs are attached *via* pH, enzyme and redox (glutathion) sensitive linkers.

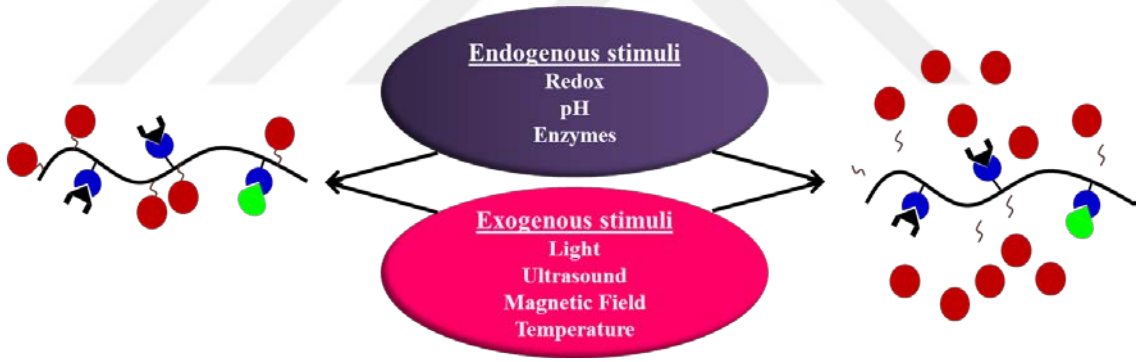

Figure 1.15. Stimuli responsive controlled drug release.

1.11.1. Ph Responsive Polymer Drug Conjugates

In the nanostructure design process, pH differences can be considered as important release triggers of drugs in tumor tissue. So that, too many studies about pH responsive molecules such as micelles [177], nanogels [178], dendrimers [179], liposomes [180] have been investigated. Most common model of polymeric structure that bears chemotherapy agent by using pH-sensitive linker is illustrated in Figure 1.16.

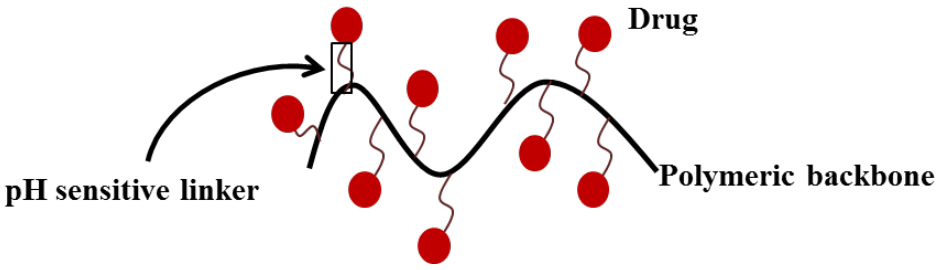

Figure 1.16. pH-sensitive linker bearing polymer drug conjugate.

When utilizing from pH sensitivity, acid labile linkers between drug and polymeric backbone are used in polymer drug conjugation systems in general. By using acid sensitive linker systems, not only therapeutic efficacy of drugs is improved, and increased cell uptake profiles are observed, but also healthy cells damage is minimized. More importantly, using acid labile linkers may provide well biodistribution in the body and specific delivery to tumor due to pH of normal cells or healthy tissue is 7.4 which means polymer can't release its cargo in bloodstream. However, polymer or/and attached drugs may not have specific reactive groups for formation of pH sensitive chemical bond. In that case, sometimes special spacers can be used. In principle, to obtain best release profile, selected linker should response to all pH changes in targeted region that will facilitate cleavage of linker hydrolytically. Prepared macromolecules are administered intravenously because of their poor oral bioavailability as a result, drug goes in bloodstream quickly [181]. During transition process, linker is expected to stay stable to achieve safe access to tumor tissue. As soon as polymer drug conjugate reaches to morbid tissue, it is uptaken by cells through endocytosis which has two separate categories namely phagocytosis and pinocytosis [182]. When drug enters to cancer cell, it encounters with several environments with different pH values. At first, it goes through cytosol that has neutral pH (7.4) and then it is taken in to endosomal compartment with 5.0-6.0 pH value. Finally, polymer is exposed to low pH (4.5-5.0) in lysosome, so pH sensitive linker is expected to be cleaved because of acidic condition. pH responsive polymer drug conjugate is firstly designed and implemented by Shen and Ryser in 1981 [183]. Currently, so many pH responsive polymer drug conjugation systems are applied by organic and polymer chemists. Among all linkers, hydrazone [87], ester [146], acetal [184] bonds can be quoted.

Utilized polymers containing pH sensitive linker are widely used in clinical trials. The most common carrier backbones are HPMA and PEG based molecules. Because of their non-degradable backbone features, their sizes and molecular weights should be kept under 50 kDa at least for achieving safe renal elimination [185]. Kopecek and his crew prepared HPMA based polymeric structure that contains doxorubicin as a chemotherapy drug. In their design, drug was attached to backbone *via* cis-acetonityl bond between amino group of polymer and carbonyl group of drug [186]. Another application of pH responsive polymer is promoted by using hydrazone bond. Especially, HPMA based doxorubicin conjugate is most popular counterpart because they are capable of releasing doxorubicin pH dependently.

On the other hand, according to *in vitro* results, polymeric structure was more toxic than free drug unexpectedly. Nevertheless, because of their large sizes and high molecular weights, prolonged blood circulation time was observed when compared to free DOX. As for *in vivo* studies, this pH responsive polymer drug conjugate exhibited improved tumor accumulation, correspondingly well tumor growth inhibition was achieved. Furthermore as a latter study, monoclonal antibody (anti-CD20 mAb) was conjugated to increased molecular weight version of that HPMA polymeric backbone [187]. Another important polymeric backbone that is used in pH dependent macromolecule applications is PEG. The use of PEG is based on modifying it to form block, random, grafted or star shaped copolymers [188, 189]. Owing to their hydrophilic morphology, PEG molecules can be used for micelle preparation in aqueous solution. Moreover, by using PEG molecule in the synthesis of micelles may enhance inhibition of P-glycoprotein efflux pump which causes drug resistance in cancer cells. As an illustration, Yang prepared promising micelles by conjugating PEG-poly carbonate block and DOX *via* pH sensitive Schiff base linker [188]. According to release results, micelles which have 100 nm of sizes showed better release behavior in acidic pH (5.0) when compared to neutral pH (7.4). In acidic environment, approximately 50% of DOX was released from micelles whereas 23% of DOX was released in neutral condition. Additionally, cellular drug accumulation was better in micellar form than free DOX that resulted in more cell death because of their suppressing capability of DOX resistant MCF-7/Adr cells proliferation. Besides from these, pH sensitive linkers with PEG are also used for preparing quantum dots (QDs). In one of the examples, DOX was conjugated to Poly (glycidyl methacrylate)-ethane diamine-PEG based grafted copolymer by using Schiff base. This prepared conjugate was used for coating QDs surface to improve tumor imaging and

treatment [190]. More currently, Kwon and his crew studied on micelles which are consisting of two different block copolymers. It was discovered that, combining two different copolymers to form micelle, affects release behavior by changing ratios of consisting copolymers in the structure [191]. As mentioned previously, our group also designed PEG based polymer drug conjugate in which antiangiogenic drug was attached *via* pH labile ester linker. In our study, we observed satisfying release profiles in rat plasma for our structure that carries its drug with ester linker. The release results were attributed to esterase enzymes presented in plasma [146].

1.11.2. Enzyme Responsive Polymer Drug Conjugates

In healthy tissues, presence of some specific enzymes is expected and normal phenomenon. But in cancerous tissues, these enzymes are overexpressed and thus they can be used as release triggers and assistant for tumor penetration of drug in cancer treatment area. Different from pH responsive polymers that can degrade in physiological conditions, enzyme responsive counterparts remain stable in the absence of their specific enzymes. For instance, Matrix-metalloproteinases (MMP) is in a kind of specific enzyme and it has leading role on tumor metastasis [192]. Torchilin and his co-workers prepared a macromolecule with GPLG*IAGQ peptide sequence which is cleavable with MMP enzymes [193]. In 2014, the same group synthesized micelle containing PEG-Peptide-PEI-1,2-dioleoyl-sn-glycero-3-phosphoethanolamine (PEG-Peptide-PEI-PE) copolymers. As expected, cleavage of peptide was achieved by using MMP enzyme. *In vivo* results on non-small lung cancer (NSCLC) xenograft displayed better results for MMP sensitive micelles in terms of cell internalization studies [194]. For glioblastoma therapy, Chen used MMP sensitive biodegradable PEG-*b*-PCL nanoparticles. They made modification of their copolymer with low molecular weight protamine. According to their results, cytotoxicity profile of PTX loaded modified nanoparticle was lower when compared to free drug and enzyme insensitive counterpart molecule. In addition to this, tumor accumulation and survival rate of enzyme sensitive structure was better again [195]. One of the vastest groups in cancer research platform, Kopecek and his crew reported compelling study on MMP enzyme cleavable HPMA based copolymer containing CXCR4 antagonist (BKT40) by using reversible addition fragmentation chain transfer (RAFT) copolymerization technique.

Experiments were performed on PC-3 human prostate carcinoma cells. Cytotoxicities of both polymer bearing BKT40 and free BKT40 were observed as similar whereas CXCL12 induced cell migration rate was higher with polymeric structure [196]. Except all these examples, there are some other enzymes presented in liposome and they are responsible for digesting. This kind of enzymes are including lycosidases, proteases and sulfatases [197]. Famous researchers Duncan, Kopecek and Ulbrich utilized from applications of these enzymes. Especially, all of them used HPMA backbone-based copolymer drug conjugates and they benefited from special four aminoacid containing peptide GFLG linker. GFLG peptide linker can be cleaved by lysosomal enzyme cathepsin K, in this manner most of the researchers have been using that linker for conjugation of drugs to polymeric carrier [198]. As mentioned previously, these designed copolymers remain stable in blood circulation due to absence of specific enzyme cathepsin K. Kopecek and his group performed a study about HPMA based copolymer carrying DOX in which drug was attached to polymer *via* GFLG linker. On the other hand, targeting group iRGD was attached by using another peptide PLGAG. Dual enzyme responsive structure displayed sufficient tumor accumulation and cytotoxicity profiles on prostate cancer cells were satisfying [199]. In 2014, release studies were achieved between PEGylated dendron bearing DOX *via* GFLG linker and enzyme insensitive counterpart to emphasize effect of GFLG on drug release. According to results which were carried out by using papain enzyme, GFLG bearing structure exhibited 80% of drug release in 15 h although 30% of release was observed in enzyme insensitive version [200]. As latter studies, *in vivo* experiments were performed as well.

Enhanced tumor accumulation and prolonged blood circulation time were observed on 4T1 murine breast cancer xenografts [201]. For enzyme sensitive linkers application in cancer treatment platform, another peptide sequences that can be cleaved by using cathepsin B enzyme is drawing attention. These peptides are consisting of two amino acids and the most encountered substrates are, valine-citrulline (VC) and phenylalanine-arginine. In this thesis, one of our chapters is about synthesizing novel monomer containing VC as a linker. According to latest researches, using these dipeptides with special spacers enhance release profiles of drugs from macromolecules. In case of studies that was used VC as a linker, spacer p-aminobenzyl alcohol is used for enhancing release behavior of molecules. According to some researchers, if PABA is not used, cathepsin B enzyme can’t affect VC linker hence release of drug doesn’t occur. In general papers, VC is conjugated to some

desired molecule from its amine moiety. After that, it is attached with amine group of PABA from its acid group that resulted in formation of stable amide bond. This new formed amide bond is crucial because of being cleavage point for cathepsin B enzyme [202]. One of the most encouraging studies on VC containing nanoparticles was reported in 2002 by Dubowchik *et al*. [203]. In their study, DOX was conjugated to antibody BR96 *via* two different dipeptides, valine-citrulline and phenylalanine-lysine. Prepared structures were treated with cathepsin B enzyme alone and phenylalanine-lysine substrate displayed better release behavior in comparison with valine-citrulline. However, in rat liver with the presence of more than one enzyme, their release profiles were similar. Both conjugates have similar toxicities against tumor cells as well. In later years, this time phe-lys was used for utilization of preparing antibody-drug conjugates [204, 205]. In 2009, HPMA polymer was attached with phe-lys linker and linker was ended with spacer p-aminobenzyl alcohol (PABA) [206]. More interestingly, used spacer was dendronized up to three arms and each of them was conjugated with drug PTX *via* carbonate linker. Design of prepared structure was shown in Figure 1.17.

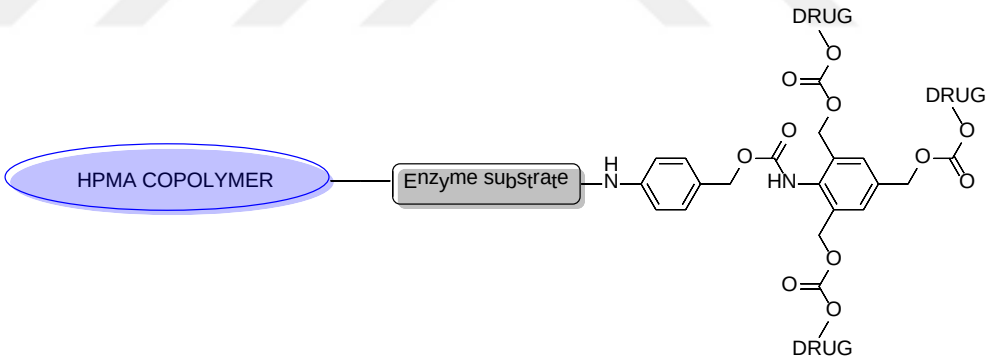

Figure 1.17. Schematic illustration of dendritic structure bearing enzymatically cleavable phe-lys linker.

Furthermore, counterpart molecule was also prepared which doesn't contain phe-lys linker but carrying non-cleavable peptide sequence. As expected, phe-lys linker containing structure showed better releasing behavior while another molecule didn't release any drug. In a more recent study that was reported in 2012, PTX was utilized again [207]. PEG was used as a polymeric carrier this time and conjugated to VC linker. Drug PTX was conjugated to spacer *via* carbonate linker like in previous work. As control, PEG-PTX molecule was

also prepared. According to release studies in the presence of cathepsin B enzyme, VC linker containing structure exhibited well release profile whereas control didn't release any drug on it. On the other hand, while control structure was inefficient on anti-tumor, anti-angiogenesis and anti-proliferation studies, prepared novel structure displayed satisfactory results as *in vivo* studies. VC bearing molecules gained attention in last decades by researchers due to encouraging results. Except of the studies mentioned above, there are some examples on preparing micellar structures with VC dipeptide sequence also [208].

1.11.3. Redox Responsive Polymer Drug Conjugates and Glutathion Sensitive Structures

When considering internal stimuli drug delivery systems, redox responsive materials are the most known examples that come to mind because of glutathion (GSH) presence inside the cells. Glutathion is a kind of protein composed from three amino acids which are γ-glutamyl-cysteinyl-glycine. It has low molecular weight and it can be reduced by using NADPH and glutathion reductase. As it is well known, tumor cells are different from healthy cells in terms of their morphology, nature and contents. Like as some special enzymes are overexpressed in the tumor cells, glutathion also exists in the tumor cells more than usual and its reducing potential is approximately 10-1000 times higher in cancer cells [209]. As a result, polymers containing disulfide bond have been investigating widely by chemists. On the other hand, using disulfide bearing molecules can be regarded as more beneficial when compared to pH responsive counterparts because disulfide bond degradation is not expected in physiological conditions. Disulfide bonds are converted to sulfhydryl groups in intracellular reducing environments. The most popular application area of redox sensitive drug delivery systems is micelle preparation. Especially, micelles that have disulfide bond between hydrophilic and hydrophobic blocks in the core are very noteworthy molecules and they are named as shell-sheddable micelles. For hydrophobic blocks, polypeptides [210], polyesters [211], polyanhydrides [212] are being utilized in general.

In one study, ator vastatin calcium that is used for prevention of metastasis in some cancer types, was loaded in to shell-sheddable type micelle [213]. According to tumor accumulation studies *in vivo*, micellar structures accumulated in the tumor more than free

ator vastatin after 12 h from administration. In connection with this phenomenon, ator vastatin loaded micelles inhibited tumor metastasis 4T1 orthotropic mammary tumor metastatic cancer model. In 2013, instead of ator vastatin, galactose decorated micelles were prepared *via* same technique. After 12 h, SS bond bearing shell-sheddable micelles showed good release profile, more than 75% of DOX was released from micelle in 10 mm dithiothreitol (DTT) containing solution. Another conjugate which doesn't contain SS bond, showed very small amount of drug release [214]. As different strategies, drugs can be conjugated to side chain of copolymer by using multiple disulfide bond or disulfide bonds can be placed in the main chain of the hydrophobic polymer. For illustration of that strategy, Kataoka's research can be showed. They reported a study on micelles which are constructed from PEG-PLL copolymer and reducible disulfide bond was attached. Chemotherapy drug Campthotesin (CPT) was also linked *via* disulfide bond. The experiments on AY27 rat urothelial xenografts exhibited high accumulation behavior and enhanced blood circulation time of micelle [215]. Drug resistant MCF-7 / ADR cells were treated with DOX loaded and disulfide linker containing α-amino acid- poly(ester amide) based nanoparticle and according to results nanoparticle was more toxic than free DOX [216]. Other version of this nanoparticle which is three blocks containing micelles were also displayed better release and internalization behaviors in the nuclear and perinuclear regions of the same cells [217]. One more approach on building reduction responsive nanoparticles is using disulfide bonds as crosslinkers. This approach may provide stability for the nanotherapeutics before they are de-crosslinked in the cytosol. For instance, Lee and his crew proved that their shell-crosslinked micelles can deliver higher amount of drug to the tumor region according to non-crosslinked micelles and they can also remain stable during transportation in blood.

Consequently, M109 tumor growth regression in mice was observed after 14 days of treatment with crosslinked micelles [218]. Using hyaluronic acid (HA) hydrogels as crosslinkers are shown as the most applied methods for preparation of hydrogels. Due to HA is a natural linear polysaccaride, obtaining HA hydrogels by attaching disulfide bonds and crosslinking them is general used method. One of the examples of this studies is reported in 2015. Shell-crosslinked HA hydrogels were treated with 10 mM of glutathion resulted in quick release. Tumor accumulation and cell internalization studies were also performed with shell-crosslinked HA hydrogels and satisfied results were obtained. Tumor growth regression was better with crosslinked version in comparison with free drug and non-

crosslinked counterpart [219]. HA acid was conjugated with lysine and lipoic acid (HA-Ly-LA) and DOX was loaded in. Like as previous works, enhanced blood circulation time, better tumor accumulation and tumor growth inhibition (12.71% ID/g) were obtained in that study as well [220]. Except all mentioned studies above, disulfide linker containing prodrug designs were utilized in different diseases other than cancer such as influenza. Another similarity of that research with our study is disulfide bearing drug was attached to polymer chains from pendant groups [221]. More recently, HPMA backbone was attached with AMD3465 drug *via* disulfide bond. Prepared polymer displayed effective release of drug following treatment with glutathion [222].

2. TARGETING TO THE BONE: ALENDRONATE DIRECTED COMBRETASTATIN BEARING ANTI-ANGIGENIC POLYMER DRUG CONJUGATES

The materials in this chapter have been adapted from the following article: Karacivi, M., Sumer Bolu, B., and Sanyal R. "Targeting to the bone: Alendronate-Directed Combretastatin A-4 Bearing Anti-Angiogenic Polymer Drug Conjugates", *Mol. Pharm.*, Vol. 14, No. 5, pp. 1373–1383, March 2017.

2.1. Introduction

Among various strategies currently under investigation to increase the efficacy of therapeutic agents to combat complex diseases like cancer, targeted delivery presents an attractive and viable option [223]–[228]. Design of current drug delivery systems often incorporates both “passive” and “active” targeting modes to achieve maximum benefit. In this regard, macromolecular drug delivery platforms have been widely investigated since their large size alone or that of their assemblies enables accumulation of therapeutic agents in tumor tissues through “passive” targeting mediated through the enhanced permeation and retention (EPR) effect [229]. Appropriate design of polymeric macromolecules also allows conjugation of targeting moieties that further enhance preferential accumulation in disease tissues where unhealthy cells present an overexpression of certain biomarkers. The two common approaches that are employed to facilitate transport and delivery of drugs to the disease site involve either noncovalent encapsulation of drugs in a polymeric assembly such as micelle or nanogels, or covalent conjugation of the drug to the polymer [230, 231]. While the first approach offers advantages like utilization of drug without any modification, the system needs to be designed to suppress premature release before reaching the target and burst release at the site. The later approach, although involves more synthetic steps, often allows one to design systems that can suppress drug release during transport to site of accumulation. Furthermore, utilization of specific linkers to conjugate the drugs to the

polymeric backbone can allow preferential release upon exposure to biological cues that are present in the tumor environment. Above-mentioned assets of polymer−drug conjugates have led to a flurry of research in this area over the past decades [232].

Specific targeting of polymer−drug conjugates to various tumors can be realized by covalent attachment of particular ligands or biomolecules onto these constructs. The choice of targeting moiety varies depending upon the type of tissue that is targeted since different tissues present different chemical and biological environments. Among various organs, development of strategies to target drugs to bone tissues is quite important since apart from bone cancers, in many other types of cancers, the spread of the disease occurs through metastasis to bones. The high mineral content of bones allows targeting of polymer−drug conjugates by attachment of ligands with high affinity for minerals such as hydroxyapatite. Targeting groups with affinity for the bone tissue includes synthetic ligands such as polyglutamates [233]–[236], polyaspartates [237, 238] and bisphosphonates [239]–[241]. Among these, utilization of bisphosphonate based ligands have attracted attention since bisphosphonates are widely used to treat metabolic bone disorders such as osteoporosis [242]–[244]. Recent reports from Farokhzad, Ghobrial, and co-workers demonstrated bisphosphonate containing polymeric nanoparticles loaded with bortezomib, a potent antitumor agent for treatment of multiple myeloma, showed very promising results by not only increasing the survival of mice treated with these constructs but also reduced tumor burden [245].

Due to the efficient targeting, it is also expected to reduce potential toxicity of the drug at off-target sites. Likewise, Cheng, Fan, and co-workers reported doxorubicin loaded polylactide nanoparticles with bisphosphonate ligands on their surface for treatment of malignant skeletal tumors and showed enhanced accumulation and retention in bone tumors for targeting group containing delivery vehicles [246]. Apart of these recent encouraging reports, as alternatives to nanoparticle-based delivery, soluble polymers−drug conjugates containing bisphosphonate group have also been investigated as a viable approach to target therapeutics to bone. In a seminal contribution, Kopeček and co-workers demonstrated that conjugation of alendronate, a bisphosphonate group containing drug used for treatment of osteoporosis, to a dye conjugated poly(N-(2-hydroxypropyl)methacrylamide (HPMA) and linear poly(ethylene glycol) specifically accumulated in bone tissues [247]. Since then, they

reported the biodistribution and pharmacokinetics of alendronate conjugated HPMA and along with Satchi- Fainaro and co-workers showed that conjugation of an antiangiogenic agent TNP-470 to the bone targeting HPMA conjugate showed improved antiangiogenic and antitumor activity compared to the free drugs [248]. Satchi-Fainaro and coworkers also demonstrated the effectiveness of an alendronate and taxane conjugated HPMA copolymers for targeting chemotherapeutics to bone [68].

Until recently, most of the reports have focused on the HPMA polymer, and only a few reports have investigated other polymers containing bisphosphonate [98], [249]. Given the promising results of these bisphosphonate based targeting studies, expanding the tool box to include constructs based on other polymers and investigation alternative antiangiogenic agents is worthwhile. Alternatives such as polymers containing side chain poly-(ethylene glycol) units, which are potential candidates for fabrication of drug delivery vehicles due to their biocompatible nature and facile access through a variety of contemporary polymerization techniques, remain unexplored in this area [250], [251]. Among the various strategies investigated to combat a complex disease like cancer, utilization of antiangiogenic agents has been widely investigated in recent years [252]–[254]. In this approach, the cytotoxic agent inhibits formation of blood vessels around the tumor thus depriving it of nutrients and halting its growth. Recently, it has been demonstrated that, combretastatin (CA4), a potent antiangiogenic drug originally isolated from South Africa, provides suppression of tumor growth [255, 256]. Studies suggest that CA4 prevents tumor angiogenesis through inhibition of VEGF-induced endothelial cell functions [257].

In recent years, CA4 has been either encapsulated in or conjugated to various polymeric carriers either alone or along with other chemotherapeutic agents like doxorubicin to attain antiangiogenic effects [258]–[260]. It can be argued that the angiogenesis associated with metastasis lesion would facilitate the polymeric delivery system’s extravasation at the cancer lesion, and simultaneous utilization of a bisphosphonate unit will provide local retention in the hydroxyapatite-rich environment. Thus, it can be envisioned that a water-soluble copolymer bearing bisphosphonate groups along with a CA4 based antiangiogenic moieties would offer an attractive drug delivery platform that can be further appended with additional therapeutic agents to allow targeted multidrug therapy.

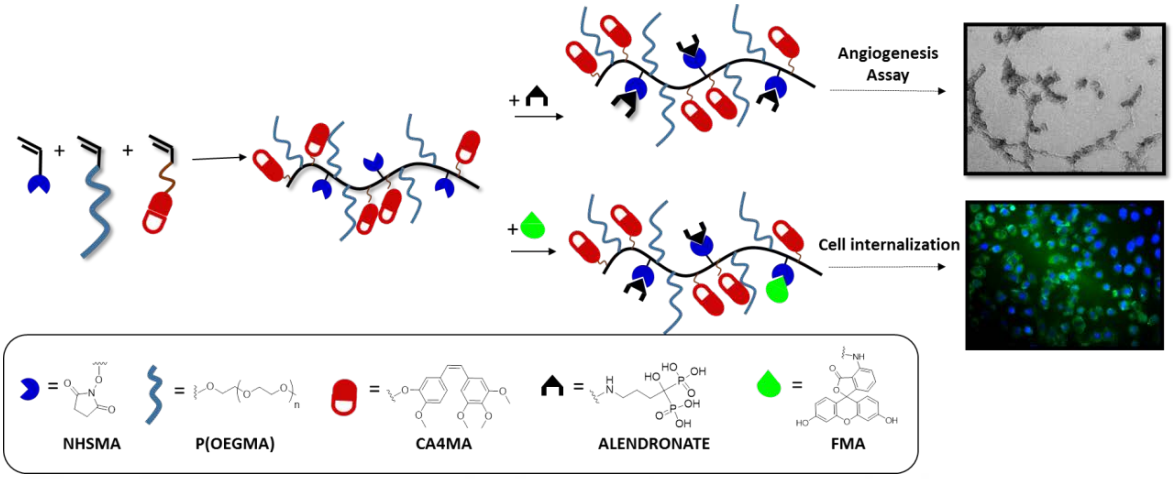

Figure 2.1. Scheme for synthesis and evaluation of bone-targeted antiangiogenic copolymers.

Herein, we report the synthesis and evaluation of a novel polymer−drug conjugate carrying two drugs, combretastatin and alendronate. While the first drug has antiproliferative activity for cancer cells, the second drug in this construct acts as a targeting ligand for directing the polymer−drug conjugate to bone tissues (Figure 2.1). A modular approach toward synthesis of poly(oligoethylene glycol) copolymer based conjugates and their evaluation toward targeting of bone materials are reported. Thereafter, in vitro studies to evaluate their cytotoxicity against various cell lines, as well assay of their antiangiogenic activity by tube formation inhibition of HUVECs were performed to probe the efficacy of such constructs.

2.2. Experimental Section

2.2.1. Materials

Methacryloyl chloride was purchased from Alfa Aesar. The solvents used thoughout this thesis was purchased from Merck. Milli-Q Water Purification System (Milli-Q system, Millipore, Billerica, MA, USA) was employed to produce ultrapure water. All the other chemicals were purchased from Sigma-Aldrich. Oligo- (ethylene glycol) methyl ether

methacrylate (OEGMA, Mn = 300 g mol^{-1}) was filtered through basic alumina column prior to use. N-Hydroxysuccinimide methacrylate (NHSMA) [261] and combretastatin A-4 (CA4) [262] were synthesized according to previously reported protocols. Fluorescein O-methacrylate (FMA) was purchased from Sigma-Aldrich. 2,2′-Azobis(2-methylpropionitrile) (AIBN) from Sigma-Aldrich was recrystallized from methanol before use. Human umbilical vein endothelial cells (HUVECs) were obtained from Lonza (Lonza Inc., Allendale, NJ). HUVECs were grown in endothelial cell growth media-2 kit (EBM-2 supplemented with EGM-2 Single Quot kit). Saos-2 and U2-OS cells were purchased from ATCC.

2.2.2. Instrumentation

^{1}H and ^{13}C NMR spectroscopy (Varian 400 MHz NMR spectrometer), Fourier transform infrared (ATR-FTIR) spectroscopy (Nicolet 380, Thermo Scientific, USA), and UV−vis spectroscopy (PerkinElmer series) methodologies were used in order to characterize synthesized monomers and polymers. The qualification and quantification of CA4 monomer (CA4MA) was achieved utilizing the liquid chromatography−mass spectrometry (LC−MS) system (LCMS 2020, Shimadzu, Japan) with a C- 18 (5 μm, 150 × 4.6 mm) column. A gradient method was utilized with acetonitrile (ACN) and deionized water supplemented with 0.05% trifluoroacetic acid (TFA) through the following program; LC: 0−3 min, 50% ACN; 3.01 min, 50% ACN; 8 min, 95% ACN; 8.01−11 min, 50% ACN; MS positive scan 100−800 m/z. The polymer molecular weights were estimated by size exclusion chromatography (SEC) using a PSS-SDV (length/ID 8 × 300 mm, 10 mm particle size) linear Mixed C column calibrated with poly(methyl methacrylate) (PMMA) standards using a refractive-index detector with a mobile phase solution of 0.05 M lithium bromide in dimethylaceteamide (DMAc) as eluent at a flow rate of 1 mL/min at 30 °C. During the internalization experiments, cells were visualized using Zeiss Observer.Z1 inverted fluorescence microscope.

2.2.3. Synthesis and Characterization of CA4MA (3)

To a solution of CA4 (0.3 g, 0.946 mmol) and triethylamine (0.197 g, 1.89 mmol) in dichloromethane (15 mL) was added methacryloyl chloride (0.197 g, 1.89 mmol) dropwise over 10 min at 0 °C. Then, reaction was stirred at rt for 24 h. Upon completion, solution was diluted with dichloromethane (5 mL), and organic phase was washed with saturated $NaHCO_3$ (2 × 40 mL) and H_2O (2 × 40 mL). Combined organic layers were dried over anhydrous Na_2SO_4 and concentrated to give a yellowish solid, which was purified by column chromatography on SiO_2 (EtOAc/hexanes, 20:80) affording 0.24 g of compound 3 (66% yield). ^{1}H NMR ($CDCl_3$, δ, ppm) 7.11 (dd, 1H, *J* = 8.4, 2 Hz), 7.03 (d, 2H, *J* = 2 Hz), 6.84 (d, 1H, *J* = 8.8 Hz), 6.50 (s, 2H), 6.44 (d, 2H, *J* = 3.2 Hz), 6.28 (s, 1H), 5.70 (s, 1H), 3.81 (s, 3H), 3.78 (s, 3H), 3.69 (s, 3H), 2.01 (s, 3H). ^{13}C NMR ($CDCl_3$, δ, ppm): 165.3, 152.9, 150.4, 139.6, 135.5, 132.4, 130.1, 129.4, 128.6, 127.7, 127.2, 123.2, 123.1, 112.0, 105.9, 61.0, 56.0, 18.4. FT-IR (cm^{-1}) 1737, 1577. LC−MS expected [M + H] m/z = 385 and observed [M + H] m/z = 385.

2.2.4. Synthesis and Characterization of P(OEGMA-CA4-NHS) (4)

OEGMA (1 g, 3.33 mmol), CA4MA (0.36 g, 0.952 mmol), and NHSMA (0.0120 g, 0.066 mmol) were dissolved in anhydrous dioxane (5 mL). To the polymer solution was added AIBN (6.24 mg, 0.038 mmol) as initiator and the reaction mixture was stirred under N_2 for 30 min. Reaction was sealed and heated at 65 °C for 24 h. The copolymer was purified via precipitation in diethyl ether, dissolved in CH_2Cl_2, and reprecipitated. After drying under vacuo, product 4 was obtained as a colorless, viscous liquid (0.1 g, 67%) M_n = 50 kDa, M_w/M_n = 1.9. ^{1}H NMR (D_2O, δ, ppm) 7.10 (bs, 3H), 6.55 (bs, 4H), 4.18 (bs, 2H), 3.67 (bs, 20H), 3.37 (bs, 3H), 2.75 (bs, 4H), 1.91 − 0.90 (m, $-CH_2$ and CH_3 along with backbone).

2.2.5. Synthesis and Characterization of P(OEGMA-CA4-ALN) (6)

Copolymer 4 (400 mg, 0.008 mmol) was dissolved in ACN (0.4 mL), and alendronate sodium (25 mg, 0.077 mmol) was dissolved in PBS (2 mL) in a separate vessel. Copolymer

solution was added dropwise into the alendronate solution, and pH was adjusted to 8.0−9.0 by addition of NaOH (1.0 M). Then, the reaction was stirred for 4 d at 45 °C. The product was dialyzed using 3.5 kDa cutoff regenerated cellulose acetate membrane in water (200 mL) for 2 d. Pure product 6 was lyophilized and obtained as a viscous liquid (0.28 g, 71%). ^{1}H NMR (D_2O, δ, ppm) 7.07 (bs, 3H), 6.52 (bs, 4H), 4.19 (bs, 2H), 3.70 (bs, 20H), 3.39 (bs, 3H), 2.59 (bs, 2H), 1.93 − 0.92 (m, −CH_2 and CH_3 along with backbone).

2.2.6. Synthesis and Characterization of P(OEGMA-CA4) (7)

To a solution of compound 4 (400 mg, 0.008 mmol) in DMF (0.4 mL) was added 1-amino-2-propanol (8.0 mg, 0.1 mmol) in DMF (0.1 mL). Reaction was stirred at rt for 24 h. After dialysis using 3.5 kDa cutoff regenerated cellulose acetate membrane in water (200 mL) for 2 d, viscous and colorless product 7 was obtained by lyophilization (0.3 g, 75%). ^{1}H NMR (D_2O, δ, ppm) 7.00 (bs, 3H), 6.45 (bs, 4H), 4.11 (bs, 2H), 3.61 (bs, 20H), 3.31 (bs, 3H), 2.50 (bs, 2H), 1.81 − 0.85 (m, −CH_2 and CH_3 along with backbone).

2.2.7. Synthesis and Characterization of P(OEGMA-NHS) (8)

OEGMA (0.5 g, 1.66 mmol) and NHSMA (0.034 g, 0.184 mmol) were dissolved in anhydrous dioxane (2.5 mL). After addition of AIBN (4.32 mg, 0.0263 mmol), the solution was purged with N_2 for 30 min. Reaction was carried out at 65 °C, under N_2 for 24 h. Copolymer was purified via precipitation in ice-cold diethyl ether. After drying under vacuo, product 8 was obtained as a colorless, viscous liquid. Mn = 51 kDa, M_w/M_n = 2.0 (300 mg, 57%). ^{1}H NMR (D_2O, δ, ppm) 4.18 (bs, 2H), 3.78 − 3.62 (m, 20 H), 3.39 (bs, 3H), 2.94 (bs, 4H), 1.91 − 0.91 (m, −CH_2 and CH_3 along with backbone).

2.2.8. Synthesis and Characterization of P(OEGMA-ALN-NHS) (9)

Copolymer solution was prepared by dissolving compound 8 (300 mg, 0.006 mmol) in ACN (0.3 mL). Alendronate solution was prepared by dissolving alendronate sodium

(7.18 mg, 0.022 mmol) in PBS (0.6 mL). Copolymer solution was added into the alendronate solution dropwise, and final pH was adjusted to 8.0 − 9.0 using NaOH (1.0 M). Resulting reaction mixture was stirred for 4 d at 45 °C. The product was dialyzed using 3.5 kDa cutoff regenerated cellulose acetate membrane in water (200 mL) for 2 d. Pure product 9 was lyophilized to obtain a viscous liquid (200 mg, 67%). ^{1}H NMR (D_2O, δ, ppm) 4.21 (bs, 2H), 3.81 − 3.66 (m, 20H), 3.37 (bs, 3H), 2.96 (bs, 4H), 2.53 (bs, 2H), 1.91 − 0.94 (m, −CH_2 and CH_3 along with backbone).

2.2.9. Synthesis and Characterization of P(OEGMA-ALN) (10)

To a solution of compound 9 (400 mg, 0.008 mmol) in DMF (0.4 mL) was added 1-amino-2-propanol (0.165 mg, 0.022 mmol) in DMF (0.02 mL). Reaction was stirred at rt for 24 h. After dialysis using 3.5 kDa cutoff regenerated cellulose acetate membrane in water (200 mL) for 2 d, viscous and colorless product 10 was obtained by lyophilization (0.28 g, 70%). ^{1}H NMR (D_2O, δ, ppm) 4.17 (bs, 2H), 3.78 − 3.63 (bs, 20H), 3.39 (bs, 3H), 2.57 (bs, 2H), 2.48 (bs, 2H), 1.90 − 0.91 (m, −CH_2 and CH_3 along with backbone).

2.2.10. Synthesis and Characterization of P(OEGMA-CA4-NHS-FMA) (12)

OEGMA (0.2 g, 0.66 mmol), CA4MA (0.032 g, 0.083 mmol), NHSMA (0.010 g, 0,083 mmol), and FMA (0.005 g, 0.041 mmol) were dissolved in anhydrous dioxane (1.5 mL). To the polymer solution, was added AIBN (0.672 mg, 0.0041 mmol) as initiator and mixture was stirred under N_2 for 30 min. Reaction was sealed and heated at 65 °C for 24 h. The copolymer was purified by precipitation in ether, dissolved in CH_2Cl_2, and reprecipitated. After drying under vacuo, the product 12 was obtained as a colorless, viscous liquid (0.12 g, 60%). M_n = 61 kDa, M_w/M_n = 2.1. ^{1}H NMR ($CDCl_3$, δ, ppm) 8.01 (s, 2H), 7.70 − 7.63 (m, 2H), 7.13 − 6.47 (m, 14H), 4.10 (bs, 2H), 3.65 − 3.56 (m, 20H), 3.39 (bs, 3H), 2.82 (bs, 4H), 1.98 − 0.89 (m,−CH_2 and CH_3 along with backbone).

2.2.11. Synthesis and Characterization of P(OEGMA-CA4-ALN-NHS-FMA) (13)

Copolymer solution was prepared by dissolving compound 12 (60 mg, 0.001 mmol) in ACN (0.06 mL). Alendronate solution was prepared by dissolving alendronate sodium (10 mg, 0.03 mmol) in PBS (1.0 mL). Copolymer solution was added into the alendronate solution dropwise, and final pH was adjusted to 8.0 − 9.0 using NaOH (1.0 M). Resulting reaction mixture was stirred for 4 d at 45 °C. The product was dialyzed using 3.5 kDa cutoff regenerated cellulose acetate membrane in water (200 mL) for 2 d. Pure product 12 was lyophilized to obtain a viscous liquid (0.048 g, 80%). ^{1}H NMR ($CDCl_3$, δ, ppm) 8.04 (s, 2H), 7.72 − 7.67 (m, 2H), 7.15 − 6.48 (m, 14H), 4.11 (bs, 2H), 3.85 − 3.57 (m, 20H), 3.39 (bs, 3H), 2.53 (bs, 2H), 2.03 − 0.89 (m, −CH_2 and CH_3 along with backbone).

2.2.12. Synthesis and Characterization of P(OEGMA-CA4-FMA) (14)

To a solution of compound 13 (100 mg, 0.002 mmol) in DMF (0.1 mL) was added 1-amino-2-propanol (0.041 mg, 0.0055 mmol) in DMF (10 µL). Reaction was stirred at rt for 24 h. After dialysis using 3.5 kDa cutoff regenerated cellulose acetate membrane in water (100 mL) for 2 d, viscous and colorless product 14 (0.088 g, 88%) was obtained by lyophilization. ^{1}H NMR ($CDCl_3$, δ, ppm) 8.01 (s, 2H), 7.70 − 7.63 (m, 2H), 7.11 − 6.44 (m, 14H), 4.08 (bs, 2H), 3.78 − 3.54 (bs, 20H), 3.37 (bs, 3H), 2.55 (bs, 2H), 1.89 − 0.86 (m, −CH_2 and CH_3 along with backbone).

2.2.13. Synthesis and Characterization of P(OEGMA-CA4-ALN-FMA) (15)

To a solution of compound 13 (100 mg, 0.002 mmol) in DMF (0.1 mL) was added 1-amino-2-propanol (0.041 mg, 0.0055 mmol) in DMF (10 µL). Reaction was stirred at rt for 24 h. After dialysis using 3.5 kDa cutoff regenerated cellulose acetate membrane in water (100 mL) for 2 d, viscous and colorless product 15 (0.083 g, 83%) was obtained by lyophilization. ^{1}H NMR ($CDCl_3$, δ, ppm) 8.01 (s, 2H), 7.69 − 7.62 (m, 2H), 7.12 − 6.44 (m, 14H), 4.08 (bs, 2H), 3.78 − 3.54 (bs, 20H), 3.37 (bs, 3H), 2.61 (bs, 2H), 2.56 (bs, 2H), 1.86 − 0.86 (m, −CH_2 and CH_3 along with backbone).

2.2.14. *In vitro* Drug Release

Drug release from polymer−drug conjugates were determined via LC−MS. Briefly, drug containing copolymer solutions were prepared in rat serum with total CA4 concentration of 1 mg/mL. Copolymer solutions were then incubated at 37 °C while stirring at 200 rpm for 96 h. A 200 μL sample was taken at predetermined time points, and plasma proteins were precipitated by ACN addition (800 μL). Tubes were centrifuged at 6000g for 5 min, and supernatants were analyzed for CA4 concentration by LC−MS analysis.

2.2.15. Serum Stability of CA4

CA4 (0.3 mg) was dissolved in rat plasma (1 mL) and solution was vortexed briefly. Free drug solutions were then incubated at 37 °C while stirring at 200 rpm for 96 h. A 200 μL sample was taken at predetermined time points, and plasma proteins were precipitated by ACN addition (800 μL). Tubes were centrifuged at 6000g for 5 min, and supernatants were analyzed for CA4 concentration by LC−MS analysis.

2.2.16. Hydroxyapatite Binding Assay

P(OEGMA-CA4-ALN) and P(OEGMA-CA4) copolymers containing equal amounts of drug CA4 (1 mg) were dissolved in phosphate buffered saline (PBS pH = 7.4, 1 mg / 2 mL). The conjugate solution was incubated with HA powder (200 mg), at 37 °C to mimic physiological conditions of bone tissue in body. At predetermined time points, samples were centrifuged at 6000g for 2 min, and supernatants were collected. Absorbance values at 287 nm were measured to detect CA4 amounts on unbound copolymers in the collected samples. Degree of HA binding capacity of copolymers was estimated according to formula given below:

$$\% \text{ binding} = \frac{A_{(\text{copolymer})_0} - A_{(\text{copolymer})t}}{A_{(\text{copolymer})_0}} \times 100$$

2.2.17. *In vitro* Cell Viability Assay on HUVEC's, Saos-2 and U-2 OS Human Osteosarcoma Cell Lines

Cell viabilities were determined by a formazan-based assay to quantify the mitochondrial activity (Cell Counting Kit-8 (CCK-8), Sigma). The cells were seeded at 3000 cells/well into 96-well plates and for each drug concentration they were seeded in quadruplicates. Cells were incubated overnight and after removal of their cell media fresh media containing various concentrations of conjugates, free drug, or controls was added onto the wells. CA4 stock solution was prepared in DMSO and diluted in working solutions with cell media where DMSO concentration 0.5% (v/v) and below. Subsequently treated cells were incubated continuously for 48 h. Following the treatments, drug containing media were removed and CCK-8 was applied. Briefly, 100 μL of cell culture media containing 10 μL of CCK-8 solution was added into each well and incubated for 4 h. The absorbance values at 450 nm were determined and the resulting cell viabilities of treated cells was calculated by dividing their value to the one of control cells (media only) thereby finding the percent viability. Non-linear regression analysis was utilized to calculate half maximal effective concentration (EC_{50}) values *via* Graphpad Prism v5 software.

2.2.18. Endothelial Cell Tube Formation Assay on HUVECs

Tube formation assay was done using Matrigel (BD Biosciences, USA) as reported in literature with minor modifications [263]. Briefly, OEGMA-CA4-ALN copolymer stock solution (1 μM) was prepared in EBM-2 cell media. Matrigel (75 μL/well) was added into wells of 96-well plates which was kept on ice in triplicates for each treatment concentration. Gels were let to solidify at 37 °C for 30 min and 10^4 HUVECs were seeded per well. Polymer solutions at various concentrations and free CA4 solution were added onto wells immediately. To control wells, only EBM-2 media was added. Cells were then incubated for 8 h at 37 °C. Images of formed tubes were collected using bright field microscopy. Negatives of collected images were processed using Angiogenesis Analyzer tool of ImageJ.

2.2.19. Internalization of FMA Containing Polymers

Human primary osteogenic sarcoma cell line Saos-2 cells (50.000 cells/well) were seeded in a 12-well plate as triplicate in 1000 µL of RPMI 1640 culture medium. Nontargeted copolymer 14 and targeted copolymer 15 (3 µM/mL concentration) were added onto the wells. Cells were incubated at 37 °C for 3 and 6 h for cells to adhere completely.

2.3. Results and Discussion

2.3.1. Synthesis and Characterization of CA4 Conjugated Copolymers

Copolymers containing the drug and the targeting units were synthesized by copolymerization of N-hydroxysuccinimide based activated ester containing monomer (NHSMA, 1) [129] the hydrophilic monomer oligo(ethylene glycol) methyl ether methacrylate (OEGMA, 2), and the antiangiogenic drug containing monomer (CA4MA, 3) (Figure 2.2).

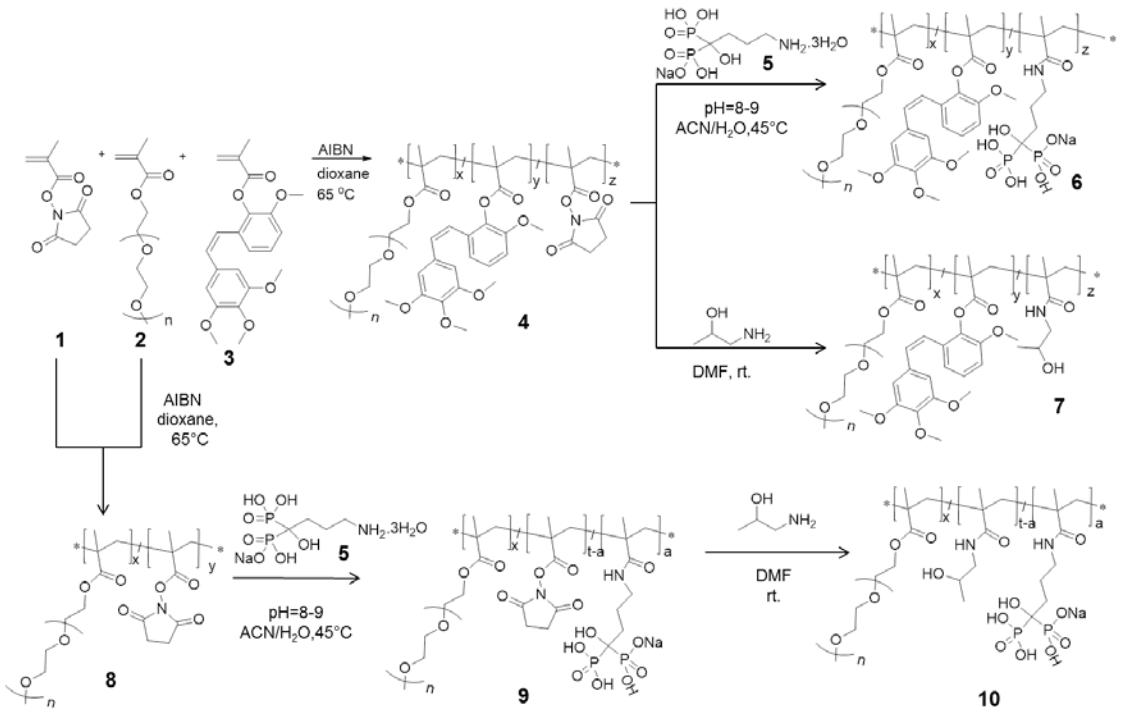

Figure 2.2. Synthetic Route for Drug and Targeting Moiety Appended Copolymers.

Table 2. 1. Polymerization Conditions and Characterization of Copolymers.

No	Copolymer	Feed Ratio				Obtained Ratio				M_n(kDa)	M_w/M_n
		1	2	3	11	1	2	3	11		
1	**4**	15	75	10	-	8.0	84.0	8.0	-	50.4	1.9
2	**8**	15	85	-	-	9.0	91.0	-	-	51.6	2.0
3	**12**	15	72	10	3	15.4	74.3	8.7	1.6	61.1	2.1

Table 2. 2. Properties of copolymers.

No	Copolymer	M_n (kDa)	M_w / M_n	CA4 wt%	ALN wt%	FMA wt%	1-amino-2 propanol wt%
1	P(OEGMA-CA4-ALN) **(6)**	50.4	1.9	13.8	3.24	-	-
2	P(OEGMA-CA4) **(7)**	50.4	1.9	16.0	-	-	3.0
3	P(OEGMA-ALN) **(10)**	51.6	2.0	-	6.96	-	1.4
4	P(OEGMA-CA4-NHS- FMA) **(14)**	61.4	2.1	8.55	-	1.77	6.90
5	P(OEGMA-CA4-ALN-NHS-FMA) **(15)**	61.4	2.1	8.58	4.16	1.40	7.88

As a subsequent step, the copolymer 4 was appended with bisphosphonate groups through conjugation of alendronate through the NHS activated ester side chain groups, as well as a copolymer devoid of any targeting unit was prepared by quenching of the activated ester groups with an amino alcohol. In particular, copolymer 4 was dissolved in acetonitrile, and a solution of sodium alendronate in PBS was added to it. The pH of the resulting mixture was adjusted between 8.0−9.0 by the addition of NaOH solution (1.0 N). The resulting copolymer was dialyzed in water using regenerated cellulose acetate membrane to remove unconjugated sodium alendronate.

The final product, P(OEGMA-CA4-ALN) (6), carrying both the drug and the targeting unit, possessed an average molecular weight of 50.4 kDa as determined using via SEC. Compositional analysis using ^{1}H NMR revealed that the copolymer contained about 14% drug by weight, while the targeting unit was about 3.24 wt % (Table 2.2, item 1). The ^{1}H NMR spectrum of the copolymer also revealed that there were no residual active NHS groups on the copolymer. The weight percentages of the monomers as determined *via* ^{1}H NMR are summarized in Table 2.2. Another portion of copolymer 4 was reacted with 1-amino-2-propanol to obtain an analogue of copolymer 6 without the targeting moiety.

The combretastatin based methacrylate monomer (CA4MA, 3) was synthesized by esterification of the hydroxyl functional group on the CA4 molecule with methacryloyl chloride. Thus, the drug moiety (CA4) is attached to the copolymer through an ester linkage, rendering the structure hydrolyzable in the presence of esterases or in acidic environment found inside the lysosomes [264, 265]. First, the drug bearing copolymer 4 was synthesized *via* AIBN initiated free radical copolymerization in dioxane. Obtained random copolymer was characterized using ^{1}H NMR to determine the composition of the monomers in the copolymer, and size exclusion chromatography (SEC) to determine its molecular weight and distribution. Using a feed ratio of 75:15:10 for monomers 1, 2, and 3, respectively, resulted in a copolymer 4 where the incorporation of monomers was 84:8:8 (Table 2.1, item 1).

A parent batch of copolymer 4 was utilized to obtain the subsequent copolymers to ensure that the copolymers 6 and 7 have the same molecular weights and distributions, as well as identical drug content for copolymers with and without the targeting unit. The use of 1-amino-2-propanol for quenching the activated ester groups along the polymer backbone yielded a hydroxypropyl methacrylamide based side chain, a well-known and widely studied building block in macromolecular drug delivery [182], [266]–[268] resulting copolymer 7 was characterized via ^{1}H NMR spectroscopy to reveal, as expected, that the construct preserved its drug content during the removal of the activated NHS esters (Table 2.2, item 2). With the purpose of synthesizing copolymers devoid of any drug unit, but bearing only the targeting moiety, monomers 1 and 2 were copolymerized to yield copolymer 8 which was further reacted with alendronate sodium salt to afford copolymer 9, followed by treatment with 1-amino-2-propanol to obtain P(OEGMA-ALN) (10). While the polyethylene glycol-based side, chains provide high aqueous solubility for the polymer−drug conjugate,

they are also known to provide an antibiofouling character due to minimal interaction with proteins and cells. Hence, we wanted to also check if these constructs are capable of undergoing cellular internalization. In order to investigate cellular internalization, fluorescein-O-methacrylate (FMA) containing fluorescent copolymers were synthesized (Figure 2.3). As with the nonfluorescent polymers, both the targeted and nontargeted copolymers stemmed from a single batch rendering them identical in size and drug content. Nontargeted copolymer 14 (Table 2.2, item 4) and targeted copolymer 15 (Table 2.2, item 5) were used for the internalization experiment.

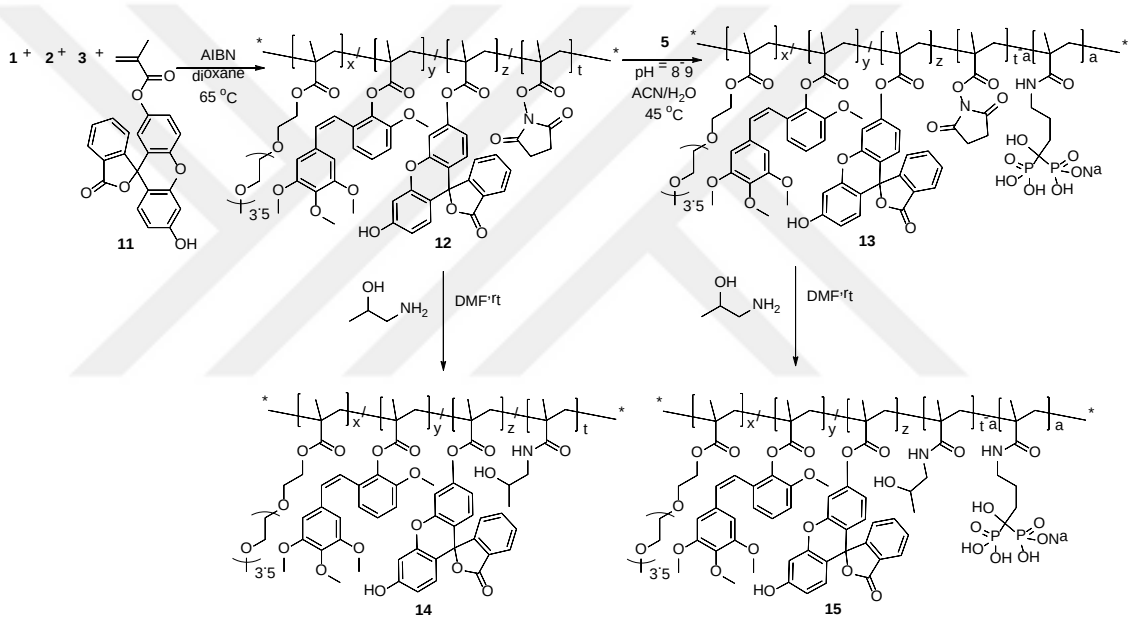

Figure 2.3. Synthetic Route for FMA Containing Fluorescent Copolymers.

2.3.2. Hydroxyapatite Binding Assay

To explore the binding capacity of alendronate bearing copolymer P(OEGCA4MA-ALN) 6 to bone tissue, its binding potency to HA was evaluated. Copolymer 6 was dissolved in PBS (pH = 7.4, 0.5 mg/mL) and incubated with HA powder (200 mg) at 37 °C. As a control experiment, to understand the role played by the ALN unit toward HA binding, HA was treated with copolymer 7, namely, P(OEGMA-CA4), in an identical manner. At predetermined time points, aliquots were collected and centrifuged at 6000g to determine

the amount of unbound conjugates using UV−vis spectroscopy. Within 20 min of incubation, 50% of copolymer 6 was bound to HA, whereas only 3% of copolymer 7 was bound to HA. The HA binding of P(OEGMA-CA4-ALN) conjugate reached a plateau around 75% after 60 min of incubation (Figure 2.4). The observed trend and extent of binding is similar to that observed for bisphosphonate containing polymeric constructs reported in the literature [98]. Binding constant values (K) of conjugates were calculated by using GraphPad Prism software version 5.03 via one-site total binding analysis. Binding isotherms of copolymers 6 and 7 in PBS exhibited correlation coefficient (R^2) of 0.985 and 0.989, respectively, with binding constant values 16.41 and 0.095 mg/L.

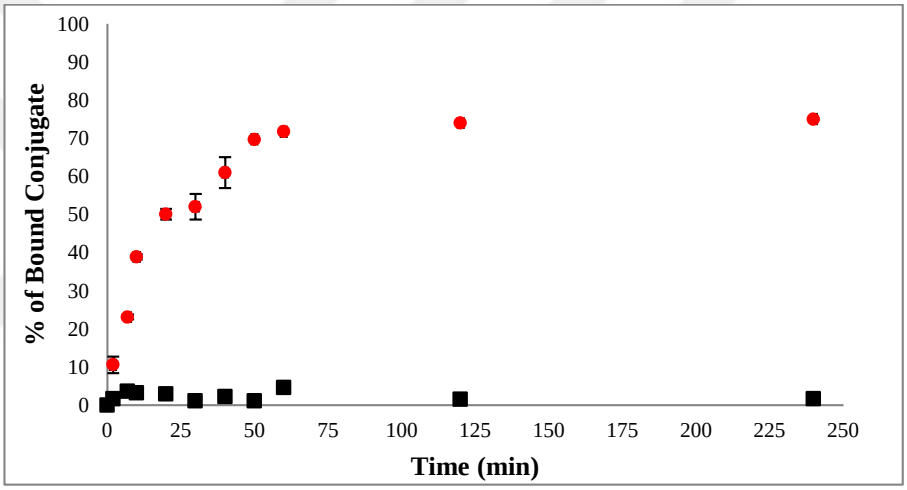

Figure 2.4. Binding kinetics of P(OEGMA-CA4-ALN) (6) (red circle) and P(OEGMA-CA4) (7) (black square) copolymers to bone mineral HA in PBS.

2.3.3. Drug Release Profiles of Copolymers

When drugs are conjugated covalently to the systems via ester-based linkers, release profiles may be improved at acidic environments or in the presence of hydrolytic enzymes like esterases. Drug conjugated copolymers were incubated at 37 °C in rat plasma, to assess enzymatic release of CA4 from copolymers (Figure 2.5). Initially, to investigate the stability of CA4 in rat plasma, free CA4 was incubated at 37 °C, and samples were collected at predetermined time points and analyzed using LC−MS to reveal that on an average about 95% of the total free drug could be determined after incubation in rat plasma, suggesting that

a small amount of free drug perhaps complexes with the plasma proteins and thus remains undetected. This underestimation was factored in while calculating the release of the drug from the copolymer. A gradual release of CA4 was observed for both copolymers with an overall release of 93% and 80% from P(OEGMA-CA4) and P(OEGMA-CA4-ALN) at the end of 5 days, respectively, while the release from P(OEGMA-CA4-ALN) plateaus at 96% after 6 days. Statistical analysis of the release data showed that there is no meaningful difference between the targeted versus nontargeted conjugates.

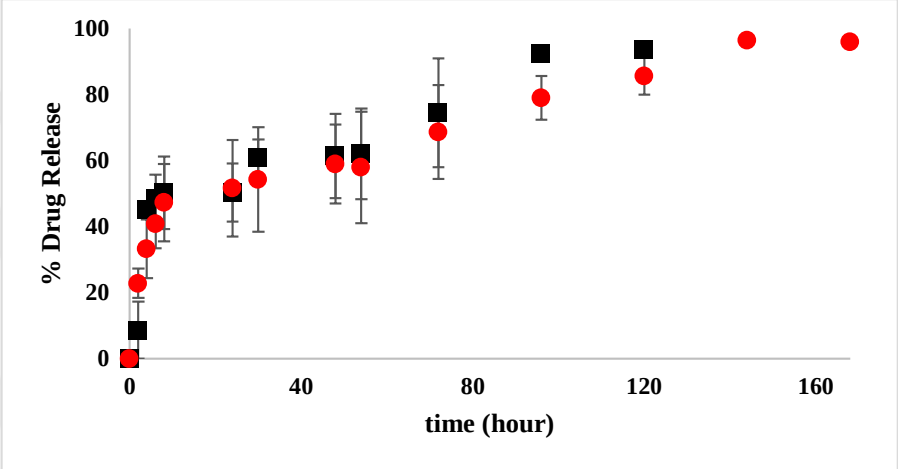

Figure 2.5. Release of CA4 from P(OEGMA-CA4-ALN) (6) (red circle) and P(OEGMA-CA4) (7) (black square) copolymers in rat plasma.

2.3.4. Determination of in vitro Cytotoxicity of Copolymers on HUVECs, Saos-2, and U2-OS Cells.

To evaluate the antiangiogenic effect of polymer conjugated CA4, a proliferation assay was performed on HUVECs by exposing them to free ALN, free CA4, P(OEGMA-CA4) (copolymer 7), and P(OEGMA-CA4-ALN) (copolymer 6). The EC_{50} estimation was performed using GraphPad Prism software version 5.03 *via* nonlinear regression with three-parameter analysis demonstrating best fit overall. Due to slow release of drug from copolymers, EC_{50} values of copolymers were higher than free CA4 as expected, and free drug was observed to be highly toxic toward HUVECs (0.107 nM) in 48 h (Figure 2.7.A). Both targeting group containing copolymer 6 and the nontargeted copolymer 7 inhibited

proliferation of HUVECs at nanomolar concentrations (Figure 2.7.A). Analysis of growth inhibition curves revealed that the targeted and nontargeted copolymers were 15−20 times less toxic than free CA4 when cells were incubated for 48 h (Table 2.3). The difference between the CA4 alone versus conjugated constructs was well within the expected range for macromolecular therapeutics [269]. In order to test the effect of ALN alone on HUVECs, free ALN and P(OEGMAALN) (10) were incubated with HUVECs. The lack of inhibitory activity at low concentrations was clearly visible (Figure 2.7.B).

Table 2. 3. Calculated EC_{50} values after continuous incubation HUVECs, U2-OS and Saos-2 cells for 48 h.

No	**Sample**	**EC_{50} value (M)**		
		HUVEC	**U2-OS**	**Saos-2**
1	CA4	1.07×10^{-10}	1.26×10^{-9}	4.39×10^{-9}
2	ALN	$> 10^{-5}$	$> 10^{-5}$	$> 10^{-5}$
3	P(OEGMA-CA4-ALN) (**6**)	1.42×10^{-9}	3.96×10^{-8}	7.30×10^{-7}
4	P(OEGMA-CA4) (**7**)	2.46×10^{-9}	8.50×10^{-8}	4.55×10^{-6}
5	P(OEGMA-ALN) (**8**)	$> 10^{-5}$	$> 10^{-5}$	$> 10^{-5}$

Comparison of effect on other cell lines revealed that HUVECs were more sensitive to CA4 compared to U2-OS and Saos-2 cells since only 10 − 20% of CA4 was required to achieve the same magnitude of cell growth inhibition (Figure 2.7.C−D). The performances of targeted copolymer 6 versus the nontargeted copolymer 7 against U2-OS cells were similar to their performance with HUVECS (Figure 2.7.D). Notably, P(OEGMA-CA4-ALN) (copolymer 6) was slightly more active (about 3-fold) than P(OEGMA-CA4) (copolymer 7), while both the constructs were at least an order of magnitude less active than CA4 alone (Table 2.3). Effect of free CA4 versus conjugated CA4 was more apparent against Saos-2 cells (Figure 2.7.C). While the growth inhibitory activity of CA4 was still in the nanomolar range (4.39 nM), the targeted conjugate 6 and nontargeted conjugate 7 were less toxic by 60 and 1000 times, respectively (Table 2.3).

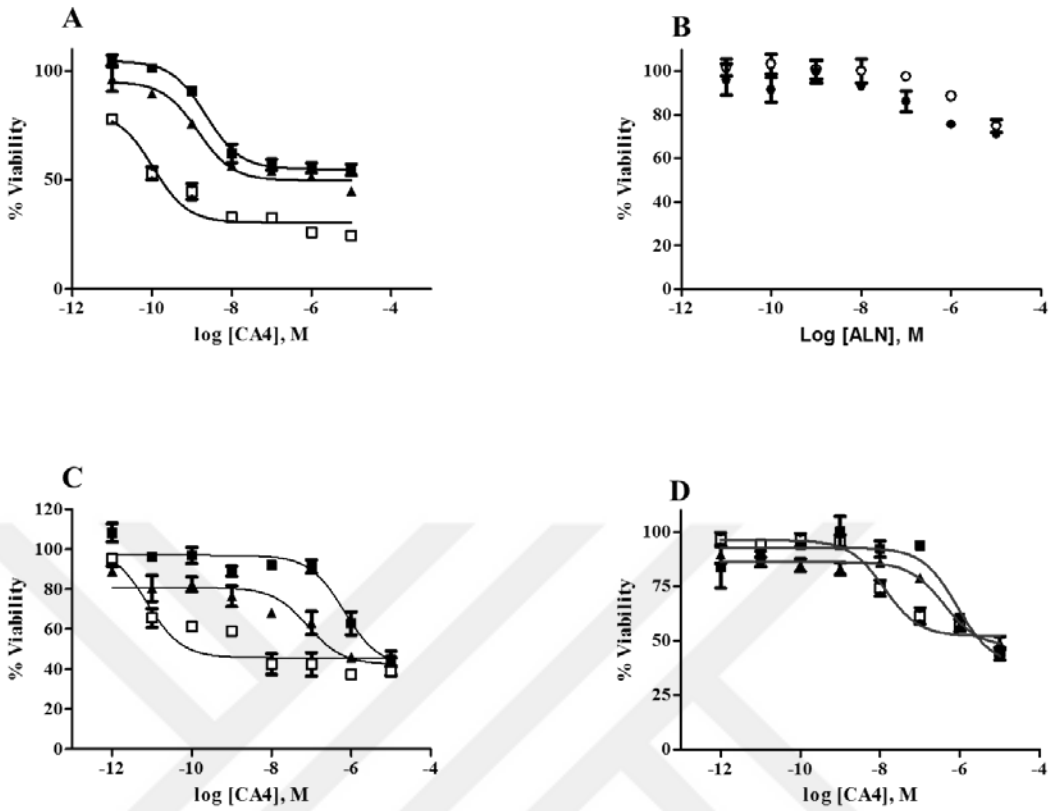

Figure 2.6. Viabilities of (A), (B) HUVECs, (C) Saos-2 and (D) U2-OS cells treated with free CA4 □, free ALN ○, P(OEGMA-CA4) ■, P(OEGMA-CA4-ALN) ▲, P(OEGMA-ALN) ●.

2.3.5. Cell Internalization Studies

Following the investigation of the in vitro cytotoxicity of the various copolymers, we wanted to see if the polymeric constructs are internalized by the cells. For this, we incubated Saos-2 cells with the targeted copolymer 13 and nontargeted copolymer 12. Green fluorescence was observed for both cell populations under the fluorescence microscopy (Figure 2.7). As expected, the degree of internalization increased with time (data not shown) but the extent of internalization was comparable for both targeted copolymer 14 and the nontargeted copolymer 15 demonstrating that the targeting group's polarity did not have a significant effect on the process.

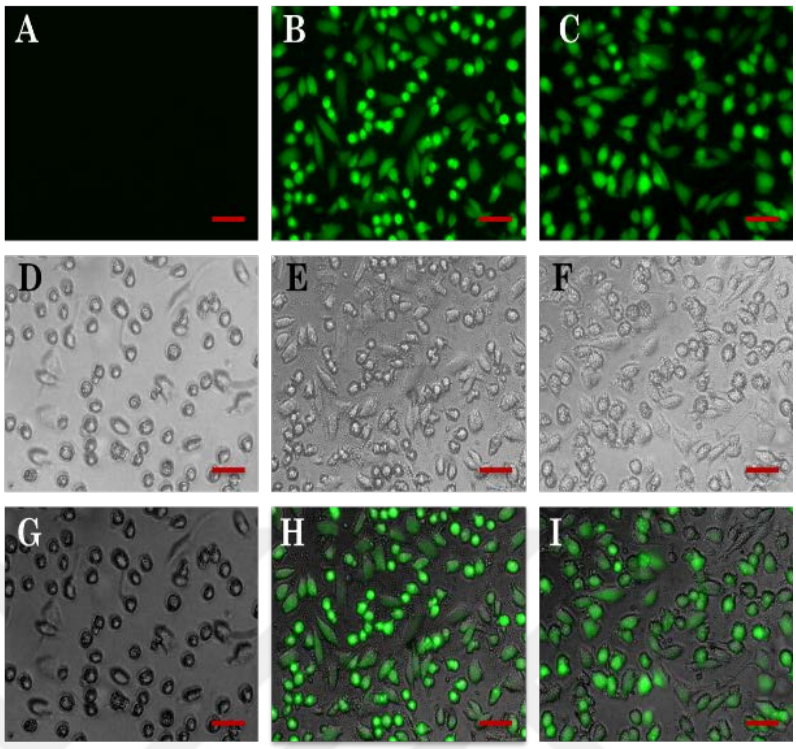

Figure 2.7. Microscopy images (fluorescence, bright field, overlap) of Saos-2 cells after 3 h incubation with fluorescently labeled copolymers.

2.3.6. Endothelial Tube Formation Assay on HUVECs.

One of the most well-established *in vitro* assays to study angiogenesis is the tube formation assay. In this assay, the ability of antiangiogenic drug bearing copolymer to inhibit tube formation was investigated using solid Matrigel, which is a growth factor reduced basement membrane. The tube formations are analyzed for segments and junctions. Segments are delimited by two junctions; master segments consist of segments where the junctions are not part of the same branch. Master junctions are junctions linking at least three master segments. In absence of any drug, vein precursor HUVECs formed three-dimensional capillary-like vasculature (Figure 2.8). However, addition of free drug decreased tube and junction formation as expected, thus highlighting CA4's antiangiogenic activity. A similar trend was observable for the drug conjugated copolymers, and a dose response was notable as well.

Number of junctions at control samples with 52.6 ± 7.9 junctions reduced to almost half of this value at wells treated with 10 nM CA4 containing conjugated polymer, 25.0 ± 7.0.

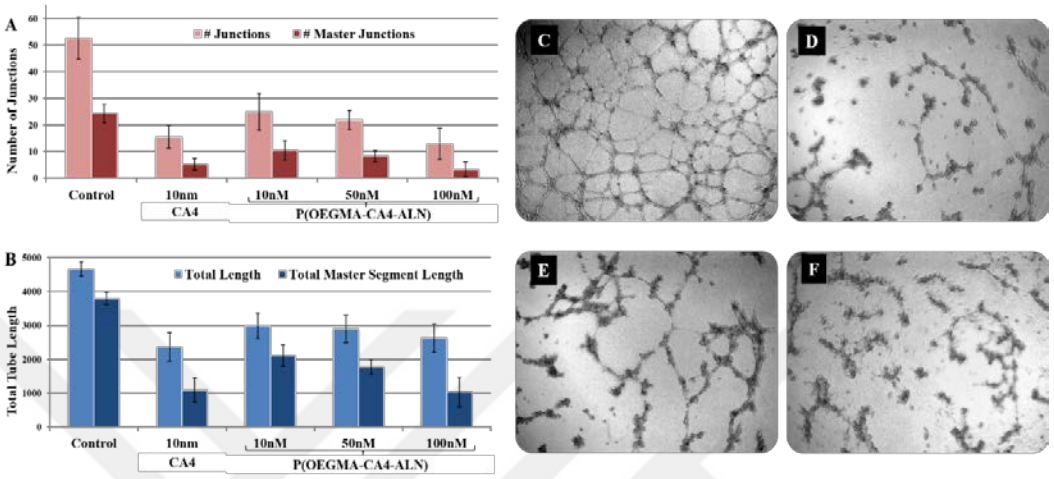

Figure 2.8. Anti-angiogenic assay using HUVECs on Matrigel. (A) Number of junctions and (B) total tube lengths.

The decline continued with 50 and 100 nM polymer−drug samples in gradual manner; number of junctions decreased to 20.0 ± 3.6 and 13.0 ± 5.8 for 50 and 100 nM samples, respectively. Furthermore, free drug at 10 nM decreased this number to 15.5 ± 4.3, which was comparable to the value of polymer conjugate at 100 nM. This effect becomes more prominent when number of master junctions was compared; a dramatic decrease in number of master junctions was observed between control wells, 24.3 ± 3.5, and 100 nM CA4 containing polymer conjugate, 3.4 ± 2.9. Change in total tube length showed similar trend for almost all wells. Total tube length at control well was measured as 4666 ± 207, and the most prominent decrease was observed at free CA4 and polymer conjugates at 100 nM to 2368 ± 419 and 2621 ± 413, respectively. However, with 500 nM copolymer solution, any measurable tube formation was not observed (data not shown). Thus, this data suggest that these polymer−drug conjugates can inhibit tube formation in vitro almost as effective as the free drug itself, thus highlighting their antiangiogenic potential *in vivo*.

2.4. Conclusions

A P(OEGMA) based polymeric carrier for targeting an antiangiogenic agent CA4 to the bone tissues was synthesized and evaluated for cytotoxicity and antiangiogenic activity. As a bone targeting unit, a small molecule amino bisphosphonate drug alendronate was conjugated to the drug-containing copolymer *via* amidation. A remarkably preferential affinity toward the bone mineral hydroxyapatite was observed for the bisphosphonate targeting group bearing polymer−drug conjugate P(OEGMA-CA4-ALN), when compared to the P-(OEGMA-CA4) copolymer devoid of any targeting unit. Effective release behavior of drug in rat plasma was observed from both targeted and nontargeted copolymers. The polymer−drug conjugates demonstrated cytotoxicity toward different HUVECs, U2-OS, and Saos-2 cell lines. Furthermore, an antiangiogenic assay with HUVECs using the drug conjugated polymers demonstrated effective inhibition of tube formation in a dose-dependent manner. These bisphosphonate functional groups bearing polymers conjugated with an antiangiogenic agent, namely, CA4, provides an attractive construct that can be further elaborated by incorporating additional drugs that act through different pathways to address challenges associated with treatment of metastatic bone cancer.

3. INTEGRIN TARGETED ANTI-ANGIOGENIC AND ANTI-NEOPLASTIC AGENT CARRYING COPOLYMERS FOR OVARIAN CANCER TREATMENT

3.1. Introduction

Ovarian cancer can be considered as one of the most dangerous cancer type due to it does not show any symptom in the early stage. It is generally diagnosed at a late stage because any effective screening strategies for ovarian cancer have not been developed yet [270] . It has different histological subtypes and each of them has different treatment ways, molecular structuring and stem cell morphology. When it is first diagnosed, cytoreductive surgery is generally applied [271]. According to latest researchers, ovarian cancer is responsible for 125.000 deaths of women in a worldwide. Most of these women die because of drug resistance after five years of diagnosis [272]. Except those, angiogenesis is so crucial and the most considerable factor in ovarian cancer treatment because follicular growth and corpus luteum development is due to angiogenesis and new blood vessel formation. In the techa layer of follicles, vascular network is formed by pre-existing endothelial cells as a result of some growth factors stimuli. These factors are including vascular endothelial growth factor (VEGF) and basic fibroblast growth factor (bFGF) [273]. Many associations have been explored between ovarian cancer and survival rate after initial antiangiogenic therapy. hence, anti-VEGF therapy became relevant strategy in ovarian cancer treatment [274]. Together with anti-angiogenic therapy, the most encountered methods for ovarian cancer treatment is drug combinations in which platinum based agents, taxanes and anti-angiogenic agents are utilized [275]. Moreover, targeted drug delivery systems are used such as integrin targeted as well.

Integrins are formed by 24 heterodimeric transmembrane proteins and they are expressed on most of the cells. They have important role on attachment to proteins of extracellular matrix to other cells. Furthermore, in some pathological diseases such as cancer, their presence is essential. It has been proved that in so many cancer cells, integrins

are overexpressed on the cell membrane hence they are very crucial constitutes in progression of angiogenesis and metastases. For instance, in angiogenesis process of cancer, $\alpha_v\beta_3$, $\alpha_v\beta_5$, and $\alpha_5\beta_1$ ligands are involved mainly. Their overexpression on cancer cell membrane, makes them very crucial and worthy tools for targeted drug delivery systems. RGD tripeptide is generally used for targeting $\alpha_v\beta_3$, $\alpha_v\beta_5$ integrins. In addition to that, α_v integrins, two β integrins and $\alpha IIb\beta_3$ integrins can recognized by RGD peptide. So that some RGD containing peptides such as cRGDfK, cRGDeV or cRGDyV are being studied for development of selective targeting to tumor site. Moreover, RGD containing macromolecules have been improved by researchers in recent years.

As for drug combination therapy, there are so many clinical trials that have been performed. In 2008, combination of bevacizumab and metronomic oral cyclophosphamide was prepared for interm clinical trials. According to results which are obtained from 70 patients, a partial response was achieved in 24% of patients [276]. In 2010, one of the studies showed that when Paclitaxel is administered to recurrent ovarian cancer patients weekly, myelosuppression can be reduced [277]. These clinical trials proved weekly paclitaxel is very effective on patients. Furthermore, it has been explored that, after treatment patients with platinum/taxane combinations, a complete remission was gained. However, relapse was observed in approximately more than 90% of these responding patients [278]. All these studies showed, each of anti-angiogenic drugs and taxane group agents are singly effective on ovarian cancer, and obtained results supported the approaches of designing combination anti-VEGF agents with chemotherapy drugs.

For example, one of the phase II studies tested imatinib with docetaxel combination on patients who have platinum-resistant ovarian cancer. While docetaxel was given to patients every week at 30 mg/m^2, imatinib was administrated every day at 600 mg. Drug administrations continued until obtaining objective response rates from patients. Among all patients, complete response was obtained from only one patient. More importantly, median overall survival length was 9.56 months [279]. In our study we are reporting the synthesis and characterizations of polymer-drug conjugates bearing both anti-angiogenic drug combretastatin A-4 and anti-neoplastic drug docetaxel. As mentioned from clinical studies above, challenging results and datas are obtained from combinations of antiangiogenic and taxane agents for ovarian cancer. In our design, we also used cRGDfK molecule for targeting

cancer cells. Our construct was gained antiproliferative activity by combretastatin for cancer cells. On the other hand, it will act as promoter for micro tubulin formation with the help of docetaxel. More importantly, due to it has targeting group on it, polymer is expected to reach tumor region directly without harming any healthy tissue. Poly(oligoethylene glycol) was used as polymeric backbone carrier. After that, in vitro experiments on ovarian cancer cell line were achieved to evaluate copolymers' toxicity.

3.2. Experimental Section

3.2.1. Materials

Methacryloyl chloride was purchased from Alfa Aesar. The solvents used throughout this thesis were purchased from Merck. Milli-Q Water Purification System (Milli-Q system, Millipore, Billerica, MA, USA) was employed to produce ultrapure water. All the other chemicals were purchased from Sigma Aldrich. Polyethylene glycol methacrylate (OEGMA M_n = 300) was filtered through basic alumina column prior to use. NHSMA (N-hydroxysuccinimide methacrylate), Combretastatin A-4 (CA4), MA-GFLG-DTX monomers and cRGDfK peptide were synthesized according to previously reported protocols [261, 262, 283]. SC-OV-3 and Caov-3 ovarian cancer cell line was purchased from ATCC.

3.2.2. Instrumentation

^{1}H and ^{13}C NMR spectroscopy (Varian 400 MHz NMR spectrometer), Fourier transform infrared (ATR-FTIR) spectroscopy (Nicolet 380, Thermo Scientific, USA), and UV−vis spectroscopy (PerkinElmer series) methodologies were used in order to characterize synthesized monomers and polymers. The qualification and quantification of CA4 monomer (CA4MA) and cRGDfK were achieved utilizing the liquid chromatography−mass spectrometry (LC−MS) system (LCMS 2020, Shimadzu, Japan) with a C- 18 (5 μm, 150 × 4.6 mm) column. A gradient method was utilized with acetonitrile (ACN) and deionized water supplemented with 0.05% trifluoroacetic acid (TFA) through the following program;

LC: 0−3 min, 50% ACN; 3.01 min, 50% ACN; 8 min, 95% ACN; 8.01−11 min, 50% ACN; MS positive scan 100−800 m/z. The polymer molecular weights were estimated by size exclusion chromatography (SEC) (Shimadzu, Japan) PSS-SDV (length/ID 8 × 300 mm, 10 mm particle size) linear Mixed C column calibrated with polymethyl methacrylate using a refractive-index detector with a mobile phase solution of 0.05 M lithium bromide in dimethylaceteamide (DMAc) as eluent at a flow rate of 1 mL/min at 30 ºC. During the internalization experiments cells were visualized using Zeiss Observer.Z1 inverted fluorescence microscope.

3.2.3. Synthesis and Characterization of P(OEGMA-CA4-NHS) (18)

Poly(ethylene glycol) methyl ether methacrylate (O(EGMA)) (1.00 g. 3.33 mmol), CA4MA (0.36 g, 0.952 mmol) and NHSMA (0.087 g, 0.475 mmol) were dissolved in anhydrous DMF (5 mL). To the polymer solution was added 4-cyano-4-(phenylcarbonothioylthio) pentanoic acid (6.2 mg, 0.0237 mmol) as chain transfer agent (CTA) and AIBN (0.78 mg, 0.00475 mmol) as initiator. Reaction mixture was stirred under N_2 for 30 min. Reaction was sealed and heated at 70 °C for 20 h. The copolymer was purified via precipitation in diethyl ether, dissolved in CH_2Cl_2 and re-precipitated. After precipitation, copolymer was washed with diethyl ether. The product was dried in high *vacuo* and obtained as viscous liquid. (0.7 g, 48 % yield). M_n = 48 kDa, M_w/M_n = 1.35). ^{1}H NMR (DMSO-*d6*, δ, ppm) 7.14 - 6.98 (m, 3H), 6.51 - 6.49 (m, 4H), 4.03 (bs, 2H), 3.51 - 3.36 (m, 20H), 3.24 (bs, 2H), 2.79 (bs, 4H), 2.08 - 0.80 (m, $-CH_2$ and CH_3 along with backbone).

3.2.4. Synthesis and Characterization of P(OEGMA-CA4-RGD) (19)

Copolymer 18 (0.35 g) and cRGDfK (97 mg, 0.16 mmol) were dissolved in DMF (0.4 mL). To the copolymer solution, DIPEA (0.3 mL, 1.6 mmol) was added dropwise. Resulting reaction mixture was stirred at ambient temperature for 24 h. Then, ethanolamine (0.9 mg, 0.16 mmol) was added to reaction mixture and reaction kept stirring at 45 °C for 1 more day. Upon completion of the reaction, resulted copolymer was purified by using 3.5 kDa cut off membrane by dialysis. Copolymer was diluted with MeOH (10 mL) and placed in a 3.5 kDa

cutoff dialysis bag. Dialysis bag was placed in a beaker containing MeOH (250 mL). Solvent was changed 3 times/day and dialysis was completed in 2 days. After dialysis, solvent was evaporated and dried under *vacuo* to obtain copolymer 19 (0.15 g, 43%). M_n = 48 kDa, M_w/M_n = 1.35). ^{1}H NMR (DMSO-*d6*, δ, ppm) 7.13 - 6.97 (m, 3.74 H), 6.50 - 6.48 (m, 4H), 4.01 (bs, 2H), 3.75 - 3.34 (m, 20H), 3.24 (bs, 2H), 1.83 – 0.80 (m, $-CH_2$ and CH_3 along with backbone).

3.2.5. Synthesis and Characterization of P(OEGMA-CA4) (20)

To a solution of compound 18 (0.35 g) in DMF (0.35 mL), was added ethanol amine (0.012 g, 0.2 mmol) in DMF (0.2 mL). Reaction was stirred at ambient temperature for 24 h. Resulted copolymer was purified by using 3.5 kDa cut off membrane by dialysis. Copolymer was diluted with MeOH (10 mL) and placed in a 3.5 kDa cutoff dialysis bag. Dialysis bag was placed in a beaker containing MeOH (250 mL). Solvent was changed 3 times/day and dialysis was completed in 2 days. After dialysis, solvent was evaporated and dried under *vacuo* to obtain copolymer 20 (0.17 g, 50%). M_n = 48 kDa, M_w/M_n = 1.35). ^{1}H NMR (DMSO-*d6*, δ, ppm). 7.13 - 6.97 (m, 3H), 6.50-6.48 (m, 4H), 4.01 (bs, 2H), 3.74 - 3.35 (m, 20H), 3.23 (bs, 3H), 1.83 - 0.79 (m, $-CH_2$ and CH_3 along with backbone).

3.2.6. Synthesis and characterization of P(OEGMA-CA4-NHS-DTX) (21)

O(EGMA) (0.5 g. 1.66 mmol), CA4MA (0.12 g, 0.266 mmol) and NHSMA (0.005 g, 0.011 mmol) were dissolved in anhydrous DMF (2.0 mL). To the polymer solution was added CTA (2.5 mg, 0.0098 mmol) as chain transfer agent and AIBN (0.32 mg, 0.0091 mmol) as initiator. Reaction mixture was stirred under N_2 for 30 min. Reaction was sealed and heated 80 °C for 1 h. Then, temperature of oil bath was decreased to 50 °C. By the time desirable heat was reached, Methacrylated Gly-Phe-Leu-Gly-Docetaxel (MAGFLGDTX) (0.22 g, 0.17 mmol) solution in anhydrous DMF (0.5 mL) was added under N_2 in 2 min. After drug adding process, reaction was left at 50 °C for 47 hours. Then, molecular weight and PDI of polymer was checked by gel permeation chromatography (GPC). Resulted copolymer was purified by using 10kDa cut off membrane by dialysis. Copolymer was

diluted with 10 mL of acetonitrile (ACN) and put in the 10kDa cutoff dialysis bag. Dialysis bag was put in beaker with 250 mL of acetonitrile. Solvent was changed 3 times in a day and dialysis was done in 2 days. After dialysis, solvent was evaporated and dried under *vacuo.* (0.3 g, 60%). M_n = 56 kDa M_w/M_n = 1.38. ^{1}H NMR (DMSO-*d6*, δ, ppm). 8.24 - 6.88 (m, 20H), 6.50 - 6.48 (m, 4H), 4.01 (bs, 2H), 3.74 - 3.35 (m, 20H), 3.23 (bs, 3H), 2.80 (s, 4H), 1.83 - 0.79 (m, $-CH_2$ and CH_3 along with backbone).

3.2.7. Synthesis and characterization of P(OEGMA-CA4-RGD-DTX) (22)

Copolymer 21 (0.15 g) and cRGDfK (43 mg, 0.07 mmol) were dissolved in DMF (0.2 mL). To the copolymer solution, DIPEA (0.012 g, 0.07 mmol) was added dropwise, resulting reaction mixture was stirred at 45 °C for 24 h. Then, ethanolamine (0.08 mmol, 5.0 mg) was added to reaction mixture and reaction kept stirring at ambient temperature for 1 more day. Resulted copolymer was purified by using 3.5 kDa cut off membrane by dialysis. Copolymer was diluted with MeOH (10 mL) and placed in a 3.5 kDa cutoff dialysis bag. Dialysis bag was placed in a beaker containing MeOH (250 mL). Solvent was changed 3 times/day and dialysis was completed in 2 days. After dialysis, solvent was evaporated and dried under *vacuo* to obtain copolymer 22. (0.6 g, 40%). M_n = 56 kDa, M_w/M_n = 1.38. ^{1}H NMR (DMSO-*d6,* δ, ppm). 8.24 - 6.88 (m, 25H), 6.50 - 6.48 (m, 4H), 4.01 (bs, 2H), 3.74 - 3.35 (m, 20H), 3.23 (bs, 3H), 1.83 - 0.79 (m, $-CH_2$ and CH_3 along with backbone).

3.2.8. Synthesis and characterization of P(OEGMA-CA4- DTX) (23)

To a solution of compound 21, (0.15 g) in DMF (0.15 mL), was added ethanol amine (0.04 g, 0.7 mmol) in DMF (0.2 mL). Reaction was stirred at ambient temperature for 24 h. Resulted copolymer was purified by using 3.5 kDa cut off membrane by dialysis. Copolymer was diluted with MeOH (10 mL) and placed in a 3.5 kDa cutoff dialysis bag. Dialysis bag was placed in a beaker containing MeOH (250 mL). Solvent was changed 3 times/day and dialysis was completed in 2 days. After dialysis, solvent was evaporated and dried under *vacuo* to obtain copolymer 23. (0.07 g, 48%). M_n = 56 kDa, M_w/M_n=1.38. ^{1}H NMR (DMSO-

d6, δ, ppm). 8.24 - 6.88 (m, 20H), 6.50 - 6.48 (m, 4H), 4.01 (bs, 2H), 3.74 - 3.35 (m, 20H), 3.23 (bs, 3H), 1.83 - 0.79 (m, $-CH_2$ and CH_3 along with backbone).

3.2.9. Synthesis and characterization of P(OEGMA-CA4-NHS-FMA) (24)

OEGMA (0.3 g, 1 mmol), CA4MA (90 mg, 0.28 mmol), NHSMA (26 mg, 0.14 mmol) and FMA 11 mg, 0.0285 mmol) were dissolved in anhydrous DMF (3 mL). To the copolymer solution was added CTA (1.8 mg, 0.0071 mmol) as chain transfer agent and AIBN (0.23 mg, 0.0014 mmol) as initiator. Reaction mixture was stirred under N_2 for 30 min. After purge process, reaction was sealed and heated at 70 °C for 20 h. The copolymer was purified *via* precipitation in diethyl ether, dissolved in CH_2Cl_2 and re-precipitated. After precipitation, copolymer was washed with diethyl ether. The product was dried in high *vacuo* and obtained as viscous liquid. (0.25 g, 64%). M_n = 48 kDa, M_w/M_n = 1.35. ^{1}H NMR (DMSO-*d6*, δ, ppm). 8.02 (bs, 1H), 7.81 - 6.51 (m, 15H), 4.03 (bs, 2H), 3.61 - 3.35 (m, 20H), 3.24 (bs, 3H), 2.78 (bs, 4H), 1.85 - 0.80 (m, $-CH_2$ and CH_3 along with backbone).

3.2.10. Synthesis and characterization of P(OEGMA-CA4-RGD-FMA) (25)

Copolymer 24 (0.12 g) and cRGDfK (46 mg, 0.077 mmol) were dissolved in DMF (0.15 mL). To the copolymer solution, DIPEA (10 mg, 0.08 mmol) was added dropwise. Resulting reaction mixture was stirred at 45 °C for 24 h. Then, ethanolamine (6.0 mg, 1 mmol) was added to reaction mixture and reaction kept stirring at ambient temperature for 1 more day. Resulted copolymer was purified by using 3.5 kDa cut off membrane by dialysis. Copolymer was diluted with MeOH (5 mL) and placed in a 3.5 kDa cutoff dialysis bag. Dialysis bag was placed in a beaker containing MeOH (250 mL). Solvent was changed 3 times/day and dialysis was completed in 2 days. After dialysis, solvent was evaporated and dried under *vacuo* to obtain copolymer 25 (0.1 g, 83%). M_n = 48 kDa, M_w/M_n = 1.35. ^{1}H NMR (DMSO-*d6*, δ, ppm). 8.02 (bs, 1H), 7.81 - 6.48 (m, 20H), 4.02 (bs, 2H), 3.60-3.34 (m, 20H), 3.23 (bs, 3H), 1.84 - 0.80 (m, $-CH_2$ and CH_3 along with backbone).

3.2.11. Synthesis and characterization of P(OEGMA-CA4-FMA) (26)

To a solution of compound 24, (0.12 g) in DMF (0.15 mL), was added ethanol amine (0.052 g, 0.7 mmol) in DMF (0.05 mL). Reaction was stirred at ambient temperature for 24 h. Resulted copolymer was purified by using 3.5 kDa cut off membrane by dialysis. Copolymer was diluted with MeOH (3 mL) and placed in a 3.5 kDa cutoff dialysis bag. Dialysis bag was placed in a beaker containing acetonitrile (100 mL). Solvent was changed 3 times/day and dialysis was completed in 2 days. After dialysis, solvent was evaporated and dried under *vacuo* to obtain copolymer 26 (0.07 g, 58%). M_n = 48 kDa, M_n/M_w = 1.35. ^{1}H NMR (DMSO-*d6*, δ, ppm). 8.02 (bs, 1H), 7.82 - 6.50 (m, 15H), 4.61 (bs, 1H), 4.02 (bs, 2H), 3.60 - 3.34 (m, 20H), 3.24 (bs, 3H), 1.80 - 0.79 (m, −CH_2 and CH_3 along with backbone).

3.2.12. Synthesis and characterization of P(OEGMA-CA4-NHS-FMA-DTX) (27)

OEGMA (0.3 g, 1 mmol), CA4MA (0.051 g, 0.133 mmol), NHSMA (0.012 g, 0.066 mmol) and FMA (0.016 g, 0.04 mmol) were dissolved in anhydrous DMF (2.5 mL). To the copolymer solution was added CTA (1.7 mg, 0.0066 mmol) as chain transfer agent and AIBN (0.21 mg, 0.00013 mmol) as initiator. Reaction mixture was stirred under N_2 for 30 min. After purge process, reaction was sealed and heated at 80 °C for 1 hour. After 1 hour, temperature of oil bath was decreased to 50 °C. By the time desirable heat was reached, Methacrylated Gly-Phe-Leu-Gly-Docetaxel (MAGFLGDTX) (0.13 g, 0.1 mmol) solution in anhydrous DMF (0.5 mL) was added under N_2 in 2 min. After drug adding process, reaction was left at 50 °C for 47 hours. Then, molecular weight and PDI of polymer was checked by gel permeation chromatography (GPC). Resulted copolymer was purified by using 10 kDa cut off membrane by dialysis. Copolymer was diluted with acetonitrile (10 mL) and placed in a 10 kDa cutoff dialysis bag. Dialysis bag was placed in a beaker containing acetonitrile (250 mL). Solvent was changed 3 times/day and dialysis was completed in 2 days. After dialysis, solvent was evaporated and dried under *vacuo* to obtain copolymer 27 (0.25 g, 83%). Mn = 75k Da, M_w/M_n = 1.48. ^{1}H NMR (DMSO-*d6*, δ, ppm). 8.19 - 6.60 (m, 30 H) 6.50 (m, 3H), 4.02 (bs, 2H), 3.60 - 3.34 (m, 20H), 3.24 (bs, 3H), 2.77 (s, 4H), 1.80 - 0.79 (m, −CH_2 and CH_3 along with backbone).

3.2.13. Synthesis and characterization of P(OEGMA-CA4-RGD-FMA-DTX) (28)

Copolymer 27 (0.12 g) and cRGDfK (16 mg, 0.026 mmol) were dissolved in DMF (0.15 mL). To the copolymer solution, DIPEA (0.4 mg, 0.03 mmol) was added dropwise. Resulting reaction mixture was stirred at 45 °C for 24 h. Then, ethanol amine (2 mg, 0.3 mmol) was added to reaction mixture and reaction was stirred at ambient temperature for 24 h. The product was dialyzed using 3.5 kDa cutoff regenerated cellulose acetate membrane in MeOH (400 mL) for 2 d. Pure product was obtained by evaporating the solvent (0.05, 83%). M_n = 75 kDa, M_w/M_n = 1.48. ^{1}H NMR (DMSO-*d6*, δ, ppm). 8.19 - 6.60 (m, 35 H) 6.50 (m, 3H), 4.02 (bs, 2H), 3.60 - 3.34 (m, 20H), 3.24 (bs, 3H), 1.80 - 0.79 (m, −CH_2 and CH_3 along with backbone).

3.2.14. Synthesis and characterization of P(OEGMA-CA4 –FMA-DTX) (29)

To a solution of compound 27 (0.12 g) in DMF (0.15 mL), was added ethanol amine (1.6 mg, 0.03 mmol) in DMF (0.05 mL). Reaction was stirred at ambient temperature for 24 h. The product was dialyzed using 3.5 kDa cutoff regenerated cellulose acetate membrane in MeOH (400 mL) for 2 d. Pure product was obtained by evaporating the solvent (0.05 g, 42%). M_n = 75 kDa, M_w/M_n = 1.48. ^{1}H NMR (DMSO-*d6*, δ, ppm). 8.19 - 6.60 (m, 30 H) 6.50 (m, 3H), 4.02 (bs, 2H), 3.60 - 3.34 (m, 20H), 3.24 (bs, 3H), 1.80 - 0.79 (m, −CH_2 and CH_3 along with backbone).

3.2.15. In vitro drug release

The *in vitro* release studies of copolymers were evaluated in both rat plasma and enzyme-containing solutions. Drug release from polymer−drug conjugates were determined *via* LC−MSMS. For determination of release profiles of copolymers, 0.1 mg of each copolymer containing solutions in rat plasma and enzyme solutions were prepared in eppendorf tubes. Copolymer solutions were then incubated at 37 °C while stirring at 250 rpm for 72 h.

At predetermined time points, ACN was added to solutions and tubes were centrifuged at 6000g for 5 min. Supernatants were analyzed for CA4 and DTX concentrations by LC−MSMS analysis.

3.2.16. In *Vitro* Cell Viability Assay on SK-OV-3 and Caov-3 Human Ovarian Cancer Cell lines

Cell number and cell viability were determined by Cell Counting Kit-8 (CCK-8, Fluka). Cells were seeded in 100 μL of culture medium at a density of 3000 cells/well for SK-OV-3 and 15000 cells/well for Caov-3 cells into 96-well plates in quadruplicates for each drug concentration. After overnight incubation cell media was replaced with fresh medium containing various concentrations of conjugates, free drug, or polymer only controls. For free drug treatments docetaxel and combretastatin A4 stock solutions were prepared in 20% DMSO in growth medium (V/V) and subsequently diluted where the final DMSO concentration was below 0.5% (V/V). All cells were incubated continuously for 48h in the presence of the micellar conjugates. For 2h+22h pulse chase drug treatment, cells were incubated 2h in drug containing solutions and incubated in fresh media for 22h before CCK-8 assay. To determine the cell viability, 100 μL of culture medium together with 10 μL of CCK-8 solution was added into each well. After 4h incubation the absorbance values at 450nm was measured with a plate reader (Multiscan FC, Thermo Scientific, USA). Viability of treated cells was expressed as percentage of control cells (cell media only). EC_{50} values were obtained from concentration response curves by nonlinear regression analysis.

3.2.17. Animal Study

Mice were intravenously injected into the lateral tail vein with a single dose of P(OEGMA-CA4-DTX-RGD). The mice were observed daily for mortality and clinical findings, and body weight was recorded. The mice were sacrificed on the fifth day with collection weighing, and preservation of major organs (liver, kidneys, spleen, heart, lung).

3.3. Results and Discussion

3.3.1. Synthesis and Characterization of CA4 and DTX Bearing Copolymers

Dual drug conjugated copolymers were synthesized *via* RAFT copolymerization of anti-angiogenic drug bearing monomer (CA4MA, 3), anti-microtubule agent and enzymatically cleavable linker bearing monomer (MAGFLGDTX, 17), amine reactive activated ester containing monomer (NHSMA, 1). Oligo (ethylene glycol) methyl ether methacrylate (OEGMA, 2) was also used for bringing hydrophilic backbone characteristic to copolymer. The first step involves preparation of targeting group and drug containing copolymers. Docetaxel bearing monomer was synthesized by attaching drug molecule to enzymatically cleavable tetrapeptide linker GFLG (Figure 3.1). For this reason, previously methacrylated GFLG linker was coupled with hydroxyl functional group of docetaxel *via* acid group on it. On the other hand, as reported in our previous study, CA4 bearing monomer was prepared *via* esterification of hydroxyl group of the CA4 drug and methacryloyl chloride molecule. Thus, we obtained copolymers that have different properties and they are also bounded to two different featured drugs with cleavable linkers which are sensitive to enzymes and acidic environment.

Basically, all the copolymers were synthesized *via* Reversible chain transfer polymerization technique and initiated with AIBN in anhydrous DMF. For attaching cRGDfK molecule to copolymers, NHSMA were utilized in all polymerization reactions. Obtained products were separated in to two batches. One batch was attached with targeting group and another batch was reacted with ethanol amine for quenching activated NHS groups. On the other hand, to generate fluorescent copolymers for investigating cellular internalization capacity, fluorescein-O-methacrylate monomer was also added to copolymerization reactions as an imaging agent.

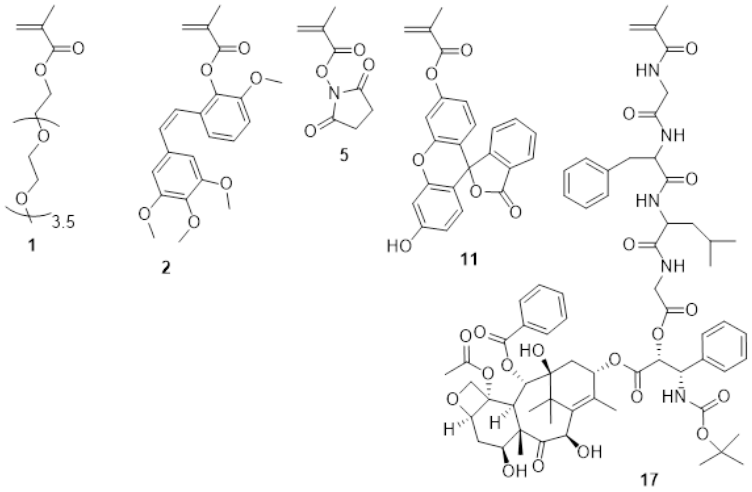

Figure 3.1. Monomers that are used in polymerization reaction.

Initially, just CA4 drug bearing copolymers were synthesized (Figure 3.2). These copolymers were separated in to two parts like as mentioned before and one part (19) was attached with cRGDfK molecule in DMF at 45 °C for 24 h. After reaction was completed, ethanol amine was added to stirring reaction *in situ* to quench remaining NHS groups. Another part was directly reacted with ethanol amine (20). Meanwhile, OEGMA, NHSMA and CA4MA monomers were copolymerized with fluorescein-O-methacrylate monomer for preparing fluorescent featured copolymers (25, 26) (Figure 3.3). The same strategy for quenching NHS groups as the latter example was followed for these reactions as well.

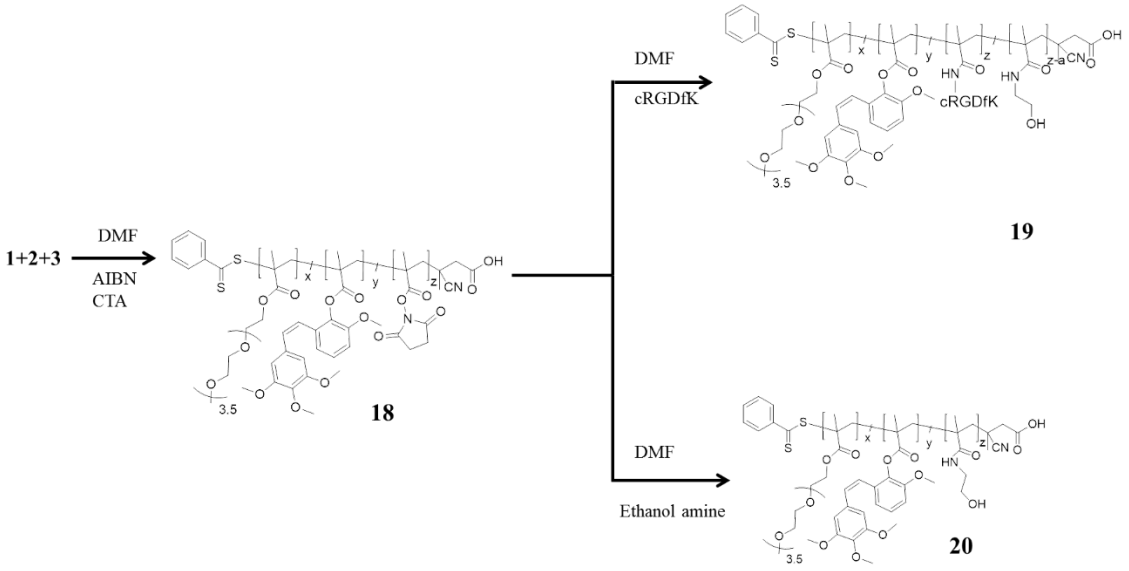

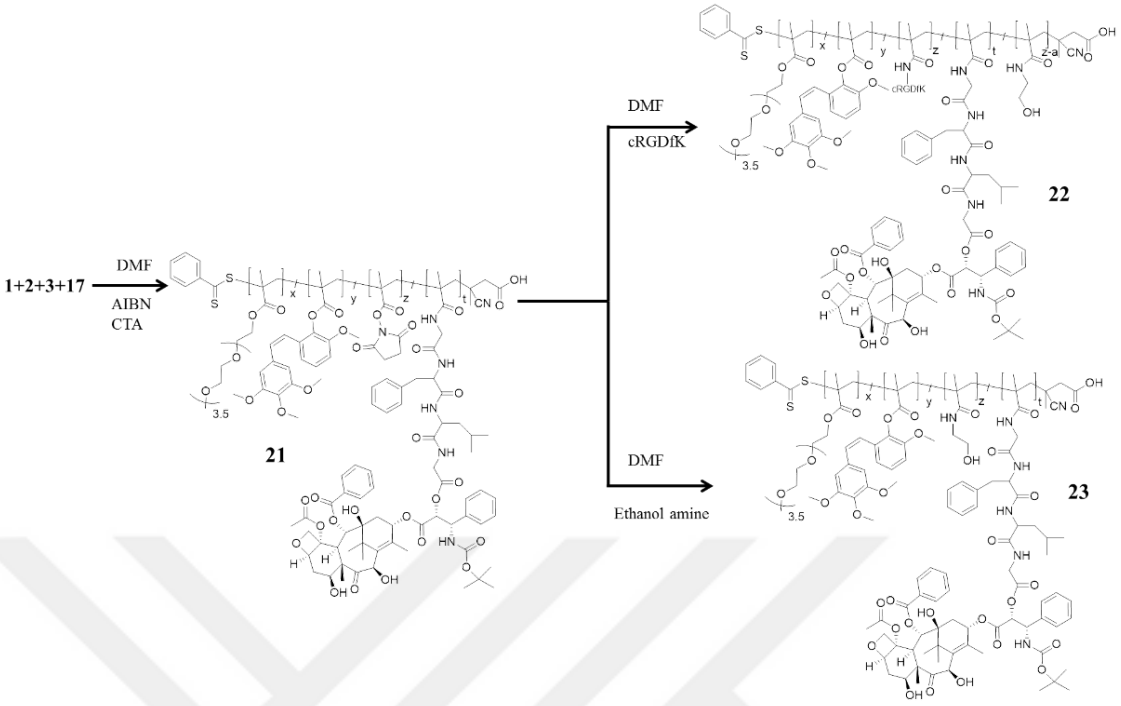

Figure 3.2. Synthetic route for drug and cRGDfK attached copolymers.

Additionally, to obtain dual drug containing copolymers, MAGFLGDTX monomer was used. By attaching another drug on copolymer molecule, achieving more effective cytotoxicity profiles on cells were aimed. Therefore, OEGMA, NHSMA and CA4MA monomers were copolymerized at 80 °C for one hour. After one hour, reaction temperature was decreased to 50 °C and MAGFLGDTX monomer was added to reaction dropwise under N_2. Like previously synthesized copolymers, dual drug containing copolymers were also separated into two parts and one part was conjugated with targeting group (22) while other part was left as non-targeted (23). Fluorescent and dual drug bearing copolymers with either targeting group containing (28) or not (29) were prepared as well. To purify resulting copolymers, they were precipitated in diethyl ether. MAGFLGDTX bearing copolymers were also dialyzed in ACN after precipitation process using 10k cutoff regenerated cellulose acetate membrane to remove free MAGFLGDTX.

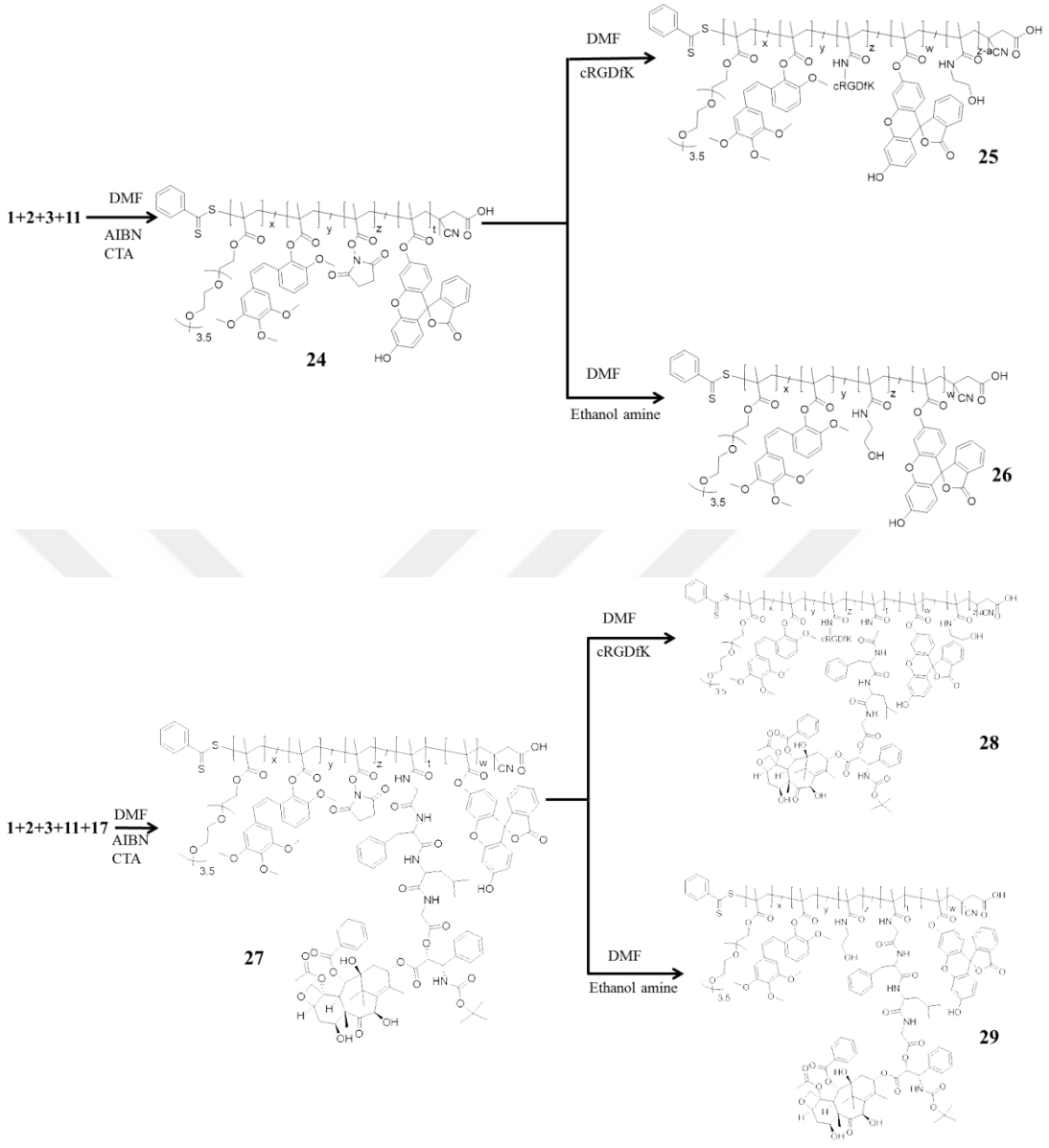

Figure 3.3. Synthetic route for dye containing copolymers.

All resulting random copolymers were characterized by using ^{1}H NMR spectroscopy. The compositions of monomers in the copolymers were determined from ^{1}H NMR spectroscopy (Table 3.2). Molecular weights and size distributions were obtained via SEC. The first copolymer among mono drug containing copolymers (Table 3.1, No:1) feed ratio of 70:20:10 was used with monomers 1, 2, 5 and it produced copolymer 18 that composed of monomers 75:12:13. Molecular weight of the copolymer was 48 kDa. Resulted product was separated into two batches and one batch was attached with cRGDfK, while second batch was treated with ethanolamine to quench remaining NHS groups, as mentioned before. At the end, according to ^{1}H NMR analysis, copolymer 19 was carrying 13.05% CA4 and

6.89 % cRGDfK by weight while amount of CA4 was 14.77% for copolymer 20. Since the phenyl peaks of CA4 and and aromatic peaks of cRGDfK were overlapping in the same region (between 7.13 - 6.97 ppm) in ^{1}H NMR spectrum, cRGDfK amount was determined by taking ^{1}H NMR spectrum of copolymer 18 as a reference. In both ^{1}H NMR spectrums of copolymers 18 and 20, there were 3 protons in the aromatic region. However, in ^{1}H NMR spectrum of copolymer 19 in the same region there were 3.74 protons. That difference can be attributed to incoming protons of cRGDfK molecule.

As for fluorescent featured version of that copolymer, feed ratio of monomers 1, 2, 11, 5 was 70:20:2:10. It was observed that, resulted copolymer 24 was composed of 80:8:2:10 ratios of monomers respectively and molecular weight was 48 kDa. Here again for determining of cRGDfK amount in the structure, ^{1}H NMR spectrums of copolymer 24, 25 and 26 were compared.

According to compositional analysis for copolymers 24 and 26, between 7.13-6.97 ppm in the ^{1}H NMR spectrum, there were 5 protons that belong to both phenyl protons of CA4 drug and fluorescent dye. But for copolymer 25, 10 protons were encountered in the same region. Drug content was similar for both copolymers which are 11.9% and 12.51% by weight respectively that means most of the drug amount was preserved after targeting group conjugation of previous molecule. On the other hand, enzymatically cleavable linker containing drug monomer was added to copolymerization reactions as a latter study. In the first batch, monomers 1, 2, 17 and 5 with feeding ratios of 75:12:8:5 were added to copolymerization reaction. In the resulted copolymer 21, incorporation of monomers was 85:5:3:7. For targeted group containing copolymer 22, drug amounts were obtained as 13.74 % and 5.83 % by weight for CA4 and DTX. For same copolymer, there was 3.16 % of cRGDfK by weight. In the nontargeted construction 23, drug amounts were not so different from other batch which is 14.56 % of CA4 and 4.95 % of DTX by weight. Final copolymer 21 which carries both targeting group and dye was obtained by using all monomers 1, 2, 17, 11, and 5 with feed ratios of 75:10:8:3:5. Resulted ratios of monomers in the product were obtained as 67:7:10:5:11. Here again, ^{1}H NMR spectrums of both targeted copolymer 22 and non-targeted copolymer 23 were compared. According to spectrum, there were two new peaks in 7.29 ppm and 7.31 ppm that are coming from RGD molecule. On the other hand, in the same region these peaks weren’t observed for copolymer 23 (Figure 3.4).

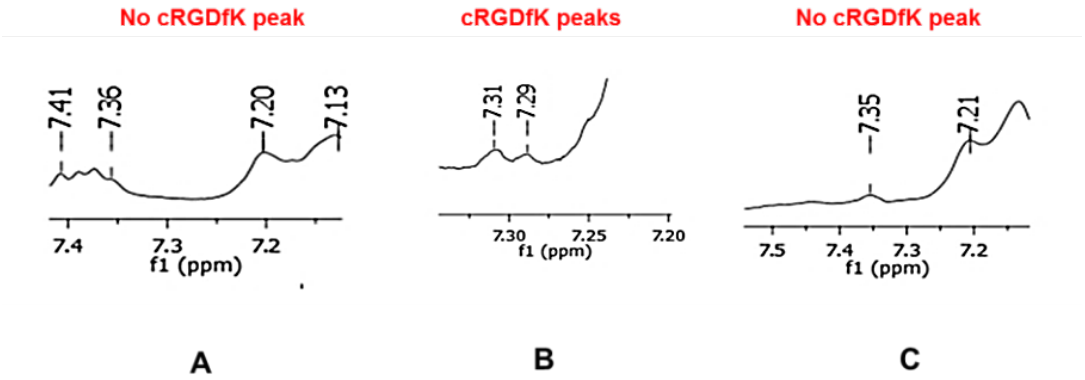

Figure 3.4. Expanded ^{1}H NMR spectrums of the constructs A) Copolymer 21 B) Copolymer 22 and C) Copolymer 23.

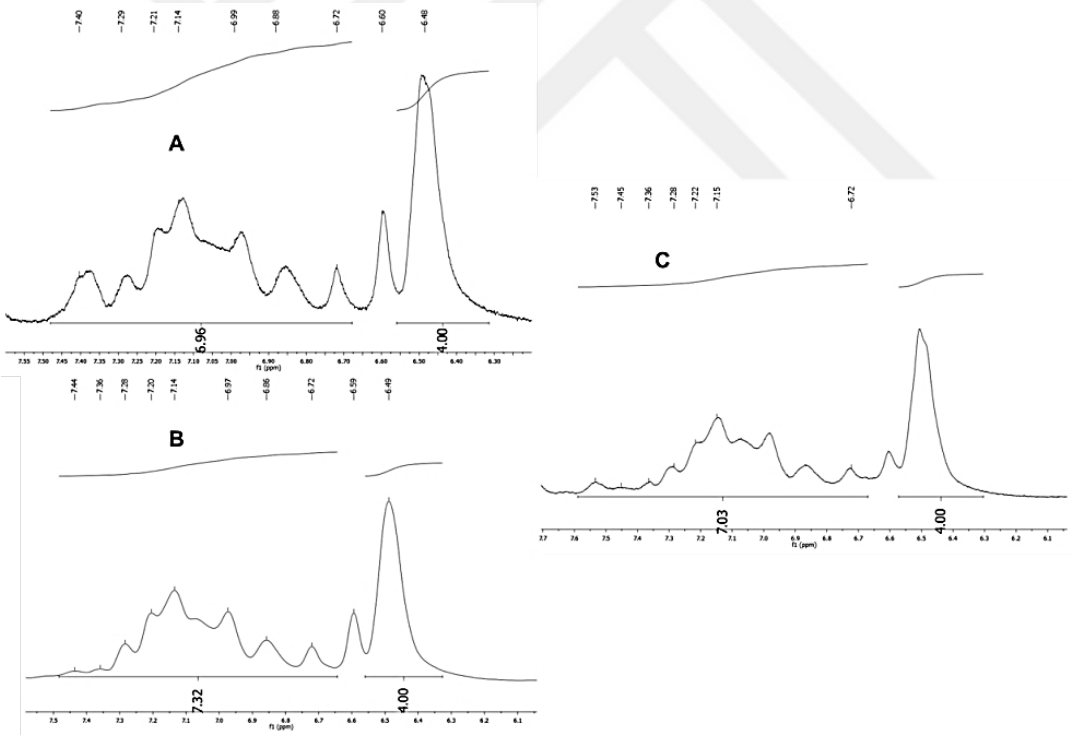

Figure 3.5. Expanded ^{1}H-NMR spectrums of structures. A) Copolymer 27 B) Copolymer 28 and C) Copolymer 29.

Table 3.1. Polymerization Conditions and Characterization of Copolymers.

		Feed ratio					Obtained ratio						
No	**Copolymer**	**1**	**2**	**3**	**11**	**17**	**1**	**2**	**3**	**11**	**17**	**Mn[c] (kDa)**	**Mw/Mn**
1	**18**	70	20	10	-	-	75.0	12.0	13.0	-	-	48	1.35
2	**21**	75	12	5	-	8	85.3	5.3	6.6	-	2.7	56	1.38
3	**24**	70	20	10	2	-	80.3	7.5	10.4	1.7	-	48	1.35
4	**27**	75	10	5	3	8	67.0	6.5	11.3	5.1	10.0	75	1.48

Table 3.2. Properties of Copolymers.

No	**Copolymer**	**Mn (kDa)**	**Mw/Mn**	**CA4 wt %**	**DTX wt %**	**cRGDfK wt %**	**FMA wt %**	**Ethanol amine wt %**
1	P(OEGMA-CA4-RGD) **19**	48	1.35	13.05	-	6.89	-	-
2	P(OEGMA-CA4) **20**	48	1.35	14.77	-	-	-	4.6
3	P(OEGMA-CA4-DTX-RGD) **22**	56	1.38	13.74	5.83	3.16	-	1.73
4	P(OEGMA-CA4-DTX) **23**	56	1.38	14.56	4.95	-	-	1.12
5	P(OEGMA-CA4-RGD-FMA) **25**	48	1.35	11.9	-	7.86	3.77	-
6	P(OEGMA-CA4-FMA) **26**	48	1.35	12.51	-	-	5.20	4.26
7	P(OEGMA-CA4-DTX-RGD-FMA) **28**	75	1.48	10.55	5.57	1.61	5.32	1.45
8	P(OEGMA-CA4-DTX-FMA) **29**	75	1.48	10.89	3.66	-	4.56	1.25

Same comparison was done for fluorescent featured copolymer 27 and copolymer 28. (Figure 3.5). As expected, there were much more protons in aromatic regions of ^{1}H NMR spectrum of targeted copolymers with regard to non-targeted ones. In addition, according to ^{1}H NMR spectrums of all copolymers, there were not any remaining NHS groups in the molecules.

3.3.2. Drug Release Profiles of Copolymers

We have chosen two different environments to investigate differences of release profiles of drugs because drugs were conjugated to polymeric carrier *via* different linkers. For docetaxel, we used enzymatically cleavable linker GFLG and we attached CA4 to copolymer *via* ester bond. The enzymatic release of DTX from both copolymers was achieved in papain enzyme containing PBS (pH=7.4) solution. On the other hand, release behaviors of both drugs in rat plasma were determined as well. According to obtained graphs, in prepared enzyme solution at 37 °C, as expected only docetaxel was able to release from both copolymers which can be attributed to DTX was attached to copolymers *via* enzymatically cleavable linker GFLG.

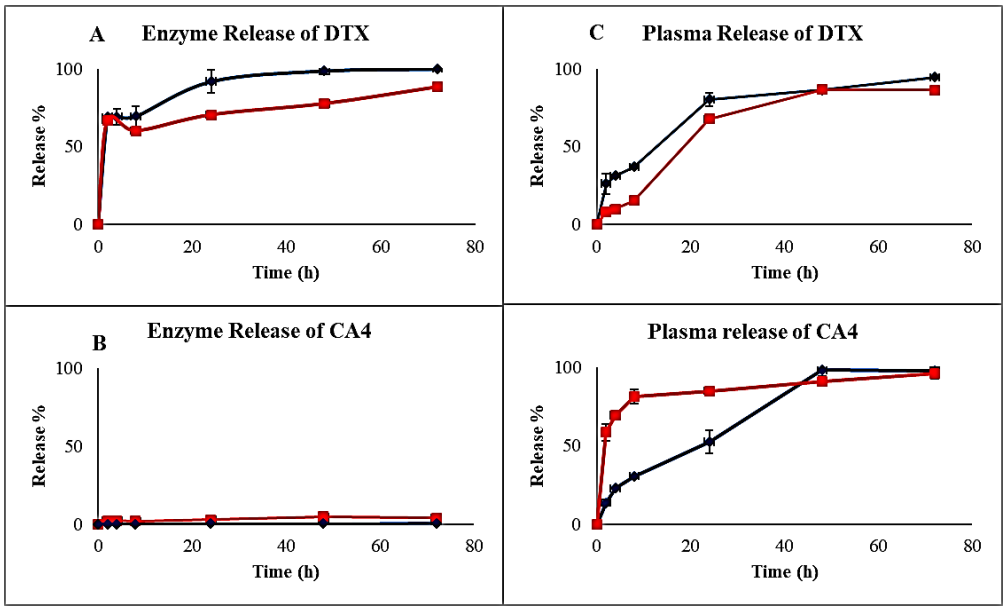

Figure 3.6. Enzymatic and plasma release of DTX and CA4 from P(OEGMA-CA4-DTX-RGD) (blue square) and P(OEGMA-CA4-DTX) (red square).

At the end of the 72 hours, approximately 100% of DTX was released from targeted copolymer whereas this ratio was 61% for nontargeted counterpart. In enzyme solution, we could observe negligible amount of CA4 release from copolymers due to neutral pH of solution and lack of esterase enzymes in the environment. In case of plasma release at 37 °C, both drugs were released from polymers. After 72 hours, 94% and 86% of DTX was released from targeted and nontargeted copolymers. Addition to that CA4 release ratio was observed as 97% for RGD containing copolymer. For nontargeted version, approximately same amount of CA4 was released which is obtained as 95%. Although almost all CA4 was released from both copolymers at the end of 72 hours, release profiles were different. While RGD containing copolymer released 52% of CA4 in 24 hours, for nontargeted copolymer 84% of CA4 was released in same time.

3.3.3. In vitro cytotoxicity profiles of copolymers on SK-OV-3 and Caov-3 human ovarian cancer cells

Effects of both DTX and anti-angiogenic drug CA4 bearing copolymers were evaluated on SK-OV-3 human cells to investigate combined effect of drugs. Cancer cells were exposed with each drug alone, free drugs together, targeted and non-targeted copolymers carrying both drugs. Free DTX was highly toxic (5.25 nM) toward SK-OV-3 cells in 48 hours (Figure 3.7A). On the other hand, free CA4 was also toxic (518 nM) to cancer cells but its toxicity was approximately 100fold less than free DTX. Although free CA4 was less toxic when compared to free DTX, it was observed that free drugs of each was more toxic according to copolymers, as expected. Together with these, free drugs were combined according to their amounts in the copolymers and treated with cells. Results were compatible with their free cytotoxicity profiles. Their combined toxicity was obtained as 2.66 nM which is slightly more toxic according to free DTX due to contribution of free CA4 (Data were not shown).

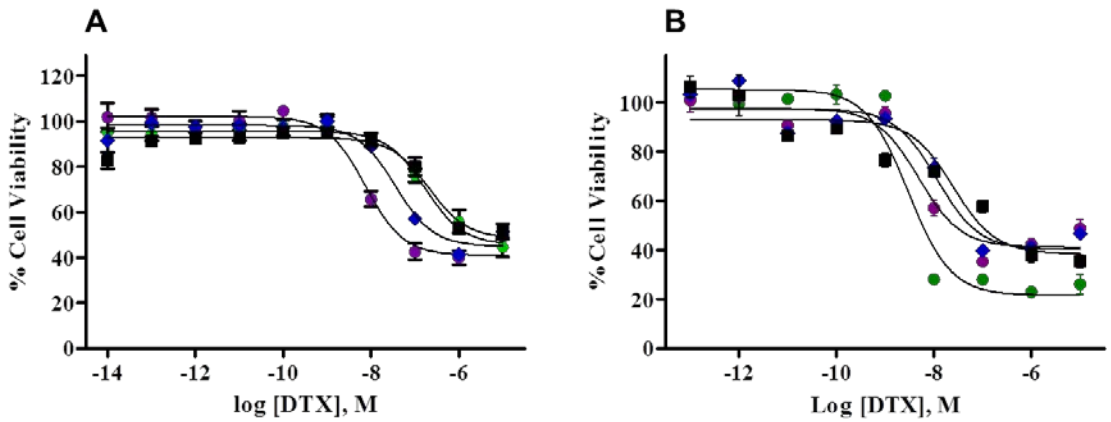

Figure 3.7. Viabilities of A) SK-OV-3 cells and B) Caov-3 cells treated with free DTX (●), free CA4 (●), P(OEGMA-CA4-DTX-RGD) (◆) and P(OEGMA-CA4-DTX) (■).

Table 3.3. EC_{50} values of free drugs and copolymers after incubation of SK-OV-3 and Caov-3 cells for 48 hours.

No	Sample	EC_{50} value (M)	
		SK-OV-3	**Caov-3**
1	CA4	5.18×10^{-7}	3.11×10^{-9}
2	DTX	5.25×10^{-9}	4.88×10^{-9}
3	P(OEGMA-CA4-DTX-RDG)	2.45×10^{-8}	1.168×10^{-8}
4	P(OEGMA-CA4-DTX)	1.36×10^{-7}	2.58×10^{-8}

The difference between drugs alone versus copolymers was within the expected ranges. At first sight, both targeted and non-targeted copolymers were less toxic than free drugs. Moreover, cRGDfK containing copolymer was 10-fold higher toxic according to its non-targeted counterpart. As for Caov-3 cells, both free drugs are more toxic than copolymers (Figure 3.7B). EC_{50} value of targeted copolymer was determined as 11 nM. On the other hand, non-targeted copolymer's EC_{50} value was 25 nM which is less toxic than

targeted copolymer. In conclusion, copolymers show toxic behaviors toward both ovarian cancer cell lines. In addition to that for both cell lines, targeted copolymer was more toxic when compared to non-targeted copolymer. All cytotoxicity values of drugs and polymers are summarized at Table 3.3.

3.4. Conclusion

A P(OEGMA) based polymeric carrier for targeting ovarian cancer, an antiangiogenic agent CA4 and anti-neoplastic agent DTX was synthesized and evaluated for cytotoxicity. As a targeting unit, cRGDfK that has high binding affinity toward $\alpha\upsilon\beta_3$/ $\alpha\upsilon\beta_5$ integrins was conjugated to the drug-containing copolymer *via* reactive NHS group through stable amide bond. Effective release behaviors of drugs in rat plasma were observed from both targeted and nontargeted copolymers. For enzyme release, just DTX release was observed due to it was conjugated to polymer *via* enzymatically cleavable bond GFLG whereas CA4 didn't show significant release profile from polymer, as expected. The polymer−drug conjugates demonstrated cytotoxicity toward different ovarian cancer cell lines, SK-OV-3 and Caov-3. These cRGDfK bearing and two different featured drugs attached copolymers are attractive candidates and they can be further used for treatment of ovarian cancer.

4. cRGDfK TARGETED REDOX RESPONSIVE 5-FU PRODRUG CONJUGATES FOR BREAST CANCER THERAPY

4.1. Introduction

Polymer drug conjugation systems are emerging as encouraging research platforms for cancer treatment because they increase bioavailability of small chemotherapy drugs and improve their pharmacokinetic behavior. Even though their *in vitro* effectiveness are demonstrated, most the cytotoxic chemicals, cannot be utilized as a drug because of their heavy side effect profiles [280]. After intravenous injection of the drug, it encounters so many obstacles such as vascular walls, interstitial spaces and cell membranes that limits the delivery of sufficient amount of the drug to the desired region. To overcome all these obstacles, targeted drug delivery has been studied by researchers [281]. For preferential accumulation in the tumor, targeting moieties are attached to macromolecules because targeting groups are expected to bind certain receptors which overexpress in tumor tissues. Especially, Arg-Gly-Asp (RGD) sequence containing peptides have been extensively studied because of their binding affinity towards $\alpha\upsilon\beta_3$/ $\alpha\upsilon\beta_5$ integrin receptors that are over-expressed in different tumor cells [282]. According to some pioneering results, $\alpha\upsilon\beta_3$ integrin overexpression in breast cancer xenografts are demonstrated [283, 284].

The most potent risk factor for breast cancer development is known as age since breast cancer rate increases regularly with increasing age [285]. Although many studies have been carried out on the subject, the cause of age-related deaths in breast cancer is not fully understood [286, 287]. For these mentioned population, the most commonly used chemotherapy drug is capecitabine. Capecitabine is an oral prodrug of 5-Fluorouracil (5-FU) that is commonly used for treatment of many types of cancers including head and neck, anal, colon and metastatic breast cancer. Especially for advanced or metastatic breast cancer which are resistant to first line treatments, effectiveness of capecitabine has been proven [288]. It has been shown that although 5-FU is more toxic than capecitabine in *in vitro* studies, especially oral use of 5-FU is limited because it rapidly dehydrates into dehydro-50

fluorouracil [289]. For example in one of the reports, researchers wanted to explore the difference between activities of capecitabine and 5-FU on MCF7 breast cancer cell line [290]. After incubation of cells with capecitabine for 48 h, EC_{50} value was obtained as 1147 µM. On the other hand, when the same experiment was carried out with 5-FU, EC_{50} was 0.38 µM, which means 5-FU is 3000 times more toxic than capecitabine. Even after 72 hours, EC_{50} value of capecitabine was 921 µM. The results of the study showed that 5-FU is much more toxic than capecitabine. On the other hand, a number of remarkable clinical trials have been carried out by researchers using capecitabine [291]. When capecitabine is taken orally by patients, it is rapidly absorbed in the digestive system and it is metabolized to 5-FU *via* three step enzymatic process at the tumor side (Figure 4.1.) In the first step, it is converted to 5-fluoro-5'-deoxycytidine (5'-DFCR) *via* carboxylesterase enzyme that exists in the liver. As a second step, 5'-DFCR is converted to 5-fluoro-5'-deoxyurudine (5'-DFUR) with the help of cytidine deaminase enzyme which exists in tumor and liver. This final metabolite is converted to drug 5-FU by thymidine phosphorylase (TP) enzyme which exists in 3-fold higher amounts in tumor tissue than in normal tissue [292].

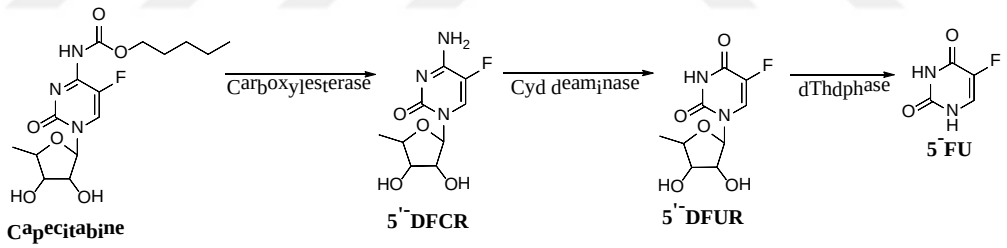

Figure 4.1. Process of turning drug capecitabine into 5-FU *via* enzymes.

Herein, we are designing the synthesis and evaluation of novel monomer and polymer drug conjugate carrying 5'-DFCR which is the active ingredient of drug capecitabine. This drug precursor was attached to a monomer *via* hydrolyzable carbamate linker. In addition to this, the linker also bears a disulfide bond that can be cleaved under reductive conditions. After the reduction process, obtained thiol-containing intermediate forms a five membered ring, namely thiolactone, as a result of intramolecular nucleophilic addition at the carbamate carbonyl (Figure 4.2.) Following thiolactone formation, 5'-DFCR is released. After synthesis and characterization of monomers and copolymers, *in vitro* cytotoxicity studies

against MDA-MB 453 breast cancer cells were carried out to evaluate the efficacy of prepared constructs.

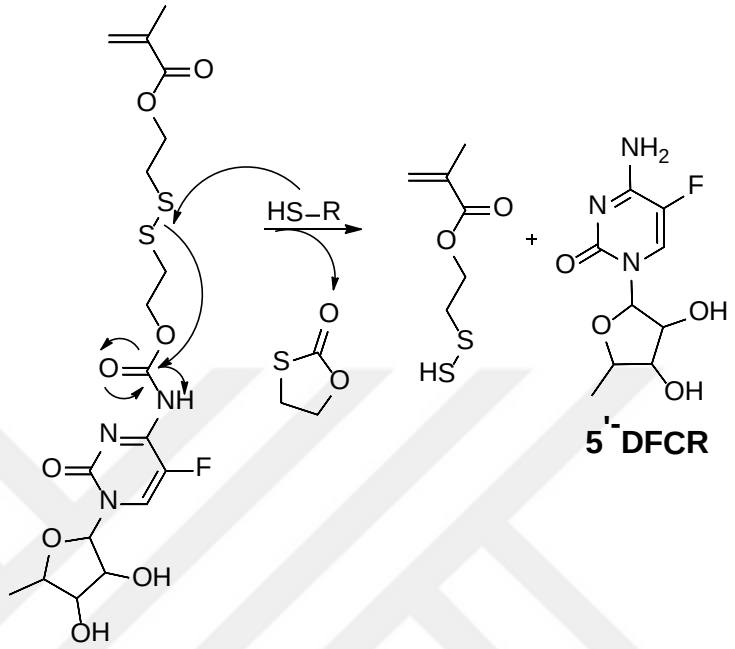

Figure 4.2. The effect of disulfide bonds on releasing 5'-DFCR.

4.2. Experimental Section

4.2.1. Materials

Methacryloyl chloride was purchased from Alfa Aesar. The solvents used throughout this thesis were purchased from Merck. Milli-Q Water Purification System (Milli-Q system, Millipore, Billerica, MA, USA) was employed to produce ultrapure water. All the other chemicals were obtained from Sigma Aldrich. Reaction conditions that require anhydrous conditions were carried out under nitrogen atmosphere. Polyethylene glycol methacrylate (OEGMA M_n = 300) was obtained from Sigma Aldrich and filtered through basic alumina column prior to use. 2-((2-hydroxyethyl)disulfonyl)ethyl methacrylate (HSEMA) (30) and NHSMA (N-hydroxysuccinimide methacrylate) (2) monomers were synthesized according to previously reported protocols [293]. Fluorescein O-Methacrylate (FMA) (11) was

purchased from Sigma Aldrich. Cyano-4-(phenylcarbonothioylthio)pentanoic acid (CPDTB) was used as chain transfer agent (CTA) and purchased from Sigma Aldrich as well. AIBN was recrystallized from methanol before use. MDA-MB-453 cells were obtained from American Type Culture Collection (ATCC). MDA-MB-453 cells were maintained in DMEM supplemented with 10% FBS. cRGDfK was synthesized according to literature example [294].

4.2.2. Instrumentation

^{1}H and ^{13}C NMR spectroscopy (Varian 400 MHz NMR spectrometer), Fourier transform infrared (ATR-FTIR) spectroscopy (Nicolet 380, Thermo Scientific, USA), and UV−vis spectroscopy (PerkinElmer series) methodologies were used in order to characterize synthesized monomers and polymers. The qualification and quantification of HSEMA (1), 2-((2-(N-succunimidylcarboxyoxy)ethyl)disulfonyl)ethyl methacrylate (SCEDEMA) (2) and protected (3) and non-protected (4) monomers were achieved utilizing the liquid chromatography−mass spectrometry (LC−MS) system (LCMS 2020, Shimadzu, Japan) with a C- 18 (5 µm, 150 × 4.6 mm) column. A gradient method was utilized with acetonitrile (ACN) and deionized water supplemented with 0.05% trifluoroacetic acid (TFA) through the following program; LC: 0−3 min, 50% ACN; 3.01 min, 50% ACN; 8 min, 95% ACN; 8.01−11 min, 50% ACN; MS positive scan 100−800 m/z. The molecular weights were estimated by Gel Permeation Chromatography (GPC, Shimadzu, Japan) with a mobile phase solution of 0.05 M lithium bromide in dimethylaceteamide (DMAc) as eluent at a flow rate of 1 mL/min at 30 ºC. GPC measurements of copolymers were carried out with PSS WinGPC Unity software. PSS Gram (10 µm - 300 × 8 mm) column was calibrated with polymethyl methacrylate standards, using refractive index detector (RID-10A).

4.2.3. Synthesis and Characterization of SCEDEMA (31)

To a solution of HSEMA monomer (30) (1.00 g, 4.5 mmol) and triethyl amine (0.68 g, 6.75 mmol) in dichloromethane (20 mL) was added N, N'-Disuccinimidyl carbonate (1.15 g, 4.5 mmol) in dichloromethane (10 mL) dropwise. Then reaction was left at ambient

conditions for 24 h. Then, solution was evaporated, and remaining TEA was removed. Product was purified by column chromatography on SiO_2 (EtOAc/DCM, 50:50) in a low yield (10-15%) assuming that it decomposes in silica column. Therefore, in subsequent experiments, we used the product without further purification. ^{1}H NMR ($CDCl_3$, δ, ppm) 6.12 (s, 1H), 5.59 (s, 1H), 4.56 (t, 2H, *J* = 8 Hz), 4.40 (t, 2H, *J* = 8 Hz), 3.02 - 2.97 (m, 4H), 2.83 (s, 4H), 1.94 (s, 3H). ^{13}C NMR ($CDCl_3$, δ, ppm) 168.5, 167.1, 151.4, 126.1, 68.7, 62.4, 37.3, 36.1, 25.4, 18.2. FT-IR (cm^{-1}) 2955, 1787, 1735.

4.2.4. Synthesis and Characterization of Compound 32

SCEDEMA (1.6 g, 4.5 mmol) and 2',3'-Di-O-acetyl-5'-deoxy-5-fluorocytidine (0.8 g, 2.5 mmol) were dissolved in dichloromethane (30 mL). After 10 min, pyridine (0.35 g, 4.5 mmol) was added dropwise to the solution. Reaction was stirred for 3 days at rt. Upon completion of the reaction, mixture was concentrated to give yellow viscous liquid. Crude product was purified by using column chromatography on SiO_2 (EtOAc/DCM, 50:50) affording 0.9 g of product (75% yield). ^{1}H NMR ($CDCl_3$, δ, ppm) 7.42 (bs, 1H), 6.13 - 6.12 (m, 1H), 5.95 - 5.94 (m, 1H), 5.59 - 5.57 (m, 1H), 5.29 - 5.26 (m, 1H), 5.01 - 4.99 (m, 1H), 4.46 - 4.39 (m, 4H), 4.29 - 4.23 (m, 1H), 3.01 - 2.97 (m, 4H), 2.11 (s, 3H), 2.09 (s, 3H), 1.95 - 1.94 (m, 3H), 1.47 - 1.45 (d, 3H, *J* = 8 Hz). ^{13}C NMR ($CDCl_3$, δ, ppm) 169.7, 169.6, 167.1, 149.6, 135.8, 126.0, 123.7, 88.1, 78.3, 73.9, 73.1, 64.1, 62.5, 37.1, 36.9, 25.4, 24.8, 20.5, 20.4, 18.7, 18.3, 14.2. FT-IR (cm^{-1}) 2979, 1745, 1714. LC−MS expected [M + H] m/z = 578 and observed [M + H] m/z = 578.

4.2.5. Synthesis and Characterization of MA-5'DFCR (33)

MA-DO-5'DFCR (0.9 g, 1.88 mmol) was dissolved in methanol (4.5 mL). To the solution, was added triethylamine (1.8 g, 18 mmol). After 10 min, 0.5 mL of distilled water was added to the mixture. Reaction was stirred at rt for 24 h. Upon completion of the reaction, methanol was evaporated, then remaining water was lyophilized to obtaine yellowish viscous liquid. Crude product was purified by using column chromatography on SiO_2 (EtOAc / CH_3OH, 90:10) affording 0.48 g of product (50% yield). ^{1}H NMR ($CDCl_3$, δ,

ppm). 7.77 (bs, 1H), 6.11 (s, 1H), 5.70 (s, 1H), 5.58 (s, 1H), 4.44 - 4.38 (m, 4H), 4.26 - 4.23 (m, 2H), 3.86 - 3.83 (m, 1H), 2.98 - 2.94 (m, 4H), 1.92 (s, 1H), 1.41 - 1.39 (d, 3H, *J* = 8 Hz). ^{1}H NMR (DMSO-*d6*, δ, ppm) 8.01 (bs, H), 6.05 (s, 1H), 5.70 (s, 1H), 5.66 (s, 1H), 5.42 - 5.41 (d, -OH), 5.07 - 5.06 (d, -OH), 4.39 - 4.29 (m, 4H), 4.10 - 4.01 (m, 1H), 3.93 - 3.87 (m, 1H), 3.70 - 3.65 (m, 1H), 3.06 - 3.01 (m, 4H), 1.88 (s, 3H), 1.31 - 1.30 (d, 3H, J = 4 Hz). ^{13}C NMR ($CDCl_3$, δ, ppm) 168.5, 167.1, 151.4, 135.9, 126.1, 68.7, 62.4, 37.3, 36.1, 25.4, 18.2. FT-IR (cm^{-1}) 3300, 2963, 1762, 1711. LC−MS expected [M + H] m/z = 494 and observed [M + H] m/z = 494.

4.2.6. Synthesis and Characterization of P(OEGMA-NHS-5'DFCR) (34)

OEGMA (0.5 g, 1.66 mmol), MA-5'DFCR (0.091 g, 0.183 mmol), NHSMA (0.033 g, 0,183 mmol), were dissolved in DMF (3 mL). To the solution was added CTA (2.58 mg, 0.0092 mmol) as chain transfer agent and AIBN (0.3 mg, 0.00184 mmol) as initiator. Reaction mixture was stirred under N_2 for 30 min. Reaction was sealed and heated 70 °C for 20 h. The copolymer was purified *via* precipitation in diethyl ether, dissolved in CH_2Cl_2 and re-precipitated. After precipitation, copolymer was washed with diethyl ether. The product was dried under *vacuo* and obtained as viscous liquid. (0.3 g, 60%). M_n = 49 kDa, M_w / M_n = 1.3. ^{1}H NMR (DMSO-*d6*, δ, ppm) 7.94 (bs, 1H), 5.66 (bs, 1H), 5.38 (bs, 1H), 5.03 (bs, 1H), 4.32 (m, 3H), 4.01 (s, 2H), 3.62 - 3.34 (m, 20H), 3.01(m, 4H), 2.80 (bs, 4H), 2.09 - 0.80 (m, $-CH_2$ and CH_3 along with backbone).

4.2.7. Synthesis and Characterization of P(OEGMA-5'DFCR-RGD) (35)

Copolymer 34 (0.15 g) and cRGDfK (0.16 mmol, 97 mg) were dissolved in DMF (0.4 mL). To the copolymer solution, DIPEA (1.6 mmol, 0.3 mL) was added dropwise. Resulting reaction mixture was stirred at ambient temperature for 24 h. Then, ethanol amine (0.16 mmol, 0.9 mg) was added to the reaction mixture and reaction was kept stirring at 45 °C for 1 d. Resulting copolymer was purified by using 3.5 kDa cut off membrane by dialysis. Copolymer was diluted with MeOH (10 mL) and placed in a 3.5 kDa cutoff dialysis bag. Dialysis bag was placed in a beaker containing MeOH (250 mL). Solvent was changed 3

times/day and dialysis was completed in 2 d. After dialysis, solvent was evaporated and dried under *vacuo* to obtain copolymer 35 (0.12 g, 80%). M_n = 52 kDa, M_w/M_n = 1.60. ^{1}H NMR (DMSO-*d6*, δ, ppm) 7.76 - 7.74 (d, 1H, *J* = 8 Hz), 8.0 (bs, -NH), 7.56 (bs, -NH), 7.32 - 7.12 (m, 5H), 5.69 (s, 1H), 5.27 - 5.25 (d, -OH, *J* = 8 Hz), 4.99 - 4.97 (d, -OH, *J* = 8 Hz), 4.36 - 4.03 (m, 4H), 3.62 - 3.34 (m, 20H), 3.26 (s, 3H), 3.03 - 2.96 (m, 4H), 2.86 - 2.81 (m, 2H), 2.09 - 0.80 (m, $-CH_2$ and CH_3 along with backbone).

4.2.8. Synthesis and Characterization of P(OEGMA-5'DFCR) (36)

Copolymer 34 (0.15 g) and ethanol amine (0.16 mmol, 0.9 mg) were dissolved in DMF (0.4 mL) and the reaction mixture was kept stirring at 45 °C for 24 h. Upon completion of the reaction, resulting copolymer was purified by using 3.5 kDa cut off membrane by dialysis. Copolymer was diluted with MeOH (10 mL) and placed in a 3.5 kDa cutoff dialysis bag. Dialysis bag was placed in a beaker containing MeOH (250 mL). Solvent was changed 3 times/day and dialysis was completed in 2 d. After dialysis, solvent was evaporated and dried under *vacuo* to obtain copolymer 36. (0.12g, 80%). Mn=52 kDa, M_w/M_n = 1.64. ^{1}H NMR (DMSO-*d6*, δ, ppm) 7.75 - 7.73 (d, 1H, *J* = 8 Hz), 7.87 (bs, -NH), 7.54 (bs, -NH), 5.69 (s, 1H), 5.26 - 5.24 (d, -OH, *J* = 8 Hz), 4.98 - 4.96 (d, -OH, *J* = 8 Hz), 4.16 - 4.02 (m, 4H), 3.61 - 3.32 (m, 20H), 3.25 (s, 3H), 2.96 (bs, 4H), 2.81 (bs, 2H), 2.09 - 0.80 (m, $-CH_2$ and CH_3 along with backbone).

4.2.9. Synthesis and Characterization of P(OEGMA-5'DFCR-NHS-FMA) (37)

OEGMA (0.3 g, 1 mmol), MA-5'DFCR (61 mg, 0.125 mmol), NHSMA (23 mg, 0,125 mmol), FMA (0.025 mmol, 10 mg) were dissolved in DMF (1 mL). To the polymer solution was added CTA (2.1 mg, 0.00078 mmol) as chain transfer agent and AIBN (0.25 mg, 0.000156 mmol) as initiator. Reaction mixture was stirred under N_2 for 30 min. Reaction was sealed and heated 70 °C for 20 h. The copolymer was purified *via* precipitation in diethyl ether, dissolved in CH_2Cl_2 and re-precipitated. After precipitation, copolymer was washed with diethyl ether. The product was dried under *vacuo* and obtained as viscous liquid (0.15 g, 50%). M_n = 59 kDa, M_w/M_n = 1.44. ^{1}H NMR (DMSO-*d6*, δ, ppm) 8.02 (bs, 1H), 7.73 -

7.72 (d, 1H, *J* = 4 Hz), 6.86-6.61 (m, 5H), 5.62 (bs, 1H), 4.09 (s, 2H), 3.85 (bs, 1H), 3.64 - 3.54 (m, 20H), 3.37 (s, 3H), 2.97 - 2.89 (m, 4H), 2.80 (bs, 4H), 1.82 - 0.87 (m, $-CH_2$ and CH_3 along with backbone).

4.2.10. Synthesis and Characterization of P(OEGMA-5'DFCR-FMA-RGD) (38)

Copolymer 37 (0.075 g) and cRGDfK (20 mg, 0.03 mmol) were dissolved in DMF (0.3 mL). To the copolymer solution, DIPEA (10 µL, 0.06 mmol) was added dropwise. Resulting reaction mixture was stirred at ambient temperature for 24 h. Then, ethanol amine (0.06 mmol, 3 µL) was added to the reaction mixture and the reaction was kept stirring at 45 °C for 1 d. Upon completion of the reaction, resulted copolymer was purified by using 3.5 kDa cut off membrane by dialysis. Copolymer was diluted with MeOH (10 mL) and placed in a 3.5 kDa cutoff dialysis bag. Dialysis bag was placed in a beaker containing MeOH (250 mL). Solvent was changed 3 times/day and dialysis was completed in 2 d. After dialysis, solvent was evaporated and dried under *vacuo* to obtain copolymer 38 (0.06 g, 80%) (M_n = 71 kDa M_w/M_n = 1.4). ^{1}H NMR (DMSO-*d6*, δ, ppm) 8.02 (bs, 1H), 7.92 - 6.55 (m, 9H), 5.60 (bs, 1H), 4.07 (s, 2H), 3.82 (bs, 1H), 3.64 - 3.54 (m, 20H), 2.93 (m, 4H), 2.55 (bs, 1H), 1.81 - 0.85 (m, $-CH_2$ and CH_3 along with backbone).

4.2.11. Synthesis and Characterization of P(OEGMA-5'DFCR-FMA) (39)

Copolymer 37 (0.075 g) and ethanol amine (0.06 mmol, 3 µL) were mixed in DMF (0.3 mL). Reaction was left at 45 °C for 1 d. Copolymer was diluted with MeOH (10 mL) and placed in a 3.5 kDa cutoff dialysis bag. Dialysis bag was placed in a beaker containing MeOH (250 mL). Solvent was changed 3 times/day and dialysis was completed in 2 d. After dialysis, solvent was evaporated and dried under *vacuo* to obtain copolymer 39. (0.055 g, 73%) (M_n = 69 kDa, Mw/Mn = 1.34). ^{1}H NMR (DMSO-*d6*, δ, ppm) 8.02 (bs, 1H), 7.92 - 6.55 (m, 9H), 5.58 (bs, 1H), 4.07 (s, 2H), 3.82 (bs, 1H), 3.64 - 3.54 (m, 20H), 2.93 (m, 4H), 2.55 (bs, 1H), 1.81 - 0.85 (m, $-CH_2$ and CH_3 along with backbone).

4.2.12. *In vitro* Drug Release

Drug release from polymer−drug conjugates was determined *via* LC−MSMS. Briefly, drug containing copolymer solutions were prepared in PBS, 10% glutathion containing PBS with total drug concentration of 0.1 mg/mL. Copolymer solutions were then incubated at 37 °C while stirring at 200 rpm for 48 h. A 100 μL sample was taken at predetermined time points, and ACN (900 μL) was added. Tubes were centrifuged at 6000 G for 5 min, and supernatants were analyzed for drug concentration by LC−MSMS analysis.

4.2.13. Cell Lines

All cell lines were incubated in a humidified incubator at 37 °C supplemented with 5% CO_2. They were kept in their logarithmic growth phase for all experiments stated here. MDA-MB-453 cells and MDA-MB-231 cells were cultured in RPMI 1640 media supplemented with 10% FBS.

4.2.14. *In vitro* Cell Viability Assay on MDA-MB-453 and MDA-M-231 Cells

Cell number and cell viability were determined by Cell Counting Kit-8 (CCK-8, Fluka). Cells were seeded in 100 μL of culture medium at a density of 15000 cells/well for MDA-MB-453 and 6000 cells/well for MDA-MB-231 cells into 96-well plates in quadruplicates for each drug concentration. After overnight incubation cell media was replaced with fresh medium containing various concentrations of conjugates, free drug, or polymer only controls. For free drug treatments 5-FU stock solutions were prepared in DMSO in growth medium (V/V) and subsequently diluted where the final DMSO concentration was below 0.5% (V/V). All cells were incubated continuously for 48 h in the presence of the micellar conjugates. For 2h+22h pulse chase drug treatment, cells were incubated 2 h in drug containing solutions and incubated in fresh media for 22h before CCK-8 assay. To determine the cell viability, 100 μL of culture medium together with 10 μL of CCK-8 solution was added into each well. After 4h incubation the absorbance values at 450 nm was measured with a plate reader (Multiscan FC, Thermo Scientific, USA). Viability of

treated cells was expressed as percentage of control cells (cell media only). EC_{50} values were obtained from concentration response curves by nonlinear regression analysis.

4.3. Results and Discussion

4.3.1. Synthesis and Characterization of 5'-DFCR Conjugated Copolymers

In this study, copolymers containing both the targeting group cRGDfK and the 5'-DFCR drug were designed and synthesized. 5'-DFCR which is prodrug of 5-FU was attached to the copolymer by using an acid sensitive carbamate linker. The drug containing monomer was designed so that it will have a reducible S-S bond which can be cleaved in the presence of thiol reducing agent as glutathion and initiate the release of the attached drug or cargo in a self-immolative manner. This drug containing monomer was obtained after multiple synthesis steps. In the first step, esterification reaction was achieved between methacryloyl chloride and hydroxide group of 2,2'-dithiodiethanol. Since only one of the hydroxide groups of 2,2'-dithiodiethanol was modified during the esterification, the remaining one would be used in the subsequent steps. Next, the free hydroxide group was modified with N,N′-Disuccinimidyl carbonate (DSC) to obtain a reactive carbonate functionality at the end of the monomer 32 (Figure 4.3). After synthesis of monomer 32, precursor of capecitabine, namely 2',3'-di-O-acetyl-5'-deoxy-5-fuluro-D-cytidine was attached to the monomer through its reactive carbonate group forming a carbamate linkage to form monomer 33. As a final step, acetate groups of prodrug's monosaccharide moiety were removed in the presence of a mixture containing TEA, water and methanol and the final monomer 34 was obtained. The carbamate linkage in the proximity of the S-S bond is particularly important since upon cleavage of this disulfide group, the thiol group that formed after reduction can further attack the carbamate linkage and trigger the release of the attached drug while forming a thiolactone as side product. This mechanism would work in theory for every drug or other cargo that contain a modifiable hydroxide or amine group that can react with the activated carbonate on the monomer thereby providing a self-immolative character to the final delivery system. As a conclusion, a novel monomer that contains cleavable disulfide and carbamate linkers was prepared for the subsequent polymerization step. All synthesized small molecules were characterized by using ^{1}H NMR, ^{13}C NMR and FT-IR^{-1} spectroscopy.

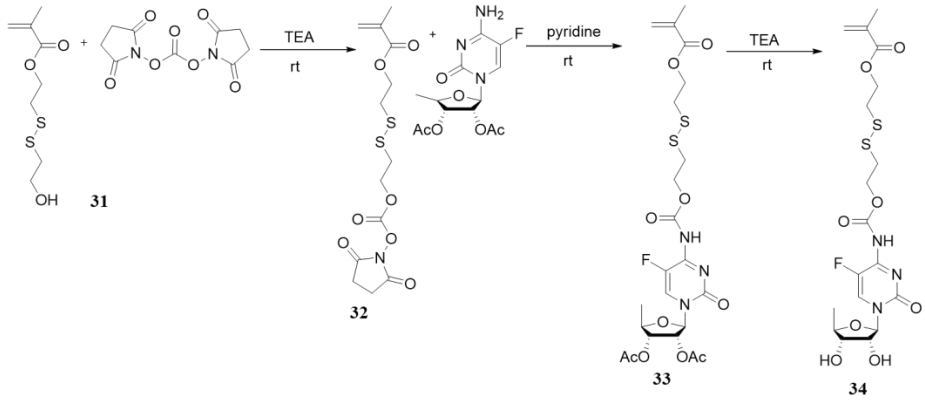

Figure 4.3. Synthetic route of 5'-DFCR bearing monomer.

Desired polymeric product was synthesized by RAFT copolymerization of activated ester containing monomer N-hydroxysuccinimide (NHSMA), hydrophilic monomer oligo (ethylene glycol) methyl ether methacrylate (OEGMA) and 5'-DFCR containing monomer 34. First, drug and activated ester bearing copolymer 35 was synthesized *via* AIBN initiated RAFT polymerization in DMF. Synthesized copolymers were characterized by using ^{1}H NMR spectroscopy to determine individual monomer compositions in the polymers. Furthermore, the molecular weight and distribution of resulting copolymers were determined through size exclusion chromatography (SEC).

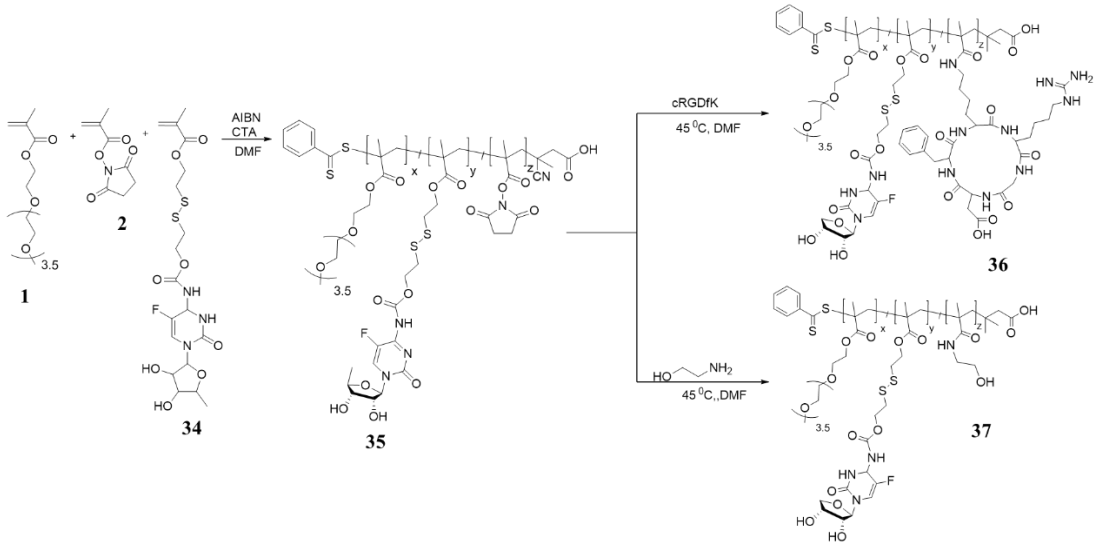

Figure 4.4. Synthesis of 5'-DFCR and cRGDfK bearing copolymers.

Table 4. 1. Polymerization conditions and obtained polymers' characterizations.

		Feed ratio				Obtained ratio					
No	**copolymer**	**1**	**2**	**34**	**11**	**1**	**2**	**34**	**11**	**M_n (kDa)**	**M_w/M_n**
1	**35**	80	10	10	-	78	13	9	-	49.0	1.34
2	**38**	80	10	10	5	72	14	10	4	36.0	1.35

According to the results, incorporation of monomers was determined as 78:13:9 for OEGMA (1), NHSMA (2) and MA5'-DFCR (34) respectively (Table 4.1, Item 1). As a following step, copolymer 35 was decorated with cRGDfK molecule through its NHS activated ester groups. At the end of the reaction, ethanol amine in DMF was added to reaction *in situ* for quenching of remaining NHS groups, thus targeting group bearing copolymer without any residual NHS groups was obtained.

Table 4. 2. Properties of Copolymers.

No	**copolymer**	**Mn (kDa)**	**Mw/Mn**	**5'-DFCR wt %[b]**	**cRGDfK wt %**	**FMA wt %[b]**	**Ethanol amine wt %[b]**
1	P(OEGMA-5'DFCR-RGD)	53.0	1.34	6.20	1.52	-	3.59
2	P(OEGMA-5'DFCR)	53.0	1.34	5.01	-	-	1.18
3	P(OEGMA-5'DFCR-RGD-FMA)	33.0	1.42	1.29	4.82	12.97	2.43
4	P(OEGMA-5'DFCR-FMA)	33.0	1.42	1.43	-	8.63	2.35

Average molecular weight of the targeted version of copolymer P(OEGMA-5'DFCR-RGD) was determined as 53 kDa as a result of SEC analysis. Deuterated DMSO was used for ^{1}H NMR analysis of copolymers since the phenyl protons of cRGDfK can't be observed

in any other solvents. According to the ^{1}H NMR spectroscopy, copolymer 36 contained 6.2% 5'-DFCR by weight while the cRGDfK amount was approximately 1.52% by weight. All determined percentages of monomers in the copolymer are summarized in Table 4.2.

For non-targeted counterpart of the copolymer, copolymer 35 was reacted with ethanol amine in DMF for 24 h, at 45 °C. The reason for doing this is to obtain copolymers with or without targeting units with identical drug contents, where they also have the same molecular weight and distribution. The product, copolymer 37, was characterized using ^{1}H NMR spectroscopy and SEC analysis. According to results, negligible amount of drug content was lost during NHS removal process.

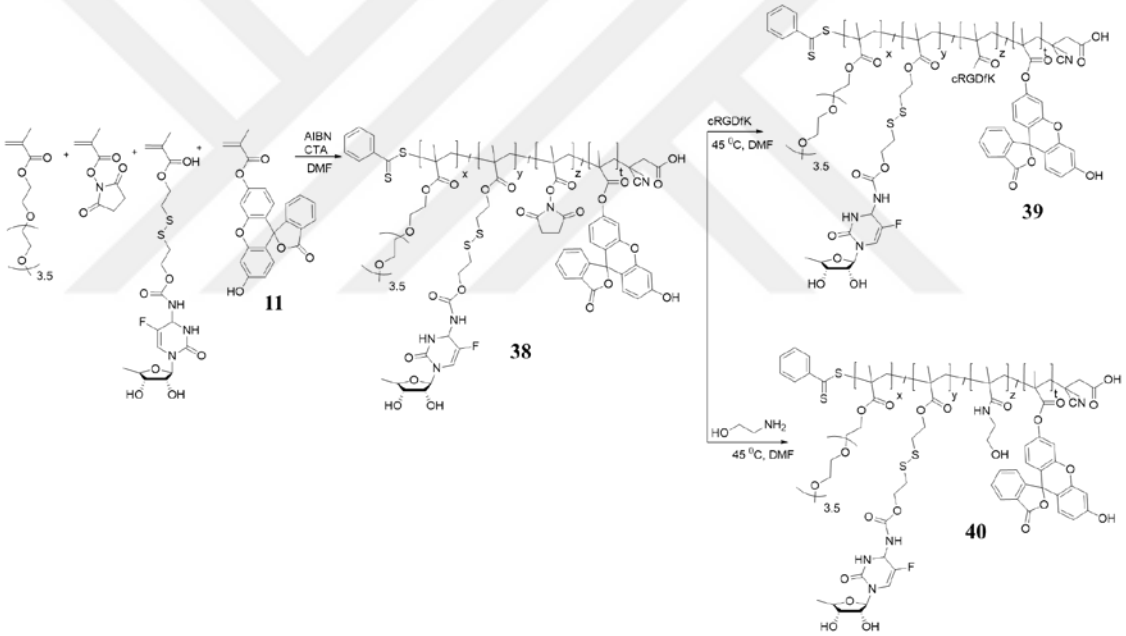

Figure 4.5. Synthesis of 5'-DFCR, FMA and cRGDfK bearing copolymers

After the above mentioned studies, we wanted to investigate if there is any difference between cell internalization capabilities of targeted and non-targeted copolymers. For internalization studies, fluorescein dye containing analogues of copolymers were also prepared (Figure 4.5). In addition to the normal polymerization reaction procedure, fluorescein methacrylate monomer was also added to reaction. Similar to nonfluorescent copolymers, fluorescein dye containing copolymers were also seperated in two batches. One batch was attached with cRGDfK and other one was reacted with just ethanol amine for preparation of non-targeted counterpart. Resulted molecules were characterized by using ^{1}H

NMR and SEC analysis. Properties of targeting group, dye and 5'-DFCR drug containing copolymers were shown in Table 4.2, items 3 and 4.

4.3.2. Drug Release Profiles of Copolymers

The *in vitro* release of 5'-DFCR from copolymers were evaluated in the presence of glutathion since it is overexpressed in tumor cells. Prodrug of capecitabine, 5'-DFCR, was conjugated to copolymer *via* carbamate linker to improve release profile of molecule in acidic environment of tumor. At the same time, reducible disulfide bond was utilized for obtaining more enhanced release behavior. Drug conjugated polymers were incubated at 37 °C in 5 mM glutathion containing PBS (pH = 7.4). For control, polymers were also incubated at 37 °C in glutathion free PBS. Samples were collected at predetermined time points and they were analyzed by using LC-MSMS. As a result, approximately 84% of drug was released from targeting group containing polymer while this amount is 88% for non-targeted counterpart in the presence of glutathion at the end of the 2 d (Figure 4.6A). On the other hand, almost any amount of drug did not release from both polymers when glutathion was not added to PBS solution as expected (Figure 4.6B).

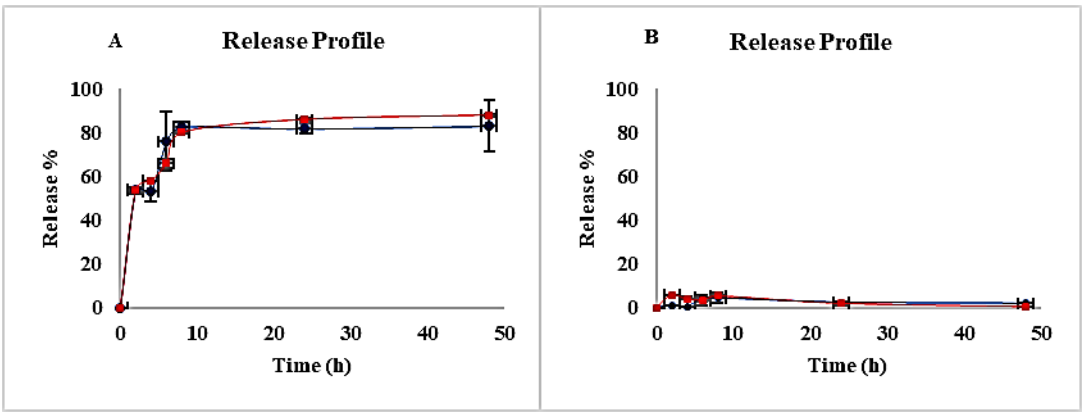

Figure 4.6. Release profiles of cRGDfK targeted copolymer 35 (blue circle) and non-targeted copolymer 36 (red square) in 5 mM glutathion containing PBS (A) and in PBS (B).

According to the results, disulfide bonds provide selectivity and enhanced release behavior to copolymers which means drug is not expected to be released from copolymers in normal body conditions and it will release its cargo after copolymer reaches to tumor tissue with the help of targeting group and EPR effect.

4.3.3. Determination of *in vitro* Cytotoxicity of Copolymers on MDA-MB-453 and MDA-MB-231 Cells

To investigate cytotoxicity effects of the 5'-DFCR bearing targeted and non-targeted copolymers, proliferation assay on MDA-MB-453 cells was performed (Figure 4.7). Cells were treated with free 5-FU, P(OEGMA-5'DFCR-RGD) (35) and P(OEGMA-5'DFCR) (36) copolymers.

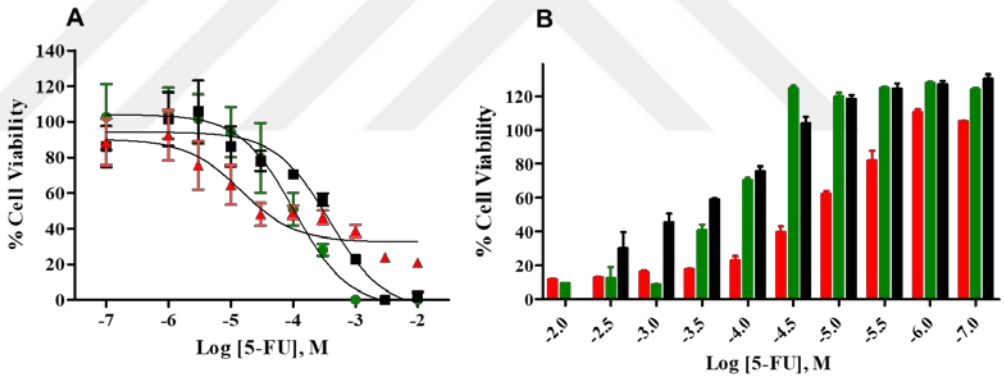

Figure 4.7. Viabilities of MDA-MB-453 and MDA-MB-231 cells treated with free 5-FU (▬), P(OEGMA-5'DFCR-RGD) (▬) and P(OEGMA-5'DFCR) (▬).

Since 5'DFCR is expected to convert into 5-FU in the tumor region ultimately, cytotoxicity of free 5-FU was determined. Because of the release process, both copolymers are less toxic compared to free 5-FU, as expected. EC_{50} value of free 5-FU was obtained as 14.6 µM in 48 h.

Table 4.3. EC_{50} values of MDA-MB-453 and MDA-MB-213 cells treated with free 5-FU, targeted and non-targeted copolymers.

No	Sample	EC_{50} values (M)	
		MDA-MB-453	MDA-MB-231
1	5-FU	1.46×10^{-5}	9.57×10^{-6}
2	P(OEGMA-5'DFCR-RGD)	1.04×10^{-4}	1.24×10^{-5}
3	P(OEGMA-5'DFCR)	3.85×10^{-4}	1.013×10^{-5}

Both targeted and non-targeted copolymers exhibited cytotoxicity effect on MDA-MB-453 cells, and they are approximately 10 times less toxic than free 5-FU. On the other hand, there is also difference between targeted and non-targeted copolymers in terms of their toxicities. According to results, cRGDfK containing copolymer is more toxic than non-targeted counterpart which are 104 µM and 385 µM, respectively. As for MDA-MB-231 cell lines, free 5-FU exhibited more toxic behavior toward MDA-MB-231 cell line when compared to both copolymers. However, when EC_{50} values of copolymers were checked, non-targeted copolymer seems more toxic but at high concentrations of drug, it was observed that targeted copolymer was more effective than non-targeted copolymer on MDA-MB-231 cells. All EC_{50} values are shown in Table 4.3.

4.4. Conclusion

A novel monomer bearing 5'-DFCR, the active moiety of the chemotherapy prodrug capecitabine, was prepared and polymerized. Design of the monomer includes a reducible S-S bond and carbamate functionality to link the active agent to the carrier. The obtained polymer was ornamented with integrin targeting cRGDfK peptide. Satisfying release profiles of 5'-DFCR was observed in PBS that has 5 mM concentration of glutathion. On the other hand, in GSH free solution, release of drug was negligible. Both targeted and nontargeted conjugates were evaluated for their toxicity toward two different breast cancer cell lines, MDA-MB-453 and MDA-MB-231. Both conjugates were toxic, with the targeted

copolymers showing slightly higher activity, against to both the cell lines. Free 5-FU was more toxic when compared to copolymers, as expected. Furthermore, for internalization studies, dye containing counterparts were prepared. This novel carbamate monomer can gain great attention since the same idea can be utilized for attachment of different drugs, as a carbamate as well as a carbonate.

5. NOVEL CATHEPSIN B LABILE DIPEPTIDE LINKER VAL-CIT AND ANTI-NEOPLASTIC DRUG DOCETAXEL CONJUGATED MONOMER FOR CANCER TREATMENT

5.1. Introduction

For obtaining effective therapy for cancer, systematic stability of used macromolecules or small drugs is very crucial and it can be provided by selective release [295]. Furthermore, clinical applications of macromolecules are limited due to their poor water solubility and short circulation time in the body. Accordingly, polymer drug conjugates together with special targeting group attachments are designed to improve blood circulation time, selective release ability and stability of macromolecules [296]. Benefiting from cleavable bonds such as pH sensitive, enzymatically cleavable or reductive bonds, can support selective release profile of macromolecules [297]. Thus, surrounding conditions of used cleavable bonds while designing the structures of polymers or macromolecules are gaining so much importance.

Among all these cleavable bonds bearing structures, using enzymatically cleavable linkers is one of the most interested type by researchers. It has been known that some lysosomal enzymes are over-expressed in the tumor tissue [197]. For instance, Cathepsin B is very well-known enzyme which exists in lysosome of cell and it is kind of cysteine protease. In addition to this, according to latest researches, it has relationship with tumor growth progression. Cathepsin B enzyme can cleave some special peptides such as phe-lys, phenylalanine-arginine and valine-citrulline (VC) [298]. When these peptides are used as linkers in conjugates or amphiphilic molecules, these structures show enhanced blood circulation time and plasma stability. As a result, polymer drug conjugates which carry their drugs *via* these cathepsin b cleavable linkers are expected to release their drug in the lysosome of cell at tumor region. Valine-citrulline dipeptide sequence is one of the most encountered cathepsin b cleavable linker in the design of polymer-drug carriers. For drug conjugation with val-cit linker, p-amino benzyl alcohol (PABC) is used as a spacer because

according to researches, macromolecules cannot release their cargo when drug was directly attached to linker due to absence of sufficient cleavage region and space for enzyme [299]. So that, cathepsin b can't penetrate in to molecule and it cannot recognize the amide bond. For example in one study which was reported in 2012, paclitaxel was attached to val-cit-pabc conjugate [300]. In addition, this prepared drug carrier was also attached with carboxyl-terminated poly(ethylene glycol) monomethyl ether (mPEG) to obtain hydrophilic character as well. As expected, hydrophilic character was gained to drug paclitaxel due to PEGylation and efficiency of VC linker containing structure was much more when compared to other construct that doesn't contain VC linker. Another micellar structure was prepared by Huang and his co-workers in 2015 [301]. One side of VC linker was PEGylated, and other side was conjugated with stearic acid (C_{18}) to obtain self-assembled ellipsoid micelles. As another step, doxorubicin was loaded into these micelles to evaluate cytotoxicities toward human pancreatic cancer cell lines BxPC-3. On the other hand there are a lot of antibody-drug conjugation (ADC) studies in which VC linker was utilized in last decades [302]. Especially some of the ADC's are incorporated with dipeptide linkers such as phenylalanine-lysine and valine-citrulline. For instance, in the use of monomethyl auristatin E (MMAE) which is so toxic towards to healthy cells and cannot be used as a chemotherapy agent alone, val-cit linker is utilized due to its 230 days of half-live in the human plasma. MMAE is conjugated with cBR96 antibody *via* val-cit linker [202]. After it's administration to body, this linker undergoes hydrolysis in the presence of cathepsin b in lysosome. Brentuximab is also used for MMAE delivery to the tumor region. In one example, MMAE was conjugated to brentuximab *via* thiol reactive spacer, val-cit linker and PABC spacer [204].

In our case, we are synthesizing a novel methacrylated monomer that contains VC linker and para aminobenzoic acid (PABA) spacer. Different from the examples that are mentioned above, we are using PABA spacer instead of PABC spacer due to obtaining ester linker between drug and spacer. We are expecting our linker to be cleaved by cathepsin b enzyme through amide bond. After that, it will hydrolyze from ester bond to release its drug under acidic conditions of the tumor. Design of the structure is illustrated in Figure 5.1.

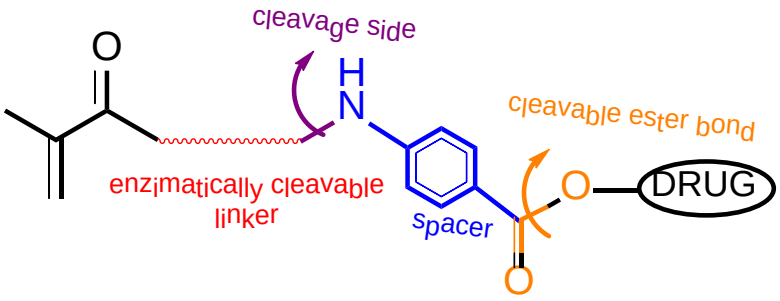

Figure 5.1. Design of methacrylated val-cit linker and PABA spacer bearing prodrug.

5.2. Experimental Section

5.2.1. Materials

Fmoc protected Valine (Fmoc-Val), N,N'-diisopropylcarbodiimide (DIC), N-(3-Dimethylaminopropyl)-N′-ethylcarbodiimide hydrochloride (EDC), L-citrulline and methacryloyl chloride were purchased from Alfa Aesar. All the other chemicals and 1-Hydroxybenzotriazole (HOBT) were obtained from Sigma Aldrich. The solvents used throughout this thesis were purchased from Merck. Milli-Q Water Purification System (Milli-Q system, Millipore, Billerica, MA, USA) was employed to produce ultrapure water. Reaction conditions that require anhydrous conditions were carried out under nitrogen atmosphere. Polyethylene glycol methacrylate (OEGMA Mn = 300) was obtained from Sigma Aldrich and filtered through basic alumina column prior to use. NHSMA (N-hydroxysuccinimide methacrylate) monomer was synthesized according to previously reported protocols [293]. Cyano-4-(phenylcarbonothioylthio)pentanoic acid (CPDTB) was used as chain transfer agent (CTA) and purchased from Sigma Aldrich as well. AIBN was recrystallized from methanol before use. cRGDfK was synthesized according to literature example.

5.2.2. Instrumentation

^{1}H and ^{13}C NMR spectroscopy (Varian 400 MHz NMR spectrometer), Fourier transform infrared (ATR-FTIR) spectroscopy (Nicolet 380, Thermo Scientific, USA), and UV−vis spectroscopy (PerkinElmer series) methodologies were used in order to characterize synthesized monomers and polymers. The qualification and quantification of all synthesized small molecules were achieved utilizing the liquid chromatography−mass spectrometry (LC−MS) system (LCMS 2020, Shimadzu, Japan) with a C- 18 (5 μm, 150 × 4.6 mm) column. A gradient method was utilized with acetonitrile (ACN) and deionized water supplemented with 0.05% trifluoroacetic acid (TFA) through the following program; LC: 0−3 min, 50% ACN; 3.01 min, 50% ACN; 8 min, 95% ACN; 8.01−11 min, 50% ACN; MS positive scan 100−2000 m/z. The polymer molecular weights were estimated by size exclusion chromatography (SEC) using a PSS-SDV (length/ID 8 × 300 mm, 10 mm particle size) linear Mixed C column calibrated with poly(methyl methacrylate) (PMMA) standards using a refractive-index detector with a mobile phase solution of 0.05 M lithium bromide in dimethylaceteamide (DMAc) as eluent at a flow rate of 1 mL/min at 30 °C. During the internalization experiments, cells were visualized using Zeiss Observer.Z1 inverted fluorescence microscope.

5.2.3. Synthesis of t-Butyl-4-aminobenzoate (41)

t-Butyl-4-aminobenzoate was synthesized via esterification of 4-amino benzoic acid and t-butyl alcohol. Briefly, 4-amino benzoic acid (2.00 g, 14.6 mmol) and EDC (2.78 g, 14.6 mmol) were dissolved in t-butyl alcohol (50 mL). The mixture was refluxed for 24 h at 90 °C. Upon reaction was complete, it was allowed to cool and water (50 mL) was added. Mixture was extracted with diethyl ether (4 x 80 mL) and organic phase was collected. Ether phase was dried over Na_2SO_4 and evaporated. Obtained yellowish solid was washed with CH_2Cl_2 three times to remove unreacted 4-amino benzoic acid. Additional purification can be achieved by recrystallization of product from ethanol (2.00 g, 71 %). ^{1}H NMR (DMSO-*d6*, δ, ppm) 7.57 - 7.54 (d, 2H, *J* = 12 Hz), 6.54 - 6.51 (d, 2H, *J* = 12 Hz), 5.88 (bs, -NH_2), 1.48 (s, 9H). LC−MS expected [M + H] m/z = 194 and observed [M + H] m/z = 194.

5.2.4. Synthesis of Fmoc-Val-Cit (42)

Fmoc-Val (3 g, 8.8 mmol) and OHSu (1.01 g, 8.8 mmol) were dissolved in anhydrous THF (20 mL). Reaction was cooled to 0 °C. N,N'-Dicyclohexylcarbodiimide (DCC) (1.8 g, 8.8 mmol) was dissolved in anhydrous THF (10 mL) and DCC solution was added dropwise to the first mixture. Reaction was left at rt for 24 h. Then, white solid was filtered and washed with THF. The solvent was removed under reduced pressure. Obtained glassy and colorless viscous liquid was used without further purification in the second step. Crude Fmoc-Val-OSu (8.8 mmol) dissolved in 1,2-dimethoxyethylene (DME). Mixture was added to a solution of $NaHCO_3$ (0.75 g, 9 mmol) and L-citrulline (1.57 g, 9 mmol) in water (20 mL). and THF (5 mL). Reaction was stirred at rt for 24 h. Then, citric acid solution (15%, 50 mL) was added to reaction mixture and extracted with isopropanol/ethyl acetate (10%, 4 x 100 mL). Organic layers were combined, dried over Na_2SO_4 and solvent was evaporated under reduced pressure. Resulted glassy and sticky product was washed and sonicated with diethyl ether. Then, white solid was washed with CH_2Cl_2 for removal of unreacted Fmoc-Val-OH. After the washing process, white solid product was filtered and dried under *vacuo* to yield 42 (3.50 g, 80%). ^{1}H NMR (DMSO-*d6*, δ, ppm) 8.16 (d, *J* = 7.2 Hz, 1H), 7.90 (d, *J* = 7.6 Hz, 2H) 7.75 (t, *J* = 7.2 Hz, 1H), 7.31 – 7.44 (m, 5H), 5.92 (t, *J* = 4.8 Hz, 1H), 5.36 (br s, 2H), 4.12 – 4.31 (m, 4H), 3.92 (t, *J* = 8.0 Hz, 1H), 2.92 – 2.97 (m, 2H), 1.94 – 2.00 (m, 1H) 1.36 – 1.73 (m, 4H), 0.89 (d, *J* = 6.4 Hz, 3H), 0.86 (d, *J* = 6.8 Hz, 3H). LC−MS expected [M + H] m/z = 497 and observed [M + H] m/z = 497.

5.2.5. Synthesis of Fmoc-Val-cit-tertiary amino benzoate (43)

Fmoc-Val-Cit (42) (2.00 g, 4.04 mmol) was dissolved in anhydrous DMF (3 mL) in a flask to which was added HOBt (0.54 g, 4.04 mmol) and EDC (0.77 g, 4.04 mmol). After 10 min, t-butyl-4-aminobenzoate (0.78 g, 4.04 mmol) and $CuCl_2$ (0.054 g, 0.404 mmol) in anhydrous DMF (6 mL) were added to the first mixture. Reaction was allowed to stir at rt for 5 d. Then, saturated K_2CO_3 solution (20 mL) was added to the mixture and extracted with ethyl acetate (4 x 100 mL). Organic phase was separated and dried with Na_2SO_4. Solvent was evaporated, yellowish product was washed with ether.

Obtained white product was dried under *vacuo* to yield 43. (1.20 g, 44%). ^{1}H NMR (DMSO-*d6*, δ, ppm) 7.90 - 7.31 (m, 12 H), 5.92 (t, *J* = 4.8 Hz, 1H), 5.36 (br s, 2H), 4.12 – 4.31 (m, 4H), 3.92 (t, *J* = 8.0 Hz, 1H), 2.92 – 2.97 (m, 2H), 1.94 – 2.00 (m, 1H), 1.53 (s, 9H), 1.36 – 1.73 (m, 4H), 0.89 (d, *J* = 6.4 Hz, 3H), 0.86 (d, *J* = 6.8 Hz, 3H). ^{13}C NMR (DMSO-*d6*, δ, ppm) 202.8, 171.6, 164.9, 159.3, 144.3, 141.2, 130.5, 128.1, 127.5, 125.8, 120.5, 118.9, 80.7, 47.1, 30.9, 29.7, 28.3, 27.3, 19.6, 18.9. FT-IR (cm^{-1}) 1698, 1644, 1115, 739. LC−MS expected [M + H] m/z = 672 and observed [M + H] m/z = 672.

5.2.6. Synthesis of Val-cit-tertiary amino benzoate (44)

Fmoc-Val-cit-tertiary amino benzoate (1.20 g, 1.78 mmol) was dissolved in DMF (1.0 mL) and pyrrolidine (3.0 mL). Reaction was stirred for 1 h. Upon completion of the reaction, volatiles were removed. Obtained brown viscous product was washed ether four times, for removal of remaining pyrrolidine. Yellowish solid was obtained and dried under *vacuo* to yield 44 (0.5 g, 63%). ^{1}H NMR (DMSO-*d6*, δ, ppm) 8.17 (bs, 1H), 7.86 (d, *J* = 7.6 Hz, 2H), 7.73 (d, *J* = 7.6 Hz, 2H), 6.03 (bs, 1H), 4.48 (bs, 1H), 3.02 - 2.95 (m, 3H), 1.92 - 1.37 (m, 14H), 0.89 - 0.77 (m, 6H). ^{13}C NMR (DMSO-*d6*, δ, ppm) 175.2, 171.8, 165.1, 159.4, 143.3, 133.3, 130.6, 126.2, 118.9, 80.8, 60.1, 53.2, 31.8, 30.3, 28.3, 27.1, 20.0, 17.4. FT-IR (cm^{-1}) 3307, 2964, 1650, 1599. LC-MS expected [M + H] m/z = 450 and observed [M + H] m/z = 450.

5.2.7. Synthesis of MA-Val-cit-tertiary amino benzoate (45)

To a solution of Val-cit-tertiary amino benzoate (0.50 g, 1.11 mmol) and triethylamine (0.112 g, 1.11 mmol) in THF (5 mL) was added methacryloyl chloride (0.115 g, 1.11 mmol) dropwise over 10 min at 0 °C. Then, reaction was stirred at rt for 24 h. Upon completion, solution was evaporated and diluted with dichloromethane (10 mL), and organic phase was washed with saturated $NaHCO_3$ (2 × 20 mL) and H_2O (2 × 20 mL). Combined organic layers were dried over Na_2SO_4 and evaporated. Crude product was purified by column chromatography on SiO_2 (EtOAc/DCM, 20:80) affording compound 45 (0.30 g, 52 %). ^{1}H NMR (DMSO-*d6*, δ, ppm) 8.17 (bs, 1H), 7.86 (d, *J* = 7.6 Hz, 2H), 7.73 (d, *J* = 7.6 Hz, 2H),

6.03 (bs, 1H), 5.70 (s, 1H), 5.43 (s, 1H), 4.40 (bs, 1H), 4.23 - 4.19 (m, 1H), 2.97 (bs, 1H), 2.05 - 1.41 (m, 14H), 0.90 - 0.85 (m, 6H). ^{13}C NMR (DMSO-*d6*, δ, ppm) 176.4, 176.3, 172.9, 169.8, 164.1, 148.2, 144.9, 135.3, 130.9, 124.6, 123.5, 85.5, 63.4, 58.6, 35.5, 34.3, 33.0, 32.0, 24.5, 23.9, 23.8. FT-IR (cm^{-1}) 3295, 2971, 1650, 1599, 771. LC-MS expected [M + H] m/z = 518 and observed [M + H] m/z = 518.

5.2.8. Synthesis of MA-Val-cit-amino benzoic acid (46)

MA-Val-cit-tertiary amino benzoate (0.30 g, 0.58 mmol) was dissolved in CH_2Cl_2 (1.0 mL) and was added trifluoroacetic acid (TFA) (2.0 mL). Reaction was stirred at rt for 1 h. Then, solvents were evaporated, crude product was washed with diethyl ether. Obtained yellowish solid was dried under *vacuo* to yield compound 46 (0.25 g, 93%). ^{1}H NMR (DMSO-*d6*, δ, ppm) 8.17 (bs, 1H), 7.86 (d, *J* = 7.6 Hz, 2H), 7.73 (d, *J* = 7.6 Hz, 2H), 5.70 (s, 1H), 5.37 (s, 1H), 4.42 (bs, 1H), 4.24 - 4.20 (m, 1H), 3.02-2.98 (m, 2H), 2.07 - 1.45 (m, 8H), 0.95 - 0.80 (m, 6H). ^{13}C NMR (DMSO-*d6*, δ, ppm) 171.6, 171.5, 168.2, 167.3, 159.4, 143.4, 140.2, 130.8, 125.6, 119.8, 118.8, 58.6, 53.8, 45.4, 42.7, 30.8, 29.6, 27.2, 19.7, 19.1. FT-IR (cm^{-1}) 3292, 2964, 1650, 15989, 772. LC-MS expected [M + H] m/z = 461 and observed [M + H] m/z = 461.

5.2.9. Synthesis of MA-Val-cit-amino benzoyl-DTX (47)

MA-Val-cit-amino benzoic acid (0.25 g, 0.54 mmol), DTX (0.43 g, 0.54 mmol) and DMAP (1.64 mg, 0.135 mmol) were dissolved in anhydrous THF. Reaction mixture was placed in an ice-bath and stirred for 10 min at 0 °C. Then, DIC (84 µL, 0.54 mmol) was added dropwise to the mixture. Upon completion of addition, reaction was stirred at rt for 24 h. Then, the solvent was removed and crude product was purified by column chromatography on SiO_2 (EtOAc/DCM, 50:50) to yield compound 47 (0.2 g, 30%). ^{1}H NMR (DMSO-*d6*, δ, ppm) 8.25 - 7.20 (m, 15H), 6.0 - 5.98 (t, *J* = 4Hz, 1H), 5.86 - 5.81 (t, *J* = 12Hz, 1H), 5.70 (s, 1H), 5.41 (s, 2H), 5.27 (s, 1H), 5.1 (s, 1H), 5.01 (d, *J* = 4Hz, 1H), 4.91 (s, 1H), 4.45 (s, 1H), 4.42 (m, 1H), 4.25 (t, *J* = 8Hz 1H), 4.08 - 3.98 (m, 2H), 3.72 (s, 1H), 3.68 (d, *J* = 8Hz, 1H), 3.17 - 2.96 (m, 1H), 2.28 (s, 3H), 2.1 – 2.03 (m, 1H), 1.98 (s, 2H),

1.87 (s, 3H), 1.75 (s, 3H), 1.65 – 1.59 (m, 2H), 1.52 (s, 3H), 1.39 (s, 9H), 0.99 (s, 6H), 0.91 – 0.81 (m, 6H). ^{13}C NMR (DMSO-*d6*, δ, ppm) 171.9, 171.7, 169.3, 168.3, 165.7, 165.1, 159.5, 144.5, 140.2, 133.8, 131.4, 130.5, 129.9, 129.1, 128.6, 128.0, 119.9, 118.9, 84.2, 80.7, 79.1, 77.3, 76.3, 75.8, 75.3, 74.1, 71.8, 71.2, 68.2, 60.2, 58.7, 57.4, 53.9, 46.4, 43.3, 30.7, 29.5, 28.6, 27.3, 26.9, 22.9, 21.2, 19.7, 19.5, 19.2, 19.1, 14.2, 10.2. FT-IR (cm^{-1}) 3341, 2964, 2354, 1704, 1651, 767. LC-MS expected [M + H] m/z = 1253 and observed [M + H] m/z = 1253.

5.2.10. Synthesis of P(OEGMA-MA-VC-benzoyl-DTX-NHS) (48)

OEGMA (0.13 g, 0.44 mmol) and NHSMA (4 mg, 0.025 mmol) were dissolved in DMF (0.2 mL). To the solution was added CTA (0.65 mg, 0.0023 mmol) as chain transfer agent and AIBN (0.084 mg, 0.00051 mmol) as initiator. Reaction mixture was stirred under N_2 for 30 min. Reaction was sealed and heated 80 °C for 1 h. Then, temperature was decreased to 50 °C and MA-VC-benzoyl-DTX (4 mg, 0.0518 mmol) in DMF (0.1 mL) was added to the mixture. The reaction was stirred at 50 °C for 47 h. Molecular weight and PDI of the polymer were checked by SEC. Copolymer was diluted with 2 mL of acetonitrile (ACN) and placed in the 10 kDa cutoff dialysis bag. Dialysis bag was placed in a beaker containing acetonitrile (25 mL). Solvent was changed 3 times/day and dialysis was completed in 2 d. Solvent was evaporated and dried under *vacuo* to yield copolymer 48 (0.055 g, 29 %) (M_n = 47k Da, M_w/M_n = 1.72). ^{1}H NMR (DMSO-d6, δ, ppm) 8.05 – 7.19 (m, 14H), 4.02 (bs, 2H), 3.64 - 3.54 (m, 20H), 3.25 (s, 3H), 2.96 (bs, 4H), 2.2 - 0.85 (m, $-CH_2$ and CH_3 along with backbone).

5.2.11. Synthesis of P(OEGMA-MA-VC-benzoyl-DTX-RGD) (49)

Copolymer 48 (0.055 g) and cRGDfK (8 mg, 0.013 mmol) were dissolved in DMF (0.1 mL). To the copolymer solution, DIPEA (0.18 mg, 0.0013 mmol) was added dropwise, resulting reaction mixture was stirred at 45 °C for 24 h. Then, ethanol amine (0.08 mg, 0.013 mmol) was added to the reaction mixture and reaction was kept stirring at ambient temperature for 24 h. Copolymer was diluted with MeOH (5 mL) and placed in a 3.5 kDa

cutoff dialysis bag. Dialysis bag was placed in a beaker containing MeOH (100 mL). Solvent was changed 3 times/day and dialysis was completed in 2 d. After dialysis, solvent was evaporated and dried under *vacuo* to obtain copolymer 49 (0.033 g, 55%) (M_n = 47 kDa, M_w/M_n = 1.72). ^{1}H NMR (DMSO-d6, δ, ppm) 8.09 – 7.18 (m, 19H), 4.02 (bs, 2H), 3.64 - 3.54 (m, 20H), 3.25 (s, 3H), 2.96 (bs, 4H), 2.2 - 0.85 (m, $-CH_2$ and CH_3 along with backbone).

5.2.12. Cell Lines

All cell lines were incubated in a humidified incubator at 37 °C supplemented with 5% CO_2. They were kept in their logarithmic growth phase for all experiments stated here. A549 cells were cultured in RPMI 1640 media supplemented with 10% FBS.

5.2.13. *In vitro* Cell Viability Assay on A549 Cells

Cell number and cell viability were determined by Cell Counting Kit-8 (CCK-8, Fluka). Cells were seeded in 100 µL of culture medium at a density of 15000 cells/well for A549 cells into 96-well plates in quadruplicates for each drug concentration. After overnight incubation cell media was replaced with fresh medium containing various concentrations of conjugates, free drug, or polymer only controls. For free drug treatments 5-FU stock solutions were prepared in DMSO in growth medium (V/V) and subsequently diluted where the final DMSO concentration was below 0.5% (V/V). All cells were incubated continuously for 48 h in the presence of the micellar conjugates. For 2h+22h pulse chase drug treatment, cells were incubated 2 h in drug containing solutions and incubated in fresh media for 22h before CCK-8 assay. To determine the cell viability, 100 µL of culture medium together with 10 µL of CCK-8 solution was added into each well. After 4h incubation the absorbance values at 450 nm was measured with a plate reader (Multiscan FC, Thermo Scientific, USA). Viability of treated cells was expressed as percentage of control cells (cell media only). EC_{50} values were obtained from concentration response curves by nonlinear regression analysis.

5.3. Results and Discussion

5.3.1. Synthesis of Val-Cit dipeptide and chemotherapy drug docetaxel bearing monomer

In this study, a special dipeptide linker Valine-Citrulline, that is sensitive to enzyme of tumor environment was utilized. Cathepsin B is known as cysteine protease enzyme that exists in the lysosome of tumor excessively. In addition to that it is found that cathepsin b can cleave some special peptide sequences including Valine-Citrulline and Phenylalanine-Arginine. Moreover, when these sequences are used as linkers of the structures in polymers, they provide enhanced plasma stability. To benefit from that knowledge, we designed a novel monomer that bears val-cit peptide sequence and chemotherapy drug on it.

Docetaxel containing and cathepsin B cleavable dipeptide val-cit bearing monomer was successfully synthesized in 7 steps (Figure 5. 2). Reactivity of amine group of spacer, during the conjugation with dipeptide val-cit, requires protection of acid moiety. Thus, 4-amino benzoic acid was reacted with tertiary buthanol to give t-Butyl-4-aminobenzoate (41). Fmoc-valine and L-citrulline conjugation was achieved by using previously mentioned protocols in the literature (42). As a third step, Fmoc-Val-Cit and t-Butyl-4-aminobenzoate were conjugated by utilization of carbodiimide coupling via EDC and HOBT in DMF to afford compound 43. To avoid racemization, catalytic amount of $CuCl_2$ was also added to the reaction mixture. After completion of the coupling, Fmoc removal was carried out in the presence of pyrrolidine in DMF to yield 44. In order to obtain the monomer, amine moiety of the valine was methacrylated in THF to obtain monomer 45. Following the monomer synthesis, tertiary buthanol moiety was removed with TFA to obtain reactive acid group for drug conjugation in the last step. Drug monomer was obtained *via* esterification reaction between acid group of citrulline and the hydroxyl group of drug docetaxel in the presence of DIC and 4-dimethylaminopyridine (DMAP) by using THF as solvent. All molecules were characterized by using ^{1}H NMR, ^{13}C NMR, FT-IR (cm^{-1}) spectroscopies and LC-MS.

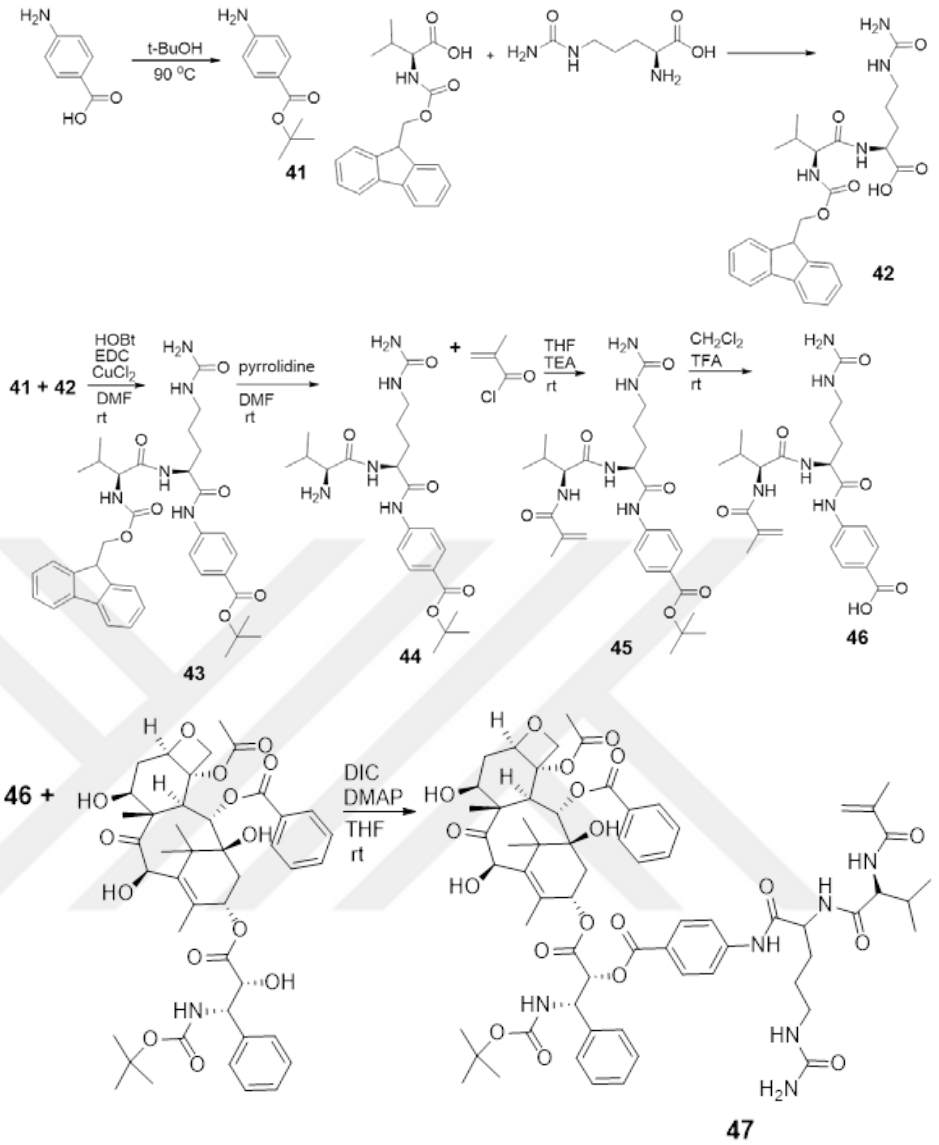

Figure 5.2. General synthesis of Val-Cit dipeptide bearing and Docetaxel containing monomer.

Following the monomer synthesis, polymerization reaction was achieved by using RAFT polymerization technique (Figure 5.4). First, drug and activated ester bearing copolymer was prepared *via* AIBN initiated RAFT polymerization in DMF to afford copolymer 48. Copolymer was characterized by using ^{1}H NMR spectroscopy to determine compositions of each monomer in the polymer. Size exclusion chromatography (SEC) was utilized for exploring of molecular weight and polydispersity index of the copolymer. According to the results, incorporation of monomers was determined as 84:7:9 for the monomers P(OEGMA), NHSMA, MA-VC-benzoyl-DTX respectively when the initial monomer ratio used was P(OEGMA):NHSMA:MA-VC-benzoyl-DTX. As a following step,

cRGDfK peptide was attached to copolymer 48 through its NHS activated ester groups. At the end of the reaction, ethanol amine in DMF was added to reaction *in situ* for quenching of remaining NHS groups, thus targeting group bearing copolymer that has no free NHS groups was obtained. Initially, copolymer 48 was dissolved in DMF and a solution of cRGDfK in DMF and DIPEA were added. The final product, copolymer 49, P(OEGMA-VC-benzoyl-DTX-RGD) was obtained. According to ^{1}H NMR spectroscopy, copolymer was containing 9.25 % DTX by weight and cRGDfK amount was 2.62 wt% approximately. (Figure 5.3).

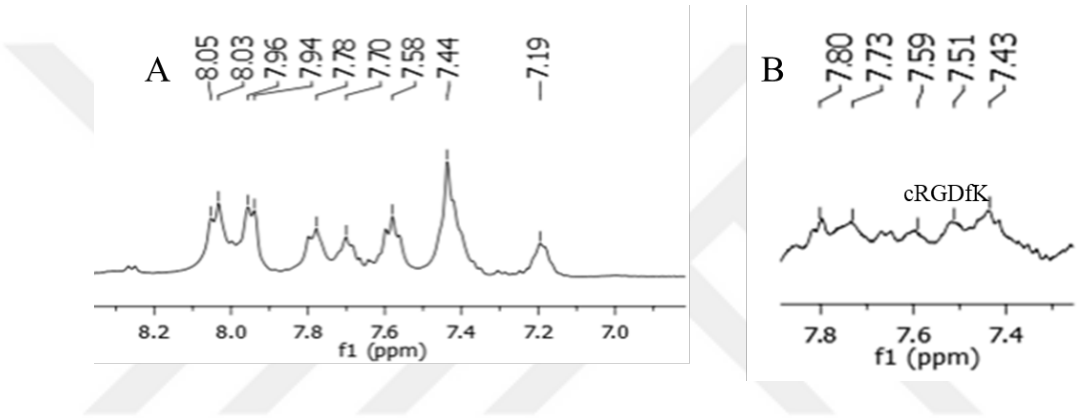

Figure 5.3. Expanded ^{1}H NMR spectrums of copolymers 48 (A) and copolymer 49 (B).

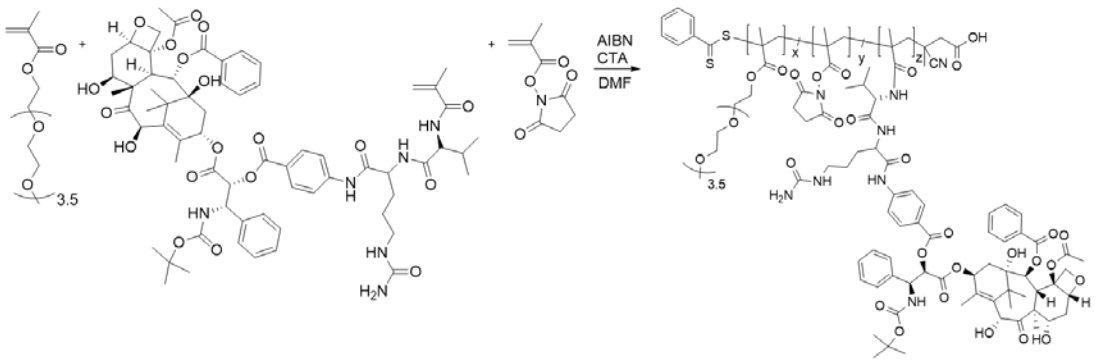

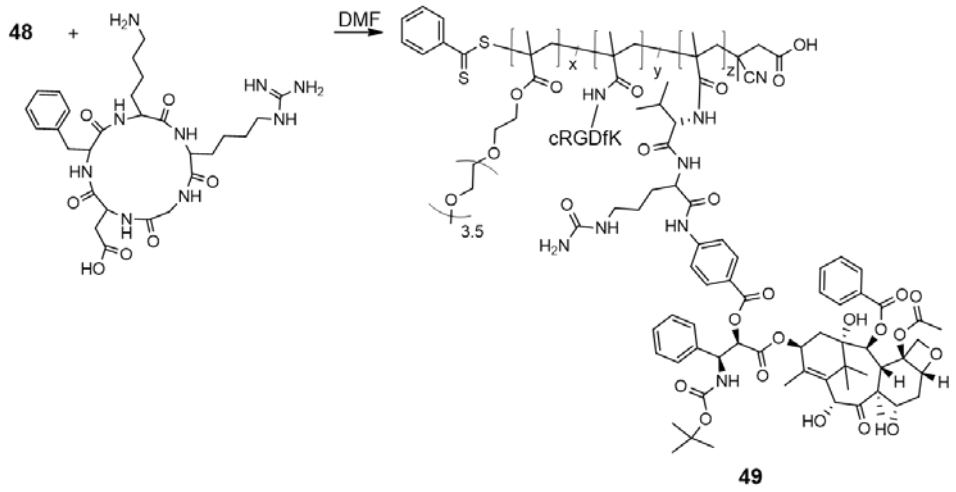

Figure 5.4. Synthesis of P(OEGMA-MA-Val-Cit-benzoyl-DTX-RGD) copolymer.

5.3.2. Determination of *in vitro* Cytotoxicity of Targeted Copolymer on A549 Cell Line

To explore cytotoxicity effects of targeted copolymer and free DTX, proliferation assay on A549 cells was performed (Figure 5.4). A549 cells were treated with free DTX and P(OEGMA-MA-Val-Cit-benzoyl-DTX-RGD). According to results, free drug DTX was 1000 times more toxic than targeted copolymer. EC_{50} values of the copolymer and DTX were obtained as 4390 nM and 2.14 nM, respectively. This difference can be attributed to the slow release behavior of the drug from the copolymer due to enzymatically cleavable linker valine-citrulline.

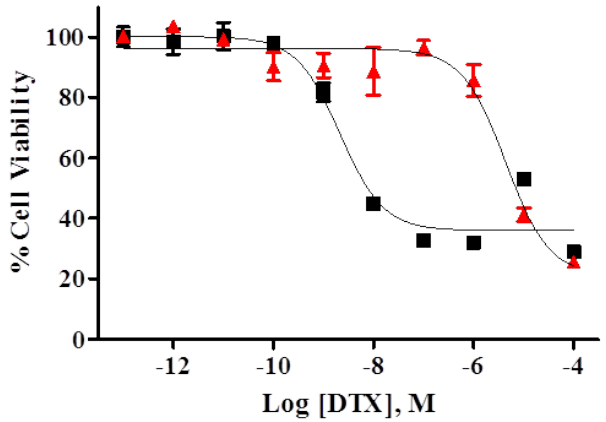

Figure 5.5. Viabilities of A549 cells treated with free DTX (black square) and P(OEGMA-CA4-DTX-RGD) (red triangle).

5.4. Conclusion

This part of the thesis is focusing on the design of a novel promising monomer that bears cathepsin B cleavable dipeptide linker and the drug docetaxel. As a linker, valine-citrulline sequence was utilized and amine moiety of valine was methacrylated. After obtaining the monomer, polymerization reaction was carried out. Like in previous studies, an amine reactive monomer NHSMA was used for attaching cRGDfK molecule *via* amide bond. Obtained molecules were all characterized and cytotoxicity behaviours of free DTX and targeted copolymer were evaluated on A549 lung cancer cell line. Release behavior under a variety of conditions will further be investigated and compared with other linkers prepared throughout this thesis.

6. CONCLUSIONS

This thesis covers the synthesis and design of polymer-drug conjugates that can be applied as therapeutic agents. As targeting moieties bisphosphonate structure alendronate and cRGDfK molecules were attached to synthesized copolymers. For control studies, non-targeted counterparts of these copolymers were also prepared. On the other hand, dye containing copolymers were also synthesized for determining cell uptake capability of the copolymers. All synthesized structures were characterized. For targeting group attachment, amine reactive monomer NHSMA was added to copolymerization reactions. In the firts project, bone targeting copolymers that bears anti-angiogenic drug CA4 were synthesized by using free radical polymerization technique. Obtained copolymers were attached with alendronate and they were evaluated on HUVECs and bone cancer cell lines Saos-2 and U2-OS. All copolymers showed toxic effect on cells. As expected, all polymers were less toxic than free drug. Internalization studies were also achieved and well uptake of copolymers into cell was observed. To better understand antiangiogenic effect of the copolymers, cell tube formation assay was carried out. According to the results, copolymers inhibited tube formation with the increasing concentration of drug CA4 in the polymer.

Second study involves targeted delivery of two combined drugs for ovarian cancer. In this project, copolymers were prepared by using RAFT polymerization technique and by using two different drug containing monomers which are antiangiogenic CA4 and antineoplastic docetaxel. DTX was conjugated polymer *via* enzymatically cleavable linker GFLG and CA4 was attached with hydrolyzable ester bond. Prepared constructs were also conjugated with targeting group cRGDfK. On SC-OV-3 and Caov-3 ovarian cancer cell lines, copolymers were evaluated according to their toxicities. Both targeted and nontargeted copolymers showed toxic effect on cells, additionally targeted polymer was more toxic than non-targeted polymer. On the other hand, both free drugs were more toxic in comparison with copolymers. For release studies, approximately 70-80% of both drugs released from copolymers in the rat serum. However, when enzymatic release study was achieved, just dtx release was observed due to it was conjugated to polymer enzymatically cleavable GFLG linker. In addition to these studies, acute toxicity study of targeted copolymer on mice was

also tested. In conclusion, there was no statistically significant differences between the organ weights of mice injected with targeted copolymer at 14 mg/kg, 40 mg/kg and 80 mg/kg which means polymer does not release its drug more than MTD dose of drug in the normal body condition.

In the third study a novel monomer that bears both reducible S-S bond in the middle and hydrolyzable carbonate group in the end was designed and synthesized for breast cancer treatment. After monomer synthesis, amine containing drug which is metabolite of drug capecitabine was attached to monomer. Obtained monomer was then used for polymerization reaction by using RAFT method again. cRGDfK was used as a targeting group. Copolymers were experimented on MDA-MB-453 and MDA-MB-231 breast cancer cell lines in terms of their toxicity. Free 5-FU was also tested on cells. For both polymers, free drug was more toxic than copolymers. On MDA-MB-453 cell line EC_{50} value of targeted copolymer was less than nontargeted copolymer as expected but on MDA-MB-231 cells, there was no significant differences. However, at high concentrations of drug, toxicity of targeted copolymer was better. Release studies of polymers were also tested to understand if S-S bond in the monomer really effects the release of drug. So that two different solutions which contains glutathion or not were utilized. As a result, both polymers released their drugs in the presence of GSH whereas this amount was negligible in GSH free solution.

In the last study, a novel enzymatically cleavable dipeptide linker containing monomer was designed. For this purpose, Valine-Citrulline dipeptide sequence was utilized due to it can be cleaved by cathepsin B enzyme. Linker was methacrylated and PABA was attached as a spacer. The purpose of using PABA was to attach drug via hydrolyzable ester linker. Docetaxel was attached to monomer as a chemotherapy agent. After monomer synthesis, copolymerization reaction was achieved by using RAFT technique. As a last step, cRGDfK was attached to copolymer.

REFERENCES

1. Seyfried, T. N. and L. M. Shelton, "Cancer as a metabolic disease", *Carcinogenesis*, Vol. 35, No. 3, pp. 515-527, 2013.
2. Anand, P., A. B. Kunnumakara, C. Sundaram, K. B. Harikumar, S. T. Tharakan, O. S. Lai, B. Sung, and B. B. Aggarwal, "Expert Review Cancer is a Preventable Disease that Requires Major Lifestyle Changes", *Pharmaceutical Research*, Vol. 25, No. 9, 2008.
3. Siegel, R. L., K. D. Miller. and Jemal, A. "Cancer Statistics , 2017", *Cancer*, Vol. 67, No. 1, pp. 7–30, 2017.
4. Caldas, C., "Cancer sequencing unravels clonal evolution", *National Biotechnologies*, Vol. 30, pp. 408-410, 2012.
5. Hayat, J., Howlader, N., Reichmann, M. E., Edwards, B. K. "Cancer Statistics, Trends and Multiple Primary Cancer Analyses from the Surveillence, Epideomology and End Results Program", *The Oncologist*, Vol. 37, pp. 12-20, 2007.
6. Yokota, J., "Tumor progression and metastasis", *Carcinogenesis*, Vol. 21, No. 3, pp. 497–503, October, 2000.
7. Weilbaecher, K. N., Guise T. A. and Mccauley, L. K. "Cancer to bone : a fatal attraction", *Nature Reviews*, Vol. 11, No. 6, pp. 411–425, 2011.
8. Rizov, M., Andreeva, P. and Dimova, I. "Taiwanese Journal of Obstetrics & Gynecology Molecular regulation and role of angiogenesis in reproduction", *Taiwan Journal of Obstetrics*, Vol. 56, No. 2, pp. 127–132, 2017.
9. Chen, S., Gao, Z. Zhou, J. Liang, M. Gong, X. Dai, T. Liang, J. Ye, G. Wu, L. Zou, Y. Wang, and X. Zou, "Journal of Materials Science & Technology Opposite Regulation of Chondrogenesis and Angiogenesis in Cartilage Repair ECM Materials under Hypoxia", *Journal of Material Science and Technologies*, Vol. 32, No. 9, pp. 978–985, 2016.
10. Kwak, G., Jo, S. D., Kim, D., Kim, H., Kim, M. G., Kim, K., Kwon, I. C. and Kim, S. H. "Synergistic antitumor effects of combination treatment with metronomic

Doxorubicin and VEGF targeting RNAi nanoparticles", *Journal of Controlled Release*, Vol. 267, pp. 203-213, 2017.

11. Plummer, M., De Martel, J. Vignat, J. Ferlay, F. Bray, and S. Franceschi, "Global burden of cancers attributable to infections in 2012 : a synthetic analysis", *Lancet Global Health*, Vol. 4, No. 9, pp. 609–616, 2015.
12. Marasini, N., S. Haque, and L. M. Kaminskas, "Current Opinion in Colloid & Interface Science Polymer-drug conjugates as inhalable drug delivery systems : A review", *Current Opinion in Colloid and Interface Science* Vol. 31, pp. 18–29, 2017.
13. Bahrami, B., M. Hojjat-farsangi, H. Mohammadi, and E. Anvari, "Nanoparticles and targeted drug delivery in cancer therapy", *Immunoligy Letters*, Vol. 190, pp. 64–83, 2017.
14. Haley, B. and E. Frenkel, "Nanoparticles for drug delivery in cancer treatment", *Urologic Oncology: Seminers and Original Investigations*, Vol. 26, No. 1, pp. 57–64, 2017.
15. Maeda, H., "The enhanced permeability and retention (EPR) effect in tumor vasculature: the key role of tumor-selective macromolecular drug targeting", *Advanced Enzyme Regulations*, Vol. 41, No. 1, pp. 189–207, 2001.
16. Horst, J., "Über den Einbau physiologisch wirksamer Substanzen in ein kollodiales Blutplasma-Ersatzmittel", *Hoppe-Seyler´s Zeitschrift für physiologische Chemie*, Vol. 297. pp. 149, 1954.
17. Ringsdorf, H., "Structure and properties of pharmacologically active polymers", *Polymer*, Vol. 153, No. 51, pp. 135–153, 1975.
18. Harris, J. M. and R. B. Chess, "Effect of Pegylation on Pharmaceutıcals", *Nature Reviews of Drug Discovery*, Vol. 2, pp. 214–221, 2003.
19. Wonganan, P. and M. A. Croyle, "PEGylated Adenoviruses: From Mice to Monkeys" Vol. 2, No. 2, pp. 468-502, 2010.
20. Li, W., P. Zhan, E. De Clercq, H. Lou, and X. Liu, "Current drug research on PEGylation with small molecular agents", *Progression in Polymer Science*, Vol. 38, No. 3, pp. 421–444, 2013.
21. Obereigner, B., M. Burešová, A. Vrána, and J. Kopeček, "Preparation of

polymerizable derivatives of N-(4-aminobenzenesulfonyl)-n′-butylurea", *Journal of Polymer Science Polymer Symposia*, Vol. 66, No. 1, pp. 41–52, 1979.

22. Conjugates, A. D., P. A. Vasey, S. B. Kaye, R. Morrison, C. Twelves, P. Wilson, R. Duncan, A. H. Thomson, L. S. Murray, T. E. Hilditch, T. Murray, S. Burtles, D. Fraier, and E. Frigerio, "Phase I Clinical and Pharmacokinetic Study of PK1 [N- (2-Hydroxypropyl) methacrylamide Copolymer Doxorubicin]: First Member of a New Class of Chemotherapeutic", *Clinical Cancer Research*, Vol. 5, pp. 83–94, 1999.

23. Markovsky, E., H. Baabur-cohen, A. Eldar-boock, L. Omer, G. Tiram, S. Ferber, P. Ofek, D. Polyak, A. Scomparin, and R. Satchi-fainaro, "Administration , distribution , metabolism and elimination of polymer therapeutics", *Journal of Controlled Release*, Vol. 161, No. 2, pp. 446–460, 2012.

24. Etrych, T., V. Šubr, J. Strohalm, M. Šírová, B. Říhová, and K. Ulbrich, "HPMA copolymer-doxorubicin conjugates : The effects of molecular weight and architecture on biodistribution and in vivo activity", *Journal of Controlled Release*, Vol. 164, No. 3, pp. 346–354, 2012.

25. Pan, H., M. Sima, and J. Yang, "Synthesis of Long-Circulating , Backbone Degradable HPMA Copolymer–Doxorubicin Conjugates and Evaluation of Molecular-Weight-Dependent Antitumor Efficacy", Vol. 13, No. 2, pp. 155–160, 2013.

26. Hongrapipat, J. and P. Kopec, "Combination Chemotherapy and Photodynamic Therapy with Fab ′ Fragment Targeted HPMA Copolymer Conjugates in Human Ovarian Carcinoma Cells", *Molecular Pharmaceutics*, Vol. 3, No. 5, pp. 351–362, 2008.

27. Vicent, M. J., F. Greco, R. I. Nicholson, A. Paul, P. C. Griffiths, and R. Duncan, "Polymer Therapeutics Designed for a Combination Therapy of Hormone-Dependent Cancer", *A Journal of the German Chemical Society*, Vol. 44, No. 26, pp. 4061–4066, 2005.

28. Muggia, F., "Platinum compounds 30 years after the introduction of cisplatin : Implications for the treatment of ovarian cancer", *Gynecological Oncology*, Vol. 112, No. 1, pp. 275–281, 2009.

29. Berhoune, M., E. Banu, F. Scotte, P. Prognon, S. Oudard, and B. Bonan, "Therapeutic

Strategy for Treatment of Metastatic Non-Small Cell Lung Cancer", *Annals of Pharmacotherapy*, Vol. 42, No. 11, pp. 1640–1652, 2008.

30. Ducreux, M., E. Van Cutsem, J. L. Van Laethem, T. M. Gress, and K. Jeziorski, "A randomised phase II trial of weekly high-dose 5-fluorouracil with and without folinic acid and cisplatin in patients with advanced biliary tract carcinoma : results of the 40955 EORTC trial", *European Journal of Cancer*, Vol. 41, pp. 398–403, 2005.

31. Kraković, H. and K. Ulbrich, "European Journal of Pharmaceutical Sciences HPMA-based polymer conjugates with drug combination", *European Journal of Pharmaceutical Sciences*, Vol. 37, pp. 405–412, 2009.

32. Lammers, T., V. Subr, K. Ulbrich, P. Peschke, P. E. Huber, W. E. Hennink, and G. Storm, "Biomaterials Simultaneous delivery of doxorubicin and gemcitabine to tumors in vivo using prototypic polymeric drug carriers", *Biomaterials*, Vol. 30, No. 20, pp. 3466–3475, 2009.

33. Ju, E., K. Park, K. Su, J. Kim, J. Yang, J. Kong, M. Young, A. S. Hoffman, and S. Kwang, "Target specific and long-acting delivery of protein , peptide , and nucleotide therapeutics using hyaluronic acid derivatives", *Journal of Controlled Drug Release*, Vol. 141, No. 1, pp. 2–12, 2010.

34. Auzenne, E., S. C. Ghosh, M. Khodadadian, B. Rivera, D. Farquhar, R. E. Price, M. Ravoori, V. Kundra, R. S. Freedman, and J. Klostergaard, "Hyaluronic Acid–Paclitaxel : Antitumor Efficacy against CD44 (+) Human Ovarian Carcinoma Xenografts 1", *Neoplasia*, Vol. 9, No. 6, pp. 479–486, 2007.

35. Luo, Y., N. J. Bernshaw, Z. Lu, J. Kopecek, and G. D. Prestwich, "Targeted Delivery of Doxorubicin by HPMA Copolymer-Hyaluronan Bioconjugates", Vol. 19, No. 4, pp. 396–402, 2002.

36. Anwar, M., M. H. Warsi, N. Mallick, S. Akhter, S. Gahoi, G. K. Jain, S. Talegaonkar, F. J. Ahmad, and R. K. Khar, "Enhanced bioavailability of nano-sized chitosan – atorvastatin conjugate after oral administration to rats", *European Journal of Pharmaceutical Sciences*, Vol. 44, No. 3, pp. 241–249, 2011.

37. Jiang, G., Z. Lin, X. Xu, H. Zhang, and K. Song, "Stable nanomicelles based on chitosan derivative : In vitro antiplatelet aggregation and adhesion properties", *Carbohydrate Polymers*, Vol. 88, No. 1, pp. 232–238, 2012.

38. Zeng, R., Z. Wang, H. Wang, L. Chen, L. Yang, R. Qiao, L. Hu, and Z. Li, "Effect of bond linkage on in vitro drug release and anti-HIV activity of chitosan-stavudine conjugates", *Macromolar Research*, Vol. 20, No. 4, pp. 358–365, 2012.

39. Links, D. A., "Lab on a Chip Microfluidic approach for highly efficient synthesis of heparin-based bioconjugates for drug delivery ", *Royal Society of Chemistry*, Vol. 12, No. 3, pp. 589–594, 2012.

40. Danhauser-riedl, S., E. Hausmann, H. Schick, R. Bender, H. Dietzfelbinger, J. Rastetter, and A. Hanauske, "Phase I clinical and pharmacokinetic trial of dextran conjugated Doxorubicin", *Investment of New Drugs*, Vol. 11, pp. 187–195, 1993.

41. Matthes, S., D. Gustafson, M. Long, A. E. Barón, and R. B. Jones, "Phase I and Pharmacokinetic Study of Docetaxel Combined with Melphalan and Carboplatin, with Autologous Hematopoietic Progenitor Cell Support in Patients with Advanced Refractory Malignancies", *Biology of Blood and Marrow Transplantation*, Vol. 11, No. 4, pp. 297–306, 2005.

42. Gaur, S., Y. Wang, L. Kretzner, L. Chen, T. Yen, X. Wu, Y. Yuan, M. Davis, and Y. Yen, "Pharmacodynamic and pharmacogenomic study of the nanoparticle conjugate of camptothecin CRLX101 for the treatment of cancer", *Nanomedicine Nanotechnology, Biology and Medicine*, Vol. 10, No. 7, pp. 1477–1486, 2014.

43. Zhang, L., T. Su, B. He, and Z. Gu, "Self-assembly Polyrotaxanes Nanoparticles as Carriers for Anticancer Drug Methotrexate Delivery", *Nano-micro letters*, Vol. 6, No. 2, pp. 108–115, 2014.

44. Cai, X., L. Yang, L.-M. Zhang, and Q. Wu, "Synthesis and anaerobic biodegradation of indomethacin-conjugated cellulose ethers used for colon-specific drug delivery", *Bioresource Technologies*, Vol. 100, No. 18, pp. 4164–4170, 2009.

45. Li, F., H. Zhang, C. Gu, L. Fan, Y. Qiao, Y. Tao, C. Cheng, H. Wu, and J. Yi, "Self-assembled nanoparticles from folate-decorated maleilated pullulan–doxorubicin conjugate for improved drug delivery to cancer cells", *Polymer International*, Vol. 62, No. 2, pp. 165–171, 2013.

46. Zhang, W., K. M. Mahuta, B. A. Mikulski, J. N. Harvestine, J. Zachary, J. C. Lee, M. G. Kaltchev, and C. S. Tritt, "Novel pectin-based carriers for colonic drug delivery", *Pharmaceutical Development and Technology*, Vol. 21, No. 1, pp. 127–130, 2016.

47. Zamboni, W. C., J. L. Eiseman, S. Strychor, P. M. Rice, E. Joseph, B. A. Zamboni, M. K. Donnelly, J. Shurer, R. A. Parise, M. E. Tonda, N. Y. Yu, and P. H. Basse, "Tumor disposition of pegylated liposomal CKD-602 and the reticuloendothelial system in preclinical tumor models", *Journal of Liposome Researches*, Vol. 21, No. 1, pp. 70–80, 2011.

48. Zhang, S., J. E. I. Wright, N. Özber, and H. Uludağ, "The Interaction of Cationic Polymers and Their Bisphosphonate Derivatives with Hydroxyapatite", *Macromolar Bioscience.*, Vol. 7, No. 5, pp. 656–670, 2007.

49. Melancon, M. P. and C. Li, "Cancer Therapeutic and Imaging Agents", *Drugs*, Vol. 10, No. 1, pp. 28–42, 2011.

50. Canal, F. and J. Sanchis, "Polymer – drug conjugates as nano-sized medicines", *Current Opinion in Biotechnologies*, Vol. 22, No. 6, pp. 894-900, 2011.

51. Eldar-boock, A., K. Miller, J. Sanchis, R. Lupu, M. J. Vicent, and R. Satchi-fainaro, "Biomaterials Integrin-assisted drug delivery of nano-scaled polymer therapeutics bearing paclitaxel", *Biomaterials*, Vol. 32, No. 15, pp. 3862–3874, 2011.

52. Svenson, S. and D. A. Tomalia, "Dendrimers in biomedical applications-reflections on the field", *Advanced Drug Delivery Reviews*, Vol. 64, pp. 102–115, 2012.

53. Nanoparticles, D., T. P. Thomas, A. K. Patri, A. Myc, M. T. Myaing, J. Y. Ye, T. B. Norris, and J. R. B. Jr, "In Vitro Targeting of Synthesized Antibody-Conjugated", *Biomacromolecules*, Vol. 5, No. 6, pp. 2269–2274, 2004.

54. Li, Y., H. He, X. Jia, W. Lu, J. Lou, and Y. Wei, "Biomaterials A dual-targeting nanocarrier based on poly (amidoamine) dendrimers conjugated with transferrin and tamoxifen for treating brain gliomas", *Biomaterials*, Vol. 33, No. 15, pp. 3899–3908, 2012.

55. Kukowska-latallo, J. F., K. A. Candido, Z. Cao, S. S. Nigavekar, I. J. Majoros, T. P. Thomas, L. P. Balogh, M. K. Khan, and J. R. Baker, "Nanoparticle Targeting of Anticancer Drug Improves Therapeutic Response in Animal Model of Human Epithelial Cancer", *Cancer Researches*, Vol. 65, No. 12, pp. 5317–5325, 2005.

56. Mignani, S., S. El, M. Bousmina, and J. Majoral, "Expand classical drug administration ways by emerging routes using dendrimer drug delivery systems : A concise overview ", *Advanced Drug Delivery Reviews*, Vol. 65, No. 10, pp. 1316–

1330, 2013.

57. Broxterman, H. J. and N. H. Georgopapadakou, "Anticancer therapeutics: “Addictive” targets, multi-targeted drugs, new drug combinations", *Drug Resistant Updates*, Vol. 8, No. 4, pp. 183–197, 2005.

58. Gaetano Donati, K., R. Rabagliati, L. Iacoviello, and R. Cauda, "HIV infection, HAART, and endothelial adhesion molecules: current perspectives", *Lancet Infectious Diseases*, Vol. 4, No. 4, pp. 213–222, 2004.

59. Orjuela, P., I. J. González, and L. Osório, "Combination therapy as a strategy to prevent antimalarial drug resistance", *Biomedical*, Vol. 24 No. 4, pp. 423–437, 2004.

60. Suarez-Pinzon, W. L., R. F. Power, H. Yan, C. Wasserfall, M. Atkinson, and A. Rabinovitch, "Combination therapy with glucagon-like peptide-1 and gastrin restores normoglycemia in diabetic NOD mice", *Diabetes*, Vol. 57, No. 12, pp. 3281–3288, 2008.

61. Gee, J. M. W., A. Howell, W. J. Gullick, C. C. Benz, R. L. Sutherland, R. J. Santen, L.-A. Martin, F. Ciardiello, W. R. Miller, M. Dowsett, P. Barrett-Lee, J. F. R. Robertson, S. R. Johnston, H. E. Jones, A. E. Wakeling, R. Duncan, and R. I. Nicholson, "Epigenetic alterations in Endocrin Related Cancer", *Endocrin Related Cancer*, Vol. 12, No. 1, pp. 1–7, 2005.

62. Li, C. and S. Wallace, "Polymer-drug conjugates: recent development in clinical oncology", *Advanced Drug Delivery Reviews*, Vol. 60, No. 8, pp. 886–898, 2008.

63. Greco, F., M. J. Vicent, N. A. Penning, R. I. Nicholson, and R. Duncan, "HPMA copolymer–aminoglutethimide conjugates inhibit aromatase in MCF-7 cell lines", *Journal of Drug Targeting*, Vol. 13, No. 8–9, pp. 459–470, 2005.

64. Santucci, L., A. Mencarelli, B. Renga, G. Pasut, F. Veronese, A. Zacheo, A. Germani, and S. Fiorucci, "Nitric oxide modulates proapoptotic and antiapoptotic properties of chemotherapy agents: The case of NO-pegylated epirubicin", *FASEB Journals*, Vol. 20, 2006.

65. Santucci, L., A. Mencarelli, B. Renga, D. Ceccobelli, G. Pasut, F. M. Veronese, E. Distrutti, and S. Fiorucci, "Cardiac safety and antitumoral activity of a new nitric oxide derivative of pegylated epirubicin in mice", *Anticancer Drugs*, Vol. 18, No. 9, 2007.

66. Satchi-Fainaro, R., M. Puder, J. W. Davies, H. T. Tran, D. A. Sampson, A. K. Greene, G. Corfas, and J. Folkman, "Targeting angiogenesis with a conjugate of HPMA copolymer and TNP-470", *Nature Medicine*, Vol. 10, No. 3, pp. 255-261, 2004.

67. Segal, E., H. Pan, P. Ofek, T. Udagawa, P. Kopec, and R. Satchi-fainaro, "Targeting Angiogenesis-Dependent Calcified Neoplasms Using Combined Polymer Therapeutics", *Plos One*, Vol. 4, No. 4, pp. 5233-5248, 2009.

68. Miller, K., R. Erez, E. Segal, D. Shabat, and R. Satchi-Fainaro, "Targeting Bone Metastases with a Bispecific Anticancer and Antiangiogenic Polymer-Alendronate-Taxane Conjugate", *Angewandte Chemie International*, Vol. 48. No. 16, pp. 2949-2954, 2009.

69. Krakovičová, H., T. Etrych, and K. Ulbrich, "HPMA-based polymer conjugates with drug combination", *European Journal of Pharmaceutical Science*, Vol. 37, No. 3, pp. 405–412, 2009.

70. Helsper, C. W., N. Van Erp, P. M. Peeters, and N. J. De Wit, "Time to diagnosis and treatment for cancer patients in the Netherlands : Room for improvement ", *European Journal of Cancer*, Vol. 87, pp. 113–121, 2017.

71. Rubin, G., A. Berendsen, S. M. Crawford, R. Dommett, C. Earle, J. Emery, T. Fahey, L. Grassi, E. Grunfeld, S. Gupta, W. Hamilton, S. Hiom, D. Hunter, G. Lyratzopoulos, U. Macleod, R. Mason, G. Mitchell, R. D. Neal, and M. Peake, "The expanding role of primary care in cancer control", *The Lancet Oncology*, Vol. 16, No. 12, pp. 1231-1272, 2010.

72. Puri, A. and R. Blumenthal, "Polymeric Lipid Assemblies as Novel Theranostic Tools", *Accounts of Chemical Research*, Vol. 44, No. 10, pp. 1071–1079, 2011.

73. Sumer, B. and J. Gao, "Theranostic nanomedicine for cancer", *Nanomedicine*, Vol. 3, No. 2, pp. 137–140, 2008.

74. Mura, S. and P. Couvreur, "Nanotheranostics for personalized medicine", *Advanced Drug Delivery Reviews*, Vol. 64, No. 13, pp. 1394–1416, 2012.

75. Guthi, J. S., S.-G. Yang, G. Huang, S. Li, C. Khemtong, C. W. Kessinger, M. Peyton, J. D. Minna, K. C. Brown, and J. Gao, "MRI-Visible Micellar Nanomedicine for Targeted Drug Delivery to Lung Cancer Cells", *Molecular Pharmaceutics*, Vol. 7, No. 1, pp. 32–40, 2010.

76. Ling, Y., K. Wei, Y. Luo, X. Gao, and S. Zhong, "Dual docetaxel/superparamagnetic iron oxide loaded nanoparticles for both targeting magnetic resonance imaging and cancer therapy", *Biomaterials*, Vol. 32, No. 29, pp. 7139–7150, 2011.

77. Yang, J., C. H. Lee, H. J. Ko, J. S. Suh, H. G. Yoon, K. Lee, Y. M. Huh, and S. Haam, "Multifunctional Magneto-Polymeric Nanohybrids for Targeted Detection and Synergistic Therapeutic Effects on Breast Cancer", *Angewandante Chemie International Editions*, Vol. 46, No. 46, pp. 8836–8839, 2007.

78. Ye, F., T. Ke, E.-K. Jeong, X. Wang, Y. Sun, M. Johnson, and Z.-R. Lu, "Noninvasive Visualization of in Vivo Drug Delivery of Poly(l-glutamic acid) Using Contrast-Enhanced MRI", *Molecular Pharmaceutics*, Vol. 3, No. 5, pp. 507–515, 2006.

79. Liao, Z., H. Wang, X. Wang, P. Zhao, S. Wang, W. Su, and J. Chang, "Multifunctional Nanoparticles Composed of A Poly(dl-lactide-coglycolide) Core and A Paramagnetic Liposome Shell for Simultaneous Magnetic Resonance Imaging and Targeted Therapeutics", *Advanced Functional Materials*, Vol. 21, No. 6, pp. 1179–1186, 2011.

80. Zarabi, B., A. Nan, J. Zhuo, R. Gullapalli, and H. Ghandehari, "HPMA copolymer-doxorubicin-gadolinium conjugates: synthesis, characterization, and in vitro evaluation", *Macromolar Bioscience*, Vol. 8, No. 8, pp. 741–748, 2008.

81. Li, X., Y. Qian, T. Liu, X. Hu, G. Zhang, Y. You, and S. Liu, "Amphiphilic multiarm star block copolymer-based multifunctional unimolecular micelles for cancer targeted drug delivery and MR imaging", *Biomaterials*, Vol. 32, No. 27, pp. 6595–6605, 2011.

82. Mitra, A., A. Nan, J. C. Papadimitriou, H. Ghandehari, and B. R. Line, "Polymer-peptide conjugates for angiogenesis targeted tumor radiotherapy", *Nuclear Medicinal Biology*, Vol. 33, No. 1, pp. 43–52, 2006.

83. Lammers, T., V. Subr, P. Peschke, R. Kühnlein, W. E. Hennink, K. Ulbrich, F. Kiessling, M. Heilmann, J. Debus, P. E. Huber, and G. Storm, "Image-guided and passively tumour-targeted polymeric nanomedicines for radiochemotherapy", *British Journal of Cancer*, Vol. 99, No. 6, pp. 900-910, 2008.

84. Valentini, R. C. and D. C. and C. D. and P. T. and G., "Time-resolved fluorescence imaging in biology and medicine", *Journal of Physics D: Applied Phycis.*, Vol. 35, No. 9, pp. 61-70, 2002.

85. Santra, S., C. Kaittanis, and J. M. Perez, "Cytochrome C encapsulating theranostic

nanoparticles: a novel bifunctional system for targeted delivery of therapeutic membrane-impermeable proteins to tumors and imaging of cancer therapy", *Molecular Pharmaceutics*, Vol. 7, No. 4, pp. 1209–1222, 2010.

86. Kurniasih, I. N., J. Keilitz, and R. Haag, "Dendritic nanocarriers based on hyperbranched polymers", *Chemical Society Reviews*, Vol. 44, No. 12, pp. 4145–4164, 2015.

87. Hu, X., R. Wang, J. Yue, S. Liu, Z. Xie, and X. Jing, "Targeting and anti-tumor effect of folic acid-labeled polymer–Doxorubicin conjugates with pH-sensitive hydrazone linker", *Journal of Materials Chemistry*, Vol. 22, No. 26, pp. 13303–13310, 2012.

88. Ho, Y.-P. and K. W. Leong, "Quantum dot-based theranostics", *Nanoscale*, Vol. 2, No. 1, pp. 60–68, 2010.

89. Lozano, M. V, D. Torrecilla, D. Torres, A. Vidal, F. Domínguez, and M. J. Alonso, "Highly Efficient System To Deliver Taxanes into Tumor Cells: Docetaxel-Loaded Chitosan Oligomer Colloidal Carriers", *Biomacromolecules*, Vol. 9, No. 8, pp. 2186–2193, 2008.

90. Wang, M. D., D. M. Shin, J. W. Simons, and S. Nie, "Nanotechnology for targeted cancer therapy", *Expert Review of Anticancer Therapy*, Vol. 7, No. 6, pp. 833–837, 2007.

91. Saha, R. N., S. Vasanthakumar, G. Bende, and M. Snehalatha, "Nanoparticulate drug delivery systems for cancer chemotherapy", *Molecular Membrane Biology*, Vol. 27, No. 7, pp. 215–231, 2010.

92. Swartz, M. A. and M. E. Fleury, "Interstitial Flow and Its Effects in Soft Tissues", *Annual Review of Biomedical Engineering*, Vol. 9, No. 1, pp. 229–256, 2007.

93. Hruby, M., T. Etrych, J. Kucka, M. Forsterova, and K. Ulbrich, "Hydroxybisphosphonate-containing polymeric drug-delivery systems designed for targeting into bone tissue", *Journal of Applied Polymer Science*, Vol. 101, No. 5, pp. 3192–3201, 2006.

94. Pan, H., M. Sima, P. Kopec, K. Wu, S. Gao, J. Liu, D. Wang, and S. C. Miller, "Biodistribution and Pharmacokinetic Studies of Copolymer-Alendronate Conjugates", *Molecular Pharmaceutics*, Vol. 5, No. 4, 2008.

95. Miller, E., R. Erez, E. Segal, D. Shabat, and R. Satchi-fainaro, "Targeting Bone

Metastases with a Bispecific Anticancer and Antiangiogenic Polymer Alendronate Taxane Conjugate", *Angewdante Chemie International Edition*, Vol. 48, No. 16, pp. 2949-2954, 2009.

96. Miller, K., A. Eldar-boock, D. Polyak, E. Segal, L. Benayoun, Y. Shaked, and R. Satchi-fainaro, "Antiangiogenic Antitumor Activity of HPMA Copolymer-Paclitaxel-Alendronate Conjugate on Breast Cancer Bone Metastasis Mouse Model", *Molecular Pharmaceutics*, Vol. 8, No. 4, pp. 1052–1062, 2011.

97. Eiken, P., P. Vestergaard, "Oral Bisphosphonates and Colon Cancer", T*herapeutic Advances in Musculoskeletal Disease*, Vol. 7, No. 4, pp. 160-168, 2015.

98. Salmaso, S., A. Scomparin, A. Eldar-boock, R. Satchi-fainaro, and P. Caliceti, "Novel Pullulan Bioconjugate for Selective Breast Cancer Bone Metastases Treatment", *Bioconjugate Chemistry*, Vol. 26, No. 3, pp. 489-501, 2015.

99. Firer, M. A. and G. Gellerman, "Targeted drug delivery for cancer therapy : the other side of antibodies", *Journal of Hemotological Oncology*, Vol. 5, No. 70, pp. 1–16, 2012.

100. Cox, D., M. Brennan, and N. Moran, "Integrins as therapeutic targets: lessons and opportunities", *Nature Reviews of Drug Discovery*, Vol. 9, No. 10, pp. 804-820, 2010.

101. Mas-Moruno, C. and F. R. and H. Kessler, "Cilengitide: The First Anti-Angiogenic Small Molecule Drug Candidate. Design, Synthesis and Clinical Evaluation", *Anti-Cancer Agents in Medicinal Chemistry*, Vol. 10, No. 10. pp. 753–768, 2010.

102. Ruoslahti, E., "Variants of the cell recognition site of fibronectin that retain attachment-promoting activity", *Biochemistry*, Vol. 81, No. 19, pp. 5985-5988, 1984.

103. Pierschbacher, M. D. and E. Ruoslahti, "Cell attachment activity of fibronectin can be duplicated by small synthetic fragments of the molecule", *Nature*, Vol. 309, pp. 30-33, 1984.

104. Pytela, R., M. D. Pierschbacher, and E. Ruoslahti, "Identification and isolation of a 140 kd cell surface glycoprotein with properties expected of a fibronectin receptor", *Cell*, Vol. 40, No. 1, pp. 191–198, 1985.

105. Kawasaki, K., M. Namikawa, T. Murakami, T. Mizuta, Y. Iwai, T. Hama, and T. Mayumi, "Amino acids and peptides. XIV. Laminin related peptides and their inhibitory effect on experimental metastasis formation", *Biochemical and Biophysical*

Research Communications, Vol. 174, No. 3, pp. 1159–1162, 1991.

106. Yamamoto, Y. and Y. T. and T. Mayumi, "Molecular Design of Bioconjugated Cell Adhesion Peptide with a Water-Soluble Polymeric Modifier for Enhancement of Antimetastatic Effect", *Current Drug Targets*, Vol. 3, No. 2. pp. 123–130, 2002.

107. Saiki, I., J. Yoneda, Y. Igarashi, M. Aoki, N. Kusunose, K. Ono, and I. Azuma, "Antimetastatic activity of polymeric RGDT peptides conjugated with poly(ethylene glycol)", *Japanese Journal of Cancer Researh*, Vol. 84, No. 5, pp. 558–565, 1993.

108. Komazawa, H., I. Saiki, Y. U. Igarashi, I. Azuma, M. Kojima, A. Orikasa, M. Ono, and I. Itoh, "Inhibition of Tumor Metastasis by a Synthetic Polymer Containing a Cell-Adhesive RGDS Peptide", *Journal of Bioactive Compatible Polymers*, Vol. 8, No. 3, pp. 258–274, 1993.

109. Fujii, H., H. Komazawa, H. Mori, M. Kojima, I. Itoh, J. Murata, I. Azuma, and I. Saiki, "Antimetastatic Activities of Synthetic Arg-Gly-Asp-Ser (RGDS) and Arg-Leu-Asp-Ser (RLDS) Peptide Analogues and Their Inhibitory Mechanisms", *Biological and Pharmaceutical Bulletin*, Vol. 18, No. 12, 1996.

110. Yoneda, J. and Y. C. Yoo, "Inhibition of tumor metastasis by Arg-Gly-Asp-Ser (RGDS) peptide conjugated with sulfated chitin derivative, SCM-chitin-RGDS", *Clinical and Experimental Metastasis*, Vol. 11, No. 6, pp. 482–483, 1993.

111. Komazawa, H., I. Saiki, Y. Igarashi, I. Azuma, S. Tokura, M. Kojima, A. Orikasa, M. Ono, and I. Itoh, "The conjugation of RGDS peptide with CM-chitin augments the peptide-mediated inhibition of tumor metastasis", *Carbohydrate Polymers*, Vol. 21, No. 4, pp. 299–307, 1993.

112. Polyak, D., C. Ryppa, A. Eldar-boock, P. Ofek, A. Many, K. Licha, F. Kratz, and R. Satchi-fainaro, "Development of PEGylated doxorubicin-E-[c(RGDfK)2] conjugate for integrin-targeted cancer therapy", *Polymers for Advanced Technologies*, Vol. 22, No. 1, 2011.

113. Eldar-Boock, A., K. Miller, J. Sanchis, R. Lupu, M. J. Vicent, and R. Satchi-Fainaro, "Integrin-assisted drug delivery of nano-scaled polymer therapeutics bearing paclitaxel", *Biomaterials*, Vol. 32, No. 15, pp. 3862–3874, 2011.

114. Ray, A., N. Larson, D. B. Pike, M. Grüner, S. Naik, H. Bauer, A. Malugin, K. Greish, and H. Ghandehari, "Comparison of Active and Passive Targeting of Docetaxel for

Prostate Cancer Therapy by HPMA Copolymer–RGDfK Conjugates", *Molecular Pharmaceutics*, Vol. 8, No. 4, pp. 1090–1099, 2011.

115. Tai, W., R. S. Shukla, K. Cheng, "Development of a peptide-drug conjugate for Prostate Cancer Therapy", *Molecular Pharmaceutics*, Vol. 8, No. 3, pp. 901-912, 2014.

116. Borgman, M. P., O. Aras, S. Geyser-stoops, E. A. Sausville, and H. Ghandehari, " Biodistribution of HPMA Copolymer-Aminohexylgeldanamycin-RGDfK Conjugates for Prostate Cancer Drug Delivery", *Molecular Pharmaceutics*, Vol. 6, No. 6, pp. 1836–1847, 2010.

117. Shukla, R., T. P. Thomas, J. Peters, A. Kotlyar, A. Myc, and J. Baker James R., "Tumor angiogenic vasculature targeting with PAMAM dendrimer–RGD conjugates", *Chemical Communications*, Vol. 14, No. 46, pp. 5739–5741, 2005.

118. Zhu, S., M. Hong, G. Tang, L. Qian, J. Lin, Y. Jiang, and Y. Pei, "Partly PEGylated polyamidoamine dendrimer for tumor-selective targeting of doxorubicin: The effects of PEGylation degree and drug conjugation style", *Biomaterials*, Vol. 31, No. 6, pp. 1360–1371, 2010.

119. Zhang, L., S. Zhu, L. Qian, Y. Pei, Y. Qiu, and Y. Jiang, "RGD-modified PEG–PAMAM–DOX conjugates: in vitro and in vivo studies for glioma", *European Journal of Pharmaceutics and Biopharmaceutics*, Vol. 79, No. 2, pp. 232-240, 2011.

120. Zhu, S., L. Qian, M. Hong, L. Zhang, Y. Pei, and Y. Jiang, "RGD-Modified PEG-PAMAM-DOX conjugate: In vitro and in vivo targeting to both tumor neovascular endothelial cells and tumor cells", *Advanced Materials*, Vol. 23, No. 12, pp. 84-89, 2011.

121. Wang, K., X. Zhang, L. Zhang, L. Qian, C. Liu, J. Zheng, and Y. Jiang, "Development of biodegradable polymeric implants of RGD-modified PEG-PAMAM-DOX conjugates for long-term intratumoral release", *Drug Delivery*, Vol. 22. No. 3, pp. 388-399, 2014.

122. Zhang, X., S. Yao, C. Liu, and Y. Jiang, "Tumor tropic delivery of doxorubicin-polymer conjugates using mesenchymal stem cells for glioma therapy", *Biomaterials*, Vol. 39, pp. 269–281, 2015.

123. Xu, X.-D., Y.-J. Cheng, J. Wu, H. Cheng, S.-X. Cheng, R.-X. Zhuo, and X.-Z. Zhang,

"Smart and hyper-fast responsive polyprodrug nanoplatform for targeted cancer therapy", *Biomaterials*, Vol. 76, pp. 238–249, 2016.

124. Cunningham, W. A., "Sulfur. III", *Journal of Chemical Education*, Vol. 12, No. 3, p. 120, 1935.

125. Serniuk, G. E., F. W. Banes, and M. W. Swaney, "Study of the Reaction of Buna Rubbers with Aliphatic Mercaptans1", *Journal of American Chemical Society*, Vol. 70, No. 5, pp. 1804–1808, 1948.

126. Merrifield, R. B., "Solid Phase Peptide Synthesis. I. The Synthesis of a Tetrapeptide", *Journal of American Chemical Society.*, Vol. 85, No. 14, pp. 2149–2154, 1963.

127. Pączkowski, P. and B. Gawdzik, "Modification of polymeric materials bearing pendant epoxide groups", *Annales Universitatis Mariae Curie-Sklodowska, Chemia*, Vol. 72, No. 1, pp. 105-111, 2017.

128. Blatz, P. E., "New polyelectrolytes: Synthesis and preliminary characterization", *Journal of Polymer Science.*, Vol. 58, No. 166, pp. 755–768, 1962.

129. Batz, H.-G., G. Franzmann, and H. Ringsdorf, "Model Reactions for Synthesis of Pharmacologically Active Polymers by Way of Monomeric and Polymeric Reactive Esters", *Angewandte Chemie International Edition*, Vol. 11, No. 12, pp. 1103–1104, 1972.

130. Savariar, E. N. and S. Thayumanavan, "Controlled Polymerization of N-Isopropylacrylamide with an Activated Methacrylic Ester", *Journal of Polymer Science*, Vol. 42, No. 24, pp. 6340–6345, 2004.

131. Devenish, S. R. A., J. B. Hill, J. W. Blunt, J. C. Morris, and M. H. G. Munro, "Dual side-reactions limit the utility of a key polymer therapeutic precursor", *Tetrahedron Letters*, Vol. 47, No. 17, pp. 2875–2878, 2006.

132. Wong, S. Y. and D. Putnam, "Overcoming Limiting Side Reactions Associated with an NHS-Activated Precursor of Polymethacrylamide-Based Polymers", *Bioconjugate Chemistry*, Vol. 18, No. 3, pp. 970–982, 2007.

133. Eberhardt, M., R. Mruk, R. Zentel, and P. Théato, "Synthesis of pentafluorophenyl(meth)acrylate polymers: New precursor polymers for the synthesis of multifunctional materials", *European Polymer Journal*, Vol. 41, No. 7, pp. 1569–1575, 2005.

134. Ulbrich, K., "Synthesis and properties of new N- (2-hydroxypropyl) -methacrylamide copolymers containing thiazolidine-2-thione reactive groups", Vol. 66, No. 12, pp. 1525–1538, 2006.

135. Desai, A., N. Atkinson, F. Rivera, W. Devonport, I. Rees, S. E. Branz, and C. J. Hawker, "Hybrid dendritic–linear graft copolymers: Steric considerations in “coupling to” approach", *Journal of Polymer Science. Part A*, Vol. 38, No. 6, pp. 1033–1044, 2000.

136. Nilles, K. and P. Theato, "Synthesis and polymerization of active ester monomers based on 4-vinylbenzoic acid", *European Polymer Journal*, Vol. 43, No. 7, pp. 2901–2912, Jul. 2007.

137. Cengiz, N., H. Kabadayioglu, and R. Sanyal, "Orthogonally Functionalizable Copolymers Based on a Novel Reactive Carbonate Monomer", *Journal of Polymer Science.*, Vol. 48, No. July, pp. 4737–4746, 2010.

138. Batz, H. G., G. Franzmann, and H. Ringsdorf, "Pharmakologisch aktive polymere, Modellreaktionen zur umsetzung von pharmaka und enzymen mit monomeren und polymeren reaktiven estern", *Die Makromolar Chemie*, Vol. 172, No. 1, pp. 27–47, 1973.

139. Ferruti, P., A. Bettelli, and A. Feré, "High polymers of acrylic and methacrylic esters of N-hydroxysuccinimide as polyacrylamide and polymethacrylamide precursors", *Journal of Polymer Science.*, Vol. 13, No. 10, pp. 462–464, 1972.

140. Yoshikawa, M., Y. Adachi, H. Yokoi, K. Sanui, and N. Ogata, "Synthesis of poly{1-[(2-methylpropenoyl)oxy]succinimide-co-acrylonitrile} and the selective separation of a water-ethanol mixture through its membranes", *Macromolecules*, Vol. 19, No. 1, pp. 47–50, 1986.

141. Deng, C., H. Tian, P. Zhang, J. Sun, X. Chen, and X. Jing, "Synthesis and Characterization of RGD Peptide Grafted Poly (ethylene glycol) -b-Poly (L -lactide) -b-Poly (L -glutamic acid) Triblock Copolymer", *Biomacromolecules*, Vol. 7, No. 2, pp. 590–596, 2006.

142. Biswas, S., X. Wang, A. R. Morales, H. Ahn, and K. D. Belfield, "Integrin-Targeting Block Copolymer Probes for Two-Photon Fluorescence Bioimaging", *Biomacromolecules*, Vol. 12, No. 2, pp. 441–449, 2011.

143. Bolu, B. S., B. Golba, N. Boke, A. Sanyal, and R. Sanyal, "Designing Dendron−Polymer Conjugate Based Targeted Drug Delivery Platforms with a “Mix-and-Match” Modularity", *Bioconjugate Chemistry*, Vol. 28, No. 12, pp. 2962-2975, 2017.

144. Scomparin, A., S. Salmaso, S. Bersani, R. Satchi-fainaro, and P. Caliceti, "Novel folated and non-folated pullulan bioconjugates for anticancer drug delivery", *European Journal of Polymer Sciences*, Vol. 42, No. 5, pp. 547–558, 2011.

145. Clementi, C., K. Miller, A. Mero, R. Satchi-fainaro, and G. Pasut, "Dendritic Poly (ethylene glycol) Bearing Paclitaxel and Alendronate for Targeting Bone Neoplasms", *Molecular Pharmaceutics*, Vol. 8, No. 4, pp. 1063-1072, 2011.

146. Karacivi, M., B. S. Bolu, and R. Sanyal, "Targeting to the Bone: Alendronate-Directed Combretastatin A-4 Bearing Antiangiogenic Polymer−Drug Conjugates", *Molecular Pharmaceutics*, Vol. 14, No. 5, pp. 1373-1383, 2017.

147. Zhu, J., B. Huang, S. Ding, W. Zhang, X. Ma, H. Niu, Y. Yuan, and C. Liu, " Tethering of rhBMP-2 upon calcium phosphate cement via alendronate/heparin for localized, sustained and enhanced osteo activity", *RSC Advances.*, Vol. 7, pp. 20281–20292, 2017.

148. Gao, T., W. Cui, Z. Wang, Y. Wang, Y. Liu, P. S. Malliappan, Y. Ito, and P. Zhang, "Photo-immobilization of bone morphogenic protein 2 on PLGA/HA nanocomposites to enhance the osteogenesis of adipose-derived stem cells", *RSC Advances*, Vol. 6, No. 24, pp. 20202–20210, 2016.

149. Danhier, F., E. Ansorena, J. M. Silva, R. Coco, A. Le Breton, and V. Préat, "PLGA-based nanoparticles: An overview of biomedical applications", *Journal of Controlled Release*, Vol. 161, No. 2, pp. 505–522, 2012.

150. Fang, X., J. Xie, L. Zhong, J. Li, D. Rong, X. Li, and J. Ouyang, "Biomimetic gelatin methacrylamide hydrogel scaffolds for bone tissue engineering", *Journal of Materials Chemistry B*, Vol. 4, No. 6, pp. 1070–1080, 2016.

151. Lu, S., J. Lam, J. E. Trachtenberg, E. J. Lee, H. Seyednejad, J. J. J. P. van den Beucken, Y. Tabata, M. E. Wong, J. A. Jansen, A. G. Mikos, and F. K. Kasper, "Dual growth factor delivery from bilayered, biodegradable hydrogel composites for spatially-guided osteochondral tissue repair", *Biomaterials*, Vol. 35, No. 31, pp.

8829–8839, 2014.

152. Neumann, A., A. Christel, C. Kasper, and P. Behrens, "BMP2-loaded nanoporous silica nanoparticles promote osteogenic differentiation of human mesenchymal stem cells", *RSC Advances*, Vol. 3, No. 46, pp. 24222–24230, 2013.

153. Gan, Q., J. Zhu, Y. Yuan, H. Liu, J. Qian, Y. Li, and C. Liu, "A dual-delivery system of pH-responsive chitosan-functionalized mesoporous silica nanoparticles bearing BMP-2 and dexamethasone for enhanced bone regeneration", *Journal of Materials Chemistry B*, Vol. 3, No. 10, pp. 2056–2066, 2015.

154. Shen, X., Y. Zhang, Y. Gu, Y. Xu, Y. Liu, B. Li, and L. Chen, "Sequential and sustained release of SDF-1 and BMP-2 from silk fibroin-nanohydroxyapatite scaffold for the enhancement of bone regeneration", *Biomaterials*, Vol. 106, pp. 205–216, 2016.

155. Shiels, S., S. Oh, C. Bae, T. Guda, B. Singleton, D. D. Dean, J. C. Wenke, M. R. Appleford, and J. L. Ong, "Evaluation of BMP-2 tethered polyelectrolyte coatings on hydroxyapatite scaffolds in vivo", *Journal of Biomedical Materials*, Vol. 100, No. 7, pp. 1782–1791, 2012.

156. Crouzier, T., F. Sailhan, P. Becquart, R. Guillot, D. Logeart-Avramoglou, and C. Picart, "The performance of BMP-2 loaded TCP/HAP porous ceramics with a polyelectrolyte multilayer film coating", *Biomaterials*, Vol. 32, No. 30, pp. 7543–7554, 2011.

157. Chu, W., Y. Huang, C. Yang, Y. Liao, X. Zhang, M. Yan, S. Cui, and C. Zhao, "Calcium phosphate nanoparticles functionalized with alendronate-conjugated polyethylene glycol (PEG) for the treatment of bone metastasis", *International Journal of Pharmaceutics*, Vol. 516, No. 1–2, pp. 352–363, 2017.

158. Allen, T., "Ligand-targeted therapeutics in anticancer therapy", *Nature Reviews Cancer*, Vol. 2 pp. 750-763, 2002.

159. Rasaneh, S., H. Rajabi, Ã. Mohammad, and H. Babaei, "Synthesis and biodistribution studies of 177 Lu-trastuzumab as a therapeutic agent in the breast cancer mice model", *Journal of Labelled Compounds*, Vol. 53, No. 9, pp. 575-579, 2010.

160. Alirezapour, B., A. Reza, J. Mohammad, and J. Rasaee, "Optimized preparation and preliminary evaluation of [64 Cu]– DOTA – trastuzumab for targeting ErbB2 / Neu

expression", *Journal of Radioanalytical and Nuclear Chemistry,* Vol. 295, No. 2, pp. 1261–1271, 2013.

161. Chan, L. J., J. B. Bulitta, D. B. Ascher, J. M. Haynes, V. M. Mcleod, C. J. H. Porter, C. C. Williams, and L. M. Kaminskas, "PEGylation Does Not Significantly Change the Initial Intravenous or Subcutaneous Pharmacokinetics or Lymphatic Exposure of Trastuzumab in Rats but Increases Plasma Clearance after Subcutaneous Administration", *Molecular Pharmaceutics*, Vol. 12, No. 3, pp.794-809, 2015.

162. Golani-armon, A., M. Golan, Y. Shamay, L. Raviv, and A. David, "DC3-Decorated Polyplexes for Targeted Gene Delivery into Dendritic Cells", *Bioconjugate Chemistry*, Vol. 26, No. 2, pp. 213-224, 2015.

163. Viswanath, A., Y. Shen, A. N. Green, R. Tan, A. B. Greytak, and B. C. Benicewicz, "Copolymerization and Synthesis of Multiply Binding Histamine Ligands for the Robust Functionalization of Quantum Dots", *Macromolecules*, Vol. 47, No. 23, pp. 8137-8144, 2014.

164. Matyjaszewski, K., "Overview: Fundamentals of Controlled/Living Radical Polymerization", *Controlled Radical Polymerization*, Vol. 685, pp. 1-2, 1998.

165. Puts, R. D. and D. Y. Sogah, "Control of Living Free-Radical Polymerization by a New Chiral Nitroxide and Implications for the Polymerization Mechanism", *Macromolecules*, Vol. 29, No. 9, pp. 3323–3325, 1996.

166. Chong,Y. K, T. P. T. Le, G. Moad, E. Rizzardo, and S. H. Thang, "A More Versatile Route to Block Copolymers and Other Polymers of Complex Architecture by Living Radical Polymerization: The RAFT Process", *Macromolecules*, Vol. 32, No. 6, pp. 2071–2074, 1999.

167. Mishra, V. and R. Kumar, "RAFT polymerization of N-vinyl pyrrolidone using prop-2-ynyl morpholine-4-carbodithioate as a new chain transfer agent", *Journal of Applied Polymer Science*, Vol. 124, No. 6, pp. 4475–4485, 2012.

168. Moad, G., J. Chiefari, R. T. A. Mayadunne, C. L. Moad, A. Postma, E. Rizzardo, and S. H. Thang, "Initiating free radical polymerization", *Macromolar Symposia*, Vol. 182, No. 1, pp. 65–80, 2002.

169. Moad, G., J. Chiefari, (Bill) YK Chong, J. Krstina, R. T. A. Mayadunne, A. Postma, E. Rizzardo, and S. H. Thang, "Living free radical polymerization with reversible

addition – fragmentation chain transfer (the life of RAFT)", *Polymer International*, Vol. 49, No. 9, pp. 993–1001, 2000.

170. Percec, V. and B. Barboiu, "Scope and Limitations of Functional Sulfonyl Chlorides as Initiators for Metal-Catalyzed “Living” Radical Polymerization of Styrene and Methacrylates", *Science*, Vol. 80, pp. 8526–8528, 1997.

171. Moad, G., E. Rizzardo, and S. Thang, "Radical addition-fragmentation chemistry in polymer synthesis", *Polymer*, Vol. 49, No. 5, 2008.

172. Bharthuar, A., L. Egloff, J. Becker, M. George, J. W Lohr, G. Deeb, and R. Iyer, "Rituximab-based therapy for gemcitabine-induced hemolytic uremic syndrome in a patient with metastatic pancreatic adenocarcinoma: a case report", *Cancer Chemotherapy and Pharmacology*, Vol. 64. 2009.

173. Talelli, M., M. Barz, C. J. F. Rijcken, F. Kiessling, W. E. Hennink, and T. Lammers, "Core-crosslinked polymeric micelles: Principles, preparation, biomedical applications and clinical translation", *Nano Today*, Vol. 10, No. 1. 2015.

174. Li, Y., G. H. Gao, and D. S. Lee, "Stimulus-Sensitive Polymeric Nanoparticles and Their Applications as Drug and Gene Carriers", *Advanced Healthcare Materials*, Vol. 2, No. 3, pp. 388–417, 2013.

175. Kim, C. S., B. Duncan, B. Creran, and V. M. Rotello, "Triggered Nanoparticles as Therapeutics", *Nano Today*, Vol. 8, No. 4, pp. 439–447, 2013.

176. Aili, D. and M. M. Stevens, "Bioresponsive peptide–inorganic hybrid nanomaterials", *Chemical Society Reviews*, Vol. 39, No. 9, pp. 3358–3370, 2010.

177. Liu, J., H. Li, X. Jiang, C. Zhang, and Q. Ping, "Novel pH-sensitive chitosan-derived micelles loaded with paclitaxel", *Carbohydrate Polymers*, Vol. 82, No. 2, pp. 432–439, 2010.

178. Zhang, X., K. Achazi, and R. Haag, "Boronate Cross-linked ATP- and pH-Responsive Nanogels for Intracellular Delivery of Anticancer Drugs", *Advanced Healthcare Materials*, Vol. 4, No. 4, pp. 585–592, 2015.

179. Fleige, E., K. Achazi, K. Schaletzki, T. Triemer, and R. Haag, "pH-Responsive Dendritic Core–Multishell Nanocarriers", *Journal of Controlled Release*, Vol. 185, pp. 99–108, 2014.

180. Yuba, E., A. Harada, Y. Sakanishi, and K. Kono, "Carboxylated hyperbranched poly(glycidol)s for preparation of pH-sensitive liposomes", *Journal of Controlled Release*, Vol. 149, No. 1, pp. 72–80, 2011.

181. Pang, X., X. Yang, and G. Zhai, "Polymer-drug conjugates: recent progress on administration routes", *Expert Opinion Drug Delivery*, Vol. 11, No. 7, pp. 1075–1086, 2014.

182. Kopeček, J., P. Kopečková, T. Minko, and Z.-R. Lu, "HPMA copolymer–anticancer drug conjugates: design, activity, and mechanism of action", *European Journal Pharmaceutics and Biopharmacy*, Vol. 50, No. 1, pp. 61–81, 2000.

183. Shen, W.-C. and H. J.-P. Ryser, "Cis-aconityl spacer between daunomycin and macromolecular carriers: A model of pH-sensitive linkage releasing drug from a lysosomotropic conjugate", *Biochemical and Biophysical Research Communications.*, Vol. 102, No. 3, pp. 1048–1054, 1981.

184. Gu, Y., Y. Zhong, F. Meng, R. Cheng, C. Deng, and Z. Zhong, "Acetal-Linked Paclitaxel Prodrug Micellar Nanoparticles as a Versatile and Potent Platform for Cancer Therapy", *Biomacromolecules*, Vol. 14, No. 8, pp. 2772–2780, 2013.

185. Etrych, T., V. Šubr, J. Strohalm, M. Šírová, B. Říhová, and K. Ulbrich, "HPMA copolymer-doxorubicin conjugates : The effects of molecular weight and architecture on biodistribution and in vivo activity", *Journal of Controlled Release*, Vol. 164, No. 3, pp. 346–354, 2012.

186. Choi, W.-M., P. Kopečková, T. Minko, and J. Kopeček, "Synthesis of HPMA Copolymer Containing Adriamycin Bound via an Acid-Labile Spacer and its Activity toward Human Ovarian Carcinoma Cells", *Journal of Bioactive and Compatible Polymers*, Vol. 14, No. 6, pp. 447–456, 1999.

187. Chytil, P., T. Etrych, J. Kříž, V. Šubr, and K. Ulbrich, "N-(2-Hydroxypropyl)methacrylamide-based polymer conjugates with pH-controlled activation of doxorubicin for cell-specific or passive tumour targeting. Synthesis by RAFT polymerisation and physicochemical characterisation", *European Journal of Polymer Sciences*, Vol. 41, No. 3, pp. 473–482, 2010.

188. Ke, X., D. J. Coady, C. Yang, A. C. Engler, J. L. Hedrick, and Y. Y. Yang, "pH-sensitive polycarbonate micelles for enhanced intracellular release of anticancer

drugs: a strategy to circumvent multidrug resistance", *Polymer Chemistry*, Vol. 5, No. 7, pp. 2621–2628, 2014.

189. Xiong, X.-B., Z. Ma, R. Lai, and A. Lavasanifar, "The therapeutic response to multifunctional polymeric nano-conjugates in the targeted cellular and subcellular delivery of doxorubicin", *Biomaterials*, Vol. 31, No. 4, pp. 757–768, 2010.

190. Wang, Y., X. Zhang, Z. Xu, H. Huang, Y. Li, and J. Wang, "A pH-sensitive theranostics system based on doxorubicin conjugated with the comb-shaped polymer coating of quantum dots", *Journal of Material and Science*, Vol. 49, No. 21, pp. 7539–7546, 2014.

191. Alani, A. W. G., Y. Bae, D. A. Rao, and G. S. Kwon, "Polymeric micelles for the pH-dependent controlled, continuous low dose release of paclitaxel", *Biomaterials*, Vol. 31, No. 7, pp. 1765–1772, 2010.

192. Kessenbrock, K., V. Plaks, and Z. Werb, "Matrix Metalloproteinases: Regulators of the Tumor Microenvironment", *Cell*, Vol. 141, No. 1, pp. 52–67, 2010.

193. Zhu, L., F. Perche, T. Wang, and V. P. Torchilin, "Matrix metalloproteinase 2-sensitive multifunctional polymeric micelles for tumor-specific co-delivery of siRNA and hydrophobic drugs", *Biomaterials*, Vol. 35, No. 13, pp. 4213–4222, 2014.

194. Zhu, L., T. Wang, F. Perche, A. Taigind, and V. P. Torchilin, "Enhanced anticancer activity of nanopreparation containing an MMP2-sensitive PEG-drug conjugate and cell-penetrating moiety", *Proceedings of the National Academy of Sciences*, Vol. 110, No. 42, pp. 17047-17052, 2013.

195. Gu, G., H. Xia, Q. Hu, Z. Liu, M. Jiang, T. Kang, D. Miao, Y. Tu, Z. Pang, Q. Song, L. Yao, H. Chen, X. Gao, and J. Chen, "PEG-co-PCL nanoparticles modified with MMP-2/9 activatable low molecular weight protamine for enhanced targeted glioblastoma therapy", *Biomaterials*, Vol. 34, No. 1, pp. 196–208, 2013.

196. Peng, Z.-H. and J. Kopeček, "HPMA Copolymer CXCR4 Antagonist Conjugates Substantially Inhibited the Migration of Prostate Cancer Cells", *Macro Letters*, Vol. 3, No. 12, pp. 1240–1243, 2014.

197. Fehrenbacher, N. and M. Jäättelä, "Lysosomes as Targets for Cancer Therapy", *Cancer Researches*, Vol. 65, No. 8, pp. 2993-2995, 2005.

198. Kopeček, J. and P. Kopečková, "HPMA copolymers: Origins, early developments,

present, and future", *Advanced Drug Delivery Reviews*, Vol. 62, No. 2, pp. 122–149, 2010.

199. Peng, Z.-H. and J. Kopeček, "Enhancing Accumulation and Penetration of HPMA Copolymer–Doxorubicin Conjugates in 2D and 3D Prostate Cancer Cells via iRGD Conjugation with an MMP-2 Cleavable Spacer", *Journal of American Chemical Society.*, Vol. 137, No. 21, pp. 6726–6729, 2015.

200. Li, N., N. Li, Q. Yi, K. Luo, C. Guo, D. Pan, and Z. Gu, "Amphiphilic peptide dendritic copolymer-doxorubicin nanoscale conjugate self-assembled to enzyme-responsive anti-cancer agent", *Biomaterials*, Vol. 35, No. 35, pp. 9529–9545, 2014.

201. Zhang, C., D. Pan, K. Luo, W. She, C. Guo, Y. Yang, and Z. Gu, "Peptide Dendrimer–Doxorubicin Conjugate-Based Nanoparticles as an Enzyme-Responsive Drug Delivery System for Cancer Therapy", *Advanced Healthcare Materials*, Vol. 3, No. 8, pp. 1299–1308, 2014.

202. Doronina, S. O., B. E. Toki, M. Y. Torgov, B. A. Mendelsohn, C. G. Cerveny, D. F. Chace, R. L. DeBlanc, R. P. Gearing, T. D. Bovee, C. B. Siegall, J. A. Francisco, A. F. Wahl, D. L. Meyer, and P. D. Senter, "Development of potent monoclonal antibody auristatin conjugates for cancer therapy", *Nature Biotechnology*, Vol. 21, p. 778, 2003.

203. Dubowchik, G. M., R. A. Firestone, L. Padilla, D. Willner, S. J. Hofstead, K. Mosure, J. O. Knipe, S. J. Lasch, and P. A. Trail, "Cathepsin B-Labile Dipeptide Linkers for Lysosomal Release of Doxorubicin from Internalizing Immunoconjugates : Model Studies of Enzymatic Drug Release and Antigen-Specific In Vitro Anticancer Activity", *Bioconjugate Chemistry*, Vol. 13, No. 4, pp. 855–869, 2002.

204. Jain, N., S. W. Smith, and S. Ghone, "Current ADC Linker Chemistry", *Pharmaceutical Research*, Vol. 32, No. 11, pp. 3526–3540, 2015.

205. Rago, B., L. N. Tumey, C. Wei, F. Barletta, T. Clark, S. Hansel, and X. Han, "Quantitative Conjugated Payload Measurement Using Enzymatic Release of Antibody − Drug Conjugate with Cleavable Linker", *Bioconjugate Chemistry*, Vol. 28, No. 2, pp. 620-626, 2017.

206. Erez, R., E. Segal, K. Miller, R. Satchi-fainaro, and D. Shabat, "Enhanced cytotoxicity of a polymer – drug conjugate with triple payload of paclitaxel", *Bioorganic and*

Medicinal Chemistry, Vol. 17, No. 13, pp. 4327–4335, 2009.

207. Liang, L., S. Lin, W. Dai, J. Lu, T. Yang, Y. Xiang, Y. Zhang, R. Li, and Q. Zhang, "Novel cathepsin B-sensitive paclitaxel conjugate : Higher water solubility , better ef fi cacy and lower toxicity", *Journal of Controlled Release*, Vol. 160, No. 3, pp. 618–629, 2012.

208. Huang, H., J. Geng, J. Golzarian, J. Huang, and J. Yu, "Biointerfaces Fabrication of doxorubicin-loaded ellipsoid micelle based on diblock copolymer with a linkage of enzyme-cleavable peptide", *Colloids Surfaces B: Biointerfaces*, Vol. 133, pp. 362–369, 2015.

209. Sun, H., F. Meng, R. Cheng, C. Deng, and Z. Zhong, "Reduction-sensitive degradable micellar nanoparticles as smart and intuitive delivery systems for cancer chemotherapy", *Expert Opinion Drug Delivery*, Vol. 10, No. 8, pp. 1109–1122, 2013.

210. Ding, J., J. Chen, D. Li, C. Xiao, J. Zhang, C. He, X. Zhuang, and X. Chen, "Biocompatible reduction-responsive polypeptide micelles as nanocarriers for enhanced chemotherapy efficacy in vitro", *Journal of Materials and Chemistry*, Vol. 1, No. 1, pp. 69–81, 2013.

211. Ko, N. R. and J. K. Oh, "Glutathione-Triggered Disassembly of Dual Disulfide Located Degradable Nanocarriers of Polylactide-Based Block Copolymers for Rapid Drug Release", *Biomacromolecules*, Vol. 15, No. 8, pp. 3180–3189, 2014.

212. Wang, J., G. Yang, X. Guo, Z. Tang, Z. Zhong, and S. Zhou, "Redox-responsive polyanhydride micelles for cancer therapy", *Biomaterials*, Vol. 35, No. 9, pp. 3080–3090, 2014.

213. Xu, P., H. Yu, Z. Zhang, Q. Meng, H. Sun, X. Chen, Q. Yin, and Y. Li, "Hydrogen-bonded and reduction-responsive micelles loading atorvastatin for therapy of breast cancer metastasis", *Biomaterials*, Vol. 35, No. 26, pp. 7574–7587, 2014.

214. Zhong, Y., W. Yang, H. Sun, R. Cheng, F. Meng, C. Deng, and Z. Zhong, "Ligand-Directed Reduction-Sensitive Shell-Sheddable Biodegradable Micelles Actively Deliver Doxorubicin into the Nuclei of Target Cancer Cells", *Biomacromolecules*, Vol. 14, No. 10, pp. 3723–3730, 2013.

215. Yen, H.-C., H. Cabral, P. Mi, K. Toh, Y. Matsumoto, X. Liu, H. Koori, A. Kim, K. Miyazaki, Y. Miura, N. Nishiyama, and K. Kataoka, "Light-Induced Cytosolic

Activation of Reduction-Sensitive Camptothecin-Loaded Polymeric Micelles for Spatiotemporally Controlled in Vivo Chemotherapy", *ACS Nano*, Vol. 8, No. 11, pp. 11591–11602, 2014.

216. Sun, H., R. Cheng, C. Deng, F. Meng, A. A. Dias, M. Hendriks, J. Feijen, and Z. Zhong, "Enzymatically and Reductively Degradable α-Amino Acid-Based Poly(ester amide)s: Synthesis, Cell Compatibility, and Intracellular Anticancer Drug Delivery", *Biomacromolecules*, Vol. 16, No. 2, pp. 597–605, 2015.

217. Lu, W., X. Wang, R. Cheng, C. Deng, F. Meng, and Z. Zhong, "Biocompatible and bioreducible micelles fabricated from novel α-amino acid-based poly(disulfide urethane)s: design, synthesis and triggered doxorubicin release", *Polymer Chemistry*, Vol. 6, No. 33, pp. 6001–6010, 2015.

218. Lee, Y., S. Kim, J. Y. Tyler, K. Park, and J.-X. Cheng, "Blood-stable, tumor-adaptable disulfide bonded mPEG-(Cys)4-PDLLA micelles for chemotherapy", *Biomaterials*, Vol. 34, No. 2, pp. 552–561, 2013.

219. Han, H. S., T. Thambi, K. Y. Choi, S. Son, H. Ko, M. C. Lee, D.-G. Jo, Y. S. Chae, Y. M. Kang, J. Y. Lee, and J. H. Park, "Bioreducible Shell-Cross-Linked Hyaluronic Acid Nanoparticles for Tumor-Targeted Drug Delivery", *Biomacromolecules*, Vol. 16, No. 2, pp. 447–456, 2015.

220. Zhong, Y., J. Zhang, R. Cheng, C. Deng, F. Meng, F. Xie, and Z. Zhong, "Reversibly crosslinked hyaluronic acid nanoparticles for active targeting and intelligent delivery of doxorubicin to drug resistant CD44+ human breast tumor xenografts", *Journal of Controlled Release*, Vol. 205, pp. 144–154, 2015.

221. Riber, C. F., T. M. Hinton, P. Gajda, K. Zuwala, M. Tolstrup, C. Stewart, and A. N. Zelikin, "Macromolecular Prodrugs of Ribavirin: Structure-Function Correlation as Inhibitors of Influenza Infectivity", *Molecular Pharmaceutics*, Vol. 14, No. 1, pp. 234–241, 2017.

222. Peng, Z. H., Y. Xie, Y. Wang, J. Li, and D. Oupický, "Dual-Function Polymeric HPMA Prodrugs for the Delivery of miRNA", *Molecular Pharmaceutics*, Vol. 14, No. 5, pp. 1395–1404, 2017.

223. Dohmen, C. and M. Ogris, "Receptor-Mediated Delivery of Proteins and Peptides to Tumors", *Pharmaceutical Perspectives of Cancer Therapeutics*, pp. 269–295, 2019.

224. Cisterna, B. A., N. Kamaly, W. Il Choi, A. Tavakkoli, O. C. Farokhzad, and C. Vilos, "Targeted nanoparticles for colorectal cancer", *Nanomedicine*, Vol. 11, No. 18, pp. 2443–2456, 2016.

225. Carter, T., P. Mulholland, and K. Chester, "Antibody-targeted nanoparticles for cancer treatment", *Immunotherapy*, Vol. 8, No. 8, pp. 941–958, 2016.

226. Zhong, Y., F. Meng, C. Deng, and Z. Zhong, "Ligand-Directed Active Tumor-Targeting Polymeric Nanoparticles for Cancer Chemotherapy", *Biomacromolecules*, Vol. 15, No. 6, pp. 1955–1969, 2014.

227. Xin, Y., Q. Huang, J.-Q. Tang, X.-Y. Hou, P. Zhang, L. Z. Zhang, and G. Jiang, "Nanoscale drug delivery for targeted chemotherapy", *Cancer Letters*, Vol. 379, No. 1, pp. 24–31, 2016.

228. Xu, H., H. Ma, P. Yang, X. Zhang, X. Wu, W. Yin, H. Wang, and D. Xu, "Targeted polymer-drug conjugates: Current progress and future perspective", *Colloids Surfaces B Biointerfaces*, Vol. 136, pp. 729–734, 2015.

229. Maeda, H., H. Nakamura, and J. Fang, "The EPR effect for macromolecular drug delivery to solid tumors: Improvement of tumor uptake, lowering of systemic toxicity, and distinct tumor imaging in vivo", *Advanced Drug Delivery Reviews*, Vol. 65, No. 1, pp. 71–79, 2013.

230. Greish, K., "Enhanced permeability and retention of macromolecular drugs in solid tumors: A royal gate for targeted anticancer nanomedicines", *Journal of Drug Targeting*, Vol. 15, No. 7–8, pp. 457–464, 2007.

231. Kaminskas, L. M., V. M. McLeod, C. J. H. Porter, and B. J. Boyd, "Association of Chemotherapeutic Drugs with Dendrimer Nanocarriers: An Assessment of the Merits of Covalent Conjugation Compared to Noncovalent Encapsulation", *Molecular Pharmaceutics*, Vol. 9, No. 3, pp. 355–373, 2012.

232. Lammers, T. and K. Ulbrich, "HPMA copolymers: 30 years of advances", *Advanced Drug Delivery Reviews*, Vol. 62, No. 2, pp. 119–121, 2010.

233. Larson, N. and H. Ghandehari, "Polymeric Conjugates for Drug Delivery", *Chemistry of Materials*, Vol. 24, No. 5, pp. 840–853, 2012.

234. Grigoletto, A., K. Maso, A. Mero, A. Rosato, O. Schiavon, and G. Pasut, "Drug and protein delivery by polymer conjugation", *Journal of Drug Delivery and Science*, Vol.

32, pp. 132-141, 2015.

235. Culpepper, B. K., P. P. Bonvallet, M. S. Reddy, S. Ponnazhagan, and S. L. Bellis, "Polyglutamate directed coupling of bioactive peptides for the delivery of osteoinductive signals on allograft bone", *Biomaterials*, Vol. 34, No. 5, pp. 1506–1513, 2013.

236. Culpepper, B. K., D. S. Morris, P. E. Prevelige, and S. L. Bellis, "Engineering nanocages with polyglutamate domains for coupling to hydroxyapatite biomaterials and allograft bone", *Biomaterials*, Vol. 34, No. 10, pp. 2455–2462, 2013.

237. Jiang, T., X. Yu, E. J. Carbone, C. Nelson, H. M. Kan, and K. W.-H. Lo, "Poly aspartic acid peptide-linked PLGA based nanoscale particles: Potential for bone-targeting drug delivery applications", *International Journal of Pharmaceutics*, Vol. 475, No. 1, pp. 547–557, 2014.

238. Fu, Y.-C., T.-F. Fu, H.-J. Wang, C.-W. Lin, G.-H. Lee, S.-C. Wu, and C.-K. Wang, "Aspartic acid-based modified PLGA–PEG nanoparticles for bone targeting: In vitro and in vivo evaluation", *Acta Biomaterials*, Vol. 10, No. 11, pp. 4583–4596, 2014.

239. Cole, L. E., T. Vargo-Gogola, and R. K. Roeder, "Targeted delivery to bone and mineral deposits using bisphosphonate ligands", *Advanced Drug Delivery Reviews*, Vol. 99, pp. 12–27, 2016.

240. Hirabayashi, H. and J. Fujisaki, "Bone-Specific Drug Delivery Systems", *Clinical Pharmacokinetics*, Vol. 42, No. 15, pp. 1319–1330, 2003.

241. Berenson James R., M. D. and M. D. Lipton Allan, "Bisphosphonates in the Treatment of Malignant Bone Disease", *Annual Review of Medicine*, Vol. 50, No. 1, pp. 237–248, 1999.

242. Gossiel, F., C. Hoyle, E. V McCloskey, K. E. Naylor, J. Walsh, N. Peel, and R. Eastell, "The effect of bisphosphonate treatment on osteoclast precursor cells in postmenopausal osteoporosis: The TRIO study", *Bone*, Vol. 92, pp. 94–99, 2016.

243. Miladi, K., S. Sfar, H. Fessi, and A. Elaissari, "Drug carriers in osteoporosis: Preparation, drug encapsulation and applications", *International Journal of Pharmaceutics*, Vol. 445, No. 1, pp. 181–195, 2013.

244. Luhmann, T., O. Germershaus, J. Groll, and L. Meinel, "Bone targeting for the treatment of osteoporosis", *Journal of Controlled Release*, Vol. 161, No. 2, pp. 198–

213, 2012.

245. Swami, A., M. R. Reagan, P. Basto, Y. Mishima, N. Kamaly, S. Glavey, S. Zhang, M. Moschetta, D. Seevaratnam, Y. Zhang, J. Liu, M. Memarzadeh, J. Wu, S. Manier, J. Shi, N. Bertrand, Z. N. Lu, K. Nagano, R. Baron, A. Sacco, A. M. Roccaro, O. C. Farokhzad, and I. M. Ghobrial, "Engineered nanomedicine for myeloma and bone microenvironment targeting", *Proceedings of the National Academy of Sciences*, Vol. 111, No. 28, pp. 10287-10292, 2014.

246. Yin, Q., L. Tang, K. Cai, R. Tong, R. Sternberg, X. Yang, L. W. Dobrucki, L. B. Borst, D. Kamstock, Z. Song, W. G. Helferich, J. Cheng, and T. M. Fan, "Pamidronate functionalized nanoconjugates for targeted therapy of focal skeletal malignant osteolysis", *Proceedings of the National Academy of Sciences*, Vol. 113, No. 32, p. E4601 LP-E4609, 2016.

247. Wang, D., S. Miller, M. Sima, P. Kopečková, and J. Kopeček, "Synthesis and Evaluation of Water-Soluble Polymeric Bone-Targeted Drug Delivery Systems", *Bioconjugate Chemistry*, Vol. 14, No. 5, pp. 853–859, 2003.

248. Segal, E., H. Pan, L. Benayoun, P. Kopečková, Y. Shaked, J. Kopeček, and R. Satchi-Fainaro, "Enhanced anti-tumor activity and safety profile of targeted nano-scaled HPMA copolymer-alendronate-TNP-470 conjugate in the treatment of bone malignances", *Biomaterials*, Vol. 32, No. 19, pp. 4450–4463, 2011.

249. Chen, H., G. Li, H. Chi, D. Wang, C. Tu, L. Pan, L. Zhu, F. Qiu, F. Guo, and X. Zhu, "Alendronate-Conjugated Amphiphilic Hyperbranched Polymer Based on Boltorn H40 and Poly(ethylene glycol) for Bone-Targeted Drug Delivery", *Bioconjugate Chemistry*, Vol. 23, No. 9, pp. 1915–1924, 2012.

250. Chen, B., D. G. van der Poll, K. Jerger, W. C. Floyd, J. M. J. Fréchet, and F. C. Szoka, "Synthesis and Properties of Star-Comb Polymers and Their Doxorubicin Conjugates", *Bioconjugate Chemistry*, Vol. 22, No. 4, pp. 617–624, 2011.

251. Zhuang, Y., Y. Su, Y. Peng, D. Wang, H. Deng, X. Xi, X. Zhu, and Y. Lu, "Facile Fabrication of Redox-Responsive Thiol-Containing Drug Delivery System *via* RAFT Polymerization", *Biomacromolecules*, Vol. 15, No. 4, pp. 1408–1418, 2014.

252. Abdollahi, A. and J. Folkman, "Evading tumor evasion: Current concepts and perspectives of anti-angiogenic cancer therapy", *Drug Resistance Updates*, Vol. 13,

No. 1, pp. 16–28, 2010.

253. Ferrara, N. and R. S. Kerbel, "Angiogenesis as a therapeutic target", *Nature*, Vol. 438, p. 967, 2005.

254. Matter, A., "Tumor angiogenesis as a therapeutic target", *Drug Discoveries Today*, Vol. 6, No. 19, pp. 1005–1024, 2001.

255. Griggs, J., J. C. Metcalfe, and R. Hesketh, "Targeting tumour vasculature: the development of combretastatin A4", *Lancet Oncology*, Vol. 2, No. 2, pp. 82–87, 2001.

256. Nagaiah, G. and S. C. Remick, "Combretastatin A4 phosphate: a novel vascular disrupting agent", *Future Oncology*, Vol. 6, No. 8, pp. 1219–1228, 2010.

257. Su, M., J. Huang, S. Liu, Y. Xiao, X. Qin, J. Liu, C. Pi, T. Luo, J. Li, X. Chen, and Z. Luo, "The anti-angiogenic effect and novel mechanisms of action of Combretastatin A-4", *Science Reports*, Vol. 6, p. 28139, 2016.

258. Sengupta, S., D. Eavarone, I. Capila, G. Zhao, N. Watson, T. Kiziltepe, and R. Sasisekharan, "Temporal targeting of tumour cells and neovasculature with a nanoscale delivery system", *Nature*, Vol. 436, p. 568, 2005.

259. Wang, Y., H. Chen, Y. Liu, J. Wu, P. Zhou, Y. Wang, R. Li, X. Yang, and N. Zhang, "pH-sensitive pullulan-based nanoparticle carrier of methotrexate and combretastatin A4 for the combination therapy against hepatocellular carcinoma", *Biomaterials*, Vol. 34, No. 29, pp. 7181–7190, 2013.

260. Sumer Bolu, B., E. Manavoglu Gecici, and R. Sanyal, "Combretastatin A-4 Conjugated Antiangiogenic Micellar Drug Delivery Systems Using Dendron–Polymer Conjugates", *Molecular Pharmaceutics*, Vol. 13, No. 5, pp. 1482–1490, 2016.

261. Nelson, D. M., Z. Ma, C. E. Leeson, and W. R. Wagner, "Extended and sequential delivery of protein from injectable thermoresponsive hydrogels", *Journal of Biomedicine Materials Research Part A*, Vol. 100, No. 3, pp. 776–785, 2012.

262. Gaukroger, K., J. A. Hadfield, L. A. Hepworth, N. J. Lawrence, and A. T. McGown, "Novel Syntheses of Cis and Trans Isomers of Combretastatin A-4", *Journal of Organic Chemistry*, Vol. 66, No. 24, pp. 8135–8138, 2001.

263. Arnaoutova, I. and H. K. Kleinman, "In vitro angiogenesis: endothelial cell tube

formation on gelled basement membrane extract", *Nature Protocols*, Vol. 5, p. 628, 2010.

264. Dykes, S. S., E. Friday, K. Pruitt, and J. A. Cardelli, "The histone deacetylase inhibitor cambinol prevents acidic pHe-induced anterograde lysosome trafficking independently of sirtuin activity", *Biochemistry and Biophysics Reports*, Vol. 3, pp. 83–93, 2015.

265. Appelqvist, H., P. Wäster, K. Kågedal, and K. Öllinger, "The lysosome: from waste bag to potential therapeutic target", *Journal of Molecular Cell Biology*, Vol. 5, No. 4, pp. 214–226, 2013.

266. Kopecek, J., "Biomaterials and drug delivery: past, present, and future", *Molecular Pharmaceutics*, Vol. 7, No. 4, pp. 922–925, 2010.

267. Chytrý, V., A. Vrána, and J. Kopeček, "Synthesis and activity of a polymer which contains insulin covalently bound on a copolymer of N-(2-hydroxypropyl)methacrylamide and N-methacryloyldiglycyl p-nitrophenyl ester", *Die Makromol. Chemie*, Vol. 179, No. 2, pp. 329–336, 1978.

268. Fitzpatrick, S., L. Fitzpatrick, A. Thakur, A. Mazumder, H. Sheardown, "Temperature Sensitive Polymers for Drug Delivery", *Expert Review of Medical Devices*, Vol. 9, No. 4, pp. 339-351, 2012.

269. Obereigner, B., M. Burešová, A. Vrána, and J. Kopeček, "Preparation of polymerizable derivatives of N-(4-aminobenzenesulfonyl)-N′-butylurea", *Journal of Polymer Science Polymer Symposia* , Vol. 66, No. 1, pp. 41-52, 2007.

270. Agarwal, R. and S. B. Kaye, "Ovarian cancer: strategies for overcoming resistance to chemotherapy", *Nature Reviews of Cancer*, Vol. 3, p. 502, 2003.

271. Pomel, C., A. Jeyarajah, D. Oram, J. Shepherd, D. Milliken, J. Dauplat, and K. Reynolds, "Cytoreductive surgery in ovarian cancer", *Cancer Imaging*, Vol. 7, No. 1, pp. 210–215, 2007.

272. Norouzi-Barough, L., M. R. Sarookhani, M. Sharifi, S. Moghbelinejad, S. Jangjoo, and R. Salehi, "Molecular mechanisms of drug resistance in ovarian cancer", *Journal of Cellular Physiology*, Vol. 233, No. 6, pp. 4546–4562, 2018.

273. Byrne, A. T., L. Ross, J. Holash, M. Nakanishi, L. Hu, J. I. Hofmann, G. D. Yancopoulos, and R. B. Jaffe, "Vascular Endothelial Growth Factor-Trap Decreases

Tumor Burden, Inhibits Ascites, and Causes Dramatic Vascular Remodeling in an Ovarian Cancer Model", *Clin. Cancer Res.*, Vol. 9, No. 15, p. 5721 LP-5728, 2003.

274. Hicklin, D. J. and L. M. Ellis, "Role of the Vascular Endothelial Growth Factor Pathway in Tumor Growth and Angiogenesis", *Journal of Clinical Oncology*, Vol. 23, No. 5, pp. 1011–1027, 2005.

275. Joo, W. D., J. Y. Lee, J. H. Kim, H. J. Yoo, H. J. Roh, J.-Y. Park, D.-Y. Kim, Y.-M. Kim, Y.-T. Kim, and J.-H. Nam, "Efficacy of taxane and platinum-based chemotherapy guided by extreme drug resistance assay in patients with epithelial ovarian cancer", *Journal of Gynecological Oncology*, Vol. 20, No. 2, pp. 96–100, 2009.

276. Garcia, A. A., H. Hirte, G. Fleming, D. Yang, D. D. Tsao-Wei, L. Roman, S. Groshen, S. Swenson, F. Markland, D. Gandara, S. Scudder, R. Morgan, H. Chen, H.-J. Lenz, and A. M. Oza, "Phase II Clinical Trial of Bevacizumab and Low-Dose Metronomic Oral Cyclophosphamide in Recurrent Ovarian Cancer: A Trial of the California, Chicago, and Princess Margaret Hospital Phase II Consortia", *Journal of Clinical Oncology*, Vol. 26, No. 1, pp. 76–82, 2008.

277. Baird, R. D., D. S. P. Tan, and S. B. Kaye, "Weekly paclitaxel in the treatment of recurrent ovarian cancer", *Nature Reviews Clinical Oncology*, Vol. 7, p. 575, 2010.

278. Kumar, S., H. Mahdi, C. Bryant, J. P. Shah, G. Garg, and A. Munkarah, "Clinical trials and progress with paclitaxel in ovarian cancer", *International Journal of Womens Health*, Vol. 2, pp. 411–427, 2010.

279. Yardley, D. A., H. A. Burris III, T. Markus, D. R. Spigel, F. A. Greco, M. Mainwaring, D. M. Waterhouse, C. D. Webb, and J. D. Hainsworth, "Phase II Trial of Docetaxal Plus Imatinib Mesylate in the Treatment of Patients With Metastatic Breast Cancer", *Clinical Breast Cancer*, Vol. 9, No. 4, pp. 237–242, 2009.

280. Liang, X.-J., C. Chen, Y. Zhao, and P. C. Wang, "Circumventing Tumor Resistance to Chemotherapy by Nanotechnology", *Multidrug Resistance in Cancer*, Vol. 596, pp. 467–488, 2010

281. Eckhardt, B. L., P. A. Francis, B. S. Parker, and R. L. Anderson, "Strategies for the discovery and development of therapies for metastatic breast cancer", *Nature Reviews Drug Discovery*, Vol. 11, p. 479, 2012.

282. Veneti, E., R. S. Tu, and D. T. Auguste, "RGD-Targeted Liposome Binding and Uptake on Breast Cancer Cells Is Dependent on Elastin Linker Secondary Structure", *Bioconjugate Chemistry*, Vol. 27, No. 8, pp. 1813–1821, 2016.

283. Brooks, P. C., S. Strömblad, R. Klemke, D. Visscher, F. H. Sarkar, and D. A. Cheresh, "Antiintegrin $\alpha_v\beta_3$ blocks human breast cancer growth and angiogenesis in human skin", *Journal of Clinical Investments*, Vol. 96, No. 4, pp. 1815–1822, 1995.

284. Burke, P. A., S. J. DeNardo, L. A. Miers, K. R. Lamborn, S. Matzku, and G. L. DeNardo, "Cilengitide Targeting of Integrin Receptor Synergizes with Radioimmunotherapy to Increase Efficacy and Apoptosis in Breast Cancer Xenografts", *Cancer Researches*, Vol. 62, No. 15, pp. 4263-4272, 2002.

285. Jemal, A., E. Ward, and M. J. Thun, "Recent trends in breast cancer incidence rates by age and tumor characteristics among U.S. women", *Breast Cancer Researches*, Vol. 9, No. 3, p. 28, 2007.

286. Hébert-Croteau, N., J. Brisson, J. Latreille, G. Gariépy, C. Blanchette, and L. Deschênes, "Time Trends in Systemic Adjuvant Treatment for Node-Negative Breast Cancer", *Journal of Clinical Oncology*, Vol. 17, No. 5, p. 1458, 1999.

287. Duchateau, L., J. P. Pignon, L. Bijnens, S. Bertin, J. Bourhis, and R. Sylvester, "Individual Patient- versus Literature-Based Meta-analysis of Survival Data: Time to Event and Event Rate at a Particular Time Can Make a Difference, an Example Based on Head and Neck Cancer", *Controlled Clinical Trials*, Vol. 22, No. 5, pp. 538–547, 2001.

288. Blum, J. L., S. E. Jones, A. U. Buzdar, P. M. LoRusso, I. Kuter, C. Vogel, B. Osterwalder, H.-U. Burger, C. S. Brown, and T. Griffin, "Multicenter Phase II Study of Capecitabine in Paclitaxel-Refractory Metastatic Breast Cancer", *Journal of Clinical Oncology*, Vol. 17, No. 2, p. 485, 1999.

289. Aguado, C., B. García-Paredes, M. J. Sotelo, J. Sastre, and E. Díaz-Rubio, "Should capecitabine replace 5-fluorouracil in the first-line treatment of metastatic colorectal cancer", *World Journal of Gastroenterol.*, Vol. 20, No. 20, pp. 6092–6101, 2014.

290. Akbari, R. and H. A. Javar, "Efficacy of Capecitabine and 5- Fluorouracil (5-FU) on the human breast cancer cell line (MCF7), effect of concentration", *American Journal of Research Communication*, Vol. 1, No. 6, pp. 75–91.

291. Lindgaard, S. C., C. M. Brinch, B. K. Jensen, H. H. Nørgaard, K. L. Hermann, S. Theile, F. O. Larsen, B. V. Jensen, H. Michelsen, K. M. Nelausen, V. H. Holm, L. Ekblad, P. G. Soerensen, and D. L. Nielsen, "Hepatic arterial therapy with oxaliplatin and systemic capecitabine for patients with liver metastases from breast cancer", *The Breast*, Vol. 43, pp. 113–119, 2019.

292. Van Cutsem, E., P. M. Hoff, P. Harper, R. M. Bukowski, D. Cunningham, P. Dufour, U. Graeven, J. Lokich, S. Madajewicz, J. A. Maroun, J. L. Marshall, E. P. Mitchell, G. Perez-Manga, P. Rougier, W. Schmiegel, J. Schoelmerich, A. Sobrero, and R. L. Schilsky, "Oral capecitabine vs intravenous 5-fluorouracil and leucovorin: Integrated efficacy data and novel analyses from two large, randomised, phase III trials", *British Journal of Cancer*, Vol. 90, No. 6, pp. 1190–1197, 2004.

293. Porsch, C., Y. Zhang, M. I. Montañez, J. M. Malho, M. A. Kostiainen, A. M. Nyström, and E. Malmström, "Disulfide-functionalized unimolecular micelles as selective redox-responsive nanocarriers", *Biomacromolecules*, Vol. 16, No. 9, pp. 2872–2883, 2015.

294. McCusker, C. F., P. J. Kocienski, F. T. Boyle, and A. G. Schätzlein, "Solid-phase synthesis of c(RGDfK) derivatives: on-resin cyclisation and lysine functionalisation", *Bioorganic and Medicinal Chemistry Letters*, Vol. 12, No. 4, pp. 547–549, 2002.

295. Nakayama, M., T. Okano, T. Miyazaki, F. Kohori, K. Sakai, and M. Yokoyama, "Molecular design of biodegradable polymeric micelles for temperature-responsive drug release", *Journal of Controlled Release*, Vol. 115, No. 1, pp. 46–56, 2006.

296. Meyer, D. E., B. C. Shin, G. A. Kong, M. W. Dewhirst, and A. Chilkoti, "Drug targeting using thermally responsive polymers and local hyperthermia", *Journal of Controlled Release*, Vol. 74, No. 1, pp. 213–224, 2001.

297. Gu, H., S. Mu, G. Qiu, X. Liu, L. Zhang, Y. Yuan, and D. Astruc, "Redox-stimuli-responsive drug delivery systems with supramolecular ferrocenyl-containing polymers for controlled release", *Coordination Chemistry Reviews*, Vol. 364, pp. 51–85, 2018.

298. Schuster, M., P. Wang, J. C. Paulson, and C.-H. Wong, "Solid-Phase Chemical-Enzymic Synthesis of Glycopeptides and Oligosaccharides", *Journal of American Chemical Society.*, Vol. 116, No. 3, pp. 1135–1136, 1994.

299. Dubowchik, G. M. and R. A. Firestone, "Cathepsin B-sensitive dipeptide prodrugs. 1. A model study of structural requirements for efficient release of doxorubicin", *Bioorganic and Medicinal Chemistry Letters*, Vol. 8, No. 23, pp. 3341–3346, 1998.

300. Liang, L., S.-W. Lin, W. Dai, J.-K. Lu, T.-Y. Yang, Y. Xiang, Y. Zhang, R.-T. Li, and Q. Zhang, "Novel cathepsin B-sensitive paclitaxel conjugate: Higher water solubility, better efficacy and lower toxicity", *Journal of Controlled Release*, Vol. 160, No. 3, pp. 618–629, 2012.

301. Huang, H., J. Geng, J. Golzarian, J. Huang, and J. Yu, "Fabrication of doxorubicin-loaded ellipsoid micelle based on diblock copolymer with a linkage of enzyme-cleavable peptide", *Colloids Surfaces B Biointerfaces*, Vol. 133, pp. 362–369, 2015.

302. McCombs, J. R. and S. C. Owen, "Antibody Drug Conjugates: Design and Selection of Linker, Payload and Conjugation Chemistry", *Journal of The American Association of Pharmaceutical Scientists.*, Vol. 17, No. 2, pp. 339–351, 2015.

APPENDIX A: ADDITIONAL DATA

^{1}H NMR, ^{13}C NMR, and FT-IR of the molecules are included.

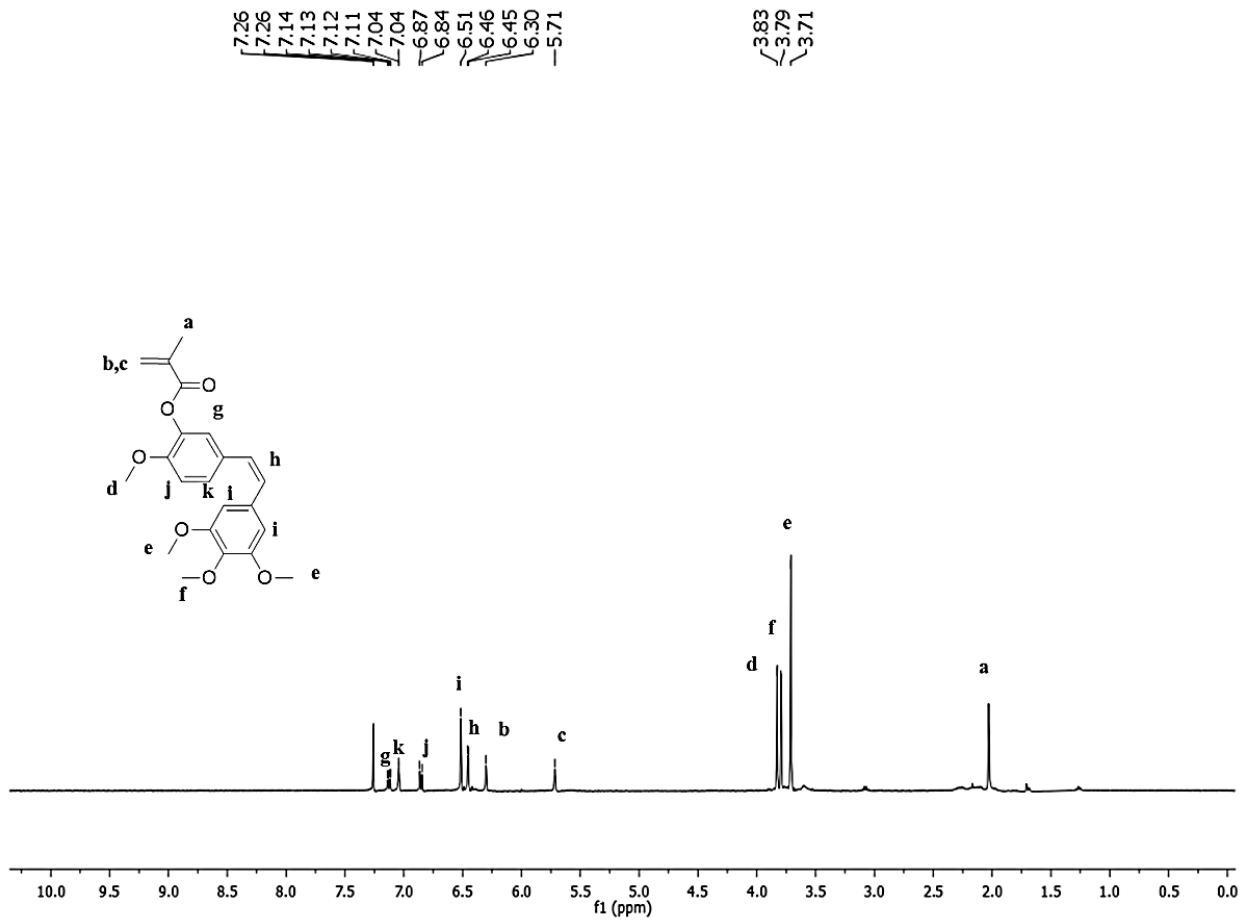

Figure A.1. ^{1}H-NMR of CA4MA (3)

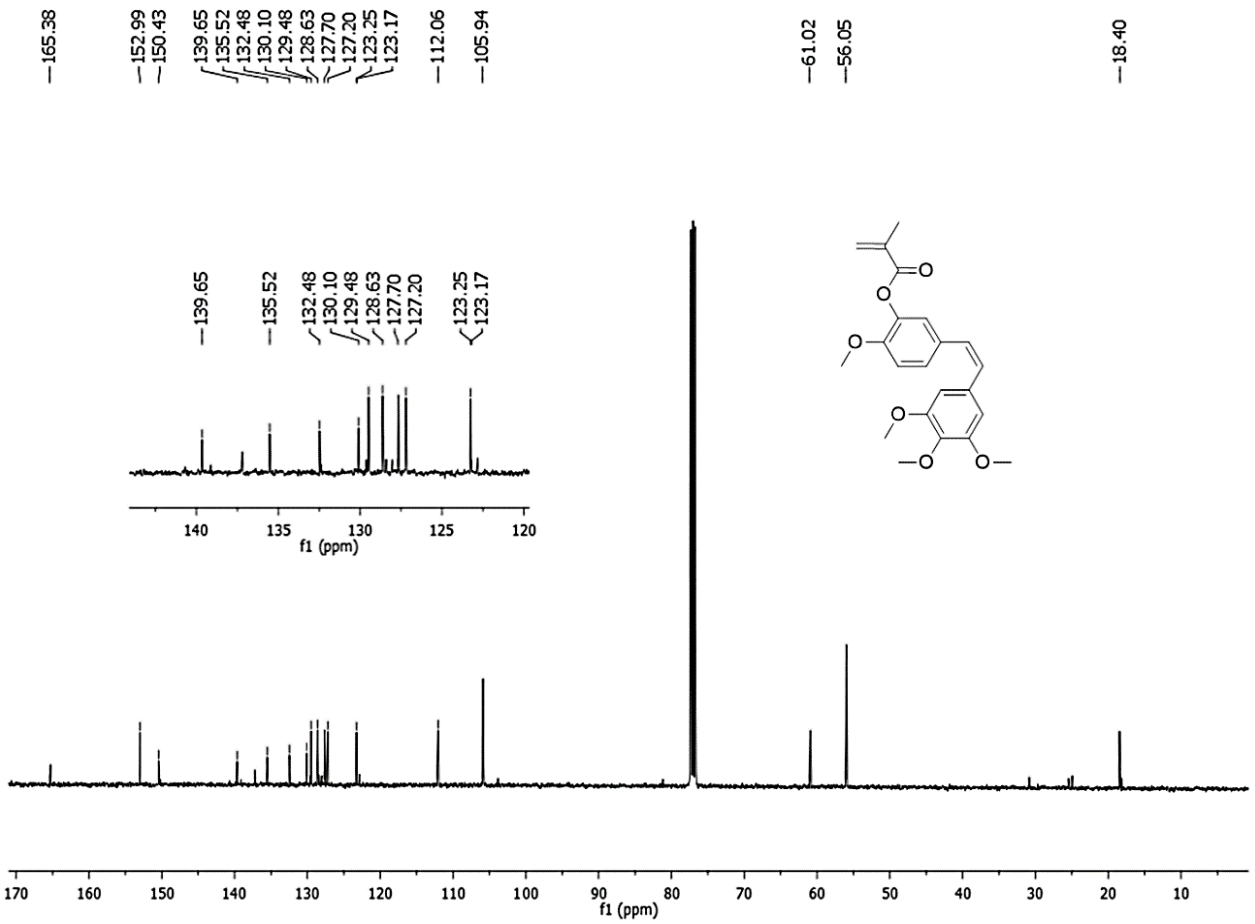

Figure A.2. ^{13}C-NMR of CA4MA (3)

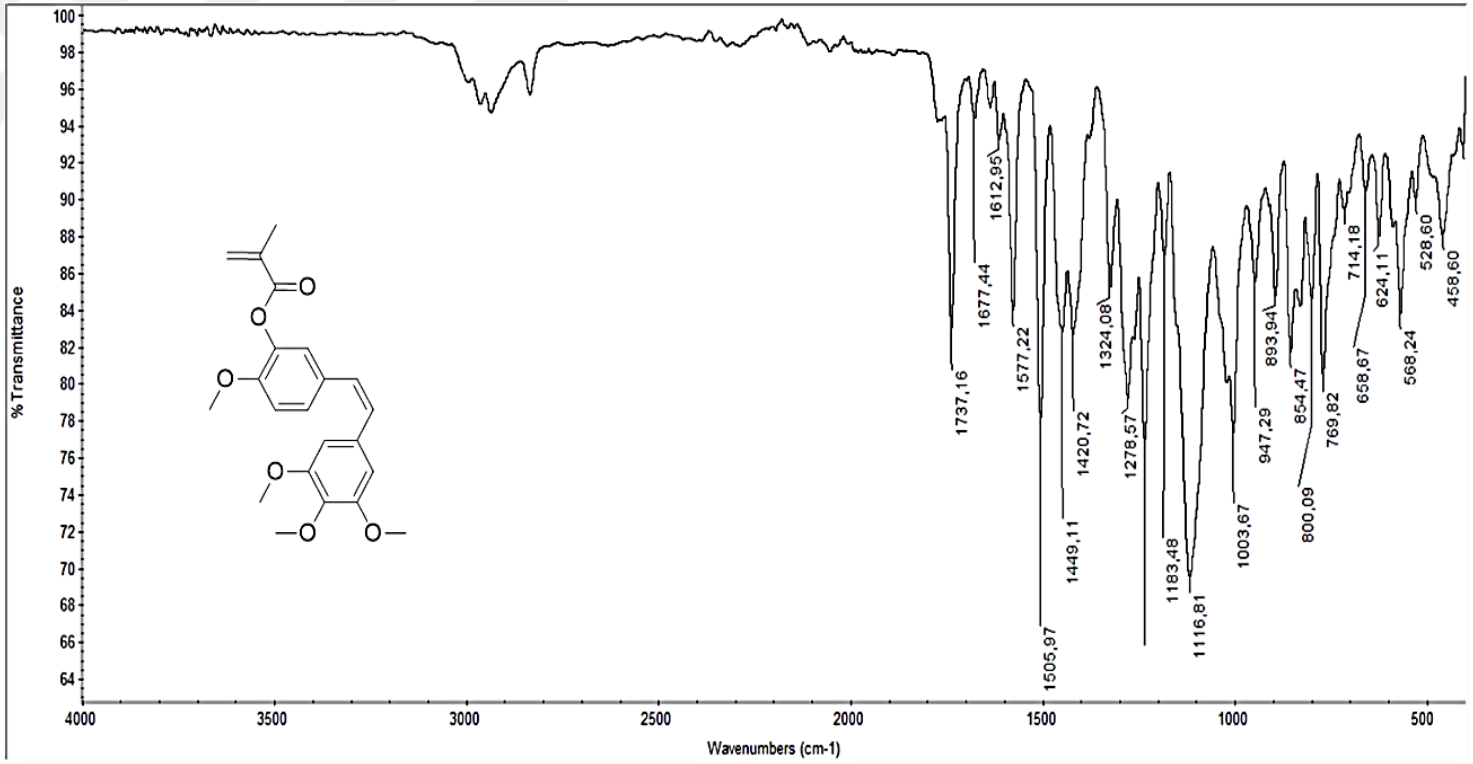

Figure A.3. FT-IR^{-1} of CA4MA (3)

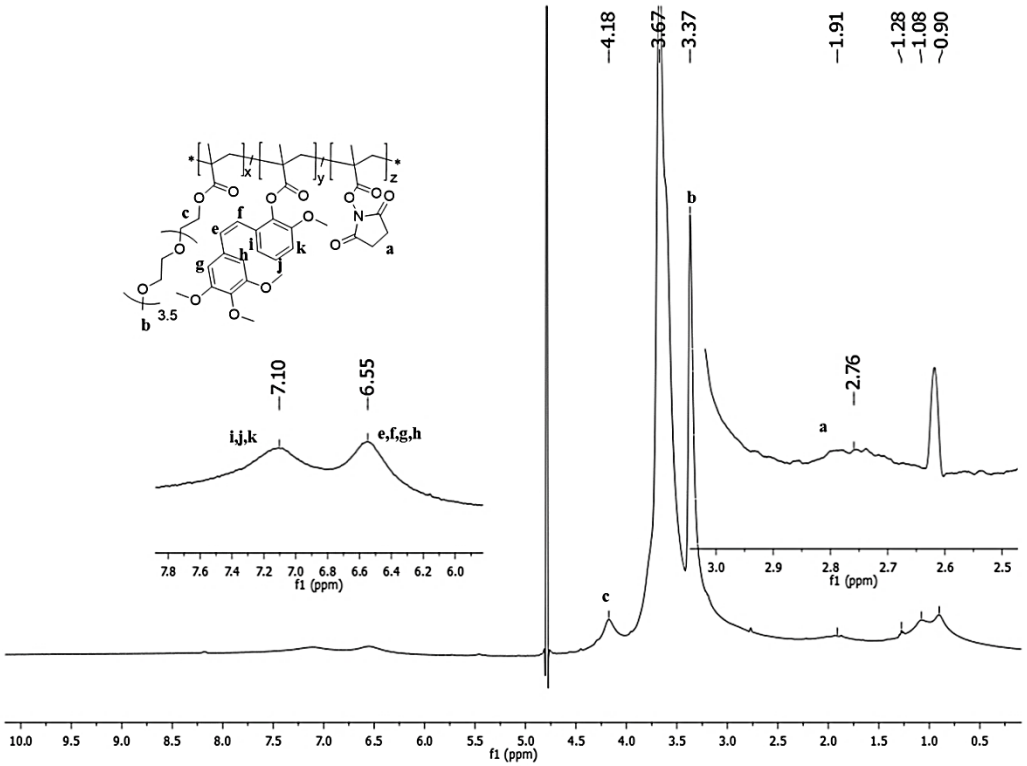

Figure A.4. ^{1}H-NMR of P(OEGMA-CA4-NHS) (4)

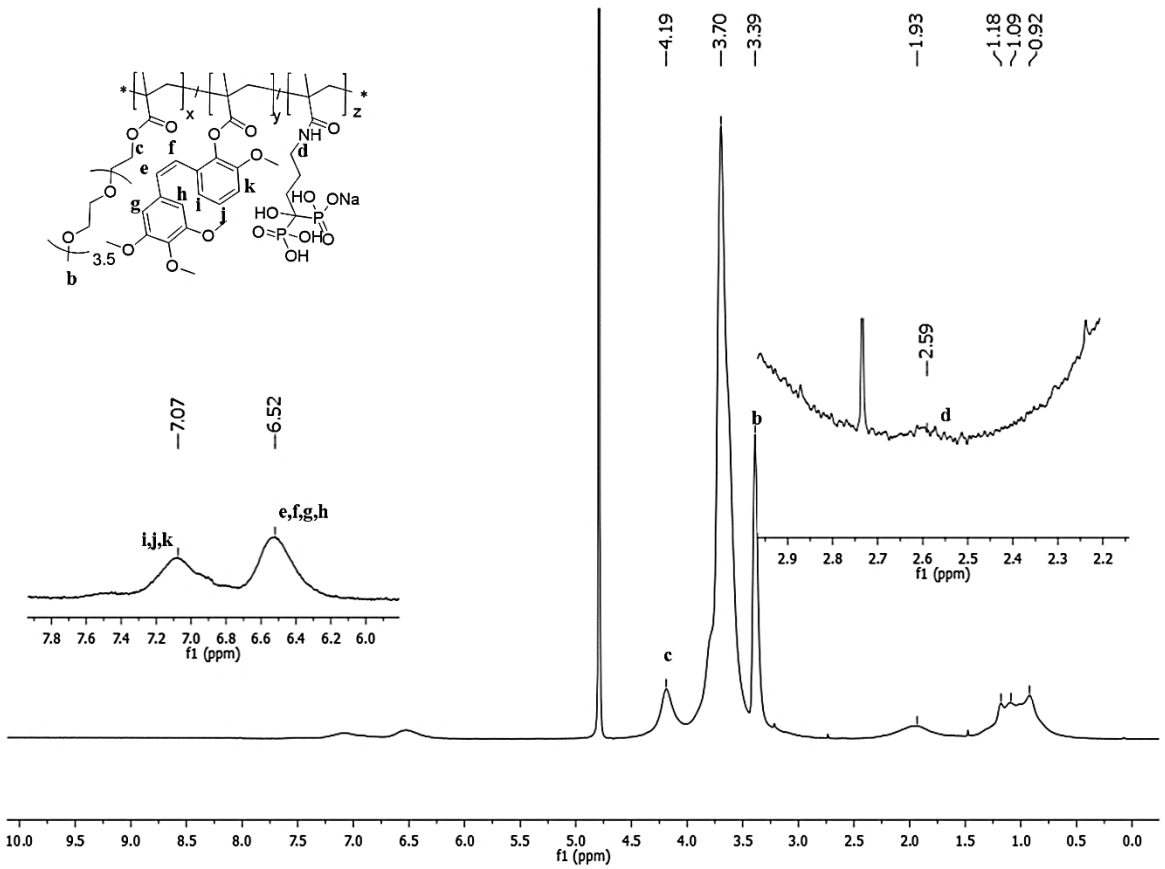

Figure A.5. ^{1}H-NMR of P(OEGMA-CA4-ALN) (6)

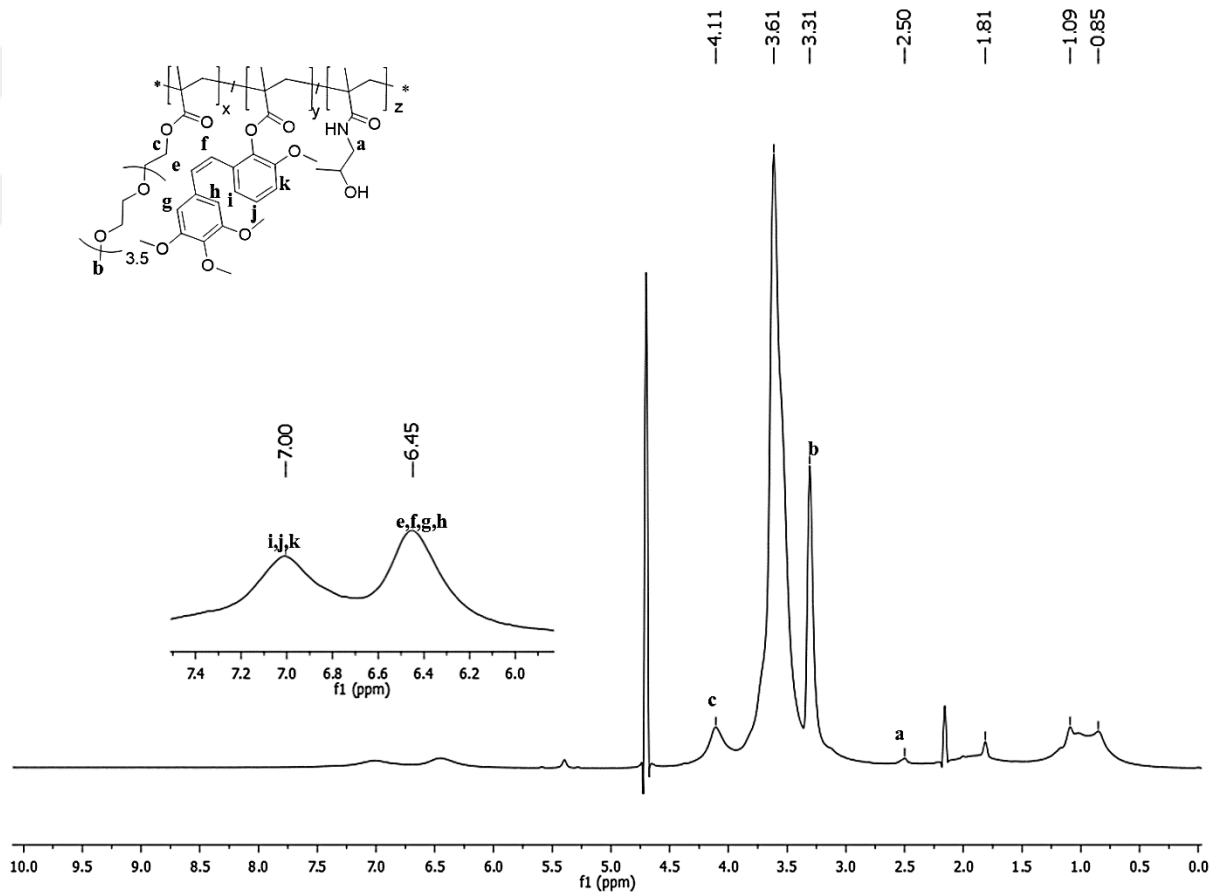

Figure A.6. ^{1}H-NMR of P(OEGMA-CA4) (7)

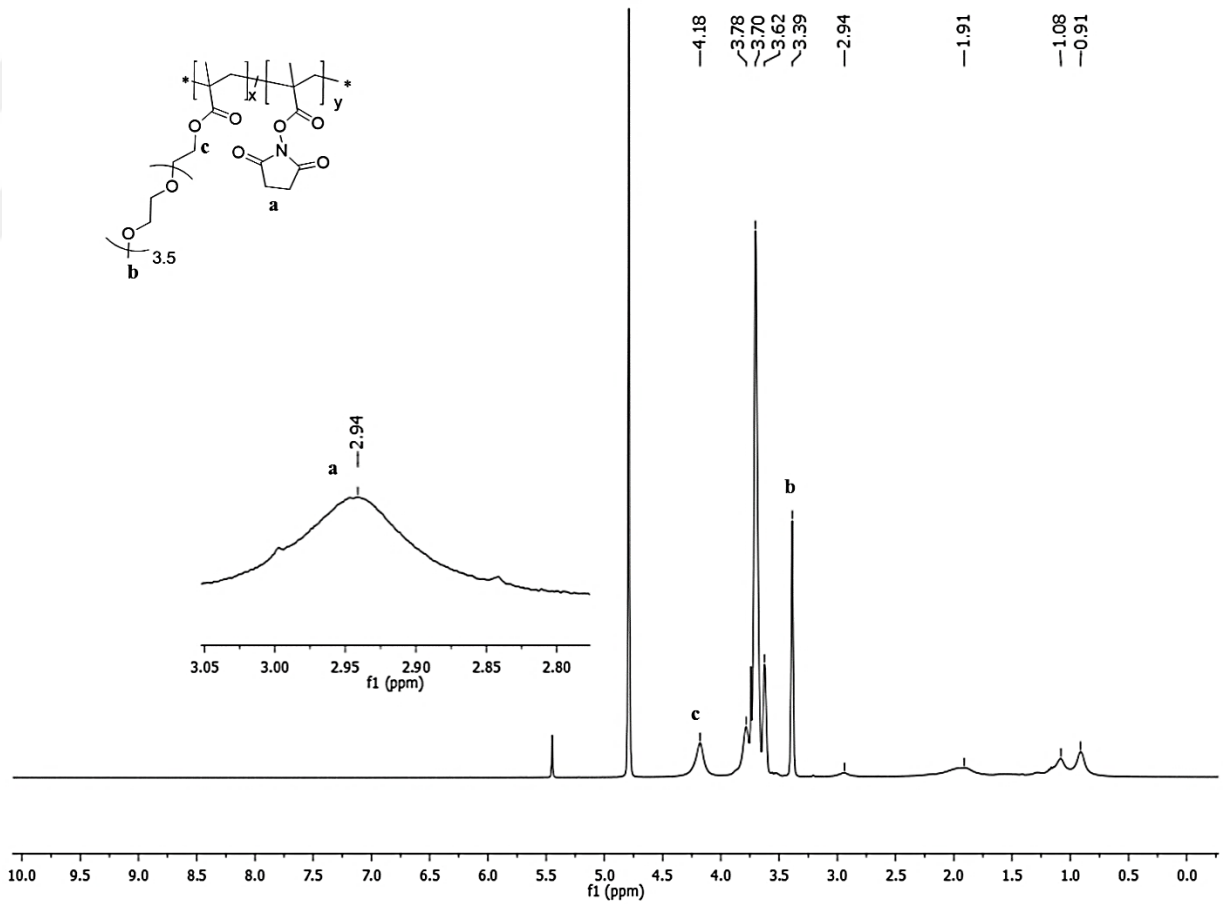

Figure A.7. ^{1}H-NMR of P(OEGMA-NHS) (8)

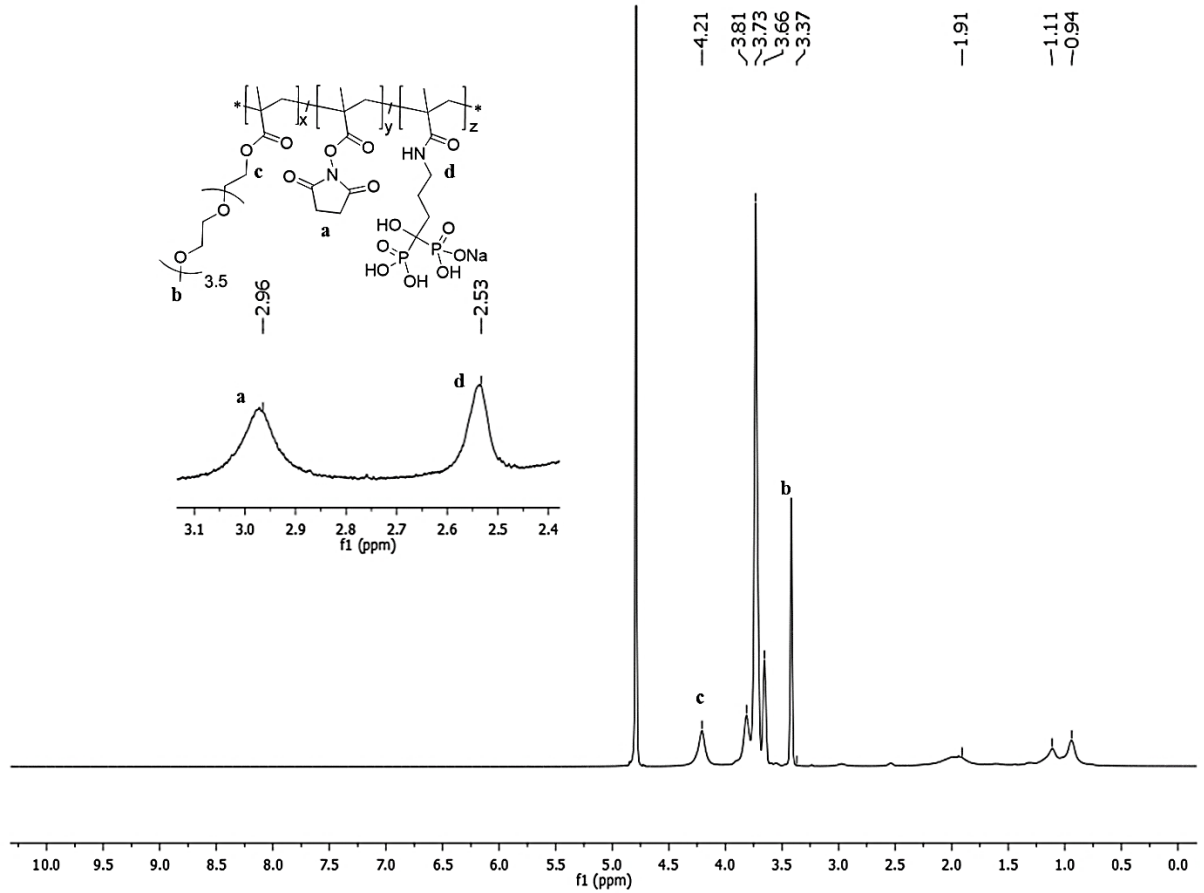

Figure A.8. ^{1}H-NMR of P(OEGMA-NHS-ALN) (9)

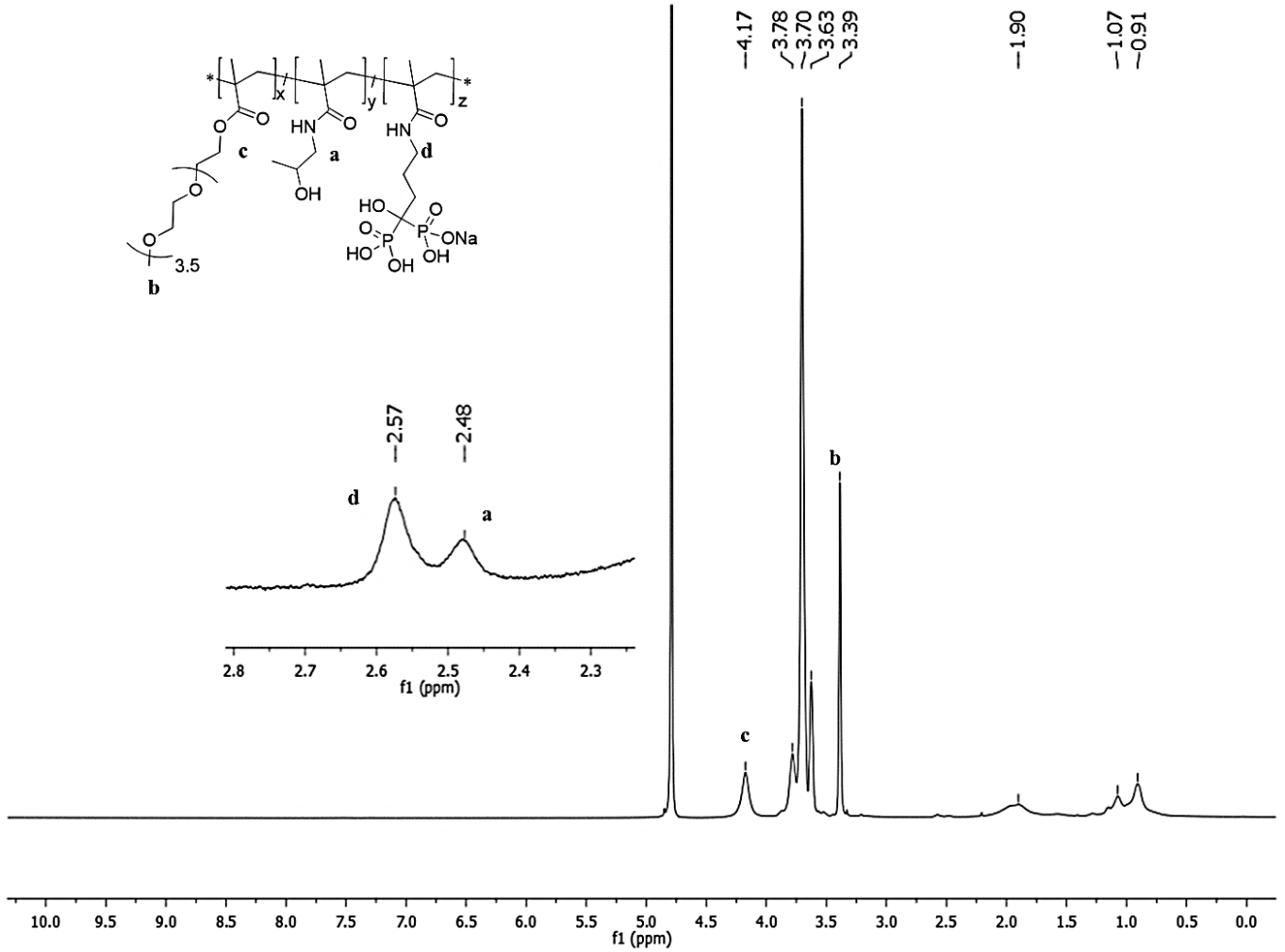

Figure A.9. ^{1}H-NMR of P(OEGMA-ALN) (10)

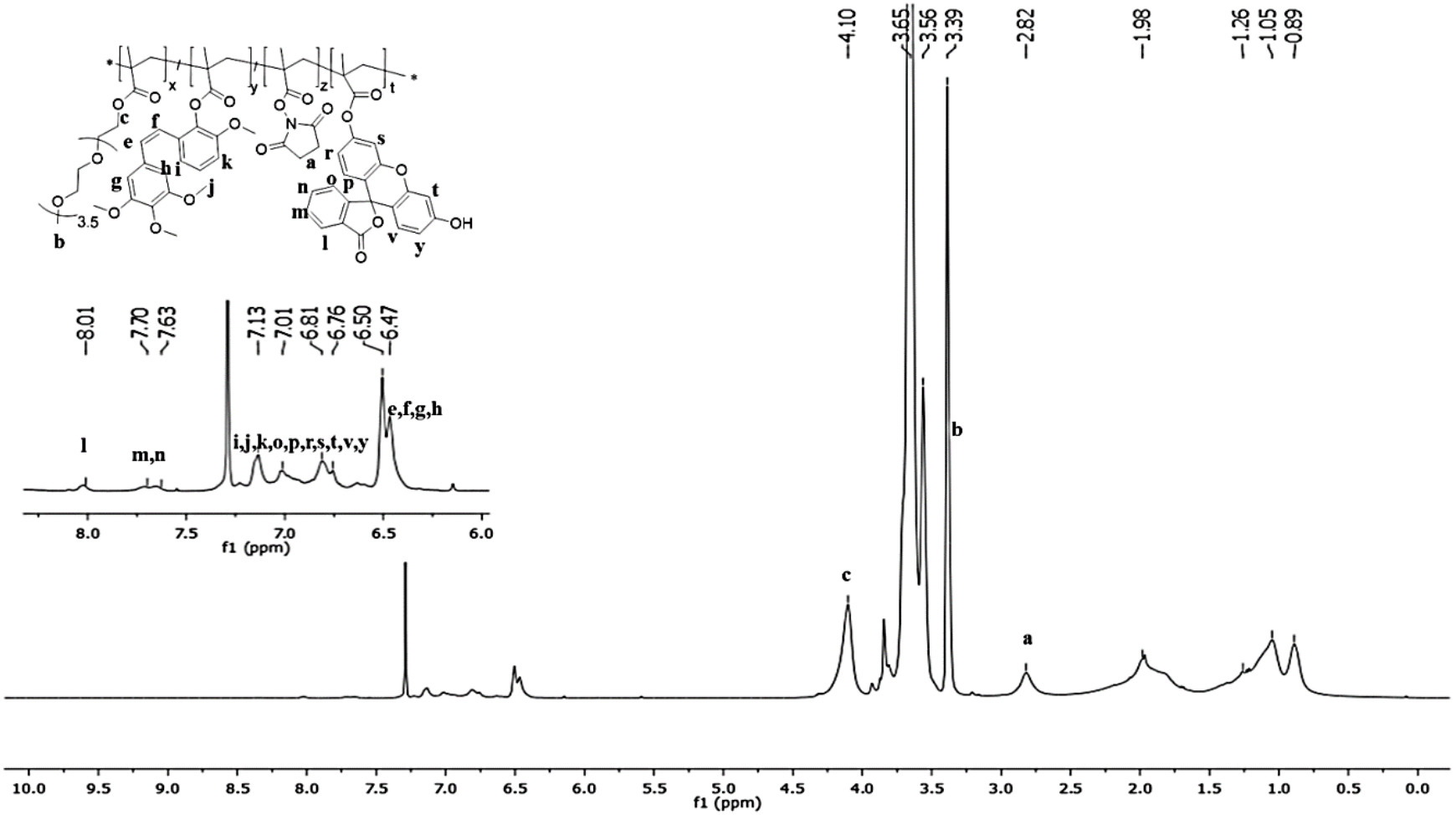

Figure A.10. ^{1}H-NMR of P(OEGMA-CA4-NHS-FMA) (12)

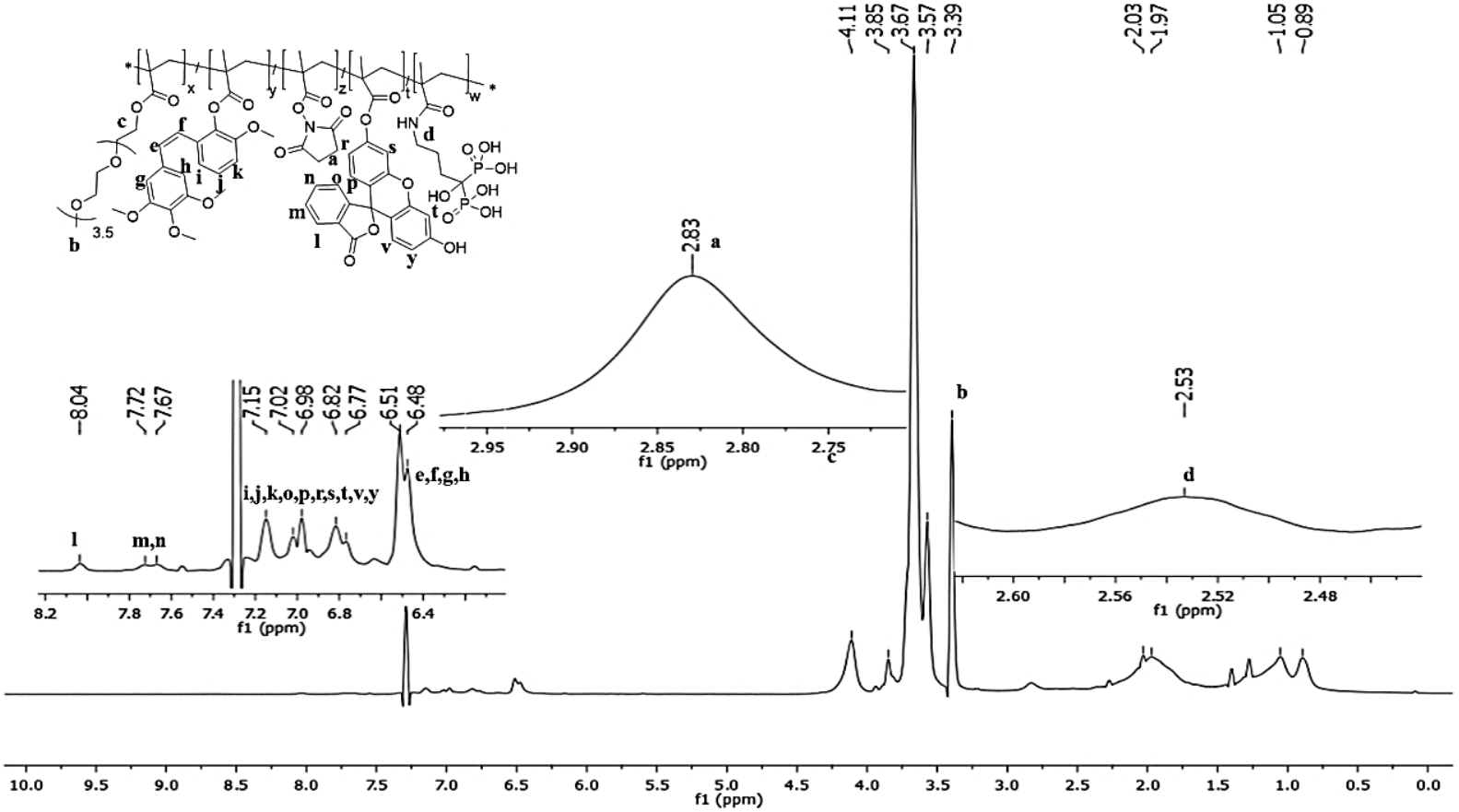

Figure A.11. ^{1}H-NMR of P(OEGMA-CA4-NHS-ALN-FMA (13)

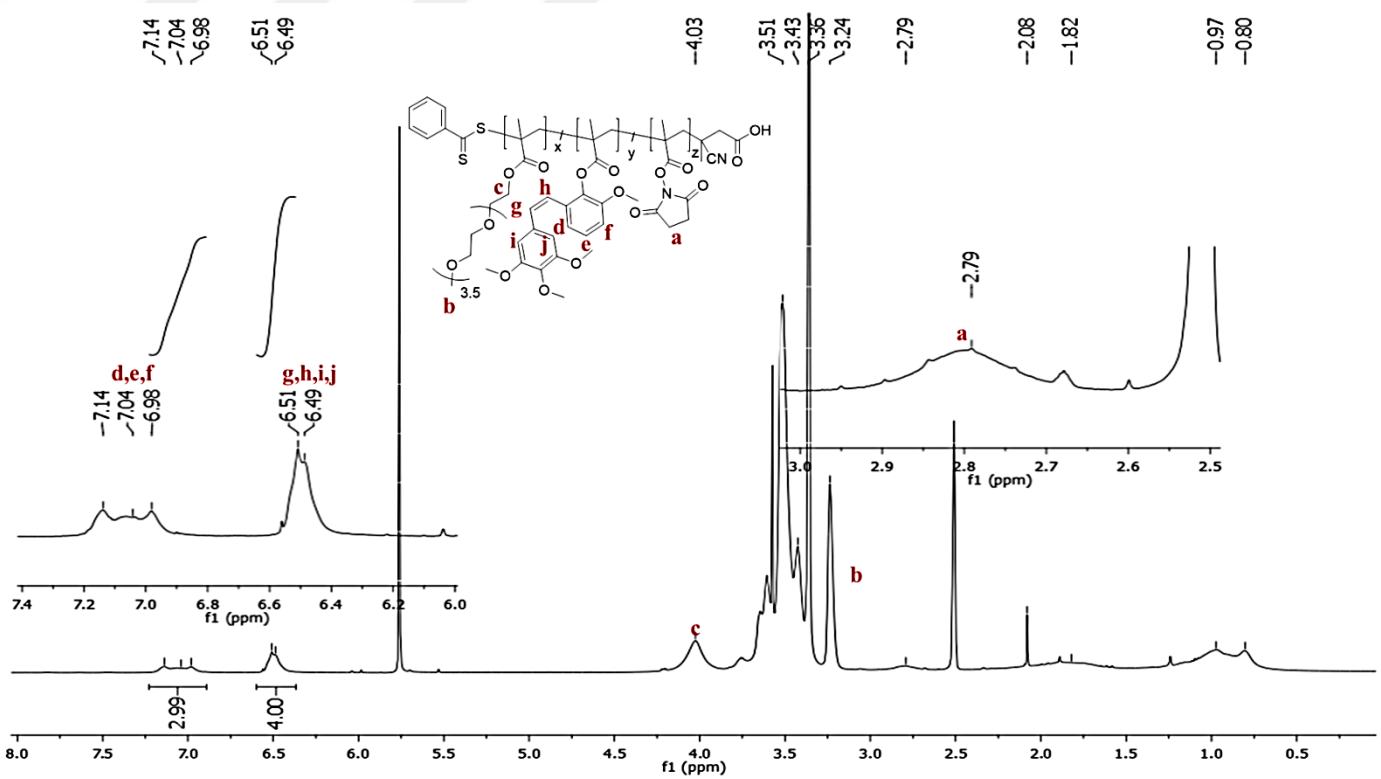

Figure A.12. ^{1}H-NMR Spectrum of P(OEGMA-CA4-NHS) (18)

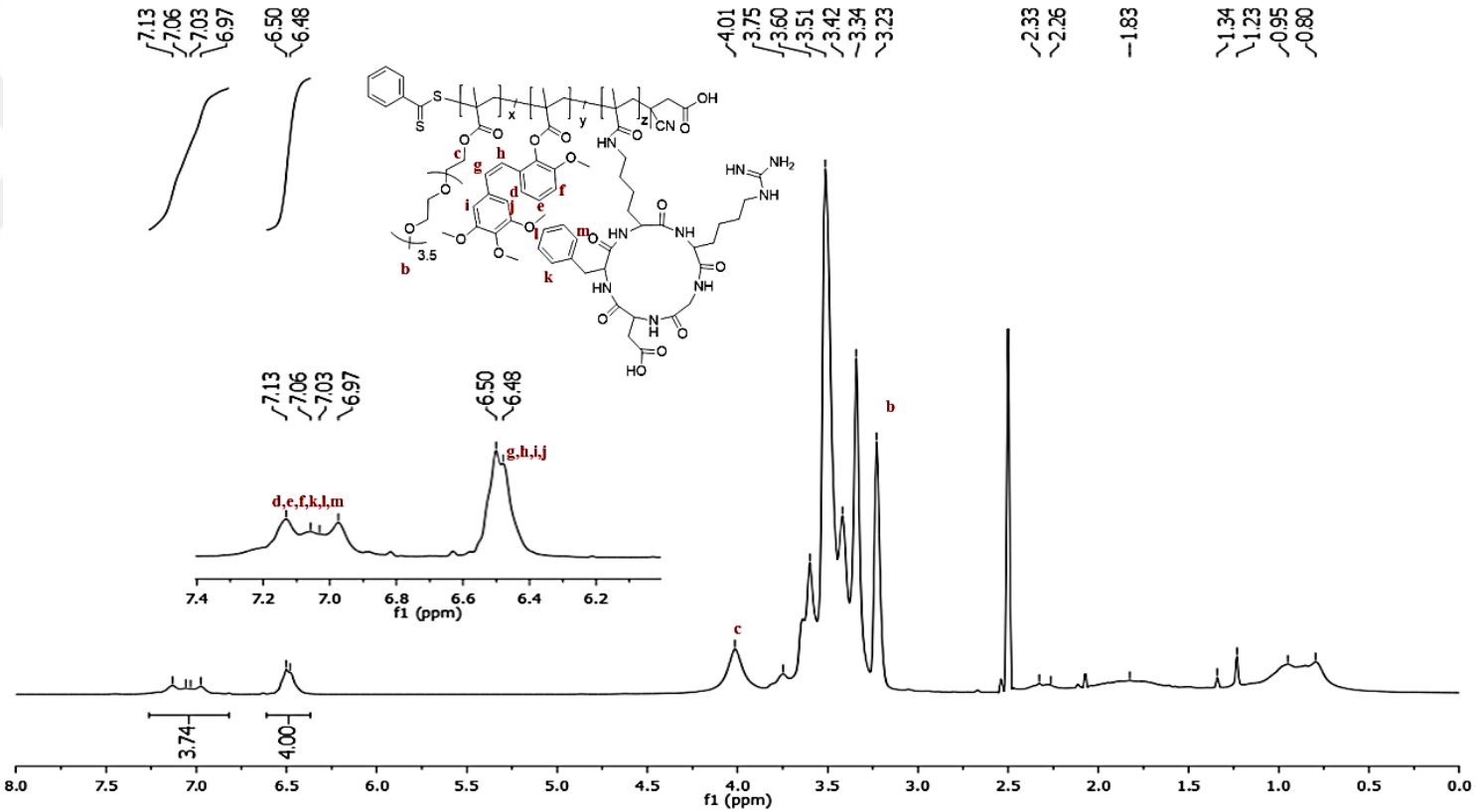

Figure A.13. ^{1}H-NMR Spectrum of P(OEGMA-CA4-RGD) (19)

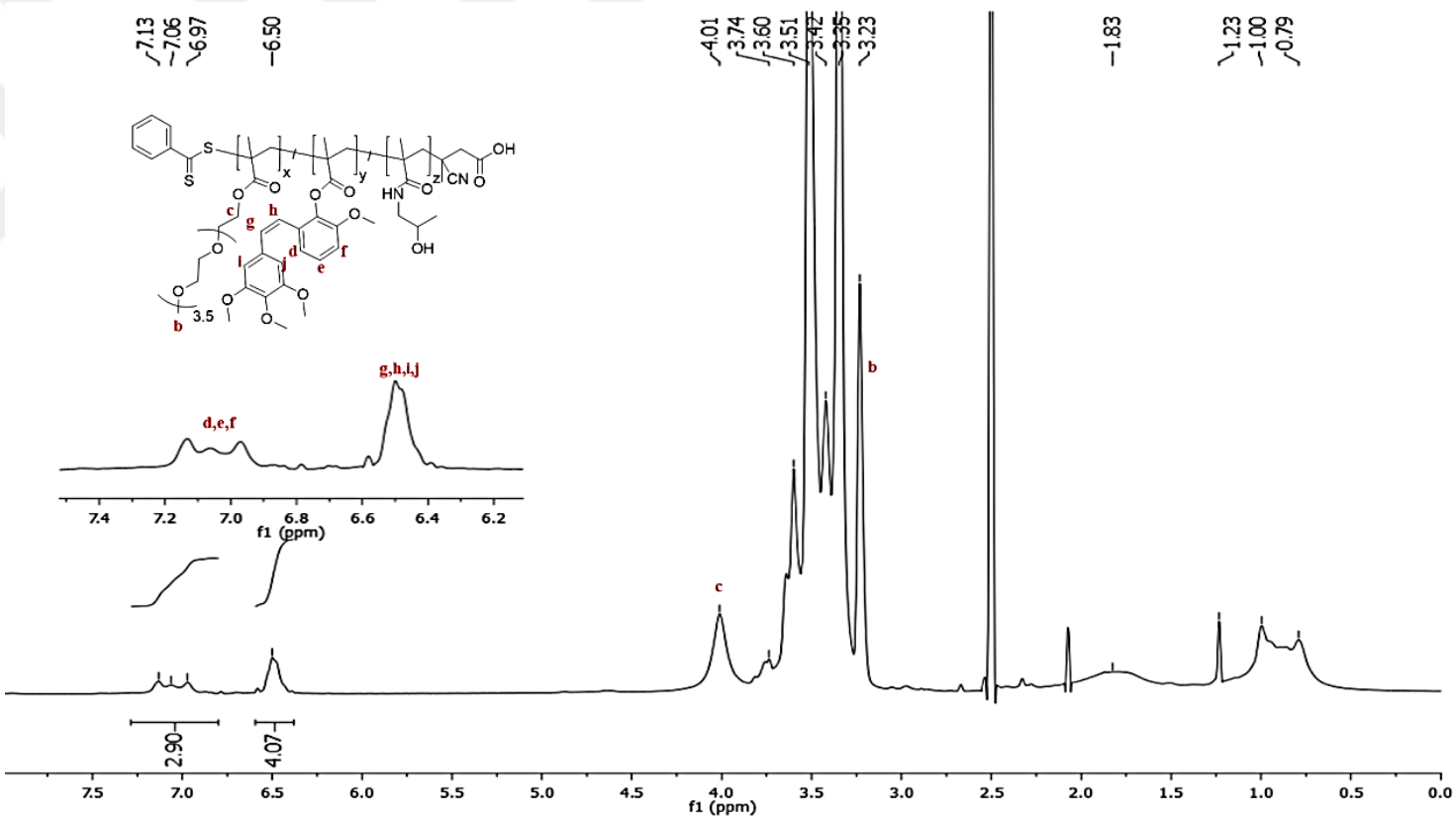

Figure A.14. ^{1}H-NMR Spectrum of P(OEGMA-CA4) (20)

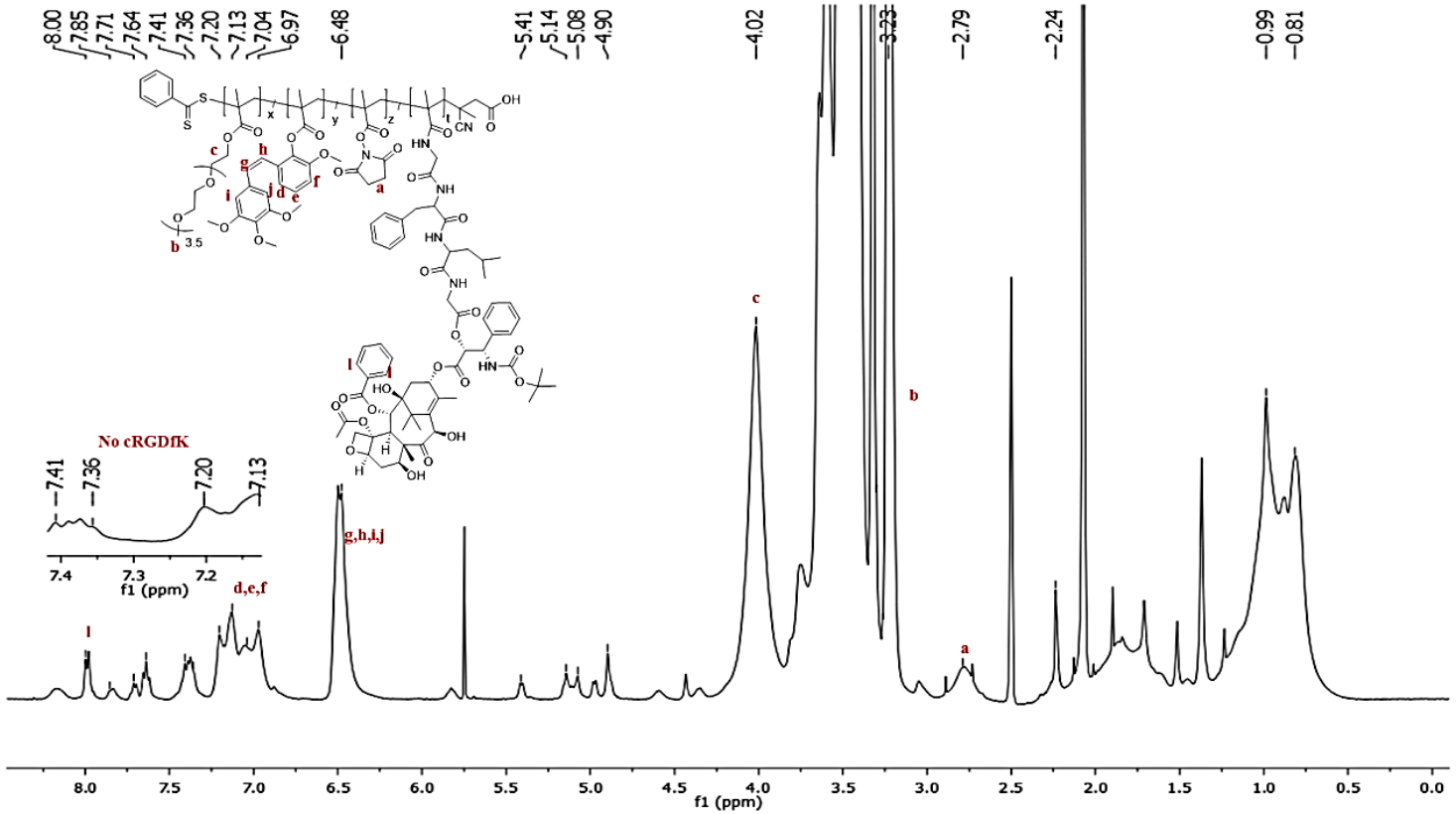

Figure A.15. ^{1}H-NMR Spectrum of P(OEGMA-CA4-NHS-DTX) (21)

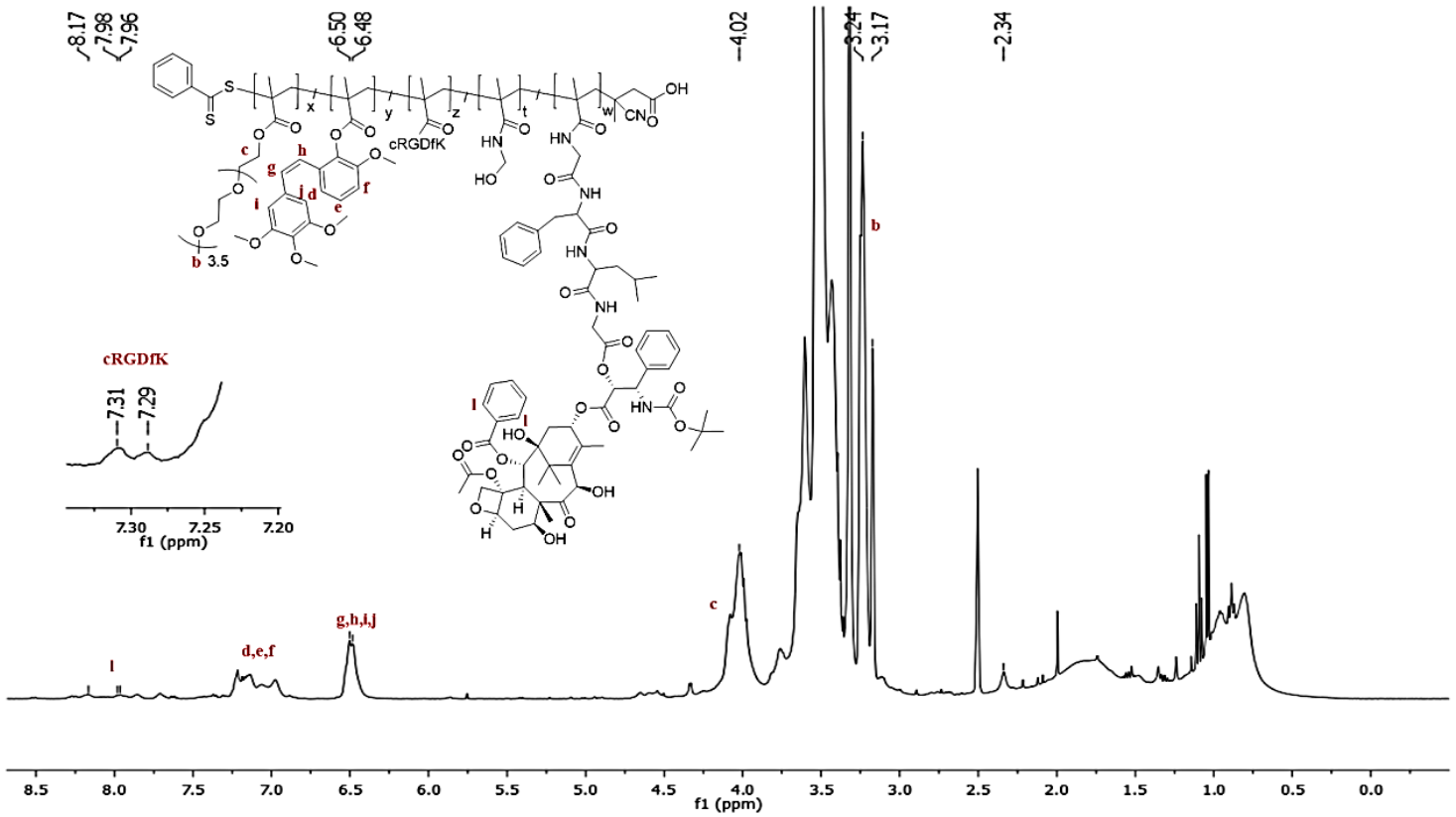

Figure A.16. ^{1}H-NMR Spectrum of P(OEGMA-CA4-RGD-DTX) (22)

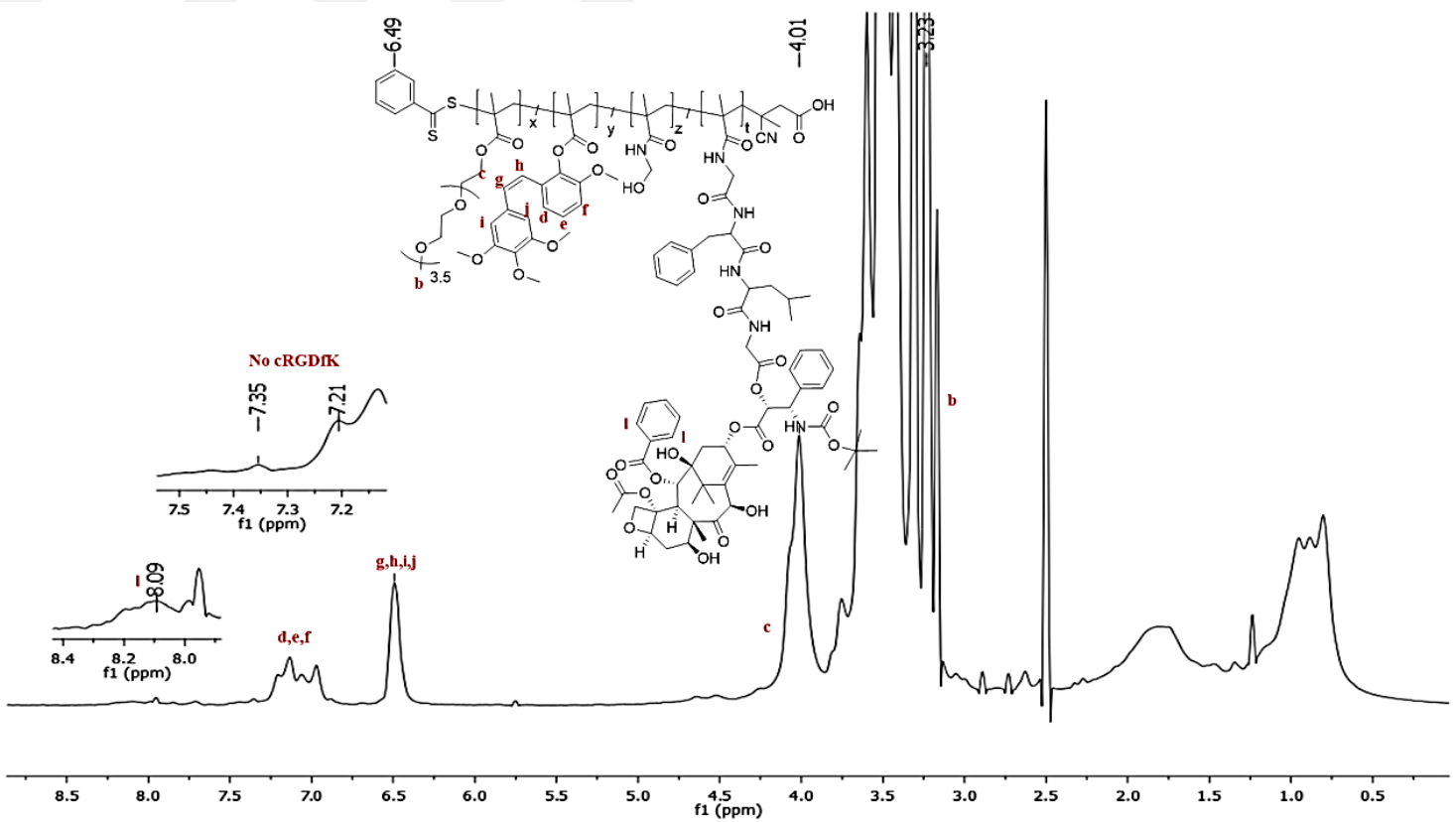

Figure A.17. ^{1}H-NMR Spectrum of P(OEGMA-CA4-DTX) (23)

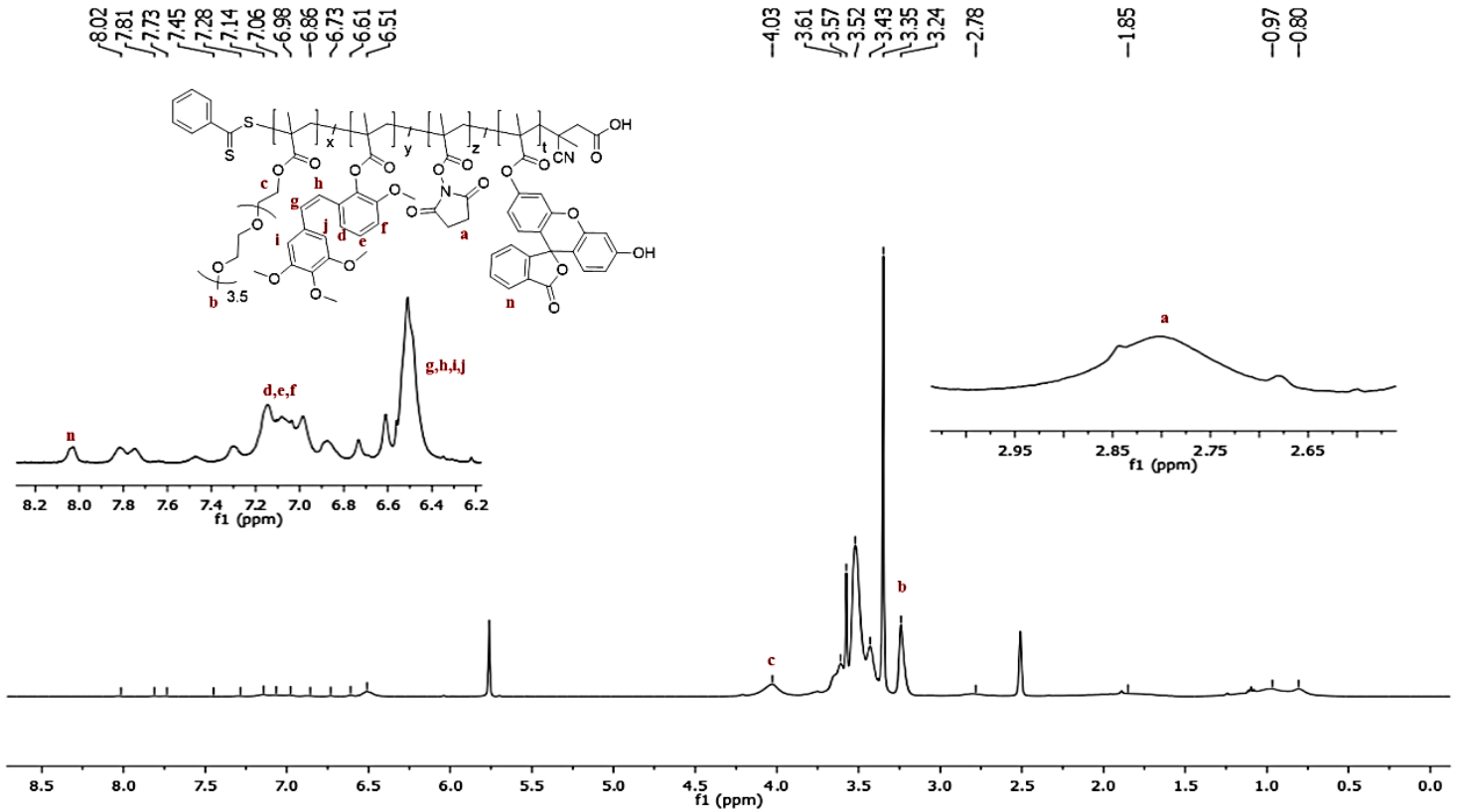

Figure A.18. ^{1}H-NMR Spectrum of P(OEGMA-CA4-NHS-FMA) (24)

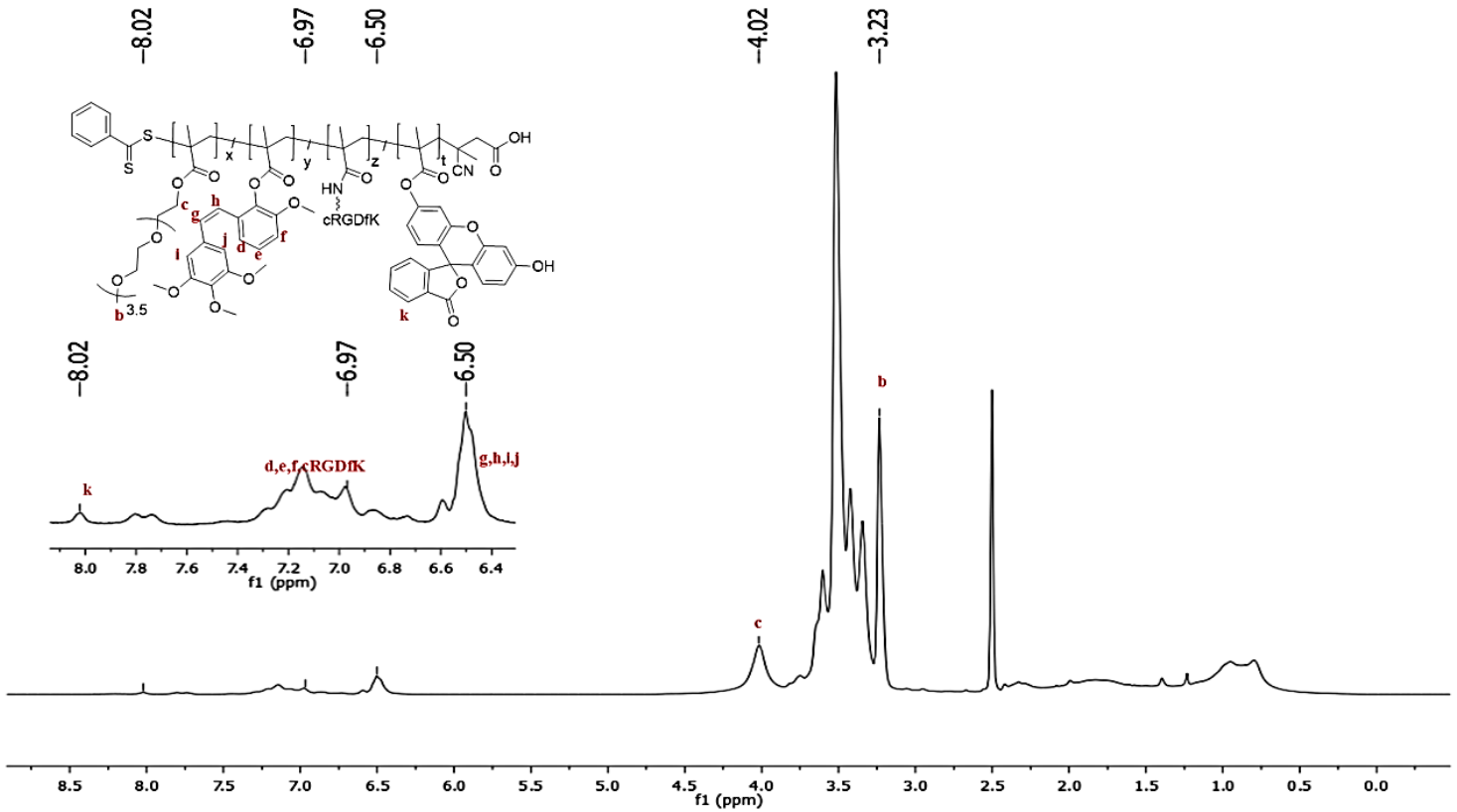

Figure A.19. ^{1}H-NMR Spectrum of P(OEGMA-CA4-RGD-FMA) (25)

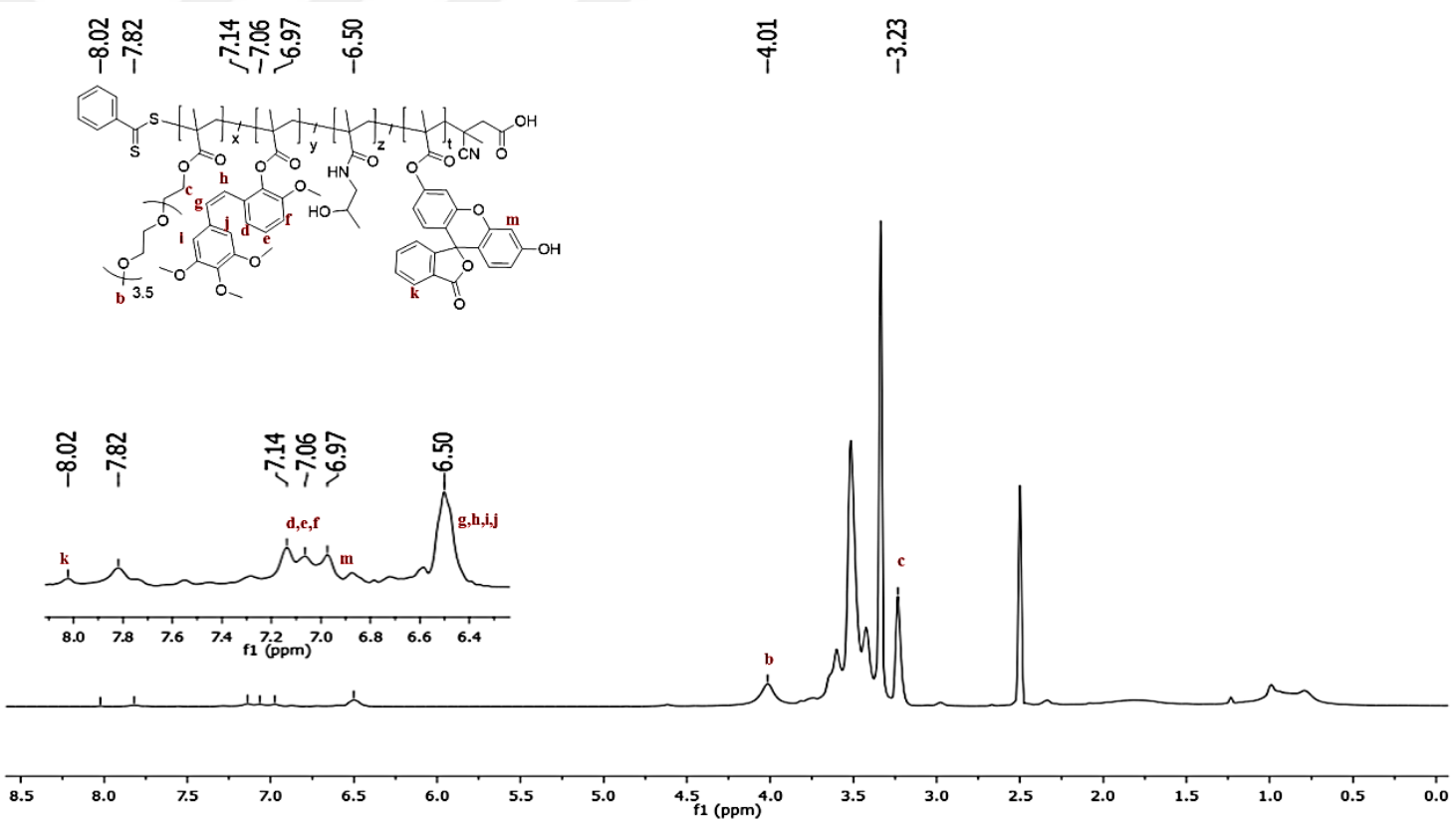

Figure A.20. ^{1}H-NMR Spectrum of P(OEGMA-CA4-FMA) (26)

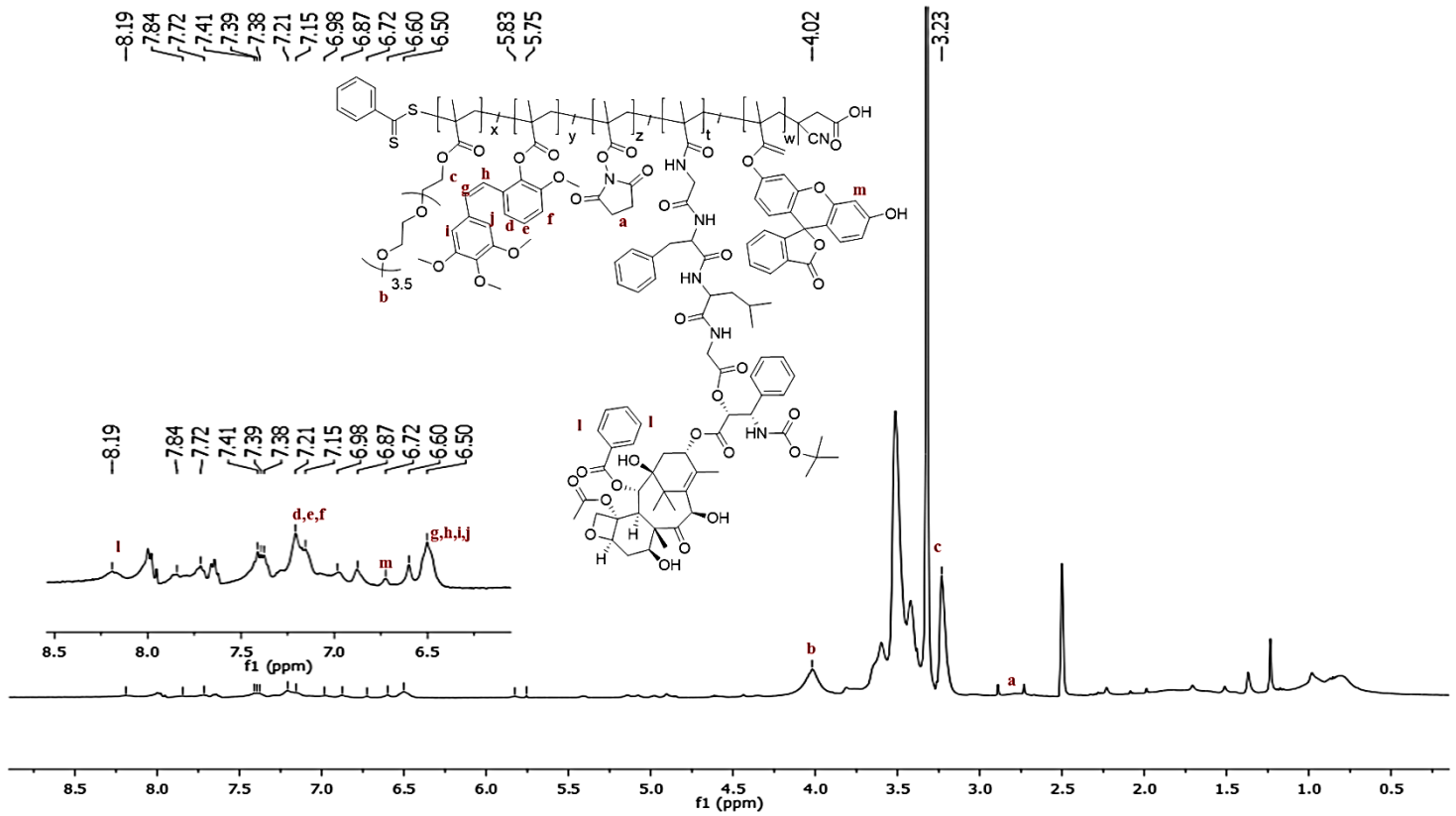

Figure A.21. ^{1}H-NMR Spectrum of P(OEGMA-CA4-NHS-DTX-FMA) (27)

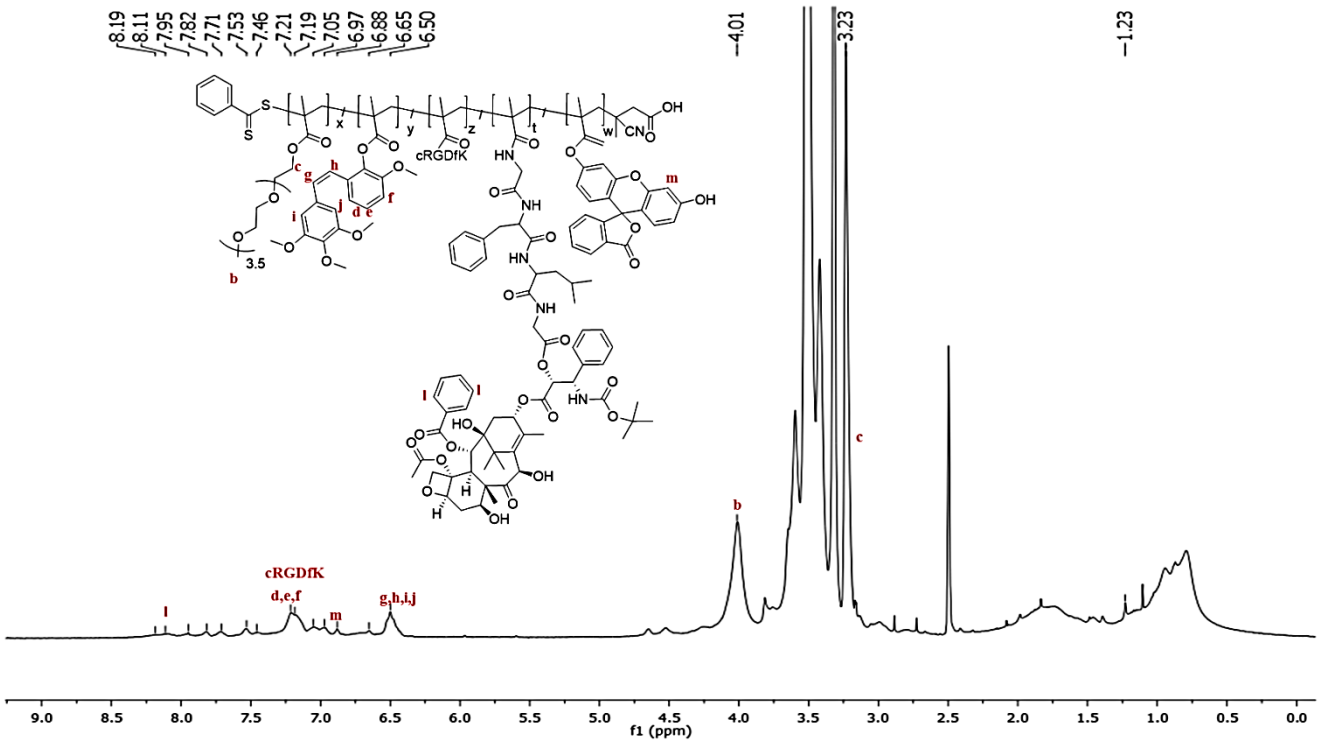

Figure A.22. ^{1}H-NMR Spectrum of P(OEGMA-CA4-RGD-DTX-FMA) (28)

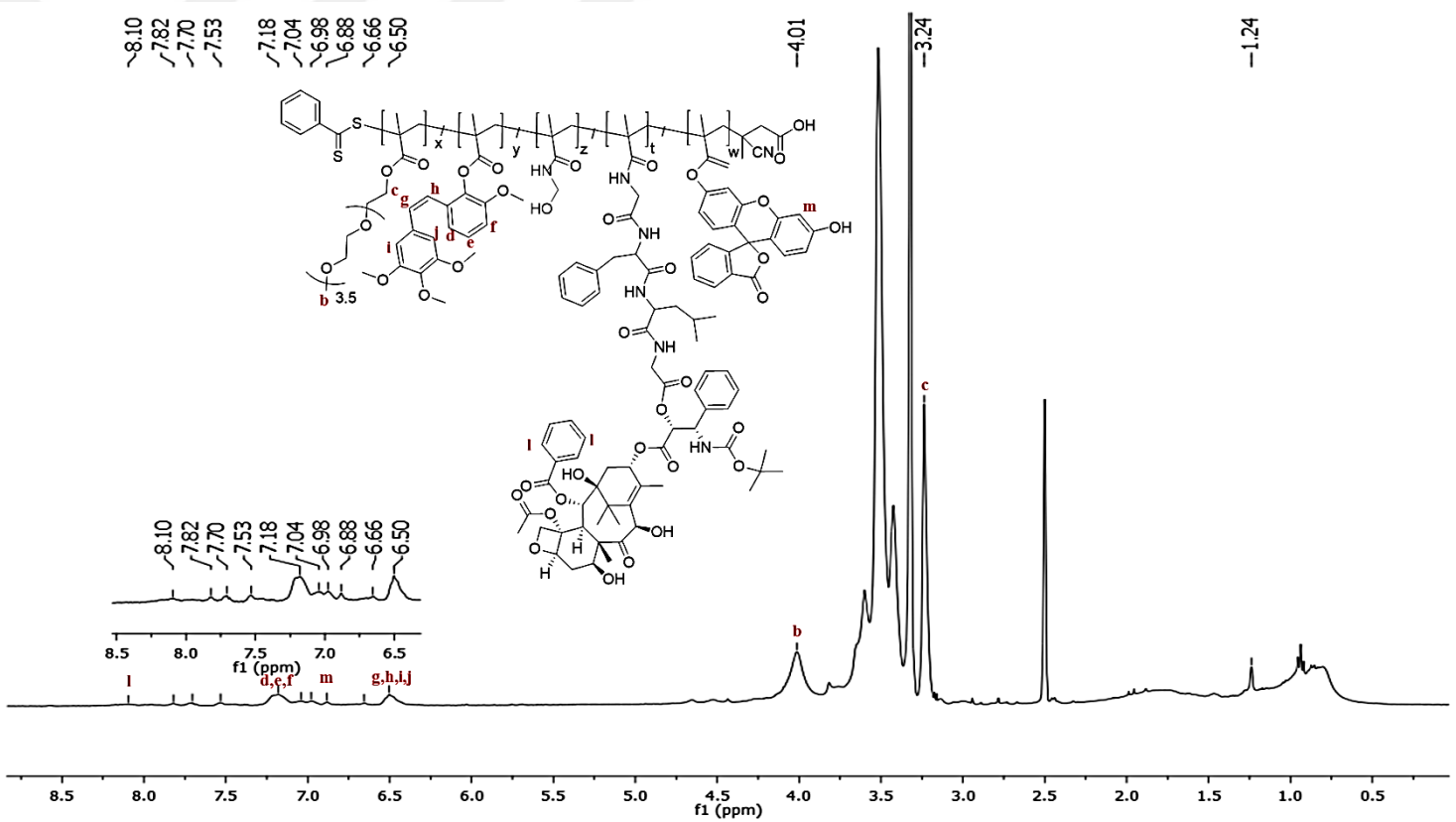

Figure A.23. ^{1}H-NMR Spectrum of P(OEGMA-CA4-DTX-FMA) (29)

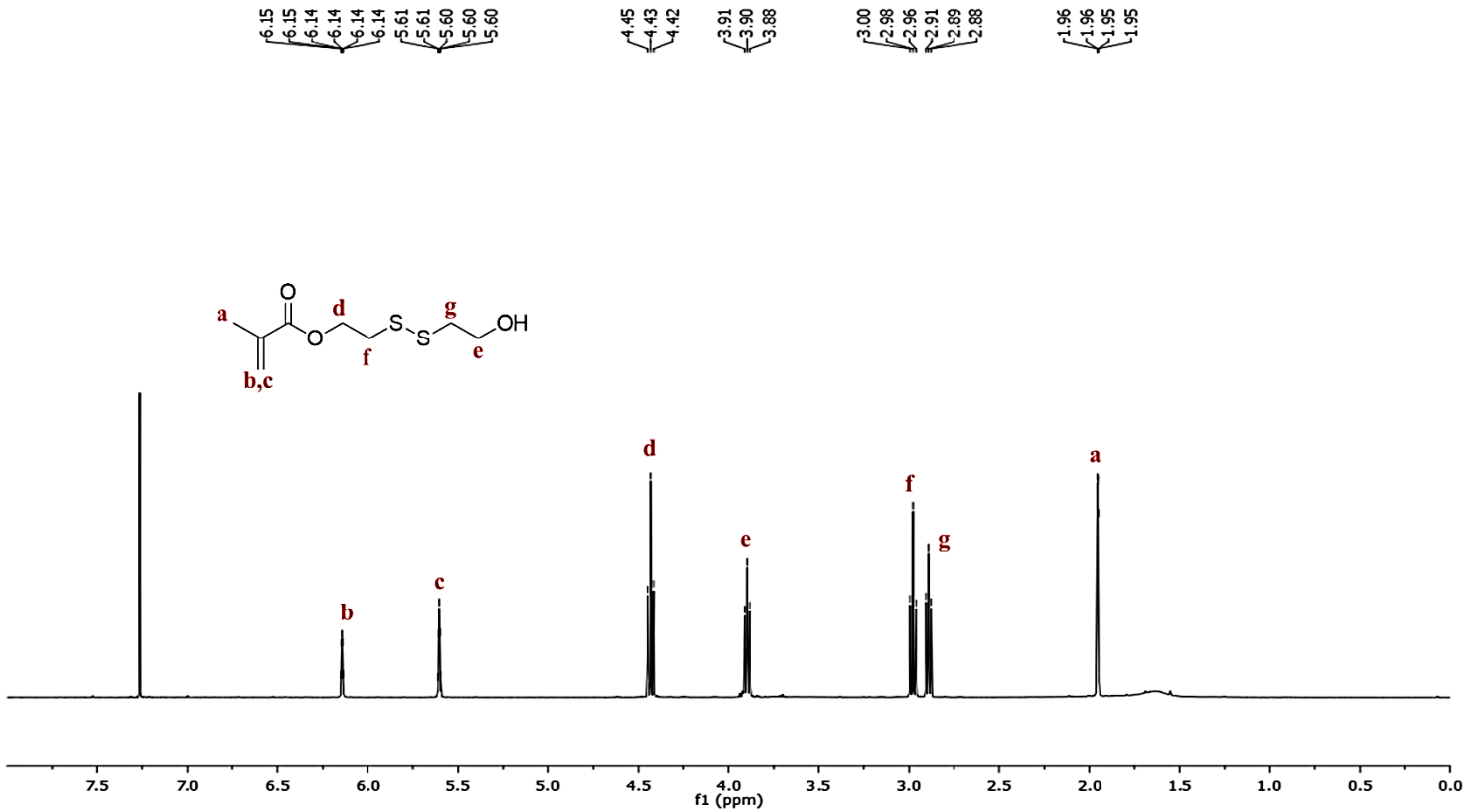

Figure A.24. ^{1}H-NMR Spectrum of HSEMA (30)

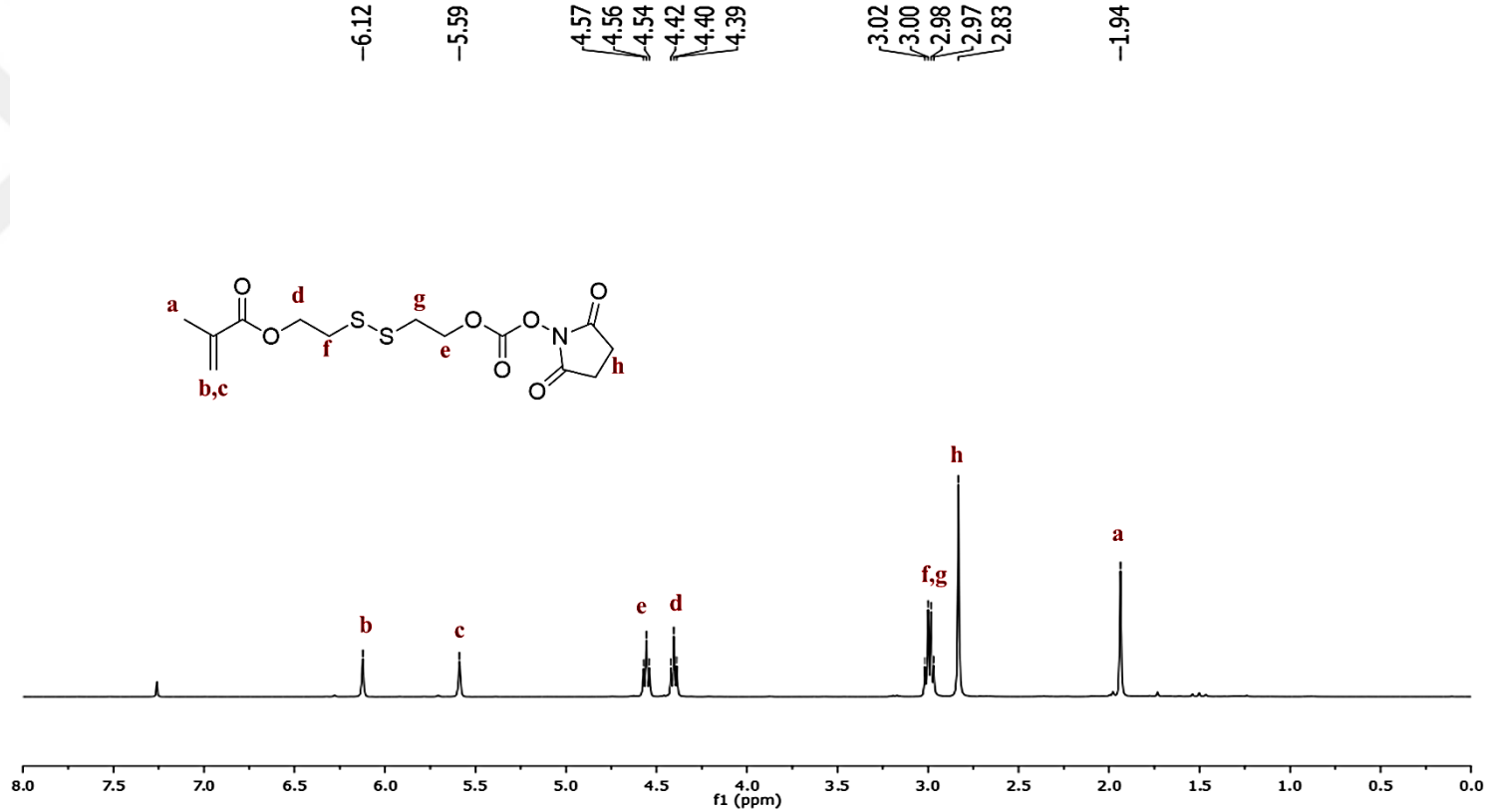

Figure A.25. ^{1}H-NMR Spectrum of SCEDEMA (31)

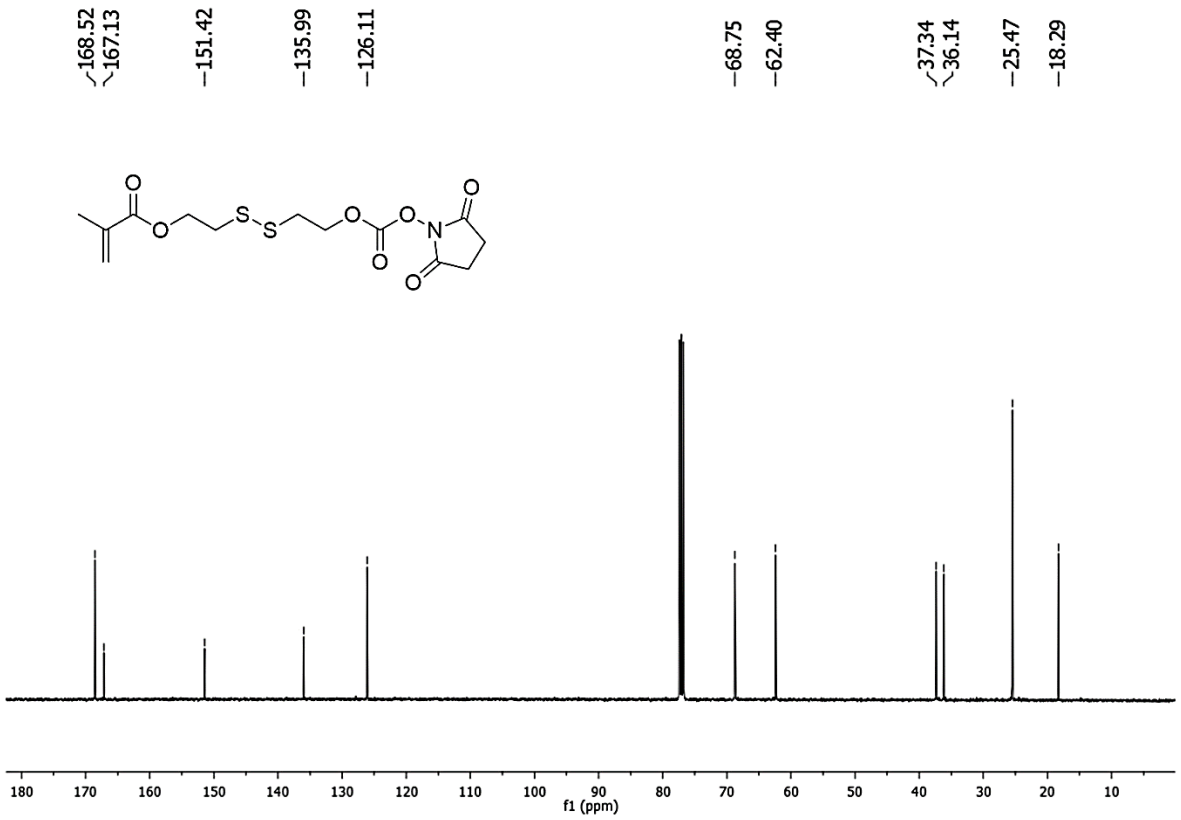

Figure A.26. ^{13}C-NMR Spectrum of SCEDEMA (31)

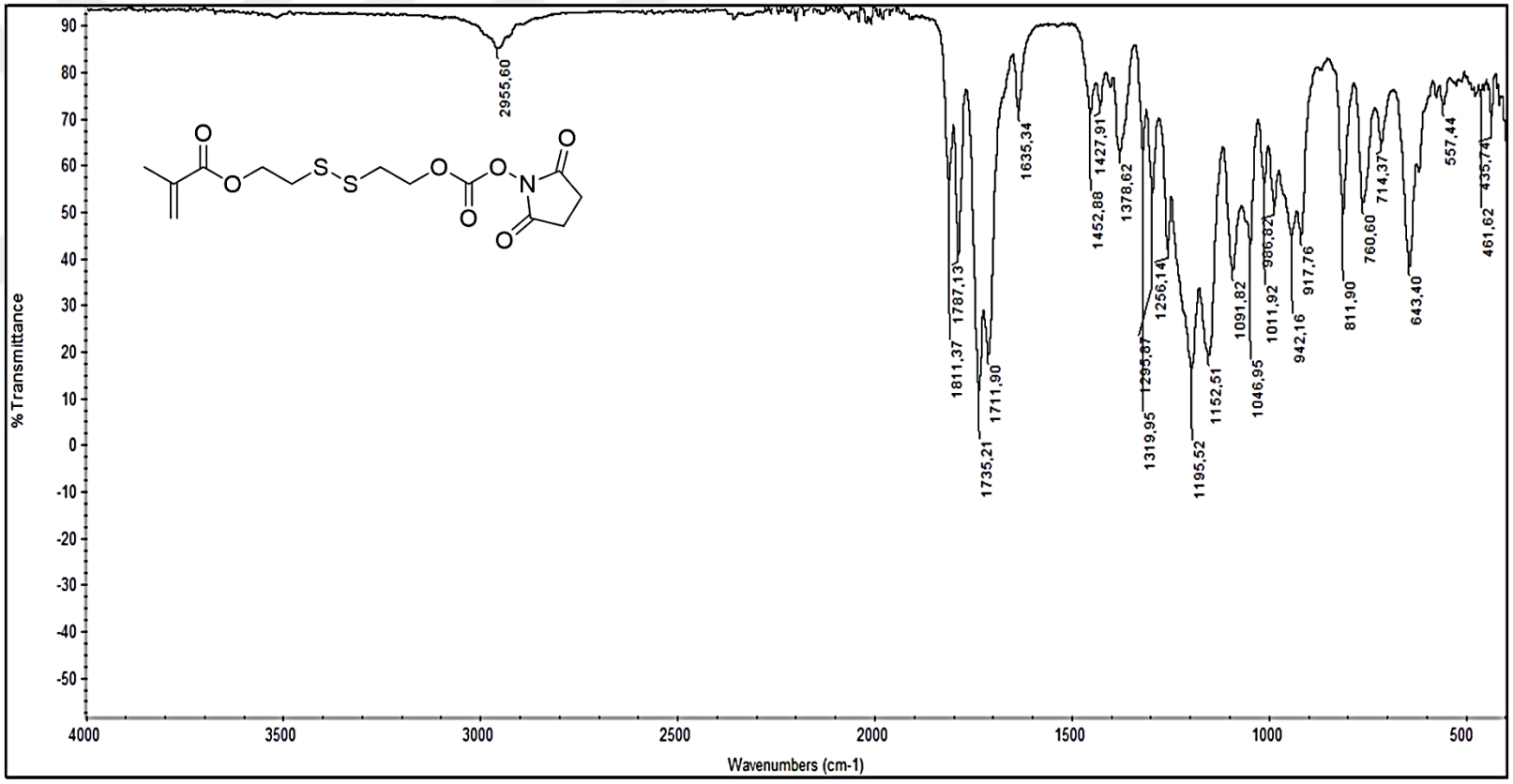

Figure A.27. FT-IR^{-1} Spectrum of SCEDMA (31)

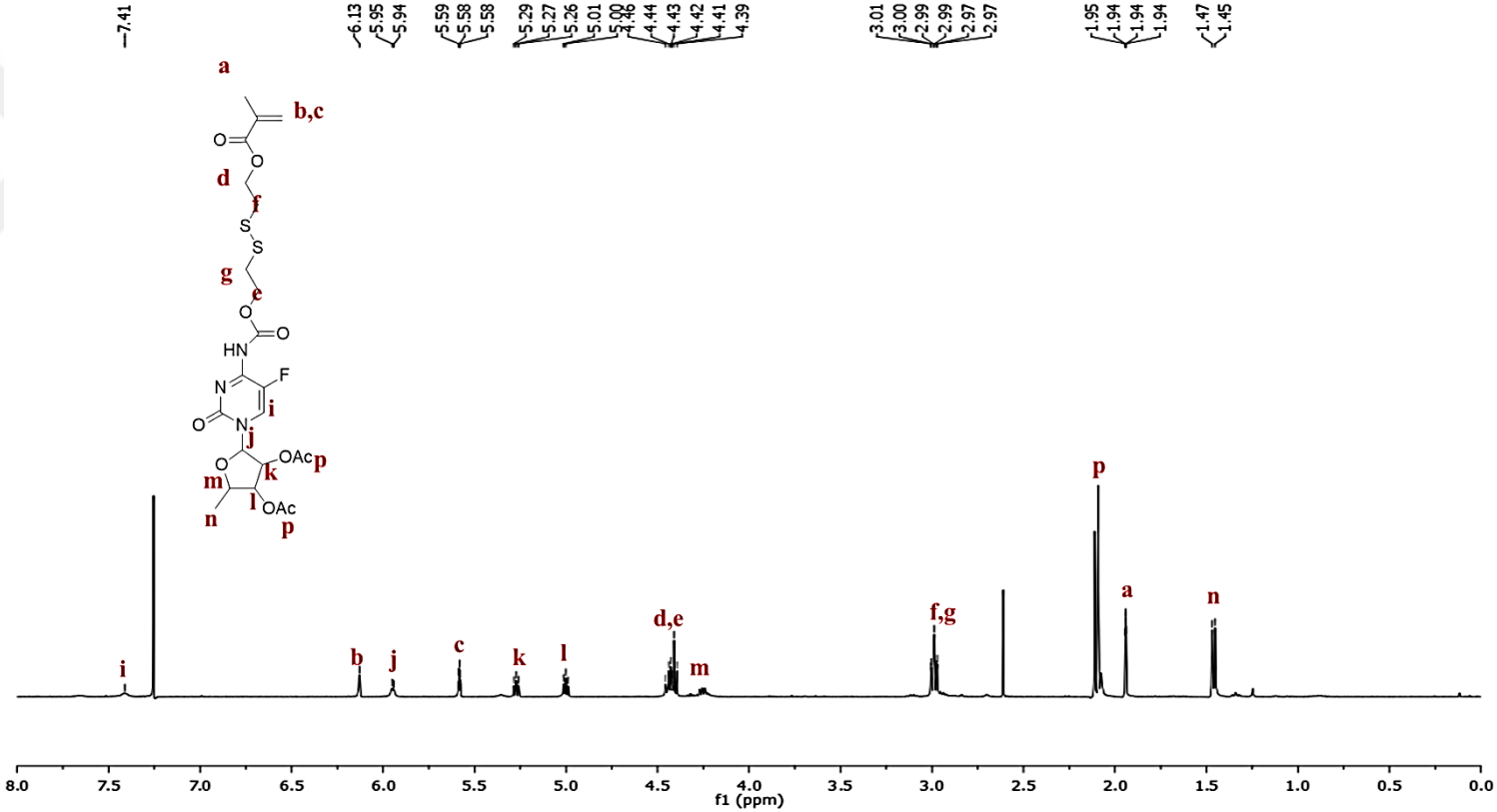

Figure A.28. ^{1}H-NMR Spectrum of MA-DO-5'DFCR monomer (32)

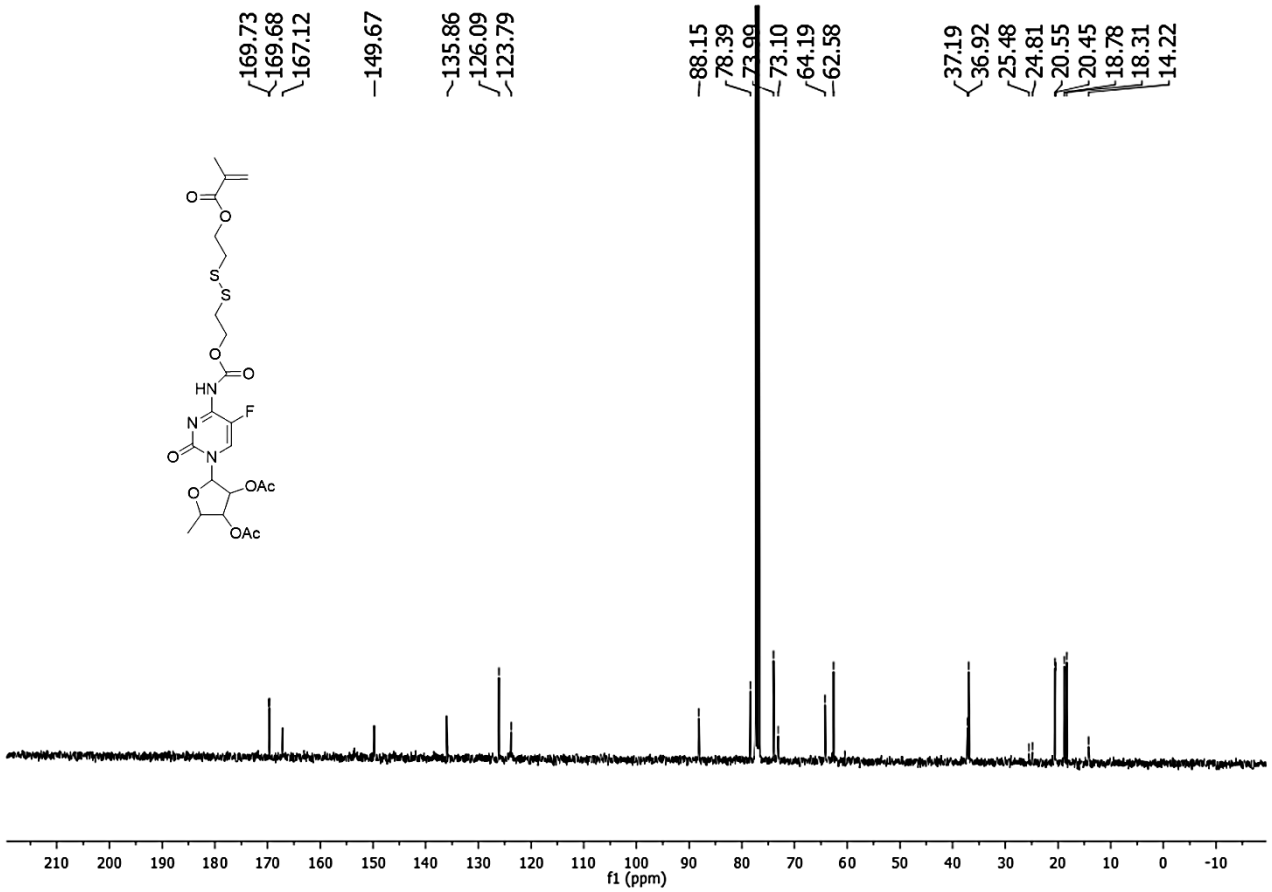

Figure A.29. ^{13}C-NMR Spectrum of MA-DO-5'DFCR monomer (32)

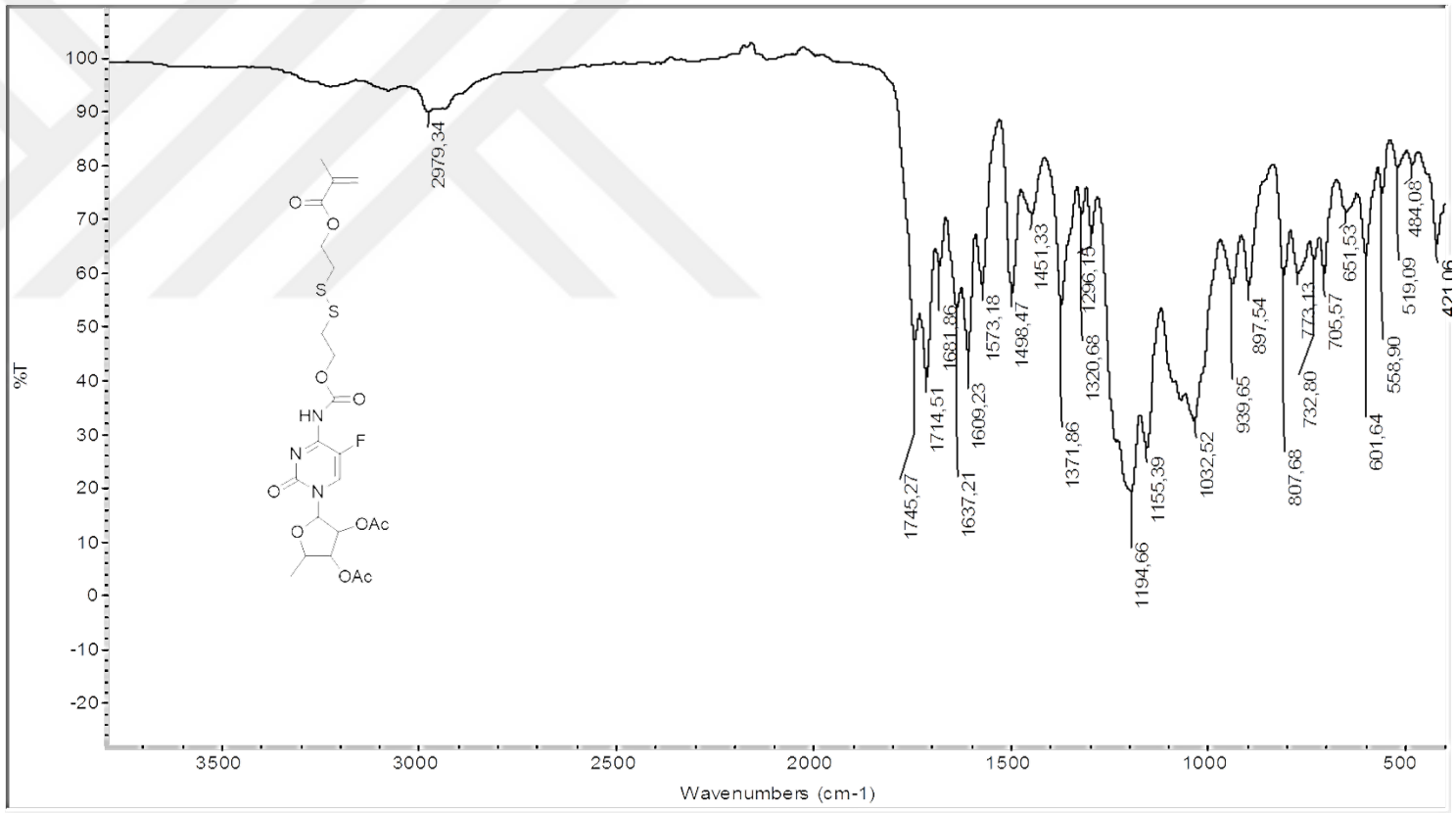

Figure A.30. FT-IR^{-1} Spectrum of MA-DO-5'DFCR monomer (32)

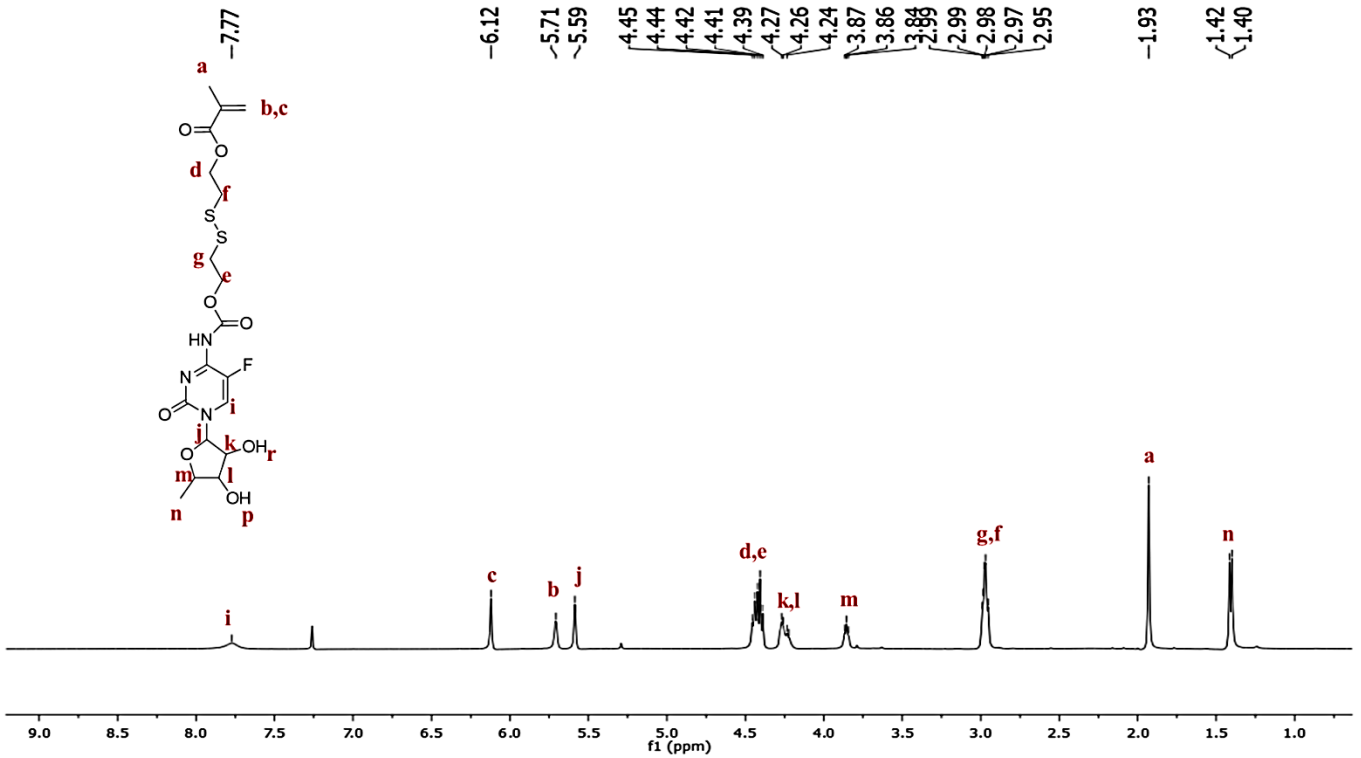

Figure A.31. ^{1}H-NMR Spectrum of MA-5'DFCR in $CDCl_3$ (33)

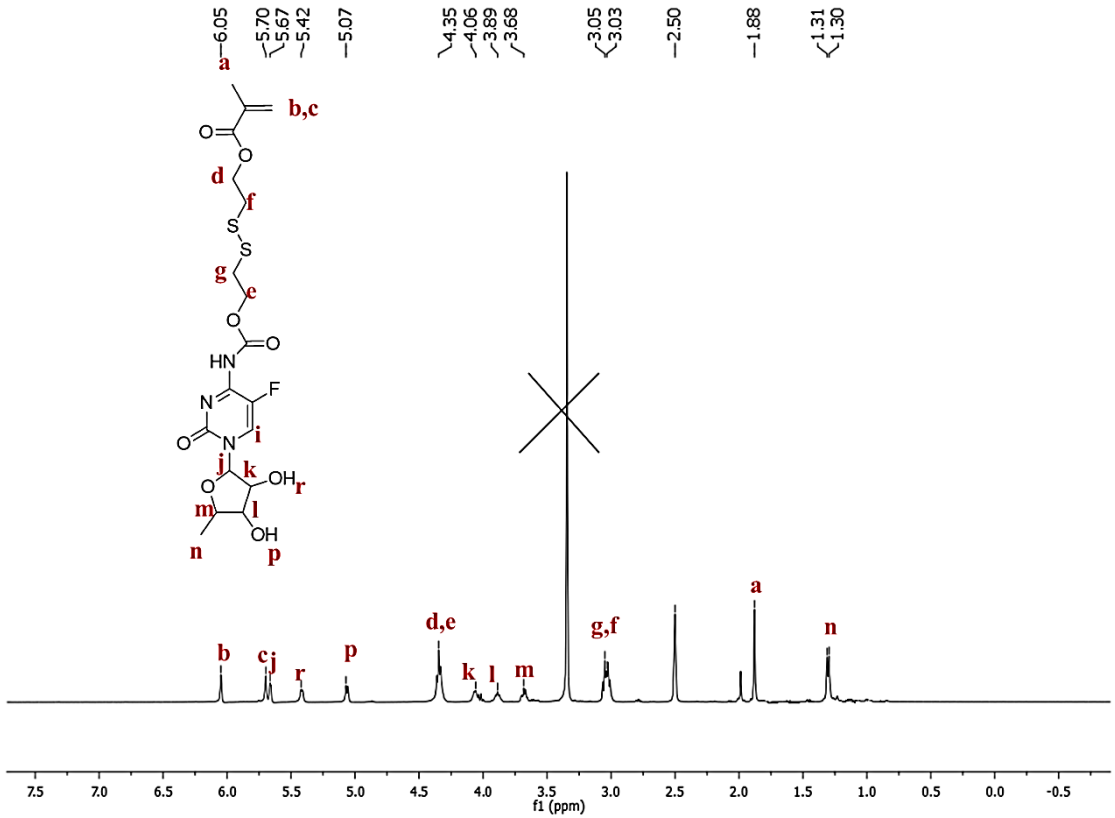

Figure A.32. ^{1}H-NMR Spectrum of MA-5'DFCR in DMSO-*d6* (33)

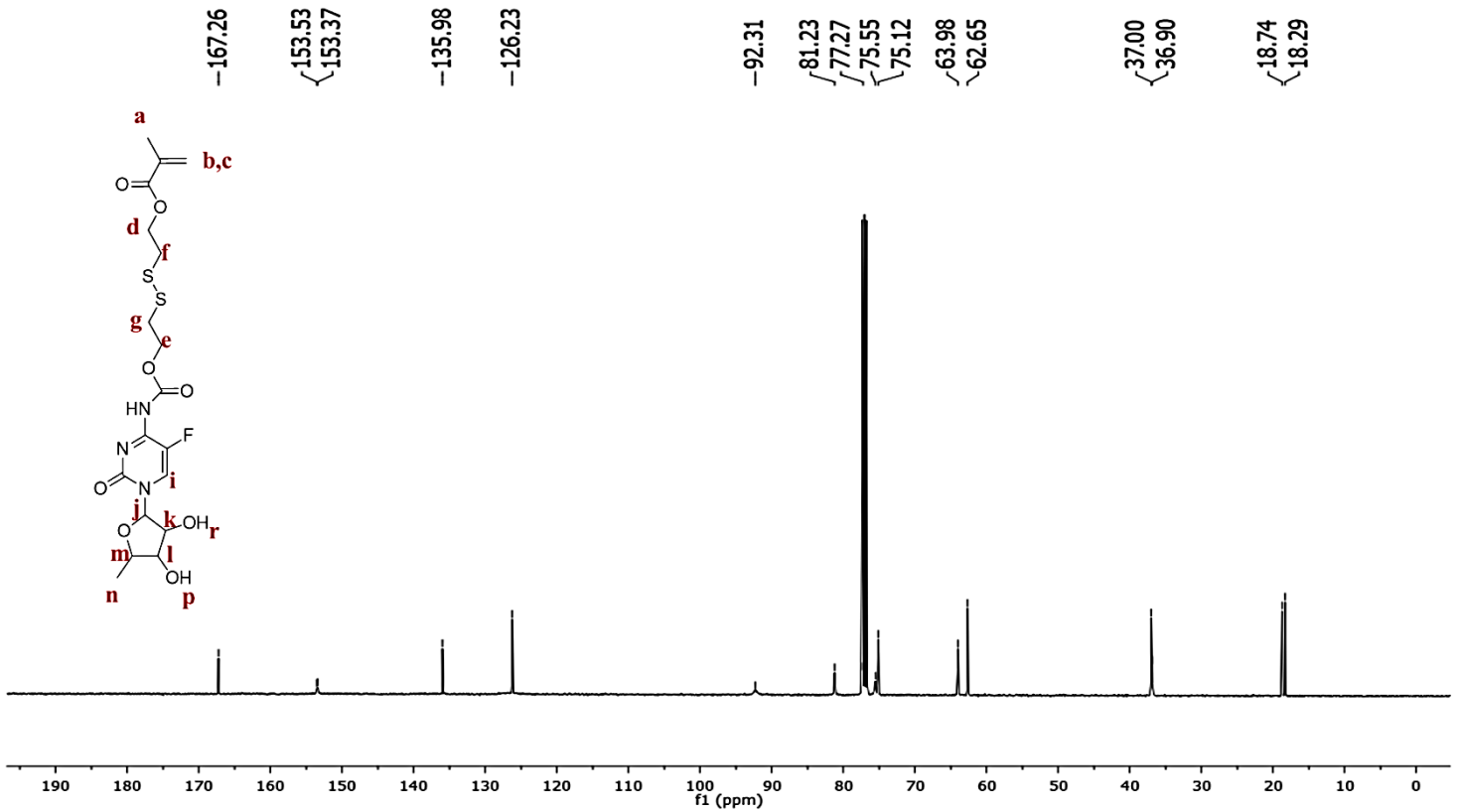

Figure A.33. ^{13}C-NMR Spectrum of MA-5'DFCR (33)

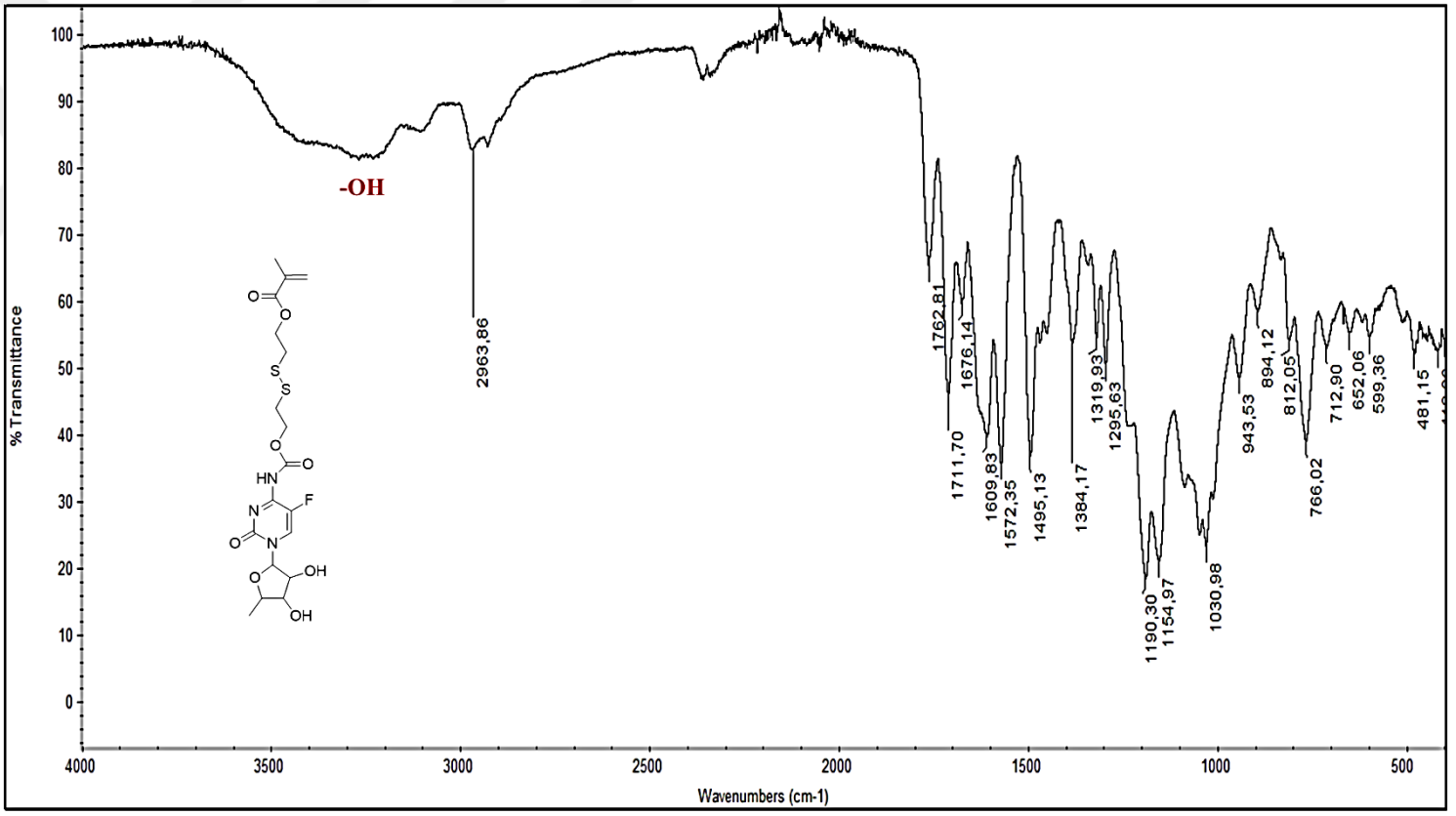

Figure A.34. FT-IR^{-1} Spectrum of MA-5'DFCR (33)

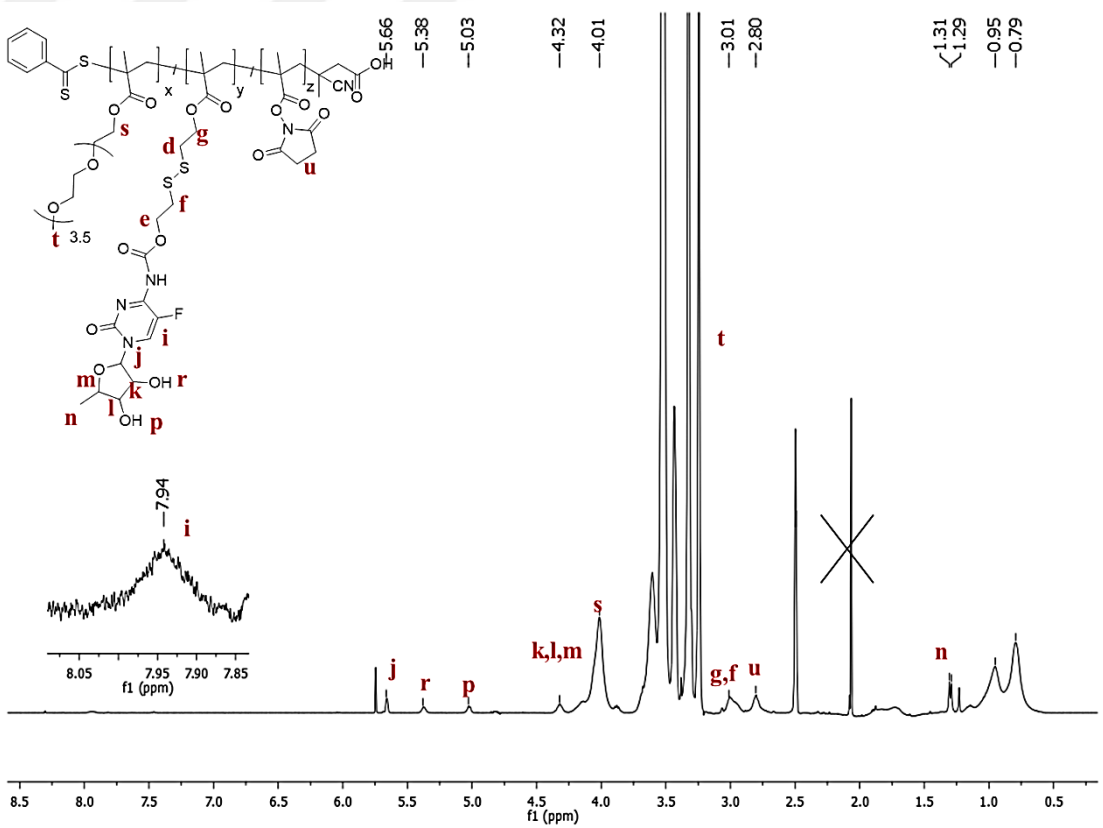

Figure A.35. ^{1}H-NMR Spectrum of P(OEGMA-NHS-5'DFCR) (35)

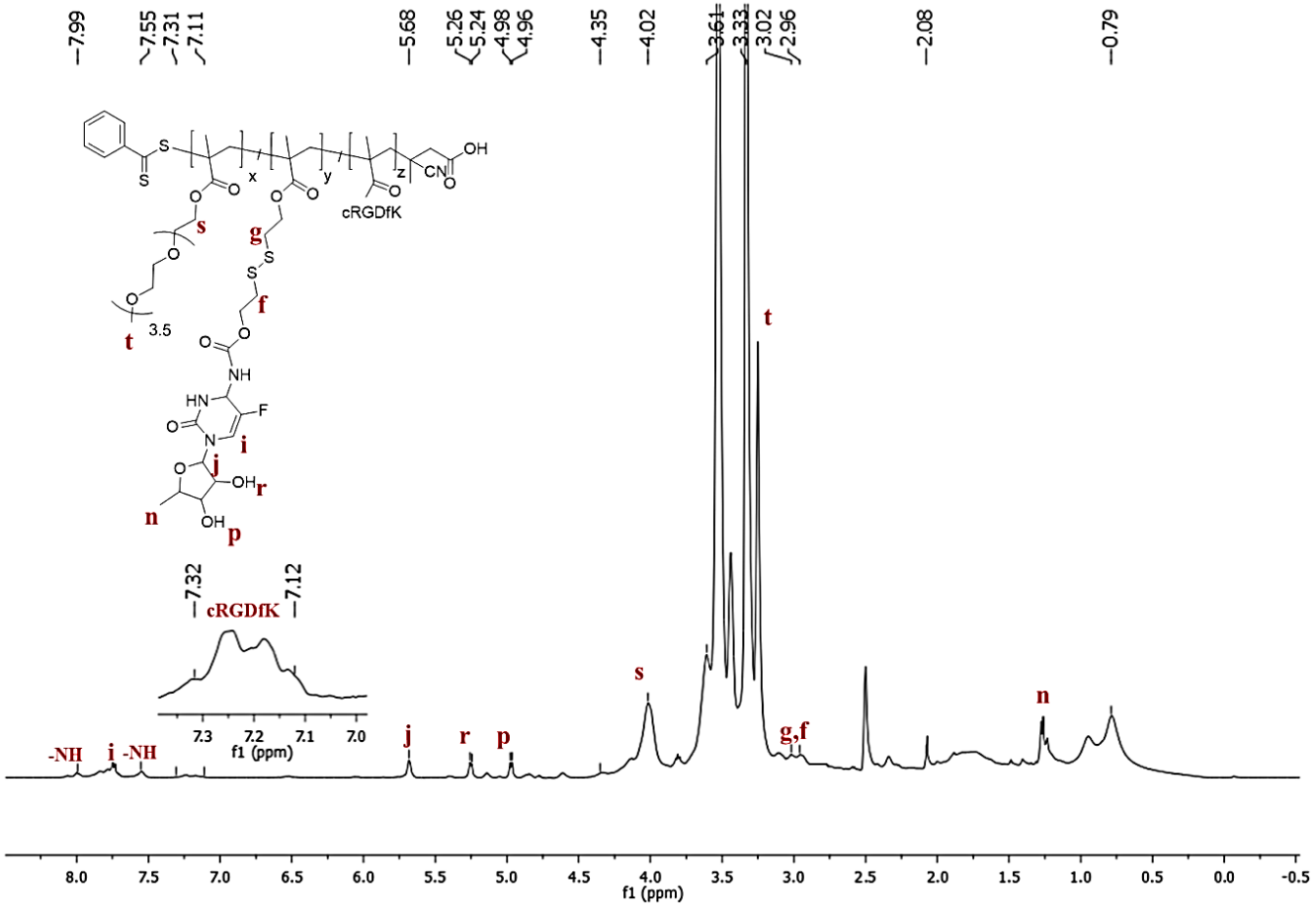

Figure A.36. ^{1}H-NMR Spectrum of P(OEGMA-RGD-5'DFCR) (36)

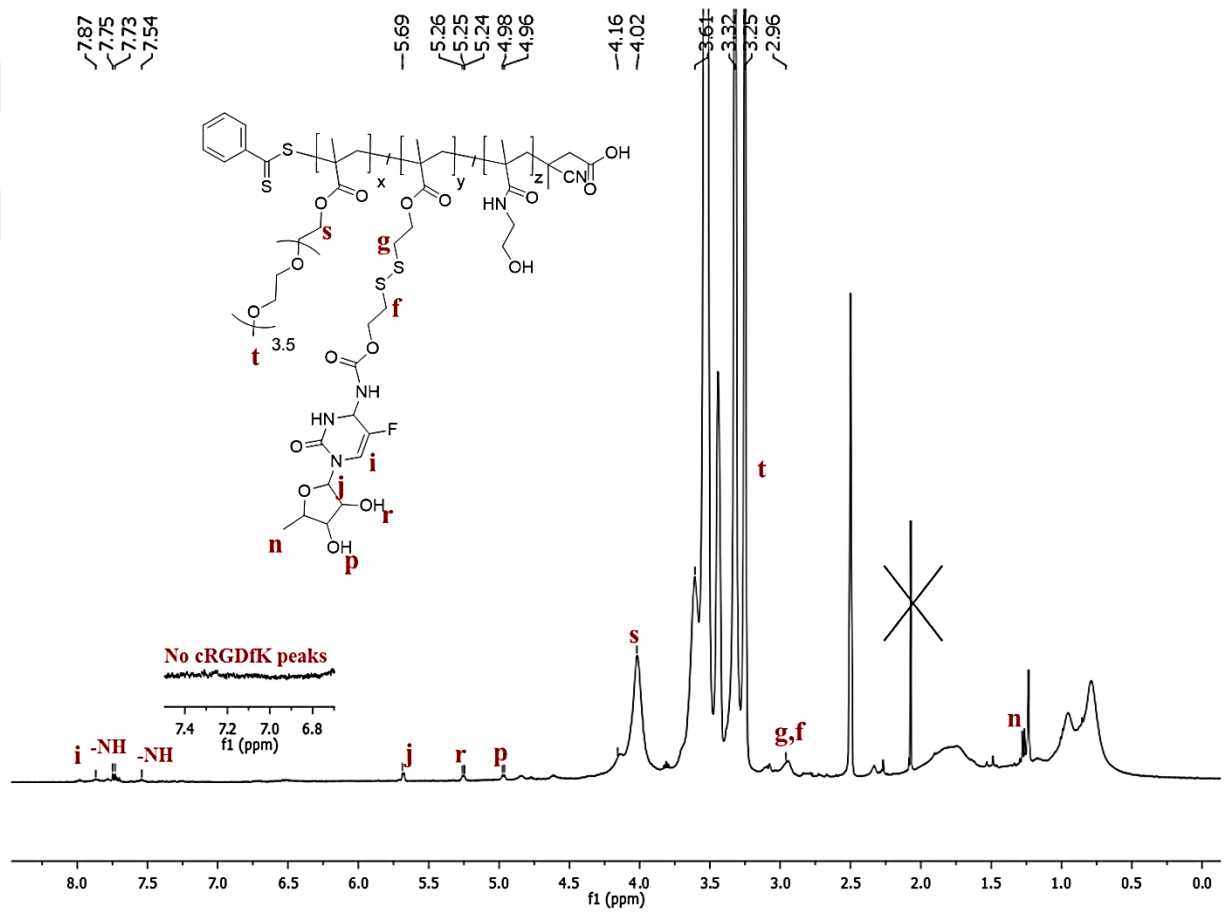

Figure A.37. ^{1}H-NMR Spectrum of P(OEGMA-5'DFCR) (37)

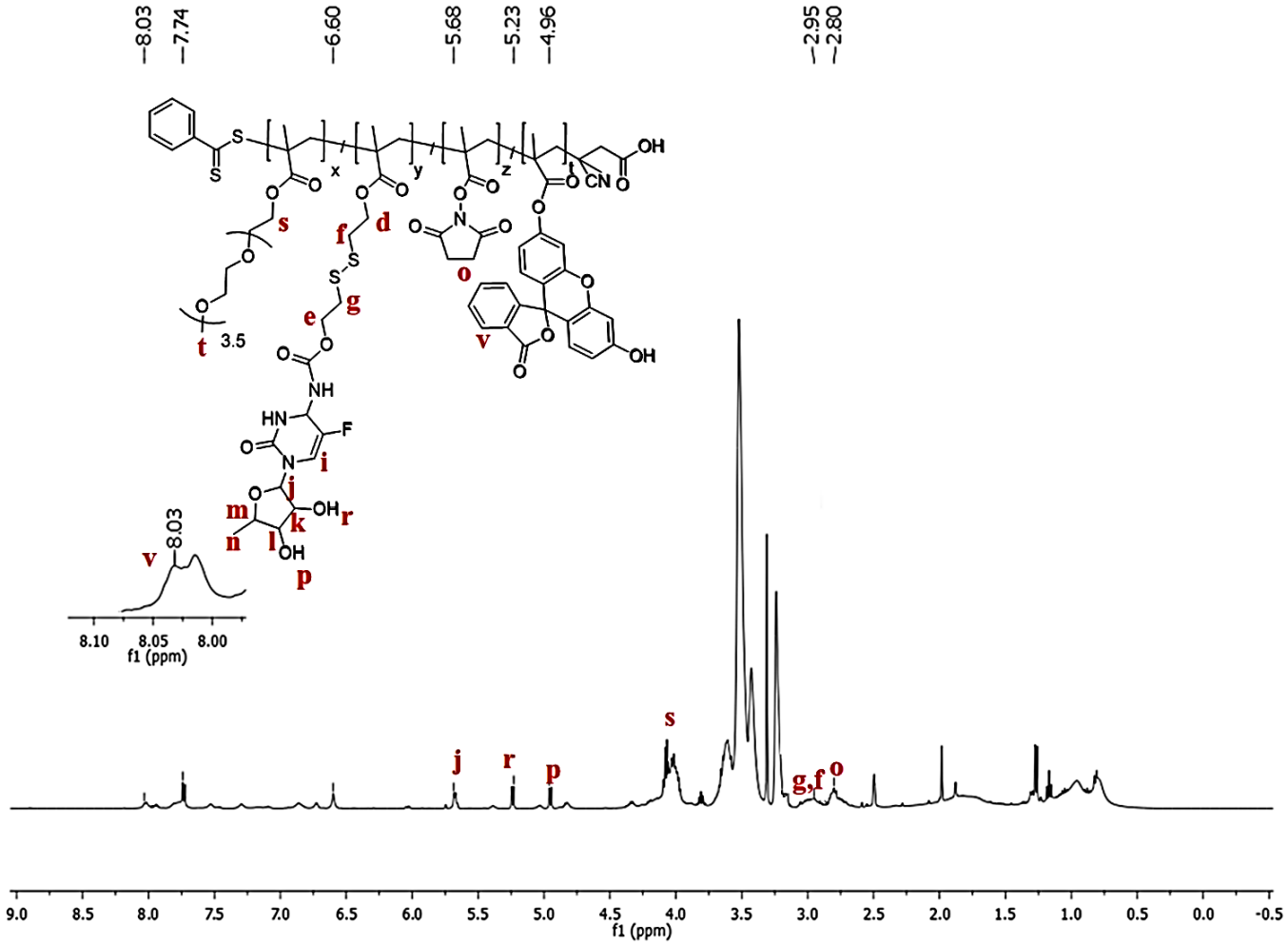

Figure A.38. ^{1}H-NMR Spectrum of P(OEGMA-NHS-5'DFCR-FMA) (38)

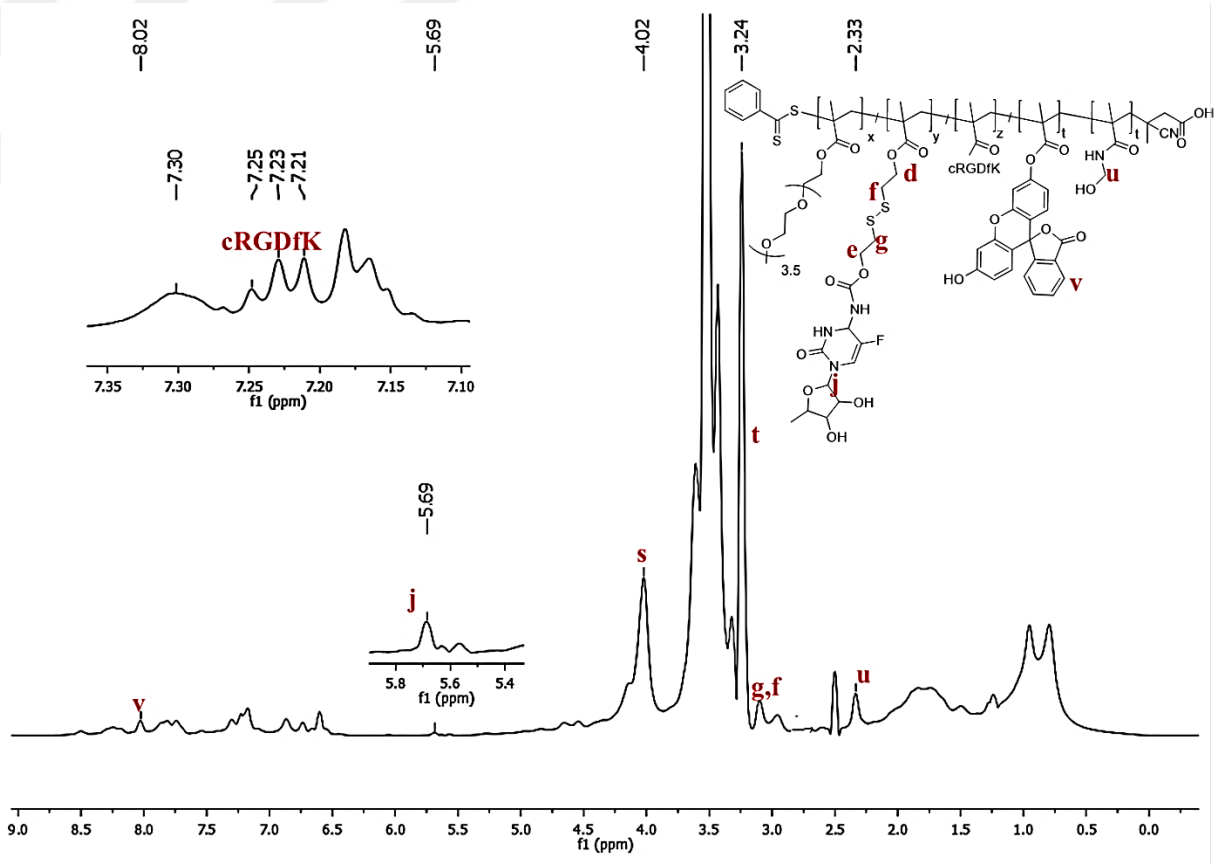

Figure A.39. ^{1}H-NMR Spectrum of P(OEGMA-RGD-5'DFCR-FMA) (39)

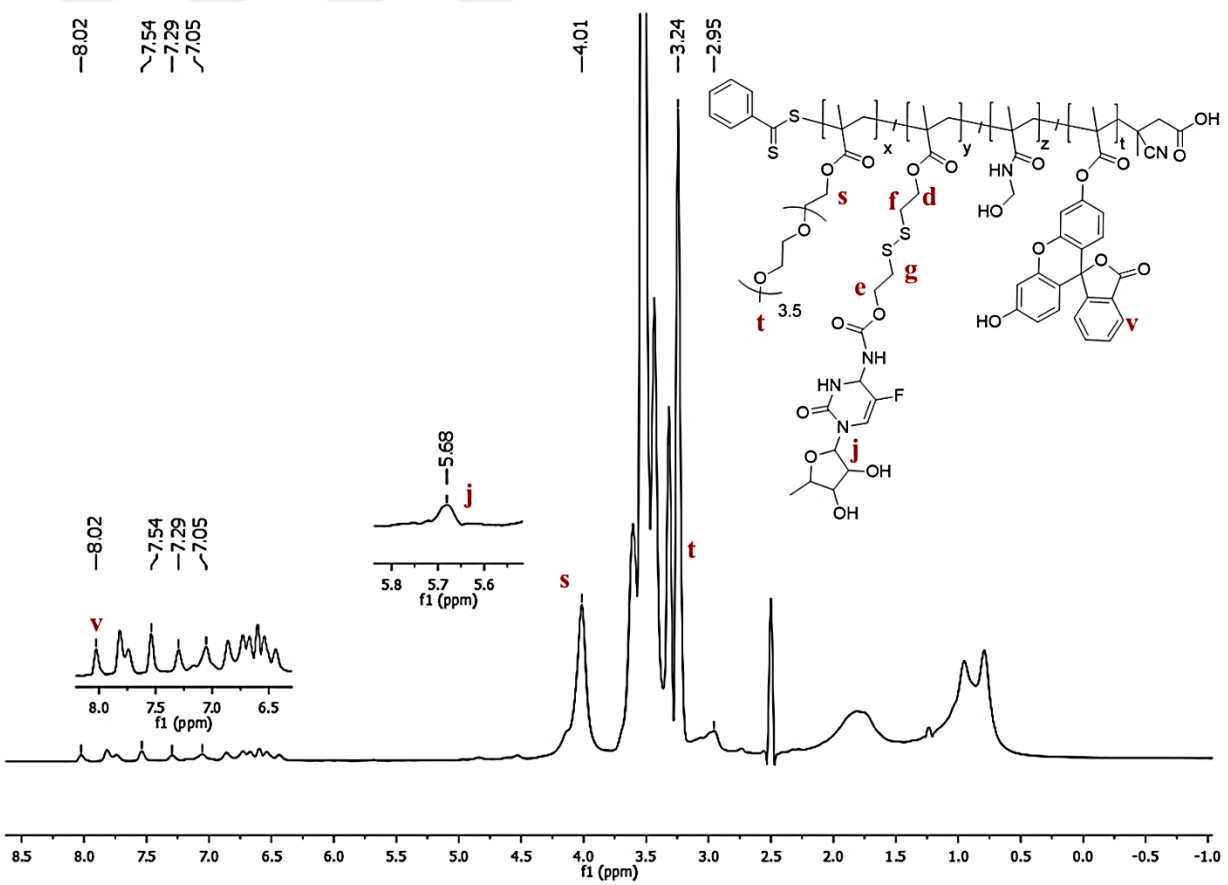

Figure A.40. ^{1}H-NMR Spectrum of P(OEGMA-5'DFCR-FMA) (40)

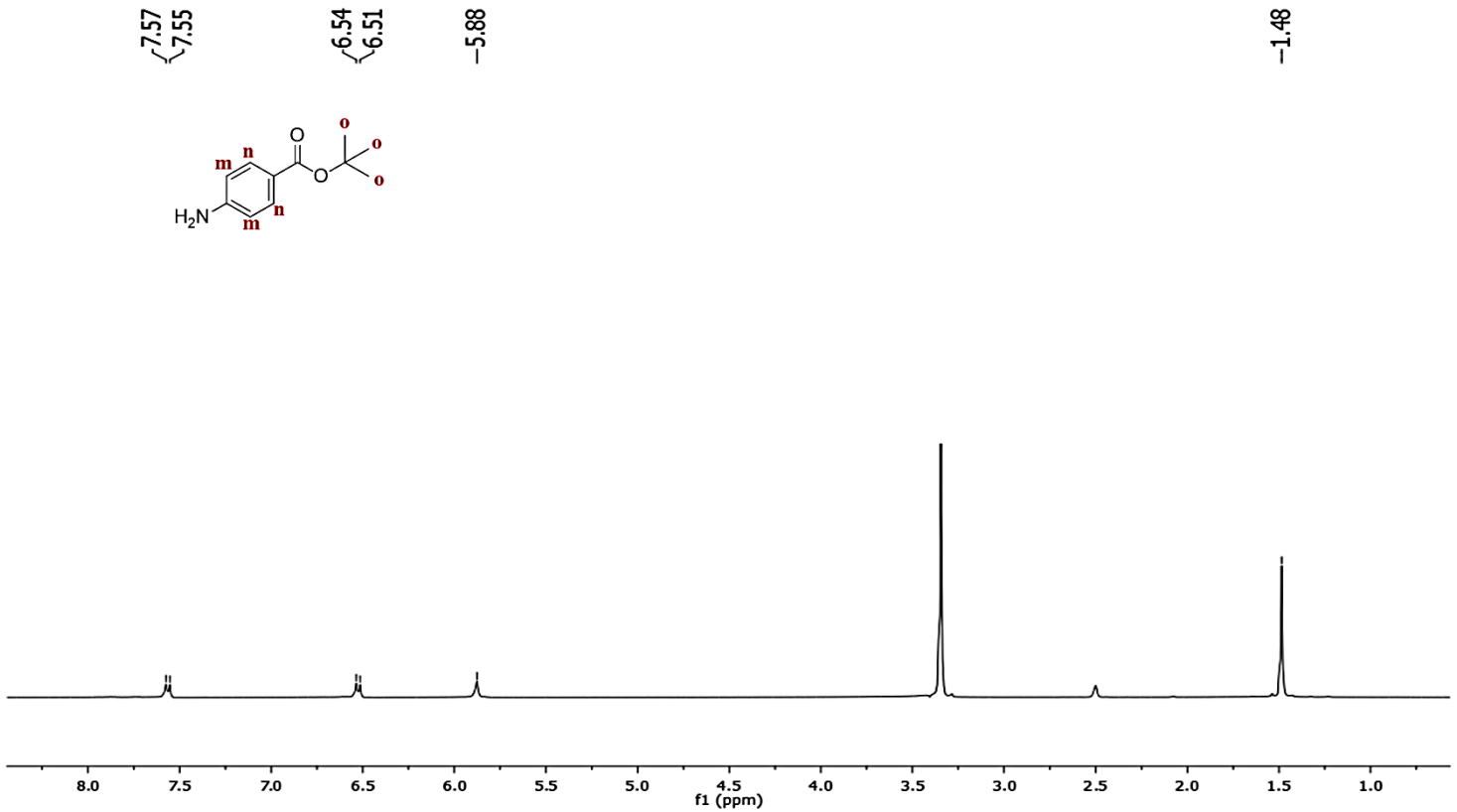

Figure A.41. ^{1}H-NMR Spectrum of tert-butyl 4-aminobenzoate (41)

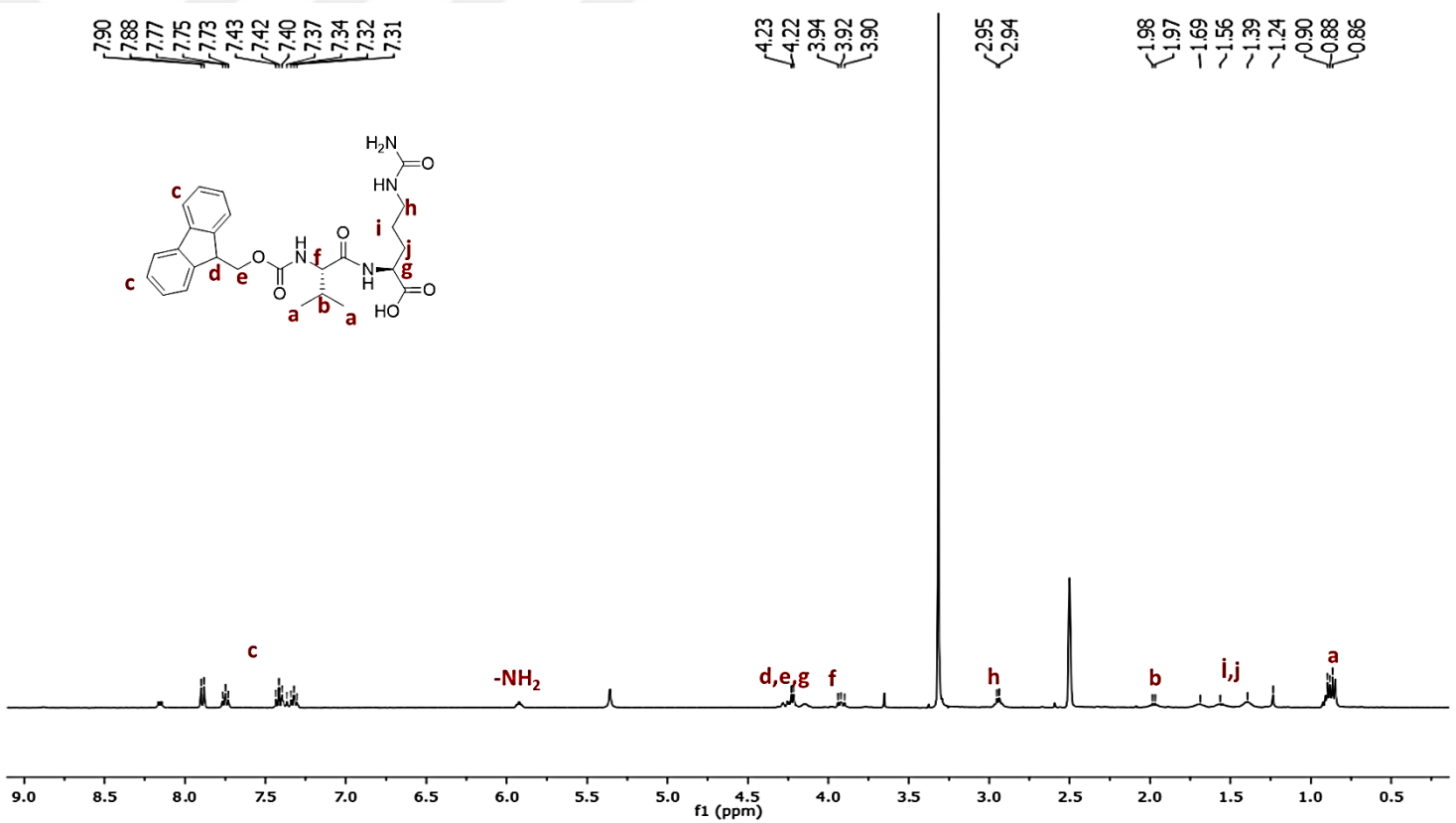

Figure A.42. ^{1}H-NMR Spectrum of Fmoc-Val-Cit (42)

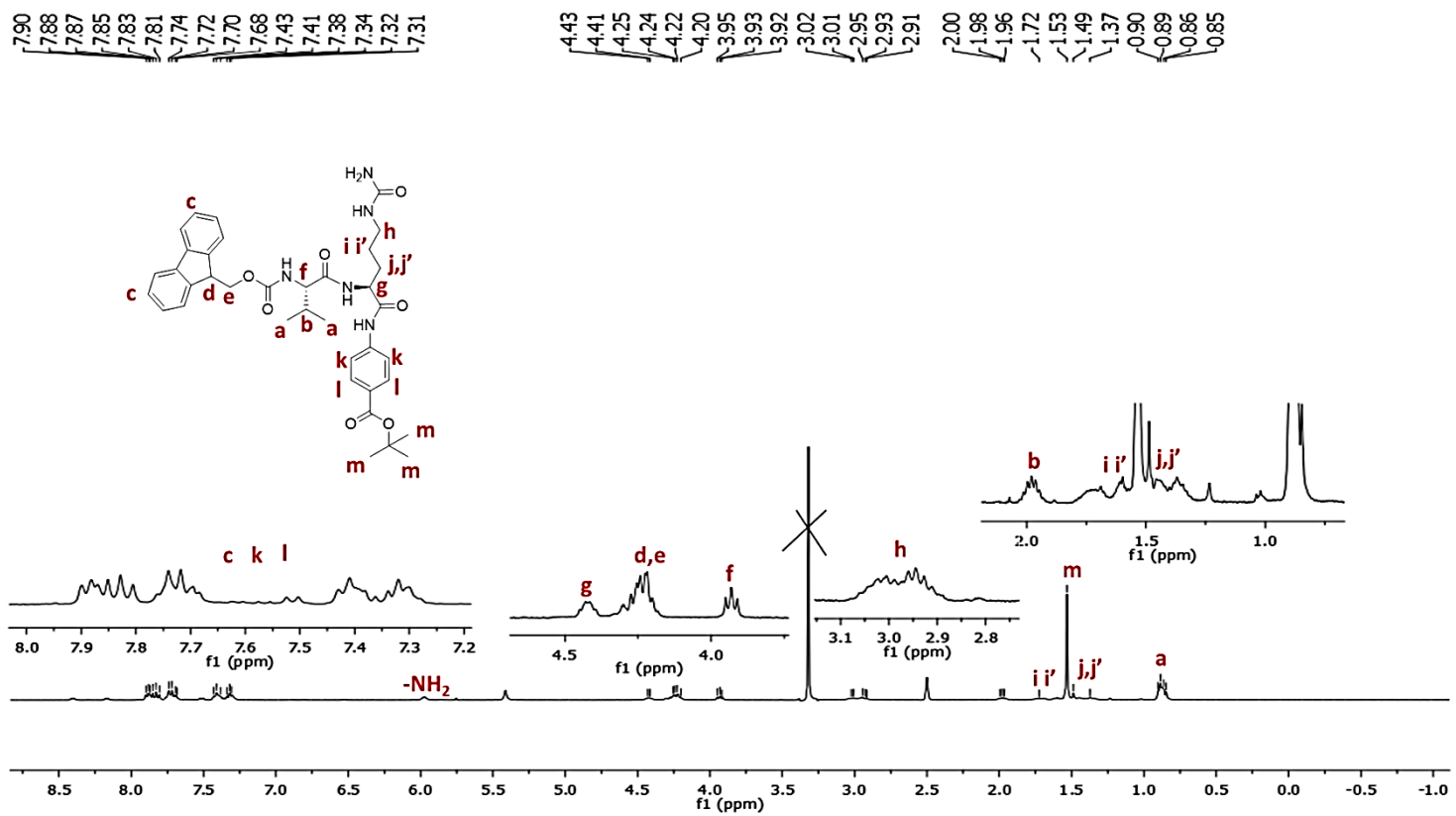

Figure A.43. ^{1}H-NMR Spectrum of Fmoc-Val-Cit-tert-butyl 4-aminobenzoate (43)

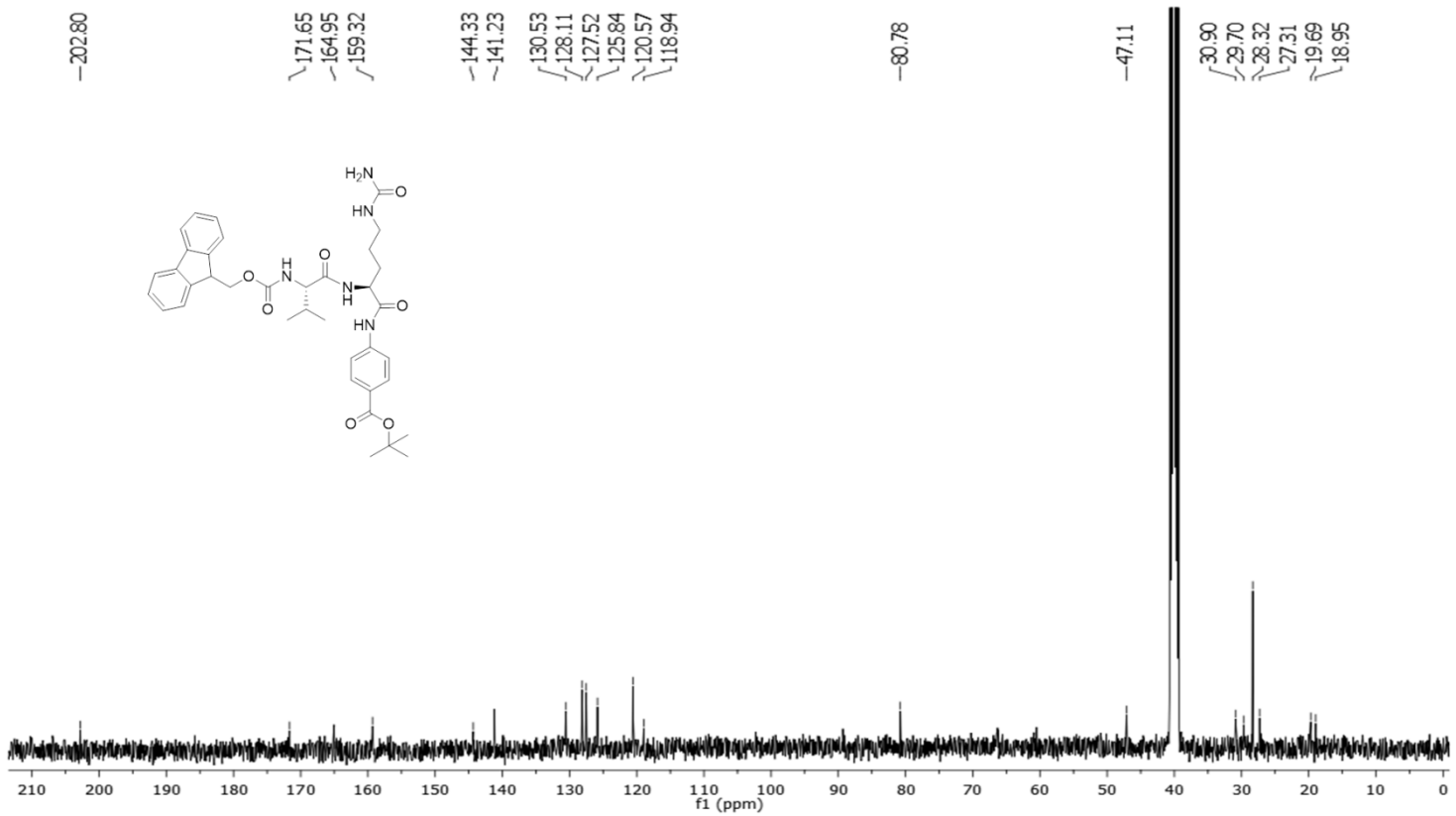

Figure A.44. ^{13}C-NMR Spectrum of Fmoc-Val-Cit-tert-butyl 4-aminobenzoate (43)

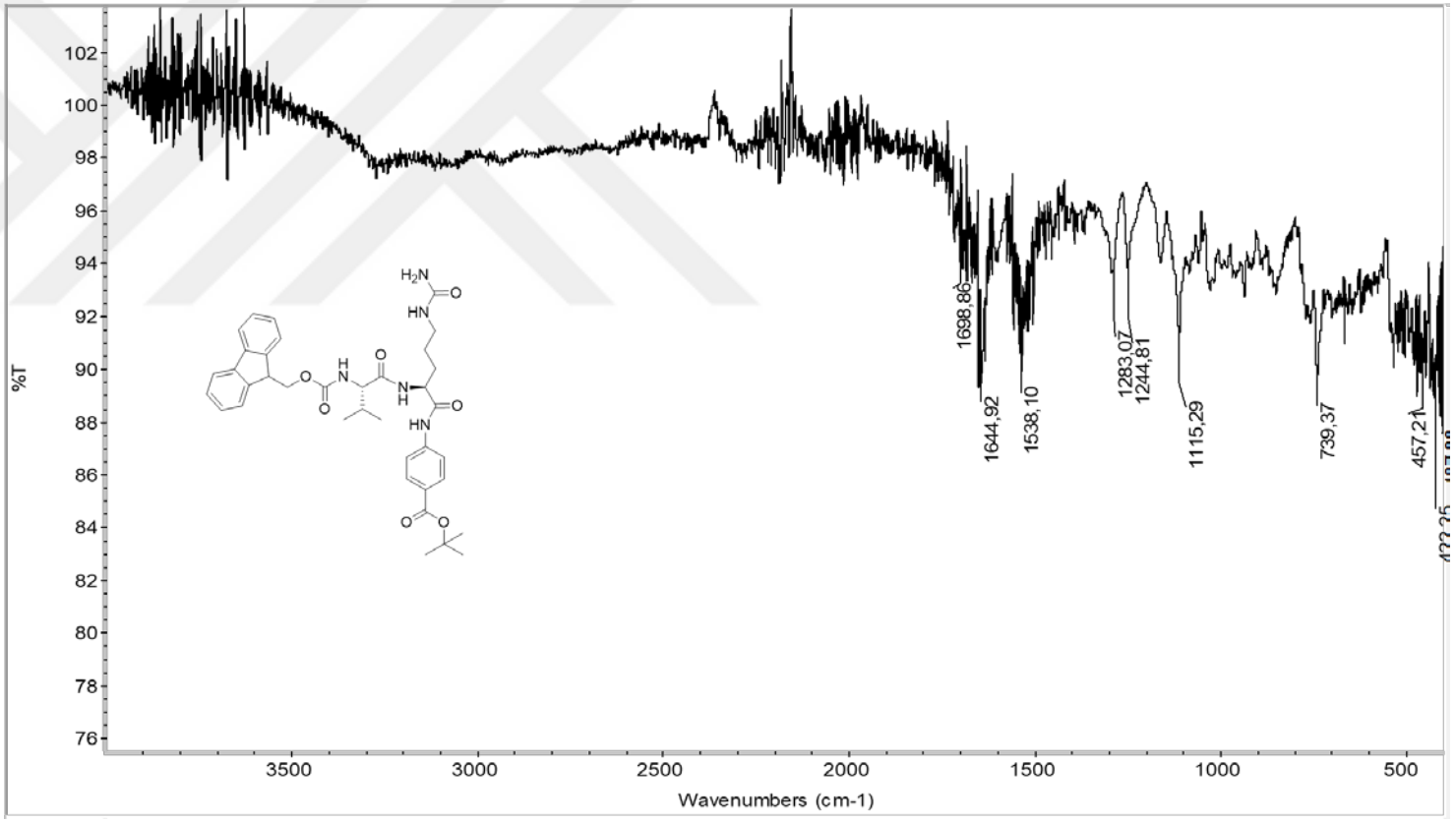

Figure A.45. FT-IR^{-1} Spectrum of Fmoc-Val-Cit-tert-butyl 4-aminobenzoate (43)

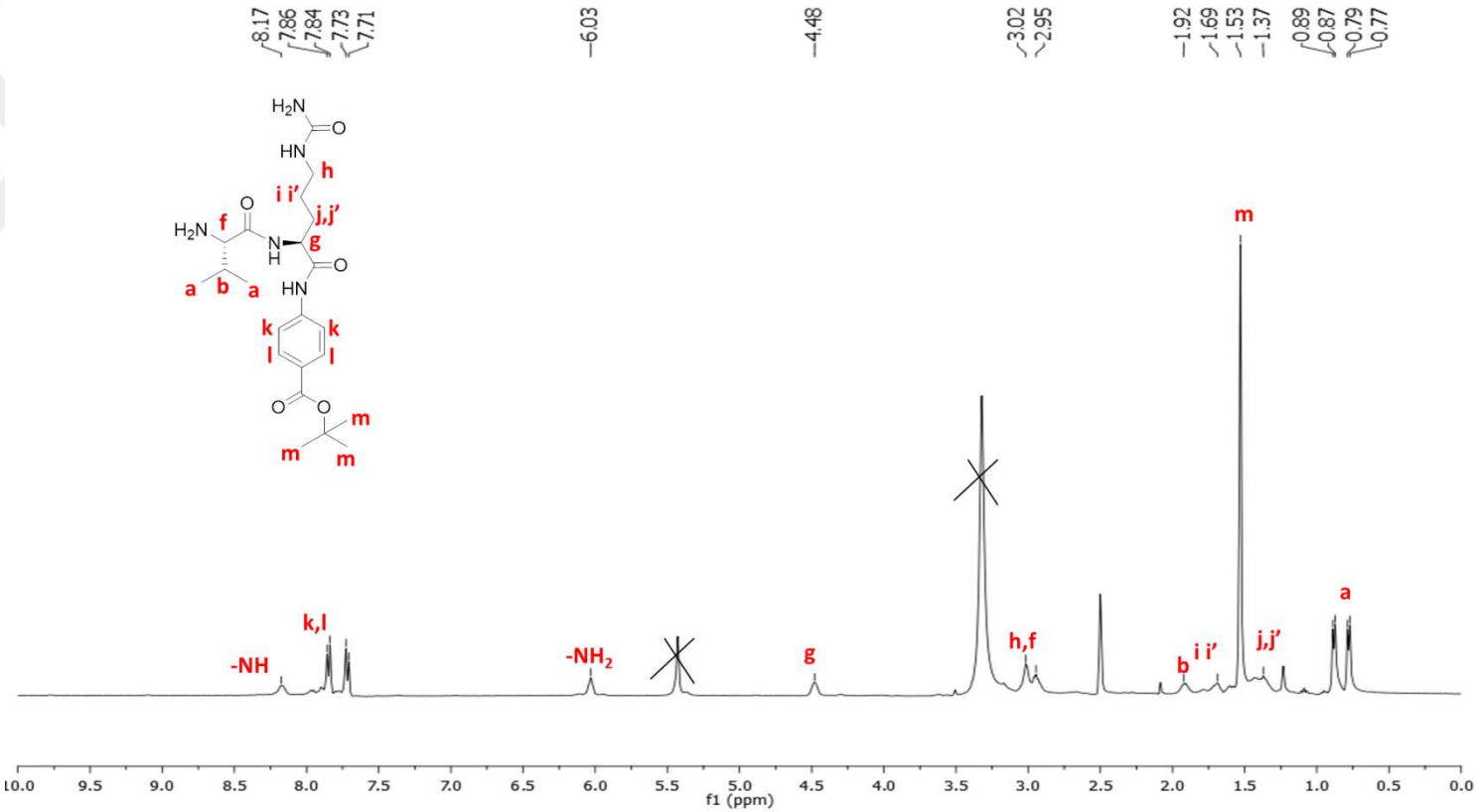

Figure A.46. ^{1}H-NMR Spectrum of Val-Cit-tert-butyl 4-aminobenzoate (44)

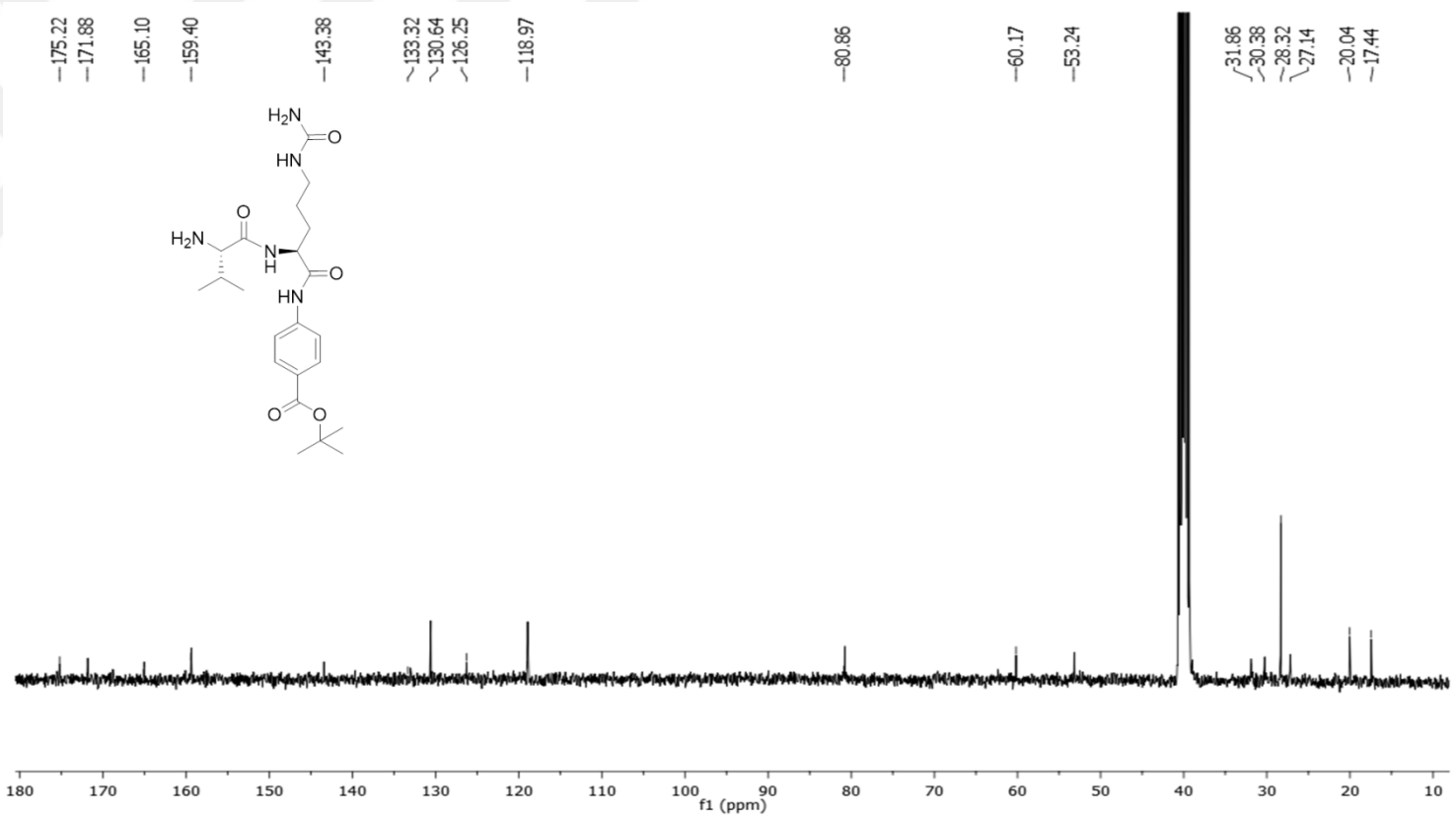

Figure A.47. ^{13}C-NMR Spectrum of Val-Cit-tert-butyl 4-aminobenzoate (44)

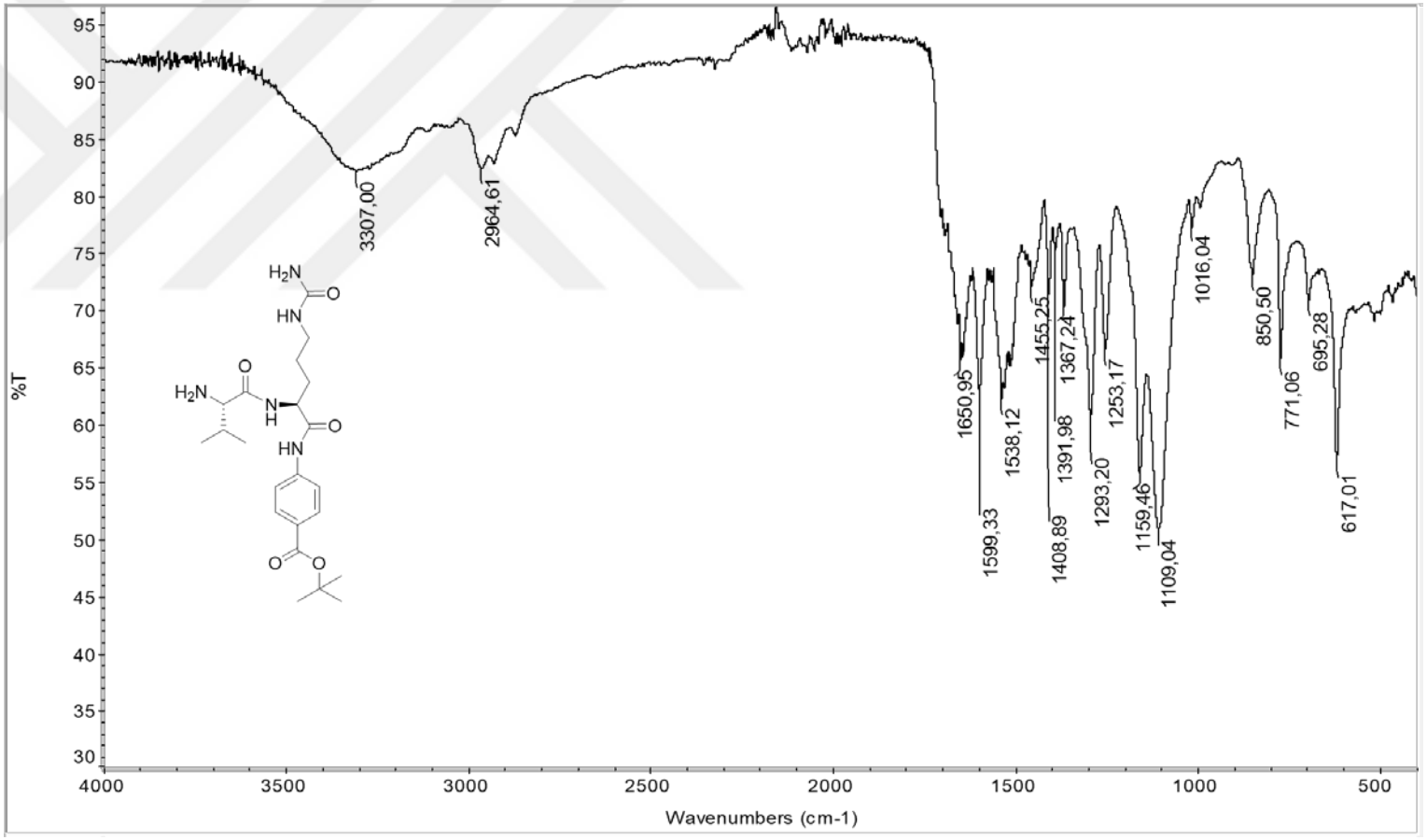

Figure A.48. FT-IR^{-1} Spectrum of Val-Cit-tert-butyl 4-aminobenzoate (44)

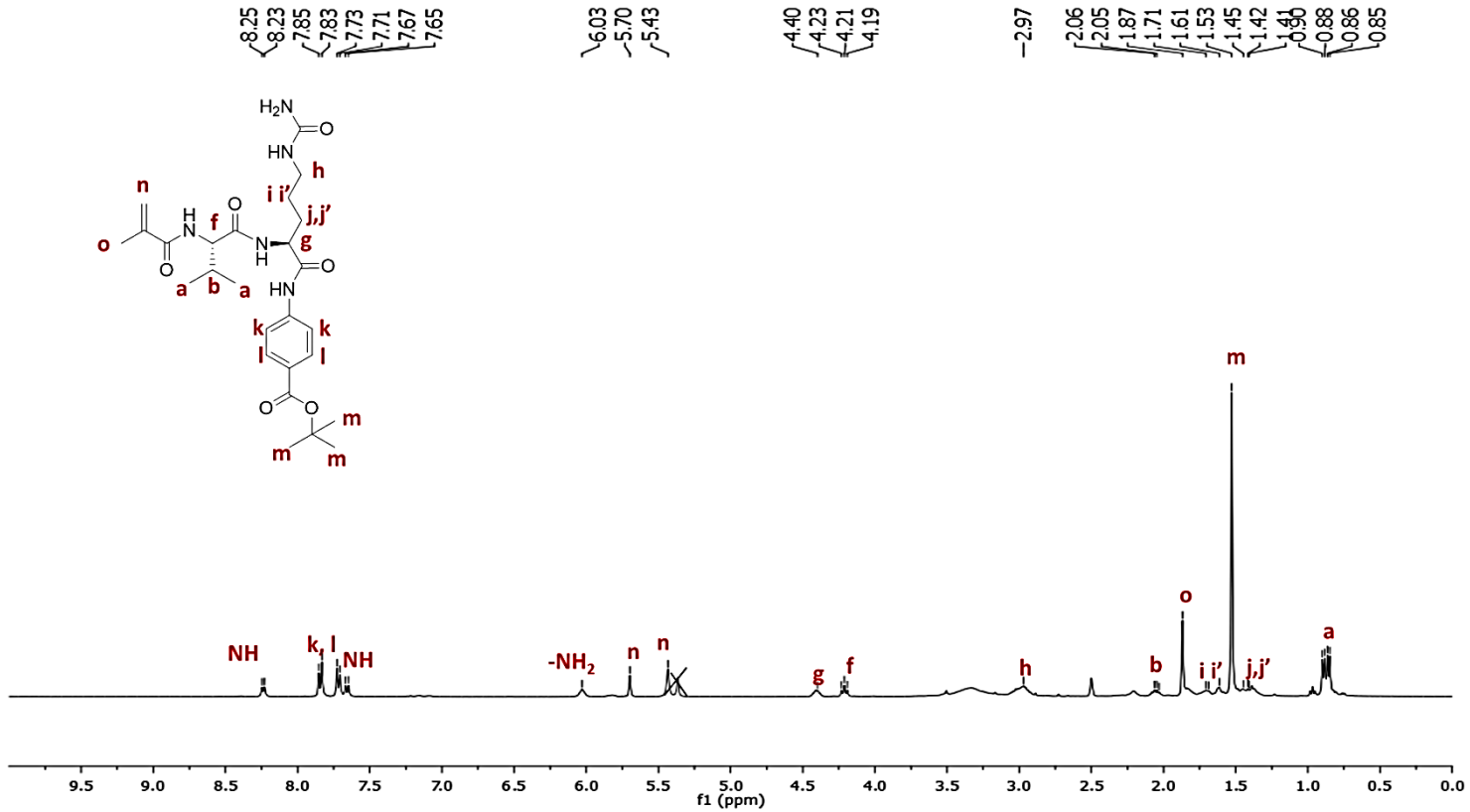

Figure A.49. ^{1}H-NMR Spectrum of MA-Val-Cit-tert-butyl 4-aminobenzoate (45)

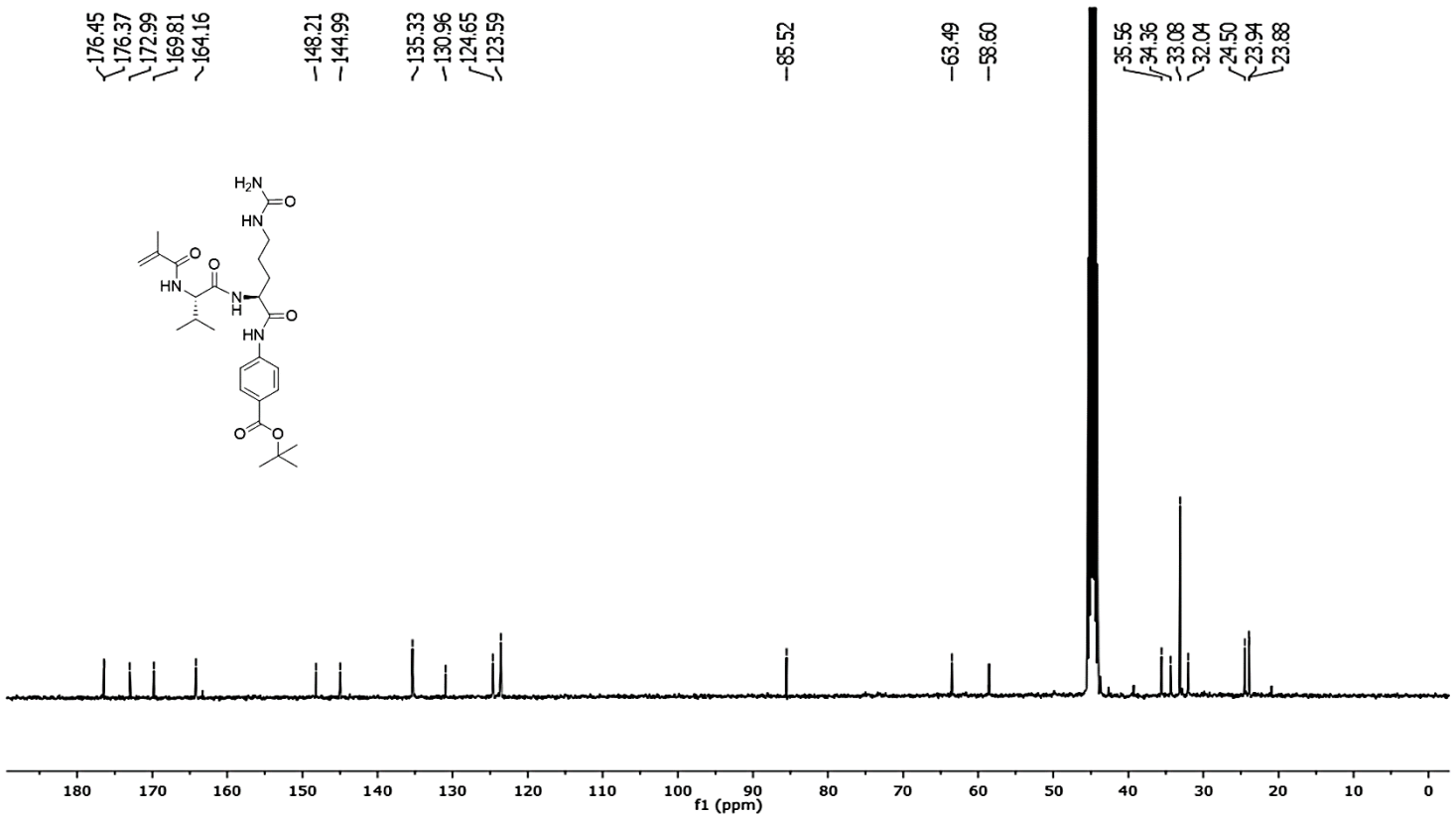

Figure A.50. ^{13}C-NMR Spectrum of MA-Val-Cit-tert-butyl 4-aminobenzoate (45)

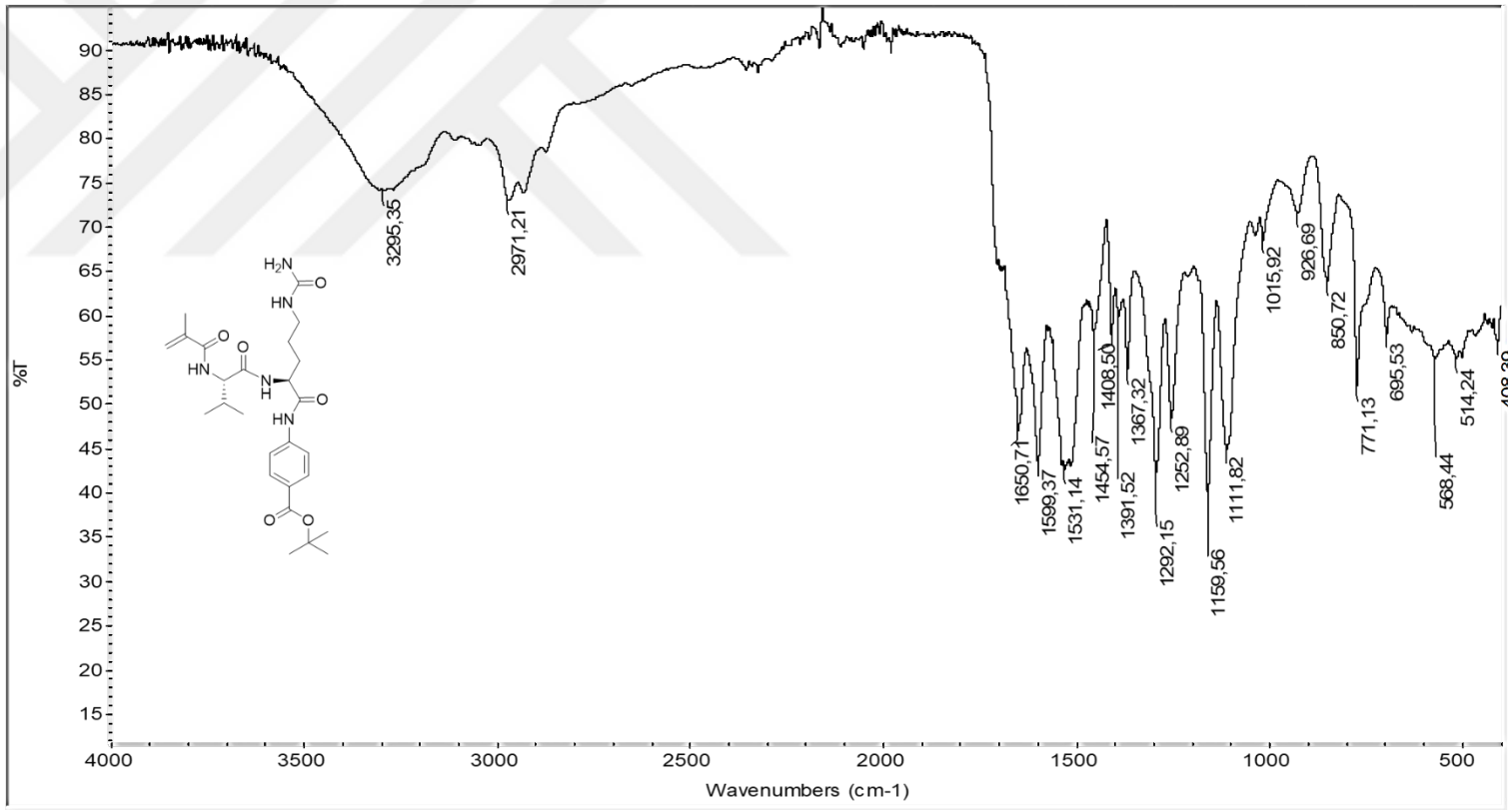

Figure A.51. FT-IR^{-1} spectrum of MA-Val-Cit-tert-butyl 4-aminobenzoate (45)

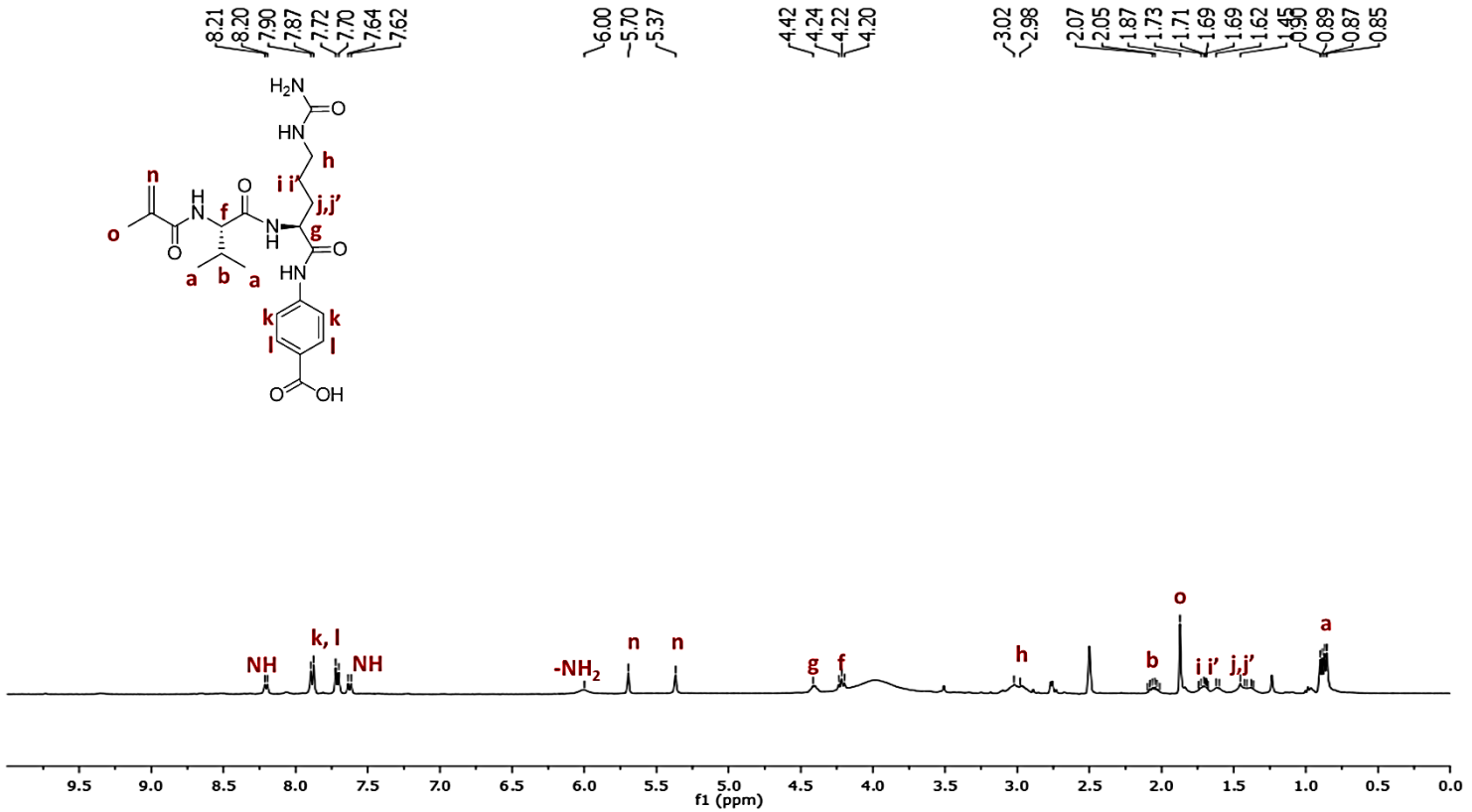

Figure A.52. ^{1}H-NMR Spectrum of MA-Val-Cit-4-aminobenzoic acid (46)

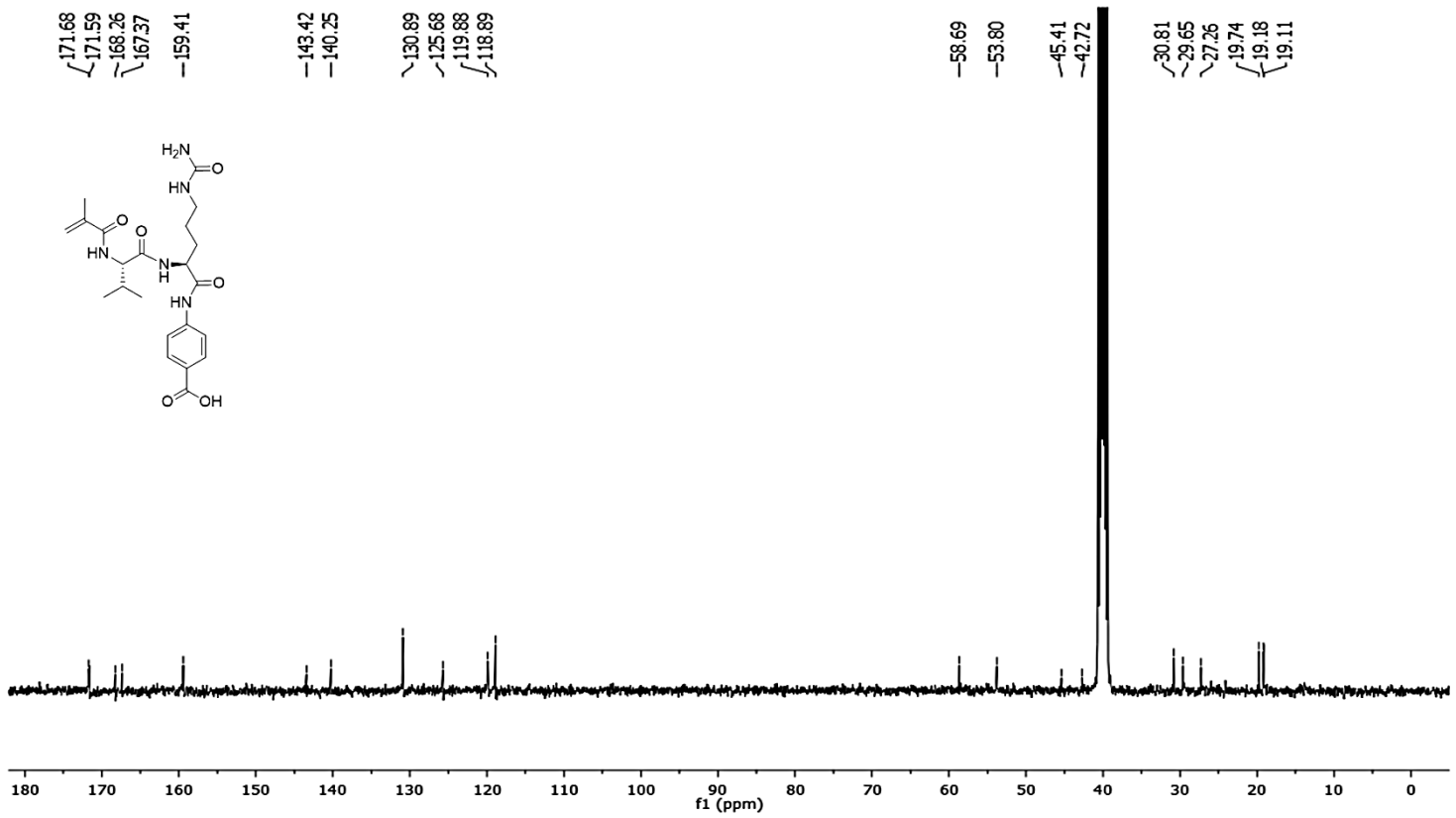

Figure A.53. ^{13}C-NMR Spectrum of MA-Val-Cit-4-aminobenzoic acid (46)

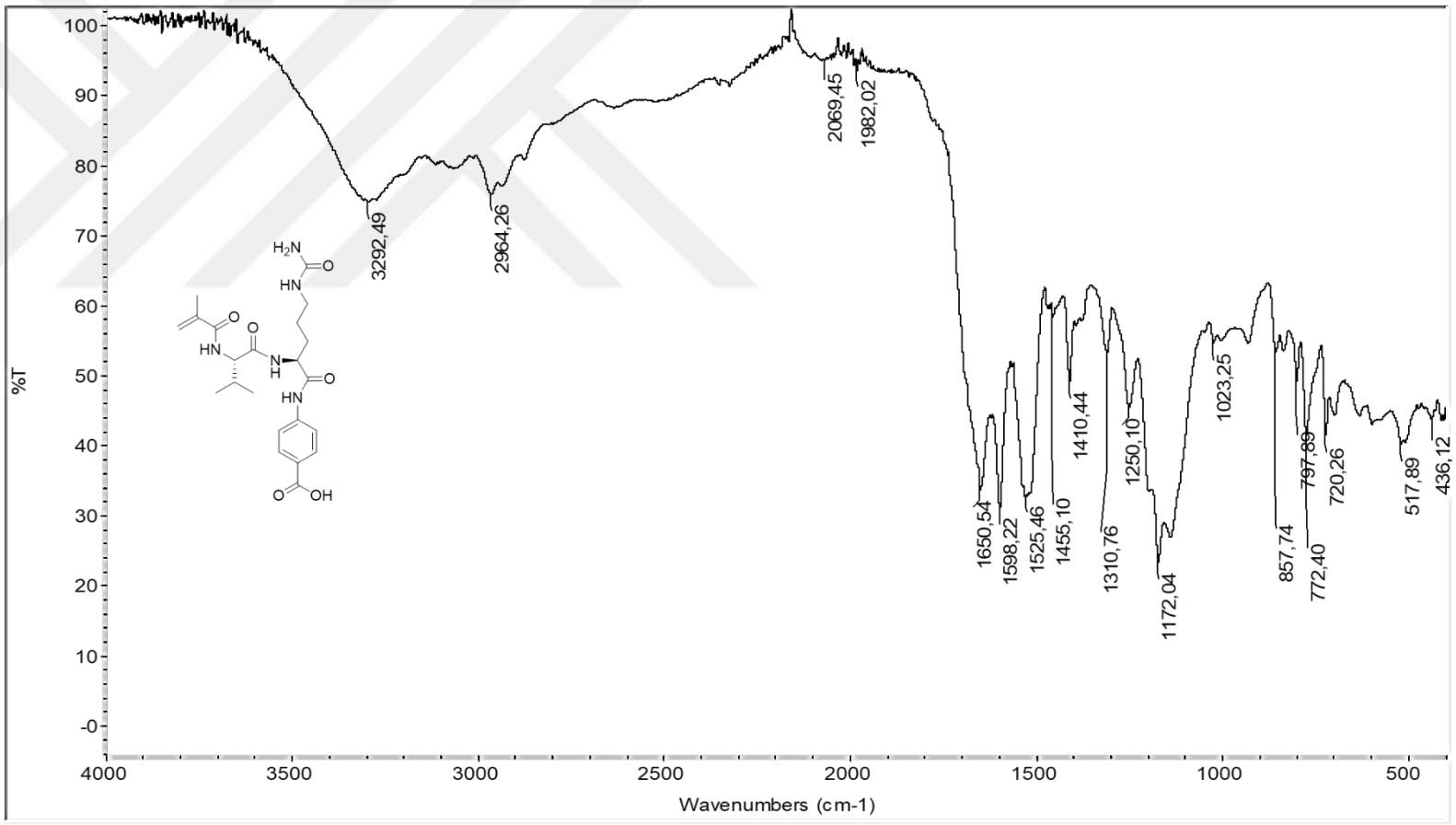

Figure A.54. FT-IR^{-1} Spectrum of MA-Val-Cit-4-aminobenzoic acid (46)

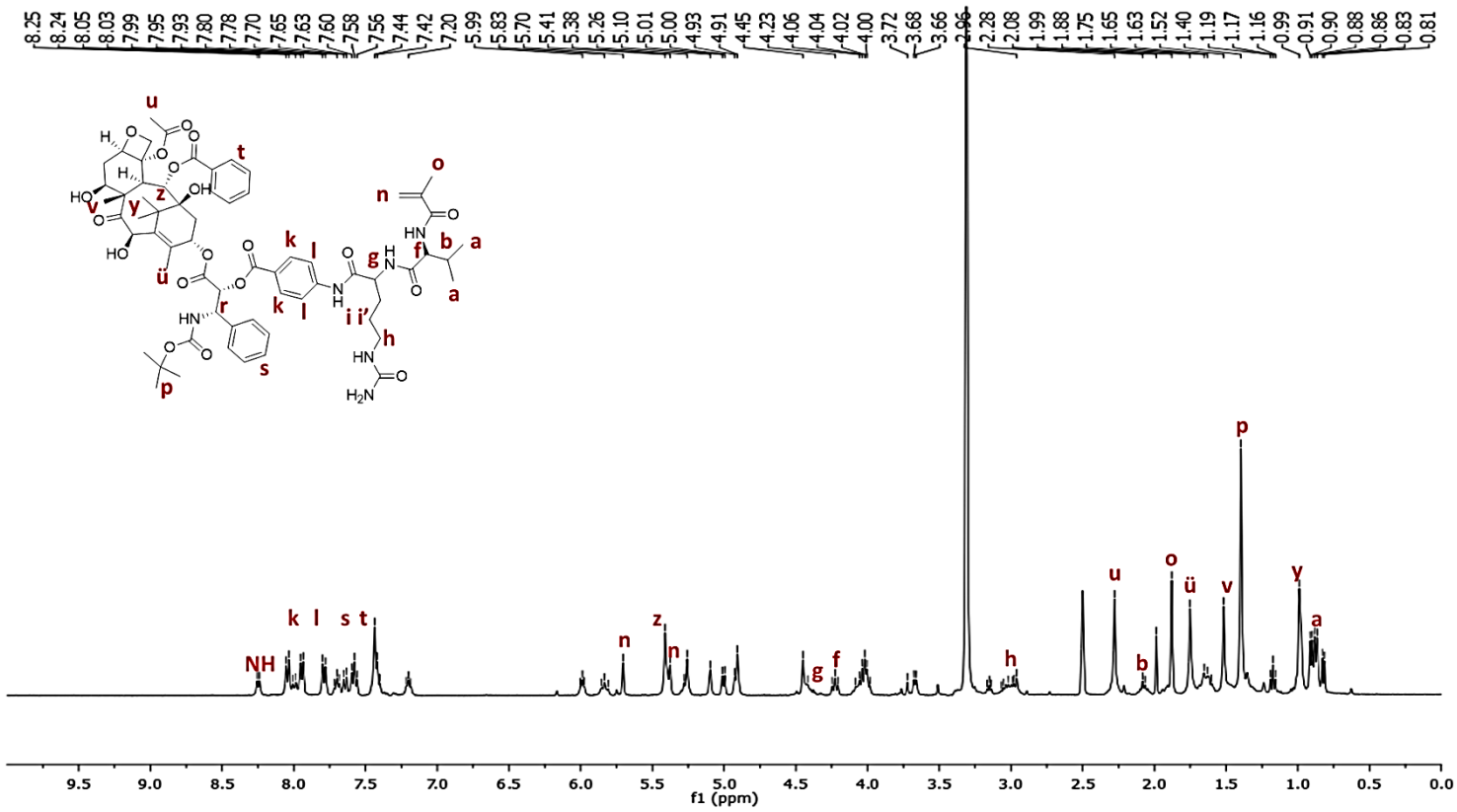

Figure A.55. ^{1}H-NMR Spectrum of MA-Val-Cit-4-aminobenzoyl-DTX (47)

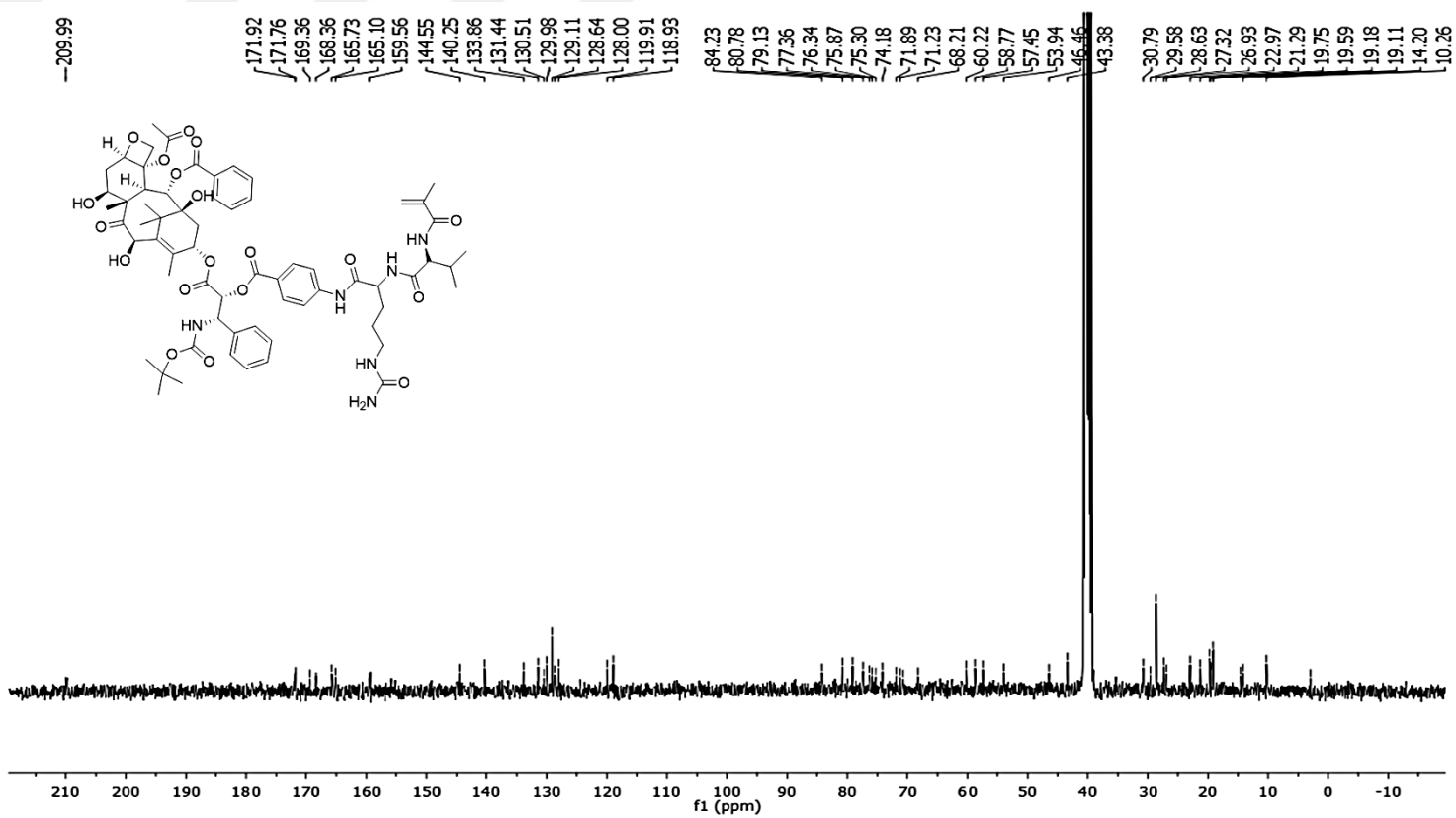

Figure A.56. ^{13}C-NMR Spectrum of MA-Val-Cit-4-aminobenzoyl-DTX (47)

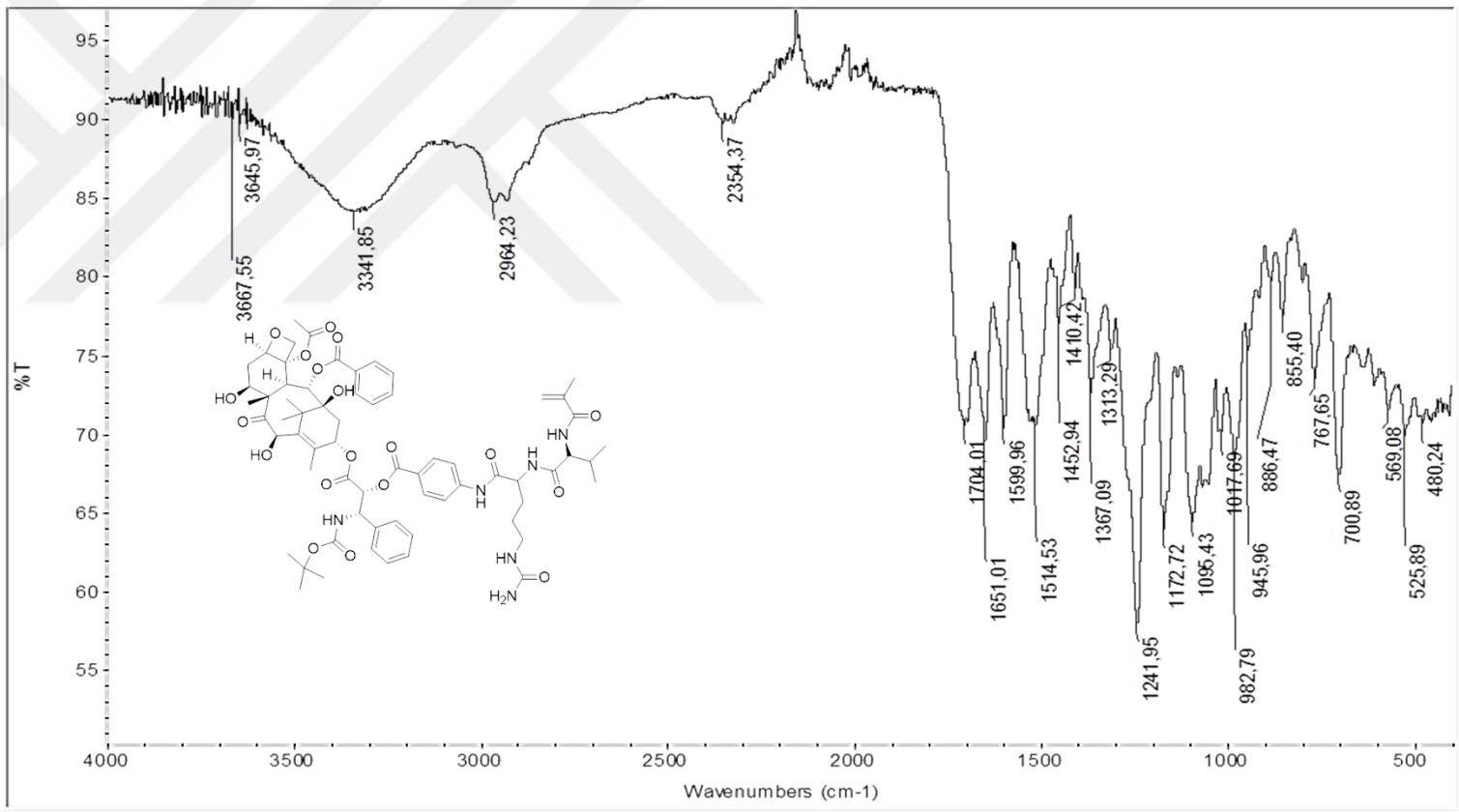

Figure A.57. FT-IR^{-1} Spectrum of MA-Val-Cit-4-aminobenzoyl-DTX (47)

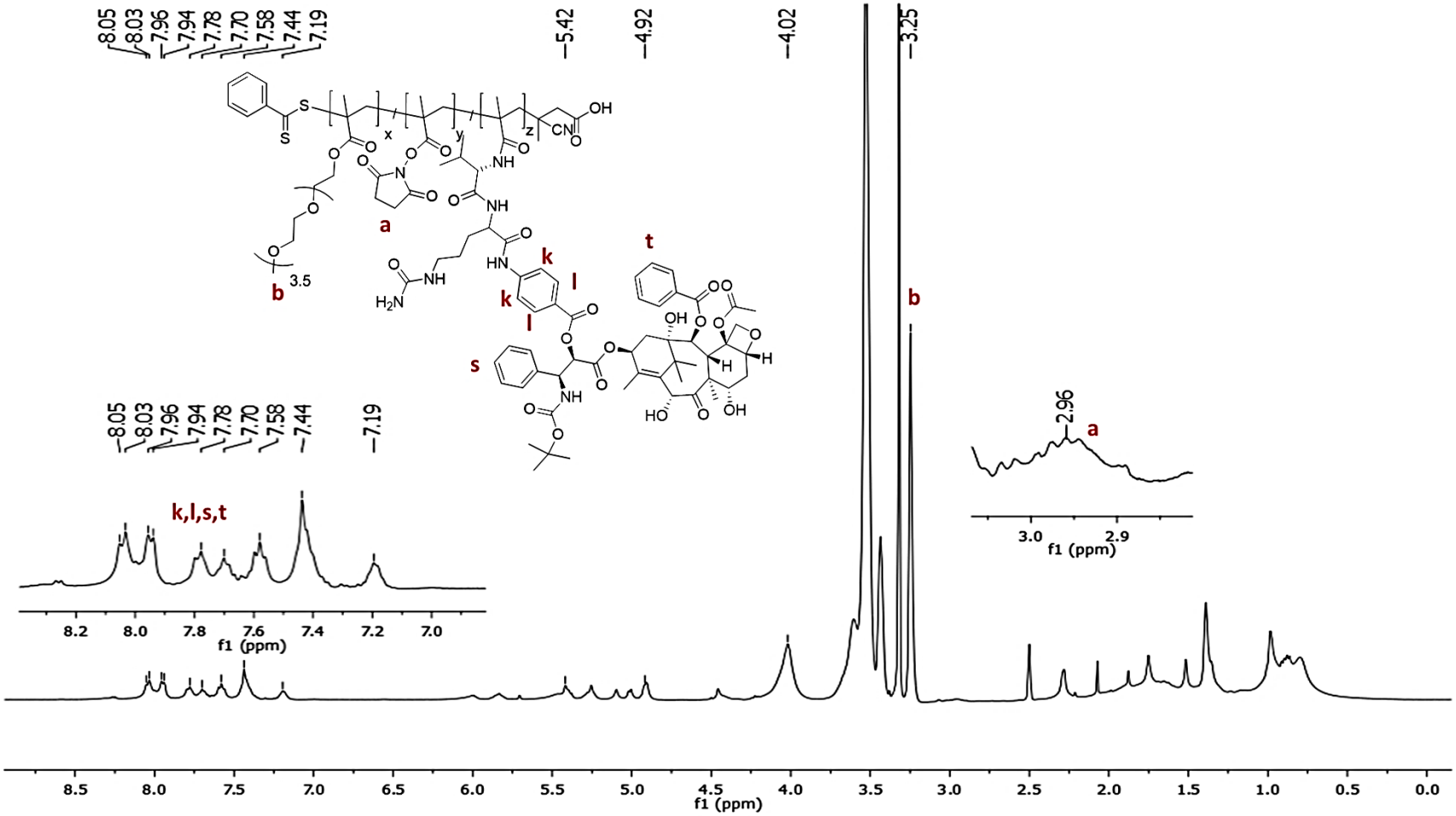

Figure A.58. ^{1}H NMR Spectrum of P(OEGMA-MA-Val-Cit-4-aminobenzoyl-DTX-NHS) (48)

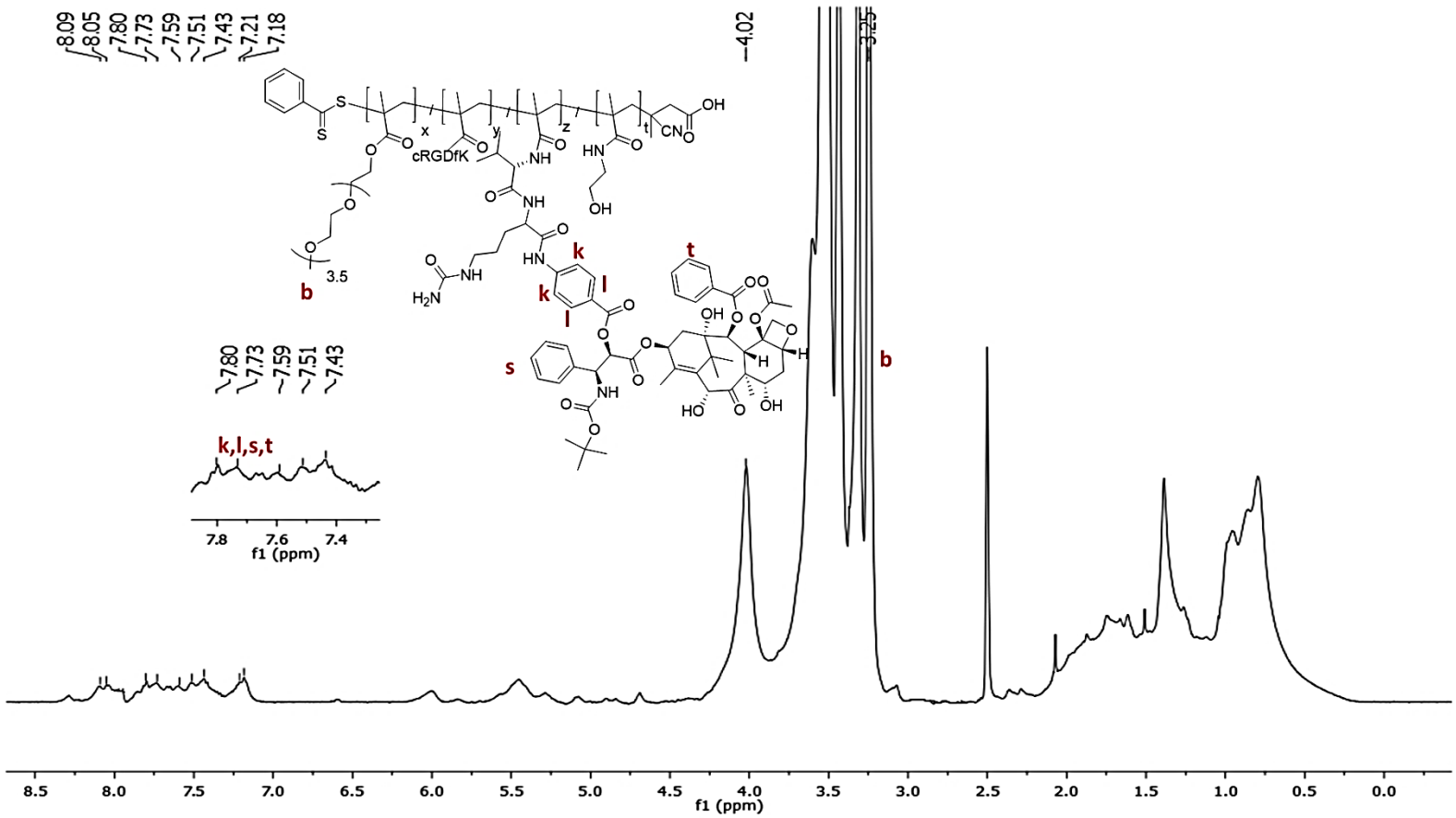

Figure A.59. ^{1}H NMR Spectrum of P(OEGMA-MA-Val-Cit-4-aminobenzoyl-DTX-RGD) (49)